

CO₂ Storage and Enhanced Oil Recovery: Bald Unit Test Site, Mumford Hills Oil Field, Posey County, Indiana

Scott M. Frailey, Ivan G. Krapac, James R. Damico, Roland T. Okwen,
and Ray W. McKaskle

Technical Editors

Jonathan H. Goodwin and Charles C. Monson

Contributing Authors

Peter M. Berger, Robert Butsch, Damon A. Garner, Jonathan H. Goodwin, John P. Grube, Keith C. Hackley,
Jessica S. Hinton, Abbas Iranmanesh, Christopher P. Korose, Edward Mehnert, Charles C. Monson,
William R. Roy, Steven L. Sargent, and Bracken Wimmer



Open File Series 2012-5 2012



**ILLINOIS STATE
GEOLOGICAL SURVEY**
PRAIRIE RESEARCH INSTITUTE



ILLINOIS STATE GEOLOGICAL SURVEY
Prairie Research Institute
University of Illinois at Urbana-Champaign

DISCLAIMER

This report was prepared as an account of work sponsored by an agency of the United States Government. Neither the United States Government nor any agency thereof, nor any of their employees, makes any warranty, express or implied, or assumes any legal liability or responsibility for the accuracy, completeness, or usefulness of any information, apparatus, product, or process disclosed, or represents that its use would not infringe privately owned rights. Reference herein to any specific commercial product, process, or service by trade name, trademark, or manufacturer, or otherwise does not necessarily constitute or imply its endorsement, recommendation, or favoring by the United States Government or any agency thereof. The views and opinions of authors expressed herein do not necessarily state or reflect those of the United States Government or any agency thereof.

Midwest Geological Sequestration Consortium

Final Report

October 1, 2007–March 30, 2012
Principal Investigator: Robert Finley
Illinois State Geological Survey
Prairie Research Institute
University of Illinois
(217) 244-8389
finley@illinois.edu

Report Issued: March 30, 2012

U.S. DOE Contract: DE-FC26-05NT42588

The Board of Trustees of the University of Illinois
Sandy Moulton, Director
c/o Grants & Contracts Office
1901 S. First Street, Suite A
Champaign, IL 61820
Illinois State Geological Survey
with Team Members:
Gallagher Drilling, Inc.
Trimeric Corporation

Frailey, S.M., I.G. Krapac, J.R. Damico, R.T. Okwen, R.W. McKaskle. 2012. CO₂ Storage and Enhanced Oil Recovery: Bald Unit Test Site, Mumford Hills Oil Field, Posey County, Indiana. J.H. Goodwin and C.C. Monson (eds.): Illinois State Geological Survey, Open File Series 2012-5, 172 pp.

CO₂ Storage and Enhanced Oil Recovery: Bald Unit Test Site, Mumford Hills Oil Field, Posey County, Indiana

Scott M. Frailey, Ivan G. Krapac, James R. Damico, Roland T. Okwen,
and Ray W. McKaskle

Technical Editors

Jonathan H. Goodwin and Charles C. Monson

Contributing Authors

Peter M. Berger, Robert Butsch, Damon A. Garner, Jonathan H. Goodwin, John P. Grube, Keith C. Hackley,
Jessica S. Hinton, Abbas Iranmanesh, Christopher P. Korose, Edward Mehnert, Charles C. Monson,
William R. Roy, Steven L. Sargent, and Bracken Wimmer



ILLINOIS STATE GEOLOGICAL SURVEY
Prairie Research Institute
University of Illinois at Urbana-Champaign
615 E. Peabody Drive
Champaign, Illinois 61820-6964
<http://www.isgs.illinois.edu>

CONTRIBUTORS

Robert J. Finley and Scott M. Frailey, Illinois State Geological Survey (ISGS), Prairie Research Institute, conducted the technical review of this document. Jonathan H. Goodwin and Charles C. Monson (ISGS) worked with contributors and reviewers to assemble the report. Goodwin and Frailey prepared the Abstract and Executive Summary.

Scott Frailey led the effort to find a suitable injection site as well as pilot planning, scheduling, and logistics of implementing the plan through post-carbon dioxide (CO₂) injection testing. Frailey monitored pressures and injection rates and performed real time analyses of the data for the CO₂ and water injection periods. He was the primary author for the introduction and sections on site selection, pilot site design and well arrangement, field observations during active CO₂ injection, and conclusions. Text for these sections was also contributed by James R. Damico and John P. Grube (ISGS), and Charles Monson.

Scott Frailey, Charles Monson, and Roland T. Okwen (ISGS) wrote the field history section, based largely on data provided by Mike Gallagher and Gallagher Drilling, Inc. (GDI), the operators of the field. James Damico organized and processed much of the data provided by GDI and drafted some of the figures.

James Damico and John Grube (ISGS) wrote the text for the geologic characterization section and were responsible for conceptual and geocellular modeling (including core and log analyses) as well as characterization of surface geology and bedrock.

Randy Locke (ISGS) coordinated the monitoring, verification, and accounting (MVA) program at the Bald Unit site. Ivan G. Krapac (ISGS) wrote or edited the majority of the MVA strategies and methods and MVA observations and interpretations sections. Ed Mehnert (ISGS) was responsible for groundwater modeling, write-up, and figures. Keith Hackley (ISGS) wrote the section dealing with isotopic characterization and oversaw lab work associated with this effort. Other ISGS contributors to both field and lab efforts and data analysis and interpretation included Peter Berger (geochemical modeling), Joe Chou and Shari Fanta (gas compositional analysis and isotopic characterization), Abbas Iranmanesh (data organization and presentation) and William Roy (geochemical modeling, health and human safety). Abbas Iranmanesh and Bracken Wimmer assisted with monitoring well installation and development, sample collection, and contributed to documentation of sampling methodology. Bob Butsch (Schlumberger Carbon Services) completed the cased hole log analyses and contributed the text and figures for the appendix on RST interpretation. Ray McKaskle, Kevin Fisher, Joe Lundeen, and Andrew Sexton (Trimeric) were responsible for injection equipment design, procurement, and testing; they also provided operational support. McKaskle was the primary author for the field operations section of this report. Additional contributors to this section were Scott Frailey, Damon A. Garner, Jessica Hinton, Charles Monson, and Steven L. Sargent (ISGS).

Mike Gallagher, Shawn Gallagher, Dan Gallagher, and Victor Gallagher of Gallagher Drilling, Inc. provided site and field logistic support and engineering and geologic design. Mike was the primary contact with ISGS throughout the project and provided information and feedback during the report writing stage. The Gallaghers also provided several of the figures used in this report. Ed Applegate and Billy Wormack (GDI) provided general field operations support.

Damon Garner (ISGS) provided extensive data management, archiving, and analysis tool development. Garner was also responsible for calculating gas production at the Bald Unit. Steve Sargent (ISGS) supported the data acquisition program from inception through completion, including selection, installation, calibration, and maintenance of monitoring equipment.

Roland Okwen (ISGS) was responsible for post-injection reservoir modeling and was the primary author for the CO₂ sequestration and EOR interpretation, analysis, and reservoir modeling section. Scott Frailey worked with Okwen on the modeling effort and write-up.

Scott Frailey and Charles Monson were the authors of the pilot closure and site reclamation section.

Bill Ellis, Billy Ellis, Rob Lowery, and Wayne Hammel provided field support. The ISGS well drilling crew led by Jack Aud installed the groundwater monitoring wells.

Other ISGS personnel who assisted with this report: Jessica Hinton was responsible for the early stages of report organization. Victoria Bobell, Megan Seger, Daniel Klen, Charles Monson, and Shannon Wilson

provided editing, figure drafting, unit conversions, and data compilation. Cynthia A. Briedis, Pamella K. Carrillo, and Michael W. Knapp provided figure formatting and layout of final report. Christopher Korose contributed Geographic Information Systems and volumetrics figures and images. Cheryl K. Nimz and Jon Goodwin provided technical editing.

ISGS personnel who took equipment photos include Roland Okwen, Jessica Hinton, Charles Monson, and Damon Garner.

ACKNOWLEDGMENTS

The Midwest Geological Sequestration Consortium is funded by the U.S. Department of Energy through the National Energy Technology Laboratory (NETL) via the Regional Carbon Sequestration Partnership Program (contract number DE-FC26-05NT42588) and the Illinois Department of Commerce and Economic Opportunity, Office of Coal Development through the Illinois Clean Coal Institute (cost share agreement).

Through a university grant program, Landmark Software was used for the reservoir and geologic modeling.

ABSTRACT

The Midwest Geological Sequestration Consortium (MGSC) carried out a small-scale carbon dioxide (CO₂) injection test in a sandstone within the Clore Formation (Mississippian System, Chesterian Series) in order to gauge the large-scale CO₂ storage that might be realized from enhanced oil recovery (EOR) of mature Illinois Basin oil fields via miscible liquid CO₂ flooding.

As part of the MGSC's Validation Phase (Phase II) studies, the small injection pilot test was conducted at the Bald Unit site within the Mumford Hills Field in Posey County, southwestern Indiana, which was chosen for the project on the basis of site infrastructure and reservoir conditions. Geologic data on the target formation were extensive. Core analyses, porosity and permeability data, and geophysical logs from 40 wells were used to construct cross sections and structure contour and isopach maps in order to characterize and define the reservoir architecture of the target formation. A geocellular model of the reservoir was constructed to improve understanding of CO₂ behavior in the subsurface.

At the time of site selection, the Field was under secondary recovery through edge-water injection, but the wells selected for the pilot in the Bald Unit had been temporarily shut-in for several years. The most recently shut-in production well, which was surrounded by four nearby shut-in production wells in a five-spot pattern, was converted to CO₂ injection for this pilot. Two additional wells outside the immediate five-spot pattern, one of which was an active producer, were instrumented to measure surface temperature and pressure. The CO₂ injection period lasted from September 3, 2009, through December 14, 2010, with one three-month interruption caused by cessation of CO₂ deliveries due to winter weather. Water was injected into the CO₂ injection well during this period. A total of 6,300 tonnes (6,950 tons) of CO₂ were injected into the reservoir at rates that generally ranged from 18 to 32 tonnes (20 to 35 tons) per day. The CO₂ injection bottomhole pressure generally remained at 8.3 to 9.0 MPa (1,200 to 1,300 psig). The CO₂ injection was followed by continued monitoring for nine months during post-CO₂ water injection.

A monitoring, verification, and accounting (MVA) program was designed to determine the fate of injected CO₂. Extensive periodic sampling and analysis of brine, groundwater, and produced gases began before CO₂ injection and continued through the monitored waterflood periods. Samples were gathered from production wells and three newly installed groundwater monitoring wells. Samples underwent geochemical and isotopic analyses to reveal any CO₂-related changes. Groundwater and kinetic modeling and mineralogical analysis were also employed to better understand the long-term dynamics of CO₂ in the reservoir. No CO₂ leakage into groundwater was detected, and analysis of brine and gas chemistry made it possible to track the path of plume migration and infer geochemical reactions and trapping of CO₂. Cased-hole logging did not detect any CO₂ in the near-wellbore region.

An increase in CO₂ concentration was first detected in February 2010 from the gas present in the carboy during brine sampling; however, there was no appreciable gas volume associated with the detection of CO₂. The first indication of elevated gas rates from the commingled gas of the pilot's production wells occurred in July 2010 and reached a maximum of 0.36 tonnes/day (0.41 tons/day) in September 2010. An estimated 27 tonnes (30 tons) of CO₂ were produced at the surface from the gas separator at the tank battery from September 3, 2009, through September 11, 2011, representing 0.5% of the injected CO₂. Consequently, 99.5% of the injected CO₂ was stored at the Bald Unit Field after nine months of post-CO₂ injection monitoring.

Project improved oil recovery (IOR) was estimated at 412 m³ (2,590 bbl) and CO₂ EOR as 325 m³ (2,045 bbl), although estimation of an EOR baseline was difficult because recovery was also increased by pre-project well work. These figures would have been higher if not for variations in oil production rate due to winter weather. Oil production rates did not return to pre-shut-in level after the lengthy winter injection hiatuses, but remained elevated relative to production rates immediately before the pilot.

The pilot was designed to measure and record data that could be used to calibrate a reservoir simulation model of the Clore sandstone to project the EOR potential of a larger-scale project at the Bald Unit. A model calibrated to field data (including geologic data and oil and water production) was used to assess the full-field EOR potential of the Field. Projections based on these models indicated that full-field CO₂ injection for 20 years could have 12% oil recovery or 27,000 scm (170,000 stb) with a CO₂ net utilization of 4,900 scm/scm (31,000 scf/stb). The potential CO₂ storage is estimated to be 193,600 to 277,450 tonnes (213,000 to 305,200 tons).

EXECUTIVE SUMMARY

Based on the results of the Characterization Phase (Phase I) studies carried out by the Midwest Geological Sequestration Consortium (MGSC), enhanced oil recovery (EOR) offers the most important economic offset to the costs associated with carbon storage in the Illinois Basin. As part of its Validation Phase (Phase II) studies, the MGSC carried out a small-scale carbon dioxide (CO₂) injection test in a sandstone of the Clore Formation (Mississippian System, Chesterian Series), in order to gauge the potential for EOR and concomitant large-scale CO₂ storage via miscible liquid CO₂ flooding in mature Illinois Basin oil fields.

The Bald Unit in the Mumfords Hills Field in Posey County, southwestern Indiana, was selected as the site for the MGSC EOR II pilot study. The decision was based on screening of five criteria: (1) conditions in the reservoir conducive to a miscible liquid CO₂ flood; (2) operation and development history of the Field; (3) surface conditions to allow delivery of CO₂ via tanker trucks; (4) wellbore condition of producing and injection wells, and (5) results of preliminary geologic and reservoir modeling.

Data for use in developing geocellular and conceptual models of the reservoir were relatively extensive compared with many Illinois Basin oil fields. Core analyses from 15 wells were supplied by the field operator, as well as spontaneous potential (SP) and either normal/lateral or short normal/induction log packages from 40 wells in the Field. There were also four neutron (gamma-ray) logs, one density log, and two density-neutron logs. These provided the data used to define the structure and architecture of the formation. A geocellular model of the reservoir was built for reservoir modeling to estimate CO₂ EOR and storage capacity and to quantify the distribution of CO₂ in the subsurface. The average core porosity was 19%, and the average core permeability was $1.46 \times 10^{-13} \text{ m}^2$ (148 mD).

At the time of site selection, the Field was under secondary recovery through edge-water injection to maintain reservoir pressure, but most of the wells in the Bald Unit had been temporarily shut-in for several years. The southernmost well in the unit was the single water injection well at the beginning of the water-flood history of the Bald Unit. Historically, this well was able to maintain pressure in the entire Bald Unit; water injection at this well continued throughout the CO₂ EOR pilot study.

An oil production well that had been shut-in for the last nine years was selected as the CO₂ injection well; it was surrounded by four other shut-in production wells, making an inverted five-spot injection pattern. Two other nearby production wells, one of which was an active producer, were instrumented to collect temperature and pressure response information.

The injection of CO₂ began on September 3, 2009, and when it was temporarily suspended on January 23, 2010 due to winter road restrictions, a total of 2,600 tonnes (2,860 tons) of CO₂ had been injected. From January 23 to May 3, 2010, 2,080 m³ (13,100 bbl) of water was injected through the same injection well. Another 3,700 tonnes (4,080 tons) of CO₂ was injected through the well from May 3, 2010, through December 14, 2010. Monitoring continued until September 21, 2011, during which time water was injected in the pilot's injection well. During this 281-day period, a total of 5,280 m³ (33,200 bbl) of water was injected.

The rate of CO₂ injected during the first injection period from September 3, 2009, to January 23, 2010, ranged from as low as 18 to 23 tonnes (20 to 25 tons) per day to as great as 27 to 32 tonnes (30 to 35 tons) per day. Injection rates were quite variable during this period; they were initially constrained by CO₂ deliveries (one truckload per day) and by the need for the Field operator to become familiar with the equipment. Despite the variability in rates, bottomhole injection pressures remained close to 8.6 MPa (1,250 psig). After CO₂ injection resumed on May 3, 2010, CO₂ deliveries were increased, and the injection rate remained relatively constant at 18 to 25 tonnes (20 to 28 tons) per day; average rate was 20.3 tonnes (22.4 tons) per day. At the beginning of this period, injection pressure reached a maximum of 9.8 MPa (1,420 psig), but decreased over about 3 weeks and stabilized at about 9.0 MPa (1,300 psig) and remained between 8.6 and 9.0 MPa (1,250 and 1,300 psig) until CO₂ injection ended on December 14, 2010. Injection was never constrained by the 10.3 MPa (1,500 psig) permitted maximum injection pressure. A total of 6,300 tonnes (6,950 tons) of CO₂ were injected into the reservoir.

An increase in CO₂ concentration was first detected in February 2010 from the gas liberated in the carboy during brine sampling; however, there was no appreciable gas volume associated with the detection of CO₂. Because of the direction of flow from the water injection well south of the five-spot pilot area, the first wells to show significant amounts of CO₂ in the gases coming from the wells were those north of the injec-

tion well. The evidence from gas samples, brine samples, and the modeling of the reservoir showed that all of the wells were in good communication with one another.

Because of the use of downhole packers in the producing wells, it was not possible to meter produced gas rates from individual wells. The first indication of elevated gas rates from the commingled gas of the pilot's wells occurred in July 2010 and reached a maximum of 0.36 tonnes/day (0.41 tons/day) in September 2010. An estimated 27 tonnes (30 tons) of CO₂ were produced at the surface from the gas separator at the tank battery from September 3, 2009, through September 11, 2011, representing 0.5% of the injected CO₂. Consequently, 99.5% of the injected CO₂ was stored at the Bald Unit after nine months of post- CO₂ injection monitoring.

Monitoring, verification and accounting (MVA) strategies for the pilot study included (1) developing and implementing a health and safety plan; (2) monitoring air quality at strategic locations to ensure human safety during CO₂ transfer and injection operations; (3) monitoring volumes and rates of CO₂ injection; (4) monitoring the quality of shallow groundwater before, during, and after CO₂ injection and modeling of potential CO₂-rock-water interactions; (5) monitoring volumes and chemical properties of produced oil, gas, and brine before, during, and after CO₂ injection; and (6) monitoring surface and subsurface CO₂ injection pressures and temperatures.

A simplified model of the surficial groundwater aquifer was used to find the groundwater flow direction and to determine whether, in the event of a leak, CO₂ released into the shallow groundwater would escape from the site. The model showed that in the absence of heavy groundwater pumpage, any CO₂ released into the groundwater would move no more than about 200 m (about 656 ft) to the west or northwest from the injection well in 100 years, remaining within the boundaries of the test site.

Analysis of the aqueous and gas samples from the Clore Formation sandstone for the MVA program allowed the inference of reservoir characteristics and, to a significant degree, the fate of CO₂ in the reservoir. Dissolution of CO₂ into the reservoir brine in the Clore sandstone caused the pH to decrease by about one pH unit, from approximately 6.8 to 5.8. For most wells, the pH decrease occurred about 45 days before the detection of CO₂ in gas samples collected from the wells, indicating rapid dissolution of CO₂ into the brine. The CO₂ dissolution and expected dissociation reactions increased the alkalinity of the brine somewhat, but the effects differed from well to well. Both $\delta^{13}\text{C}$ and ^{14}C were found to be viable tracers of injected CO₂, although ^{14}C was considered more effective.

The pH and alkalinity of the groundwater remained nearly constant or decreased gradually, clearly indicating that its chemistry was not being influenced by leakage of CO₂ from the reservoir. Also, the δD and $\delta^{18}\text{O}$ values of the shallow groundwater remained significantly different from the values in the brines.

Project improved oil recovery (IOR) was estimated at 412 m³ (2,590 bbl) and CO₂ EOR at 325 m³ (2,045 bbl), although estimation of an EOR baseline was difficult because recovery was also increased by well work. Oil production rates did not return to the pre-shut-in level after the lengthy winter injection hiatus, but they remained elevated relative to production rates immediately before the pilot.

The pilot test was designed to measure and record data that could be used to calibrate a reservoir simulation model of the Clore sandstone to estimate the CO₂ storage and EOR potential of a larger-scale project at the Field. A model calibrated to field data (including geologic data and oil and water production) was used to assess the full-field CO₂ storage and EOR potential of the Bald Unit. Projections based on these models indicated that full-field CO₂ injection for 20 years could have 12% oil recovery or 27,000 scm (170,000 stb) with a CO₂ net utilization of 4,900 scm/scm (31,000 scf/stb). The potential CO₂ storage is estimated to be 193,600 to 277,450 tonnes (213,000 to 305,200 tons).

CONTENTS

CONTRIBUTORS	IV
ACKNOWLEDGMENTS	V
ABSTRACT	VI
EXECUTIVE SUMMARY	VII
INTRODUCTION	1
Midwest Geological Sequestration Consortium Background	1
MGSC Phase I Illinois Basin Oil Reservoir Assessment Summary	1
Phase II EOR Pilot Objectives	2
Site Screening: General Pilot Requirements	2
CO ₂ –Crude Oil Interactions	2
Operation and Development History	2
Surface Conditions	2
Wellbore Conditions	4
Geological and Reservoir Modeling	4
SITE SELECTION	4
Oil Characteristics and Geology	4
Geographic Description and Location	5
Site Logistics	5
FIELD HISTORY	6
OOIP and Wells	6
Bald Unit Development	10
Geologic and Production Data Available	11
Well Completion Data	14
Cumulative Production and Injection Maps	17
Tank Battery and Flow Lines	17
Brine Injection Equipment and Injection Lines	19
PILOT SITE DESIGN AND WELL ARRANGEMENT	20
Returning Wells to Production	20
Observation Wells	21
Well Preparation	21
Tank Battery Site for Production and Separation	21
Chemical Corrosion Treatment Plan	21
Pre-injection Reservoir Modeling	23
CO ₂ UIC II Injection Permit	23
GEOLOGICAL CHARACTERIZATION	23
Area Geology	23
Surface Geology	23
Bedrock	23
General Site Hydrology and Hydrogeology	24
Reservoir Geology	24
Core Analyses	24
Log Analyses	24
Conceptual Geological Model	24
Geocellular Model	31

STRATEGIES AND METHODS FOR THE MONITORING, VERIFICATION, AND ACCOUNTING PROGRAM	33
Objectives	33
Sampling Priorities	37
Health and Human Safety	37
Sampling Strategies	37
Design of the Groundwater Monitoring System for the Injection Site	37
Groundwater Monitoring Well Description	38
Frequency of Sampling	38
Sample Types	40
Groundwater	40
Oil-Reservoir Brine and Gas Samples	40
Measurements and Sample Analyses	42
Bulk Chemistry and Fluid Characterization	42
Reservoir Brine Chemistry	42
Reservoir Brine Characterization	42
Reservoir Gas Chemistry	47
Groundwater Chemistry	47
Pennsylvanian Sandstone Mineralogy	51
Isotope Chemistry	51
Geochemical Modeling	51
Cased Hole Logging	51
FIELD OPERATIONS DURING CO₂ INJECTION	51
CO ₂ Pumping Equipment	51
Overview	51
Portable Storage Tanks	52
Booster Pump	52
Main Pump Skid	55
Automated Injection-Pressure Control System	55
Flow Meters	55
In-Line Heater	59
Data Acquisition Equipment	61
Pressure and Temperature Sensors	61
Data Acquisition System	61
Wellhead Design	61
General Operations	61
Operational Challenges	63
Scheduling CO ₂ Delivery	63
Winter Road Restrictions	64
Scale Accumulation	64
Booster Pump Failure	64
Corrosion and Well Work	64
FIELD OBSERVATIONS DURING ACTIVE CO₂ INJECTION	65
Overview	65
BU-1 Injection Schedule	66
CO ₂ Injection	66
Water Injection	66

Pilot Area's Oil, Gas, and Water Production and Pressure Response	60
Oil Production	69
Water Production	71
Gas Production	71
Water Injection Outside of the CO ₂ Injection Pilot Area	71
MVA OBSERVATIONS AND INTERPRETATIONS	71
Brines and Gases from Oil Production Wells	71
Bulk Chemistry	71
pH and Alkalinity	71
Hydrocarbons	74
Isotope Chemistry	74
Groundwater Monitoring Wells	80
Bulk Chemistry	80
Isotope Chemistry	85
Mineral-Fluid Equilibria	85
Cased Hole Logging	88
CO₂ SEQUESTRATION AND EOR: INTERPRETATION, ANALYSIS AND RESERVOIR MODELING	88
Bald Unit Pilot Area Reservoir Model Calibration	88
Description of the Geologic and Reservoir Models and Input Parameters	90
Description of the Calibrated Model	94
Primary Recovery	94
Waterflood Recovery	94
CO ₂ Pilot	94
Pilot Projections Using Calibrated Model to Determine CO ₂ Enhanced Recovery	97
Pilot Case 1: Continuous Production and Injection at Maximum Pressure	98
Pilot Case 2: Continuous Injection of CO ₂ for 5 years with Pilot Case 1 Conditions	101
Full-Field Projections Using Calibrated Model	101
Field Case 1: Full-Field CO ₂ Injection	101
Field Case 2: Expanded Full-Field CO ₂ Injection	101
Modeling Summary	104
PILOT CLOSURE	104
Plugging and Abandonment of Groundwater Monitoring Wells	104
Removal of Data Acquisition Equipment	104
Relocation of Injection Equipment	104
CONCLUSIONS	104
CO ₂ Storage Estimate	104
EOR Estimate	105
General Observations	105
Effectiveness of Operations	105
Effectiveness of MVA Techniques	105
RECOMMENDATIONS	106
REFERENCES	106
APPENDICES	109
1 Well permit application.	109
2 CO ₂ injection permit.	112

3	MVA methods.	118
4	Geologic logs, natural gamma logs, and well construction details of groundwater monitoring wells.	122
5	Chemistry of reservoir brine.	135
6	Chemistry of groundwater.	144
7	Gas composition corrected for air contamination.	147
8	Interpretation of the reservoir saturation tool logging data from the Bald Unit.	148
9	Equipment.	160
10	Schematics of data logger equipment.	161
11	Scale treatment.	162
12	Description of fracture stimulation treatment.	163
13	Sequence of events.	164
14	Results of all isotopic analyses.	167

LIST OF TABLES

1	Bald Unit wells (lease name, well number, and abbreviation), well type, and completion dates.	10
2	Date each well was temporarily abandoned.	12
3	Summary of sampling locations, number of sampling events, and types of samples collected in relation to operational activities at the Bald Unit CO ₂ pilot.	39
4	Sample preservation, containers, and methods.	40
5	Mineralogy of two core samples taken from the screened interval of groundwater monitoring well MH-2.	50
6	Summary of common chemical parameters for brine samples.	73
7	Summary of stable isotope results from brine and gas samples.	75
8	Summary of common water quality parameters for groundwater samples.	82
9	Summary table of stable isotope data from groundwater monitoring wells.	85
10	Mole fractions of the pseudo-components used in the five-component equation of state to match crude oil properties at Bald Unit.	92
11	Reservoir brine and rock parameters.	93
12	Saturation and relative permeability end points.	94
13	EOR and CO ₂ utilization for optimized pilot cases.	101
14	EOR and CO ₂ utilization for optimized field-wide cases.	103

LIST OF FIGURES

1	CO ₂ enhanced oil recovery (EOR) resources in the Illinois Basin, mapped by oil field (from Midwest Geological Sequestration Consortium, 2005).	3
2	Location of the Bald Unit (red rectangle) within the Mumford Hills Field.	6
3	Location map of the Mumford Hills site, Posey County, Indiana (left), and aerial orthophotograph of the site area, showing names of roads leading to the site.	7
4	The tank battery at Mumford Hills Field, including tanks and pump house.	8
5	Bald Unit Pilot area: orthophotographic map of the oil production wells, CO ₂ injection well, groundwater monitoring wells, and the tank battery.	9
6	Isopach map of gross Clore sandstone used to estimate the bulk volume of sand in acre-feet for OOIP calculation.	10
7	Map of well locations on the Bald Unit.	12
8	Bald Unit's average daily oil rate in barrels of oil per day (bopd) from the beginning of primary production through early 2009 (several months before commencement of CO ₂ injection).	13

9	Annual oil production (bbls) from the beginning of primary production through 2009.	13
10	Average daily water injection rate in barrels of water per day (bwpd) from the beginning of primary production through early 2011.	14
11	Bald Unit oil and water production and water injection bubble map for life of the Bald Unit prior to the pilot, by well.	15
12	Wellbore schematic of a typical Bald Unit production well (courtesy of Gallagher Drilling, Inc.).	16
13	Production manifold at Bald Unit tank battery.	17
14	Bald Unit tank battery.	18
15	Example of control panels for water injection equipment in the Bald Unit pump house.	19
16	Kimray cast iron back-pressure gas regulator attached to gas separator at the Bald Unit tank battery.	22
17	Teledyne Merla orifice well tester (aluminum pipe to right) attached to the liquid-gas separator at the Sugar Creek Field tank battery (a photograph of the well tester at the Bald Unit tank battery was not available).	22
18	Map of the unlithified aquifers in the Mumford Hills area (data obtained from Indiana Map Service, http://inmap.indiana.edu/viewer.htm , March 12, 2012).	25
19	Photo of a sample of the core taken from the Bald Unit #1 well at a depth of 586–587 m (1,923–1,926 ft).	26
20	A north to south geophysical log cross section showing the unit of interest, the Clore Formation, and a reference unit, the lower Kinkaid Limestone.	27
21	A west to east geophysical log cross section showing the unit of interest, the Clore Formation, and a reference unit, the Lower Kinkaid Limestone.	28
22	Structure map on the correlative top of the sandstone member of the Clore Formation.	29
23	Isopach map of the net thickness of the sandstone member of the Clore Formation.	30
24	Variogram map, on the left, and variogram with the fitted models on the right. A very strong N-S anisotropy is present in the variogram map, as expected given the geometry of the target formation indicated by the structure and isopach maps of the sandstone, shown in Figures 22 and 23. In the figure on the right, the corresponding variograms calculated in the two directions are represented by the erratic, lighter lines while the models are the smoother, darker lines.	31
25	Graphs illustrating the transforms created to convert normalized SP data into permeability (left) and permeability into porosity (right).	32
26	Top: boundary of the 3D geocellular model with a porosity cutoff applied, which shows the extent of the reservoir in the model.	33
27	North-to-south cross sections showing the distribution of permeability (top two figures) and porosity (bottom two).	34
28	West to east cross sections showing the distribution of permeability (top two figures) and porosity (bottom two).	35
29	Planar slices through the geocellular model. The upper and lower two images are taken at depths of 6 and 9 meters (20 and 30 feet) below the top of the Clore Formation, respectively.	36
30	Metal well protector (yellow) of monitoring well, with Solinst Barologger™ resting in open lid.	39
31	Equipment for measurement of brine field parameters.	41

32	Typical concentrations of sodium and chloride in brine collected from the Mumford Hills oil reservoir.	43
33	Concentration of sodium and chloride in water injected into oil reservoir at well BD-3 during water flood activities at Mumford Hills.	43
34	Concentrations of major analytes in water samples collected from well BD-3.	44
35	Typical concentrations of common constituents detected in brine samples from oil production wells.	44
36	Concentrations of sodium and chloride in brine samples collected from oil production well BA-1 do not follow trend observed in other production wells.	45
37	Concentrations of typical constituents detected in brine collected from oil production well BA-1.	45
38	Carbon dioxide concentrations in gas samples collected from BA-1, BA-2, IB-2, IB-3, and the tank battery (TB).	46
39	Carbon dioxide concentrations in gas samples collected from BA-1, BA-2, IB-2, IB-3, and the tank battery (TB).	46
40	Oxygen concentrations determined by gas chromatograph in gas samples collected from oil production wells and the tank battery (TB).	47
41	Nitrogen concentrations determined by gas chromatograph in gas samples collected from oil production wells and the tank battery (TB).	48
42	pH of shallow groundwater from the groundwater monitoring wells MH-1, MH-2 and MH-3.	48
43	Picture of core from MH-2.	49
44	Eh-pH plot showing stability field for iron compounds.	50
45	The CO ₂ injection system piping and instrument diagram.	53
46	Portable Air Liquide CO ₂ storage tanks. Tank capacity is 55 tonnes (60 tons) of CO ₂ .	54
47	Connection line between CO ₂ storage tank and injection equipment.	54
48	Booster pump (frosted over) and motor.	56
49	Injection pump skid at the Bald Unit tank battery.	56
50	CAT triplex pump in operation at Bald Unit tank battery.	57
51	Injection system control panel.	57
52	Globe Cast (BadgerMeter, Inc.) pressure control valve (red object at upper center) on return line between discharge of main pump and storage tank.	58
53	Natco 263,800 kJ/hr (250,000 Btu/hr) line heater. Inline heater's CO ₂ inlet (right) frosted over; top of this line has Siemens pressure gauge/transmitter (small box with blue circle on casing) that is connected to the Globe Cast pressure control valve. In-line heater discharges to the injection line (blue line to right).	59
54	Omega pressure controller panel cover and housing at Sugar Creek site with pressure reading shown.	60
55	Cameron NuFlo liquid turbine meter (center, immediately behind "meter valve" sign) and Siemens pressure gauge (with blue cover, immediately behind NuFlo meter) in series on frosted line.	60
56	Data acquisition and transmission enclosure at a production well, showing the solar panel, datalogger box, and battery.	62
57	A typical production wellhead (right), IB-2, at the Bald Unit. The Bald Unit tank battery and CO ₂ storage tanks are visible in the background.	63
58	BU-1 daily CO ₂ injection rates from September 3, 2009 to December 14, 2010.	67

59	BU-1 bottomhole injection pressure (datum-corrected) during first CO ₂ injection, September 3, 2009 to January 22, 2010.	67
60	BU-1 bottomhole injection pressure (datum-corrected) period during second CO ₂ injection, May 3, 2009 to December 14, 2010.	68
61	BU-1 bottomhole injection pressure (psig) and daily water injection rate (bwpd) between the two CO ₂ injection periods, January 27 and April 29, 2010.	68
62	BU-1 bottomhole injection pressure (psig) and daily water injection rate (bwpd) following second (and final) CO ₂ injection period, December 20, 2010 through September 11, 2011.	69
63	Five-spot daily oil rate (bopd) vs. time over entire monitoring period.	70
64	pH values in brine samples collected from BA-1, BA-2, IB-2, IB-3, and the tank battery (TB) over entire monitoring period.	72
65	Alkalinity concentrations in brine collected from BA-1, BA-2, IB-2, IB-3, and the tank battery (TB) over entire monitoring period.	72
66	Total hydrocarbon concentrations (C ₁ –C ₆) (corrected for air contamination) in gas samples collected during brine sampling from BA-1, BA-2, IB-2, and IB-3 over entire monitoring period.	74
67	Concentrations of propane in gas samples collected during brine sampling from BA-1, BA-2, IB-2, and IB-3 over entire monitoring period.	76
68	Concentrations of n-butane in gas samples collected during brine sampling from BA-1, BA-2, IB-2, and IB-3 over entire monitoring period.	76
69	δ ¹³ C of DIC in brine samples from BD-3, BA-1, BA-2, IB-2, IB-3, and the tank battery (TB) over entire monitoring period.	77
70	δ ¹⁸ O and δD of all aqueous samples from the five-spot production wells (BA-1, BA-2, IB-2, and IB-3), water supply well (BD-3), and the monitoring wells (MH-1, MH-2, and MH-3).	78
71	δD of aqueous samples from the five-spot production wells (BA-1, BA-2, IB-2, and IB-3), water supply well (BD-3), and the monitoring wells (MH-1, MH-2, and MH-3) over entire monitoring period.	79
72	Chloride concentration versus δD of samples from BD-3, BA-1, BA-2, IB-2, and IB-3.	79
73	Carbon isotopic composition of CO ₂ in gas samples acquired during brine sampling from BD-3, BA-1, BA-2, IB-2, and IB-3 over entire monitoring period.	80
74	Isotopic composition of methane from gas samples acquired during brine sampling showing typical compositions of different sources of methane from BD-3, BA-2, IB-2, and IB-3 over entire monitoring period.	81
75	δ ¹³ C composition of methane from BD-3, BA-2, IB-2, and IB-3 over entire monitoring period.	81
76	Sodium and chloride concentrations in groundwater samples collected from MH-2 and MH-3 over entire monitoring period.	83
77	Sodium and chloride concentrations in groundwater samples collected from monitoring well MH-1 over entire monitoring period.	83
78	Alkalinity in groundwater samples collected from MH-1, MH-2, and MH-3 over entire monitoring period.	84
79	Barium concentrations in groundwater samples collected from MH-1, MH-2, and MH-3 over entire monitoring period.	84
80	δ ¹³ C of DIC in groundwater samples collected from MH-1, MH-2, and MH-3 over entire monitoring period.	86

81	$\delta^{13}\text{C}$ of DIC plotted versus sulfate concentration for MH-1, MH-2, and MH-3.	86
82	(a) $\delta^{18}\text{O}$ and (b) δD for MH-1, MH-2, and MH-3 over entire monitoring period.	87
83	Observed and modeled concentrations of HCO_3 in groundwater collected from MH-2.	89
84	Mass of oxygen-reducing bacteria over time in the O_2 -driven model.	89
85	Measured and model-generated iron and sulfur concentrations in groundwater collected from well MH-2.	90
86	3-D geologic model of Mumford Hills depicting permeability distribution (South-North view).	91
87	(a) Water–oil and (b) gas–oil relative permeability curves used in reservoir simulations.	95
88	Comparison of simulation results and field data, by well, for cumulative oil production at the end of primary recovery.	95
89	Comparison of simulated values and field data, by well, for oil production at the end of waterflooding (secondary recovery).	96
90	Comparison of simulated values and field data, by well, for water production at the end of waterflooding.	96
91	Cumulative water injected during waterflooding via BD-5.	96
92	Simulated and field CO_2 injection rates during pilot project.	97
93	Field oil and water production rates during primary recovery, waterflooding, and CO_2 -EOR.	98
94	Areal distribution of gas (CO_2) saturation (a) at the end of CO_2 injection and (b) after one year of water injection (layer 17 in the model).	99
95	Cross-section of injected CO_2 distribution at the end of CO_2 injection viewed in (upper left) the x-y directions and (lower left) the x-direction, and cross-section of injected CO_2 distribution after one year of water injection viewed in (upper right) the x-y directions and (lower right) the x-direction. Note: All production wells in these figures are shut-in during CO_2 and chase water injection (pilot project).	100
96	(a) Comparison of simulated oil production rates of Pilot Case 1 and Pilot Case 2 to that of the calibrated model; (b) comparison of simulated oil production rates of Field Case 1 and Field Case 2 to that of the calibrated model.	102
97	Map of the wells showing the proposed changes to the well pattern according to (a) the first simulation case and (b) the second simulation case.	103

LIST OF APPENDIX TABLES

A3-1	Input parameters for GFLOW.	119
A4-1	Detailed geologic log for Mumford 1 (MH-1) groundwater monitoring well.	122
A4-2	Detailed geologic log for Mumford 2 (MH-2) groundwater monitoring well.	124
A4-3	Well construction details for MH-1. Some fields were intentionally left blank.	126
A4-4	Well construction details for MH-2. Some fields were intentionally left blank.	127
A4-5	Well construction details for MH-3. Some fields were intentionally left blank.	128
A5-1	Concentrations (in mg/L) of constituents detected in reservoir brine samples from wells BA-1 and BA-2.	135
A5-2	Concentrations (in mg/L) of constituents detected in reservoir brine samples from wells BA-1 and BA-2 (continued).	136
A5-3	Measurements of water quality parameters from reservoir brine samples from wells BA-1 and BA-2.	137
A5-4	Measurements of water quality parameters from reservoir brine samples from wells BA-1 and BA-2.	138

A5-5	Concentrations of constituents detected in reservoir brine samples from wells IB-2 and IB-3. All measurements in mg/L.	139
A5-6	Concentrations of constituents detected in reservoir brine samples from wells IB-2 and IB-3 (continued). All measurements in mg/L.	140
A5-7	Measurements of water quality parameters from reservoir brine samples from wells IB-2 and IB-3.	141
A5-8	Concentration (in mg/L) of constituents detected in reservoir brine samples from well BD-3 and the tank battery (TB-1).	142
A5-9	Measurements of water quality parameters from well BD-3 and the tank battery (TB-1).	143
A6-1	Concentrations (in mg/L) of constituents detected in groundwater samples collected from monitoring wells.	144
A6-2	Concentrations (in mg/L) of constituents detected in groundwater samples collected from monitoring wells (continued).	145
A6-3	Groundwater properties measured at monitoring wells.	146
A7-1	Composition (%) of gas samples collected at Bald Unit wellheads and tank battery, corrected for air contamination.	147
A9-1	Data monitoring and logging equipment used at the Bald Unit pilot.	160
A12-1	Stages of fracture stimulation treatment.	163
A14-1	Isotopic composition of brines from production wells at Mumford Hills site.	167
A14-2	Isotopic composition of freshwater samples from monitoring wells at Mumford Hills.	170
A14-3	Isotopic analyses of CO ₂ and CH ₄ for selected gas samples from Mumford Hills site.	172

LIST OF APPENDIX FIGURES

A4-1	Natural gamma log for Mumford 1 (MH-1) groundwater monitoring well.	129
A4-2	Natural gamma log for Mumford 2 (MH-2) groundwater monitoring well.	130
A4-3	Natural gamma log for Mumford 3 (MH-3) groundwater monitoring well.	131
A4-4	Details of groundwater monitoring well construction, MH-1.	132
A4-5	Details of groundwater monitoring well construction, MH-2.	133
A4-6	Details of groundwater monitoring well construction, MH-3.	134
A8-1	Log analysis for well BA-1.	152
A8-2	Log analysis for well BA-1 (magnified, showing a portion of the injection zone).	153
A8-3	Log analysis for well BA-2.	154
A8-4	Log analysis for well IB-2.	155
A8-5	Log analysis for well IB-2 (magnification).	156
A8-6	Log analysis for well IB-3.	157
A8-7	Log analysis for well BU-1.	158

INTRODUCTION

Midwest Geological Sequestration Consortium Background

The Midwest Geological Sequestration Consortium (MGSC) has been assessing the options for geological carbon dioxide (CO₂) storage, also called sequestration, in the 155,400-km² (60,000-mi²) Illinois Basin. Within the Basin, which underlies most of Illinois, western Indiana, and western Kentucky, there are deep, uneconomic coal resources, numerous mature oil fields, and deep saline reservoirs potentially capable of storing CO₂. The objective of the assessment is to determine the technical and economic feasibility of using these geological sinks for long-term CO₂ storage to avoid atmospheric release of CO₂ from fossil fuel combustion at electrical generation facilities and industrial sources.

The MGSC is a consortium of the geological surveys of Illinois, Indiana, and Kentucky, joined by subcontractors and consultants, to assess carbon capture, transportation, and storage processes and their costs and viability within the three-state Illinois Basin region. The Illinois State Geological Survey serves as the lead technical contractor for the MGSC. The Illinois Basin region has annual CO₂ emissions of about 265 million metric tonnes (292 million tons), primarily from 61 coal-fired electric generation facilities, some of which burn almost 4.5 million tonnes (5 million tons) of coal per year (U.S. Department of Energy, 2010).

Initial MGSC work during 2003 to 2005, termed the Characterization Phase (Phase I), involved an assessment of CO₂ capture, storage, and transportation options in the region. All available data were compiled on potential CO₂ sinks and on applicable carbon capture approaches. Transportation options focused on small-scale options for field tests and the pipeline requirements for long-term sequestration. Research primarily focused on storage reservoirs in order to assess each of the three geological sinks: coal beds, oil reservoirs, and saline reservoirs. Results were linked with integrated options for capture, transportation, and geological storage and the environmental and regulatory framework to define sequestration scenarios and potential outcomes for the region. A final task was to generate an action plan for possible technology validation field tests involving CO₂ injection, thus setting the stage for the Validation Phase (Phase II) of the project, involving small-scale field tests during 2005–2011. A 477-page final report (MGSC, 2005), plus two topical reports, on Phase I results are available at www.sequestration.org the MGSC's website.

A key conclusion of the Phase I studies was that the geology of the Illinois Basin is favorable for CO₂ sequestration. In some localities, two or more potential CO₂ sinks are vertically stacked. The primary focus of the Phase II study, however, was the properties of the rock units that control injectivity of CO₂, the total storage resources, the safety of injection and storage processes, and the security of the overlying rock units that act as seals for the reservoirs. For Phase II (2005–2011), four small-scale field tests were conducted. They included testing the ability to adsorb gaseous CO₂ (Frailey et al 2012a) in a deep, unminable coal seam and the ability to store CO₂ and enhance oil production in mature oil fields (Frailey et al 2012b). Each of these field tests had an extensive monitoring program for sampling air, shallow groundwater, and fluids from the injection zone, as well as geophysical and cased-hole logging and monitoring of pressure changes to understand the fate of injected CO₂ at the test sites. The integrity of the entire process is being scrutinized in detail to understand what contribution Illinois Basin geological sinks can make to national and international carbon sequestration goals and what technology developed here can be extrapolated to other regions.

MGSC Phase I Illinois Basin Oil Reservoir Assessment Summary

Enhanced oil recovery (EOR) offers the most important economic offset to the costs associated with CO₂ sequestration in the Illinois Basin. To assess this potential, a basin-wide EOR assessment was made based on a new understanding of the original-oil-in-place (OOIP) in the Basin, the CO₂ stored volume, the assessed CO₂ EOR resource, the geographic distribution of CO₂ EOR potential, and the type of recovery mechanism (miscible vs. immiscible).

With cumulative oil production of about 668 million standard cubic meters (scm; 4.2 billion stock tank barrels, stb), nearly 1.6 billion scm (10 billion stb) of additional oil resources remain in the Basin, primarily as unrecovered resources in known fields. To assess recovery potential of a part of this resource and the concurrent stored CO₂ volumes, reservoir modeling and computational simulations were carried out.

The resource target of CO₂ EOR is 137 to 207 million scm (860 to 1,300 million stb) with consequent sequestered CO₂ volume of 140 to 440 million tonnes (154 to 485 million tons). The distribution of the CO₂ EOR resource was mapped by field (Figure 1); the larger fields holding multiple reservoirs constitute the largest CO₂ EOR targets.

Phase II EOR Pilot Objectives

The purpose of this part of the project was to determine the CO₂ injection and storage capability and the EOR recovery potential of Illinois Basin oil reservoirs. The results of the EOR pilot tests were to validate the CO₂ storage and EOR estimates from the Phase I assessment. The prolific oil-producing reservoirs in the Basin, particularly the Mississippian-age Aux Vases and Cypress Sandstones and the Ste. Genevieve Limestone, were of primary interest.

In the Department of Energy Regional Carbon Sequestration Partnership (DOE RCSP) Phase I, about 15 to 20% of the OOIP in the Basin was found at depths that would sustain miscible CO₂ floods. Another 25 to 30% of the OOIP in the Basin was considered near-miscible and would likely have higher CO₂ EOR estimates than would immiscible floods. Miscible CO₂ EOR floods would achieve more CO₂ storage than immiscible floods.

For a miscible flood reservoirs with temperatures below the critical temperature of CO₂, the reservoir pressure must exceed the vapor pressure of pure CO₂. For a pilot project with a limited CO₂ budget, the current reservoir pressure could not be entirely depleted, or there would be inadequate CO₂ to pressurize the reservoir enough to have any significant mixing between CO₂ and the in situ crude oil. Depending on average reservoir temperature, a current average reservoir pressure of at least 5.9 MPa (850 psi) and preferably 6.9 MPa (1,000 psi) was desired.

For this pilot, MGSC EOR II, a miscible liquid CO₂ flood was planned.

Site Screening: General Pilot Requirements

MGSC solicited oil field operators within the Basin to nominate geologic formations within oil fields for consideration of a CO₂ EOR pilot. Finding an oil field operator and owner with the necessary technical and logistical capabilities was recognized as a necessity for the EOR pilot projects.

For budgetary and project timeline reasons, the plan was to convert an existing well to a CO₂ injection well. Consequently, the site screening process was based on an existing pattern of wells that could be used for a CO₂ injection pattern, e.g., a five-spot pattern. To identify the top candidates for this pilot, a five-tier screening process was used: CO₂ flood classification, operation and development history, surface conditions, well-bore conditions, and geologic and reservoir modeling.

CO₂-Crude Oil Interactions

The first tier screening was primarily designed to classify the CO₂-crude oil interaction as immiscible-gas, miscible-liquid, or miscible-critical fluid. (A fourth CO₂ flood classification for the pilot tests was for those reservoirs considered too close to the boundary between these three classifications; for pilot purposes only, these uncertain reservoirs were avoided.) The screening was primarily based on current reservoir pressure and temperature, API gravity, and geologic formation.

Operation and Development History

The second tier was the number of geologic zones open to the injector, and the presence of a centrally located injection well with preferably four existing producing wells surrounding the injection well. Surface injection pressure, water injection rate, and oil, water, and gas production at the surrounding wells were considered in this tier.

Surface Conditions

The third tier was surface conditions that could accommodate the injection and data acquisition equipment and CO₂ tank truck delivery. Other surface features considered included proximity to lakes and ponds, floodplains, homes, and major roads. Cooperation of the local road commissioner was critical. Early in the

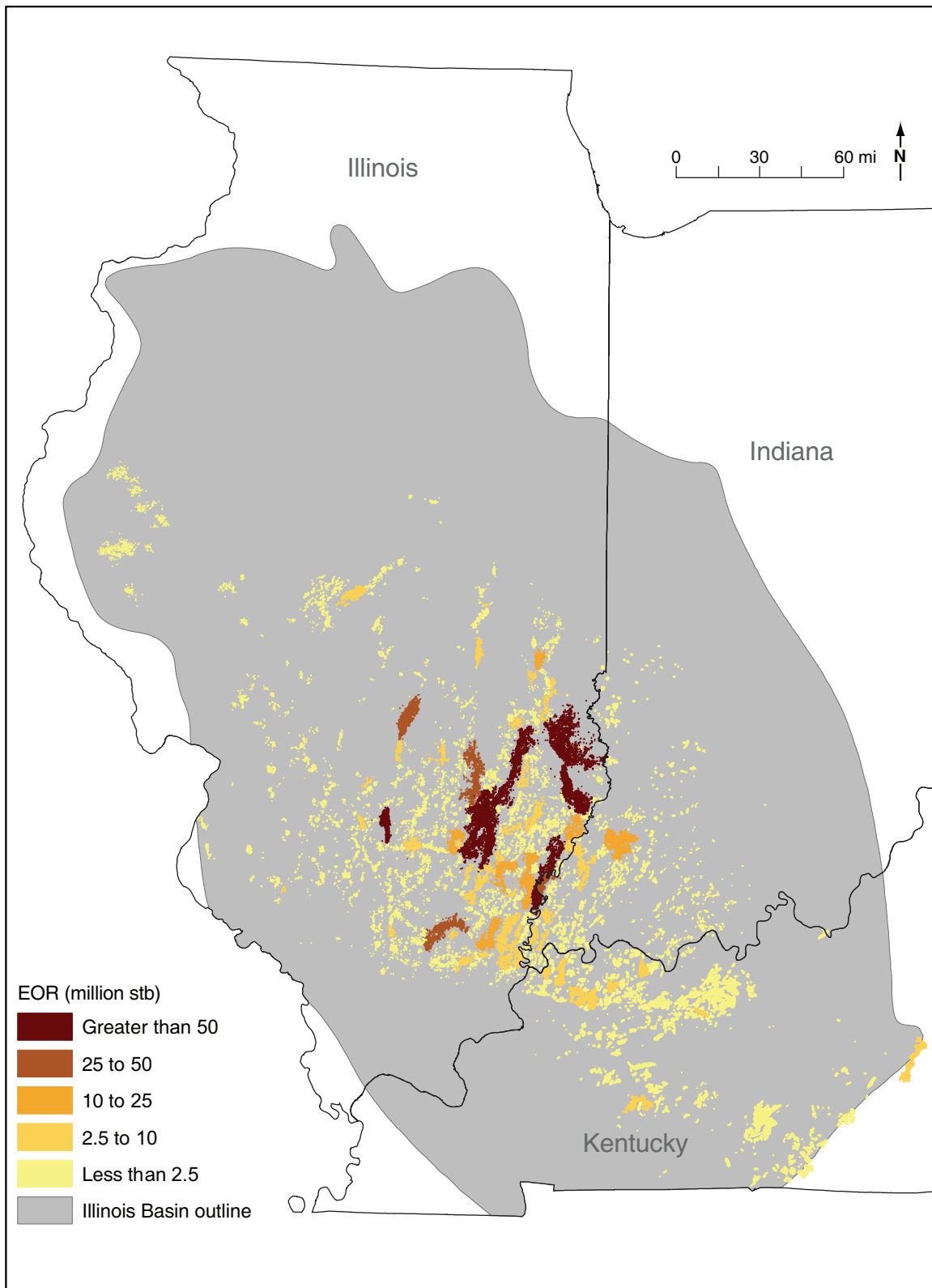


Figure 1 CO₂ enhanced oil recovery (EOR) resources in the Illinois Basin, mapped by oil field (from MGSC, 2005).

application of third-tier screening criteria it became obvious that the only oil field roads that could withstand semi-trailer tanker truckloads of CO₂ were those roads that led to the oil tank battery (separators and stock tanks) and had regular pickup of bulk crude oil via semi-trailer tanker trucks. Consequently, areas surrounding the tank battery were considered ideal for locating the surface injection equipment (e.g., CO₂ storage tanks, injection pumps, and in-line heater) and injection wells located near the tank battery were considered better choices for an EOR pilot test.

Wellbore Conditions

The depths of multiple zones currently completed in the injector, and the ability to isolate zones, were considered in the fourth tier. Therefore, type of completion (e.g., cased and perforated or open hole) was important. Injection pressure history over the preceding few months was reviewed. Work-over type and frequency were important in the screening process. Size of casing and any liners placed inside the casing were also important considerations for placement of an injection tubing packer.

Geological and Reservoir Modeling

The fifth tier was the geologic modeling and reservoir modeling results. Higher consideration was given to injection patterns and models that would give oil production and pressure results that were measurable and quantifiable within the CO₂ and time budget of the project. It was recognized that direct field data indicating increases in oil recovery were important, but a pilot to estimate EOR directly would likely require at least 2–3 years of injection and multiple injection patterns. Consequently, the CO₂ EOR estimate would be based on a reservoir model calibrated to the measured field results.

SITE SELECTION

This pilot site (designated EOR II) was screened to have current reservoir pressure and temperature sufficient to sustain a miscible flood. After applying the rigorous EOR site screening criteria, the Bald Unit within the Mumford Hills oil field in Posey County, Indiana, was chosen. The Bald Unit is owned and operated by Gallagher Drilling, Inc., based in Evansville, Indiana.

Using bottomhole pressures of the water injection well and the producing wells, the average pressure in the Bald Unit was initially estimated at 8.27 MPa (1,200 psi). The average reservoir temperature was 27°C (78°F). The Bald Unit produces from a single geologic formation with 13 wells drilled and completed, of which there was one active water injection well and one active oil production well. The CO₂ pilot area chosen was in the immediate area of the oil-producing well, Bald Unit #1, which had four oil-producing wells surrounding it. One of the wells had been plugged and abandoned recently but had no reported casing problems, so a re-entry was considered feasible.

Although several wells in the Field were temporarily or permanently abandoned, the oil field had relatively new wells and no reports of major casing leaks or other production well problems. The site's tank battery had excellent road access.

Analyses and interpretations of projections from a simplistic but representative geologic model of the Bald Unit suggested that the CO₂ injection rates and cumulative injection volume for the pilot design could be achieved in the time frame and budget allotted.

Oil Characteristics and Geology

The geologic criteria required a formation that represented the types of producing units found in fields that would be prime candidates for CO₂ EOR activities in the Illinois Basin. The geologic zone selected for the pilot study needed to represent one of the formations that account for a relatively large proportion of the Illinois Basin's oil production—the Cypress, Aux Vases, and Ste. Genevieve—or depositionally similar formations. Completion of the wells in a single geologic zone was desired. Surveillance of productivity and injectivity from wells completed in a single zone is much more certain compared to commingled production and injection in wells that are completed in multiple zones. Additionally, the amount of CO₂ injected would need to be significantly larger for a multi-zone oil field with wells completed in all zones.

The Clore Formation at the Mumford Hills Field, which lies stratigraphically above the Cypress Sandstone but closely resembles it in lithology and depositional environment, was the only formation producing at Bald Unit.

Additionally, the API gravity of the crude oil needed to be representative of the Basin's oil. A gravity value of 37° API is very common in the Basin, so a range of 35° to 40° API was considered. The gravity of the oil in the Bald Unit is 38.3° API.

Geographic Description and Location

The Mumford Hills Field is located in Posey County, Indiana, about 28 km (17.5 mi) north of the county seat, Mt. Vernon, and about 3.7 km (2.3 mi) southeast of the nearest town, Griffin. The Bald Unit is located in the southeast quarter of Section 8, Township 4S, Range 13W, in the southern part of the Mumford Hills Field (Figure 2). Figure 3a is an index map showing the location of the Mumford Hills Field near the Illinois-Indiana border near US Interstate 64. The injection well, Bald Unit #1 (BU-1), and most of the oil production and monitoring wells in this study are within 0.8 km (0.5 mile) west and southwest of the tank battery.

The Bald Unit can be accessed by taking Wilsey Rd (County Road 1100 N) east from Griffin about 3 km (2 mi), turning left onto Waller Hill Road (County Road 1050 N) after crossing under Interstate Highway 64, continuing on Waller Hill Road for 0.8 km (0.5 mi), then taking the first available right turn onto the Bald Unit's unpaved oil field road and proceeding for about 0.8 km (0.5 mi) to the Bald Unit tank battery (Figure 3b).

Physiographically, the Bald Unit is located on the eastern bluffs of the Wabash River bottom area. The area is located in moderate-relief, open farmland bordered by forest. The farmland consists of tillable acreage, pasture, and hay fields. Row-crop farming is prominent; corn and soybeans are the most common crops. Streams have moderate gradients and the area tends to be well drained, primarily due to its elevation and proximity to the river bottom area.

There is a small tilled field in the east part of the Unit (14–16 hectares [35–40 acres]) and a pasture and hay field in the west part of the Unit (6.1–8.1 hectares [15–20 acres]) in the immediate area of the tank battery and BU-1. The lease road leading to the tank battery is a rock road that runs north-south through the middle of the Unit.

Site Logistics

BU-1 was a temporarily abandoned oil-producing well drilled and completed in 1975 as an infill well. The casing integrity was considered higher because of its relative age. Bald Unit #2 (BU-2) was also drilled about the same time but was much further from the tank battery, the proposed site of the injection equipment. There were no wellbore or injection-related problems associated with BU-1, so it was chosen as the CO₂ injection well primarily based on its proximity to the oil-producing wells. However, the injection well was 170 m (550 ft) from the tank battery. The water injection pumps and accessories (e.g., filters) were located immediately adjacent to the oil tank battery (Figure 4), and the production flow line leading to BU-1 started from this location.

The lease road leading to BU-1 was not capable of supporting semi-trailer truck and tanker traffic, so the CO₂ injection equipment was placed near the tank battery to allow for regular CO₂ delivery. This required either laying a new CO₂ injection line between the injection equipment and BU-1 or using the existing production flow line to carry the CO₂. The existing production flow line was designed for much lower pressure than required for CO₂ injection so a new line was buried. The Fibersystems fiberglass pipe (1.5 inch, EUE 10 Round with integral joint) used was rated to 13.8 MPa (2,000 psig). The line was trenched to a depth of about 75 cm (30 inches) in a direct line between the tank battery and the BU-1 wellhead.

The wells surrounding BU-1 were the Inez Bailey #2 (IB-2), Inez Bailey #3 (IB-3), Bailey-Alexander #1 (BA-1), and Bailey-Alexander #2 (BA-2) (Figure 5). BU-1 was drilled slightly off center and closer to BA-1 and BA-2 because of surface topography. IB-2, IB-3, and BA-2 were temporarily abandoned when the site was initially considered. BA-1 was plugged and abandoned in 2009 due to low oil production; the casing was in good condition at that time, and reentry and completion was a viable option. All of the wells were accessible from the main lease road leading into the Unit.

FIELD HISTORY

OOIP and Wells

The first wells were drilled on their respective leases in 1974. The Bald Unit was formed at the time of the waterflood and prior to drilling BU-1 and BU-2. Gallagher Drilling, Inc. was the operator from the inception of the Unit. There are four leases in the project area: Bailey-Alexander, Bailey, Davis, and Davis Lindsey. Production throughout the history of the Field has been exclusively from the Mississippian Clore Formation sandstone.

Gallagher Drilling, Inc., provided an OOIP estimate of 333,900 scm (2,100,000 stb) for the Bald Unit. The company's formula for calculating OOIP is

$$\text{OOIP} = 7,758 V_b \phi (1 - S_w) / B_o \quad (1)$$

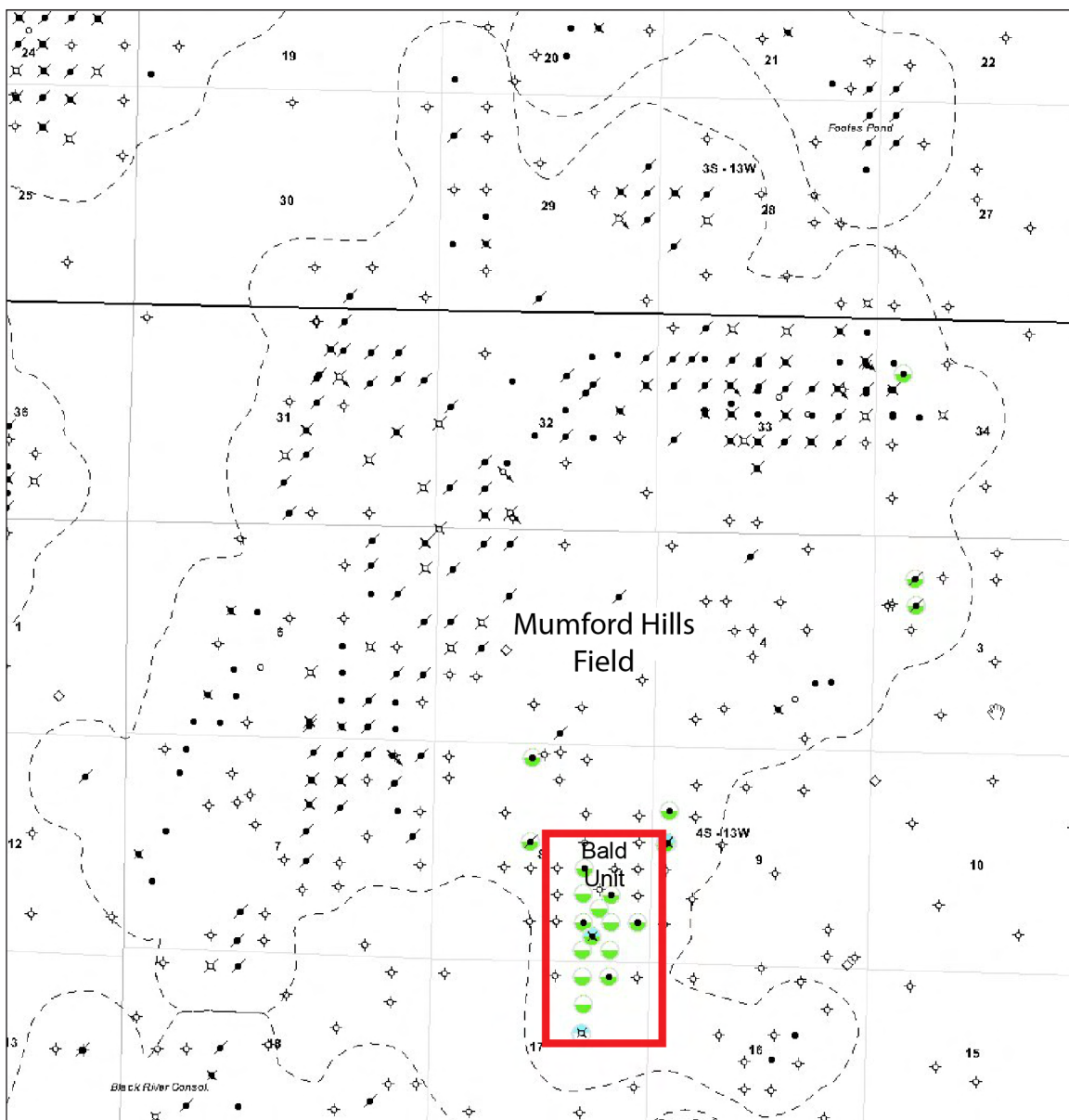


Figure 2 Location of the Bald Unit (red rectangle) within the Mumford Hills Field.

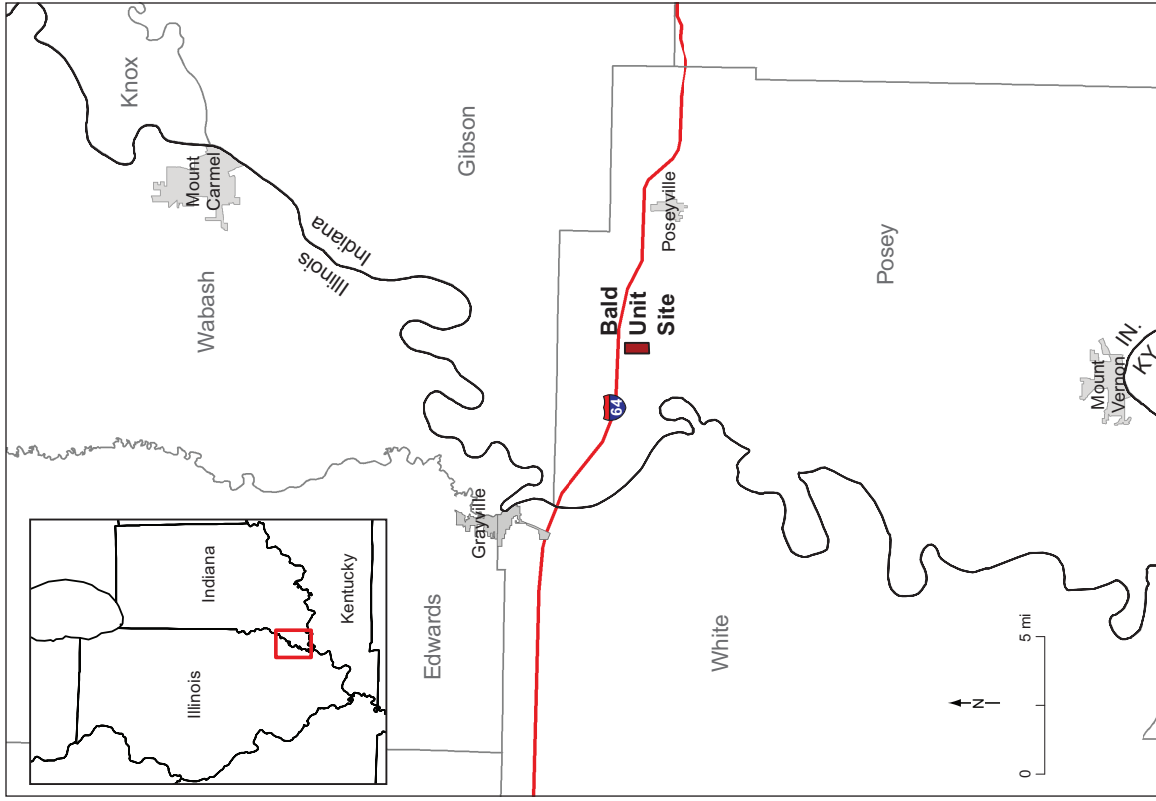


Figure 3 Location map of the Bald Unit site, Posey County, Indiana (left), and aerial orthophoto of the site area, showing names of roads leading to the site (right).



Figure 4 The tank battery at Mumford Hills Field, including tanks and pump house. Tanks are to the left, and the water injection equipment and accessories are in the white pump house at right.

where V_b is the bulk volume of sandstone reservoir in acre-feet, ϕ is porosity fraction, S_w is water saturation fraction, B_o is the oil formation volume factor, and 7,758 is a conversion factor (7,758 bbl/acre-foot equals one acre-foot per barrel). To estimate V_b , a planimeter was used to measure the area encompassed by each contour of the isopach map (Figure 6). Constant porosity of 21% and an assumed water saturation of 35% were used.

Figure 7 is a map of well locations for the Bald Unit. Historically, there were 12 oil-producing wells in the pilot project area on three leases. Twenty-eight wells were used in early modeling to construct a model of the Unit. The Unit was developed on a 0.04 km² (10 acre) spacing. A portion of the Unit is shown in an aerial photograph in Figure 5. The pilot included seven wells, including four production wells, two reservoir monitoring wells, and one water/CO₂ injection well. Wells in the pilot and in the area are listed in Table 1.

Table 1 Bald Unit wells (lease name, well number, and abbreviation), well type, and completion dates.

Well name	Well type	Completion date
Bald Unit 1 (BU-1)	Production and water/CO ₂ injection	February 12, 1975
Bald Unit 2 (BU-2)	Production	February 8, 1975
Bailey-Alexander 1 (BA-1)	Production	June 26, 1974
Bailey-Alexander 2 (BA-2)	Production	July 5, 1974
Inez Bailey 2 (IB-2)	Production	July 12, 1974
Inez Bailey 3 (IB-3)	Production	August 17, 1974
Inez Bailey 4 (IB-4)	Production	August 15, 1974
Inez Bailey 5 (IB-5)	Production	September 11, 1974
Beulah Davis 1 (BD-1)	Production	July 30, 1974
Beulah Davis 3 (BD-3)	Water supply (Pennsylvanian)	August 27, 1974
Beulah Davis 4 (BD-4)	Production	September 24, 1974
Beulah Davis 5 (BD-5)	Water injection	October 5, 1974
Davis Lindsey 1 (DL-1)	Production	August 14, 1974
Davis Lindsey 2 (DL-2)	Production	September 20, 1974



Mumford Hills Site, Posey Co., Indiana

2010 NAIP Digital Orthophoto Imagery

- CO₂ injection well
- Active oil well
- Temporarily abandoned oil well
- Water supply well
- GW monitoring well
- Brine/gas sampling location

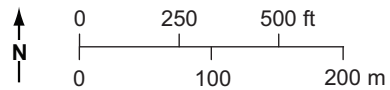


Figure 5 Bald Unit Pilot area: orthophotographic map of the oil production wells, CO₂ injection well, groundwater monitoring wells, and the tank battery.

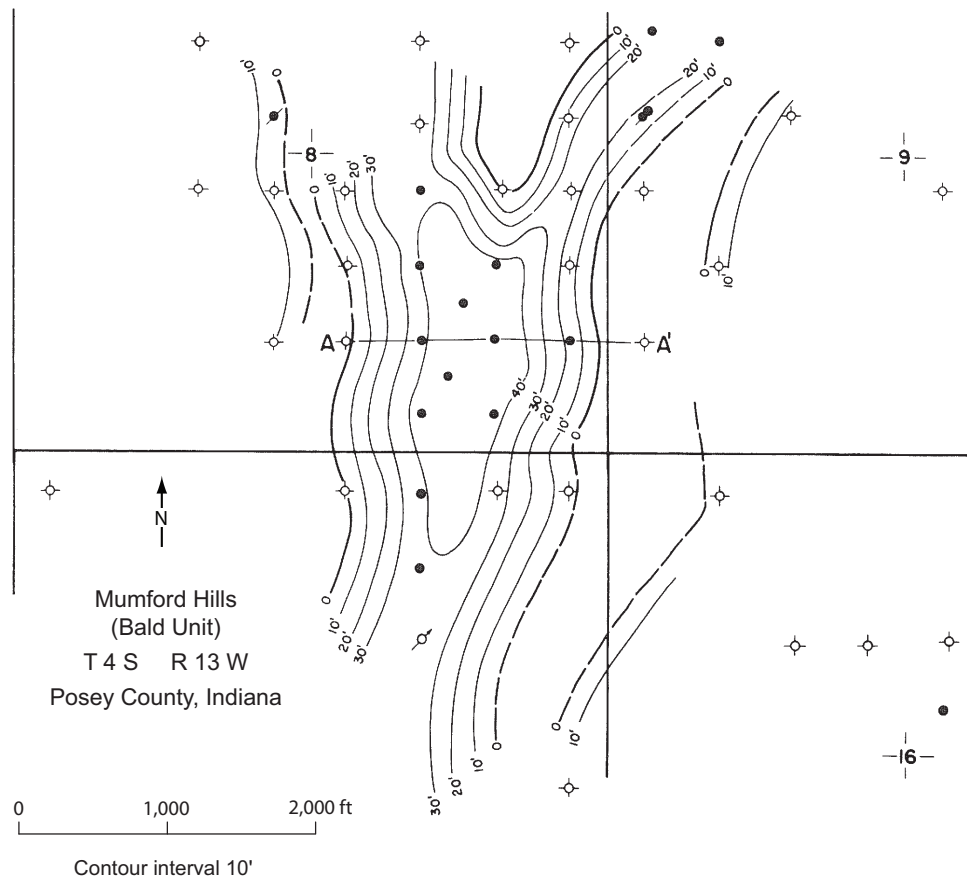


Figure 6 Isopach map of gross Clore sandstone used to estimate the bulk volume of sand in acre-feet for OOIP calculation (courtesy of Gallagher Drilling, Inc.).

Bald Unit Development

All of the wells in the Bald Unit were drilled in 1974 and 1975 (Table 1). There were 22 wells drilled in the four leases of the Bald Unit of which 13 actively produced from or injected into the Clore sandstone. The BD-3 was drilled to the Clore but completed in an overlying Pennsylvanian sandstone to produce make-up water for injection into BD-5.

The Bald Unit had a very short primary production period—less than one year—before commencement of water injection. Well BD-5 was used as a water injector for an edge waterflood beginning in March 1975. A number of wells were shut-in before the end of waterflooding or were intermittently shut-in and brought back online during waterflooding. A list of the last recorded production for each well prior to the startup of the CO₂ pilot project is in Table 2.

The average daily oil rate (Figure 8) increased significantly in 1986, 1989, 1999, and 2003. Prior to 1986, relatively high back-pressure was kept on the producing wells. In 1986 the pumping unit motors' speed was increased, which decreased bottomhole pressure and increased oil production. In 1989, IB-3 and IB-4 were acidized. BU-1 and IB-5 were treated with polymers in 1999 to reduce excessive water production. In 2003, a larger pumping unit was installed on IB-4 to increase total fluid production.

Peak annual oil production occurred in 1975: over 8,700 m³ (55,000 bbl) were produced with daily rates in excess of 30 m³/day (200 bopd) (Figures 8 and 9). The oil production for 2008 was 598 m³ (3,760 bbl). The average daily oil production for the first eight months of 2009 was 1.5 m³/day (9.7 bopd). The two lowest liquid-producing wells (oil and water) were BD-1 and BD-4 because of their early abandonment as a result of high water production caused by their relative proximity to the water injection well BD-5.

Table 2 Date each well was temporarily abandoned.

Well name	Last day of production (prior to pilot)
Bald Unit 1 (BU-1)	1/31/2003
Bald Unit 2 (BU-2)	1/31/1999
Bailey-Alexander 1 (BA-1)	5/31/1991
Bailey-Alexander 2 (BA-2)	10/31/1988
Inez Bailey 2 (IB-2)	12/31/1991
Inez Bailey 3 (IB-3)	1/31/1998
Inez Bailey 4 (IB-4)	Active producer
Inez Bailey 5 (IB-5)	4/30/2009
Beulah Davis 1 (BD-1)	1/31/1987
Beulah Davis 3 (BD-3)	1/31/1975
Beulah Davis 4 (BD-4)	6/30/1986
Beulah Davis 5 (BD-5)	Active water injection well
Davis Lindsey 1 (DL-1)	6/30/1999
Davis Lindsey 2 (DL-2)	7/31/2006

About 50% of the Bald Unit's production was allocated to the four producing wells within the proposed pilot area. The wells' average oil rates were 0.3 to 0.56 m³/day (0.2 to 3.5 bopd). The pre-CO₂ injection oil rate baseline was 0.8 m³/day (5 bopd).

BD-5 injected in excess of 1,200,000 m³ (7,500,000 bbl) water over the life of the Bald Unit. Average daily water injection rate for the first eight months of 2009 was 135 m³/day (850 bwpd) (Figure 10).

The cumulative oil production by well was between 1,590 and 24,600 m³ (10,000 and 155,000 bbl). The most prolific oil-producing wells were IB-4, BU-1, and BU-2 (Figure 11); each produced in excess of 15,900 m³ (100,000 bbl). These wells were also the largest water-producing wells, producing 40,000 to 208,000 m³ (250,000 to 1,300,000 bbls).

Total primary recovery was 6,539 m³ (41,132 bbl). Secondary (waterflooding) recovery was 126,693 m³ (793,539 bbl). This represents 37% oil recovery.

Geologic and Production Data Available

Core analyses were available from all of the active wells in the Bald Unit and provided excellent representation of reservoir permeability and porosity. Although not well preserved, a core from the injection well was available for study. From core analyses, porosity, vertical and horizontal permeability, and oil and water saturation values were available in 0.3-m (1-ft) intervals.

Only two wells had geophysical log suites that included porosity logs; most of the logs available were spontaneous potential (SP) and resistivity. As part of the CO₂ pilot MVA program, the reservoir saturation tool (RST) log was run before the pilot project began to give an estimate of porosity with a modern logging tool. Unfortunately, due to the size of the logging tool and the depth of each well with respect to the top of the Clore sandstone, only one well logged a portion of the Clore sand. As a result, the RST logging provided a porosity estimate for only one well.

Oil and water production and water injection for the life of the Field were provided by Gallagher Drilling, Inc. Early in the life of the Field (1974), a reservoir fluid study was conducted on samples from well BA-2 to find viscosity, saturation pressure, thermal expansion of saturated oil, compressibility of saturated oil at reservoir temperature, and specific volume at saturation pressure. Water-oil relative permeability was available on cores from three wells in the proposed CO₂ pilot area.

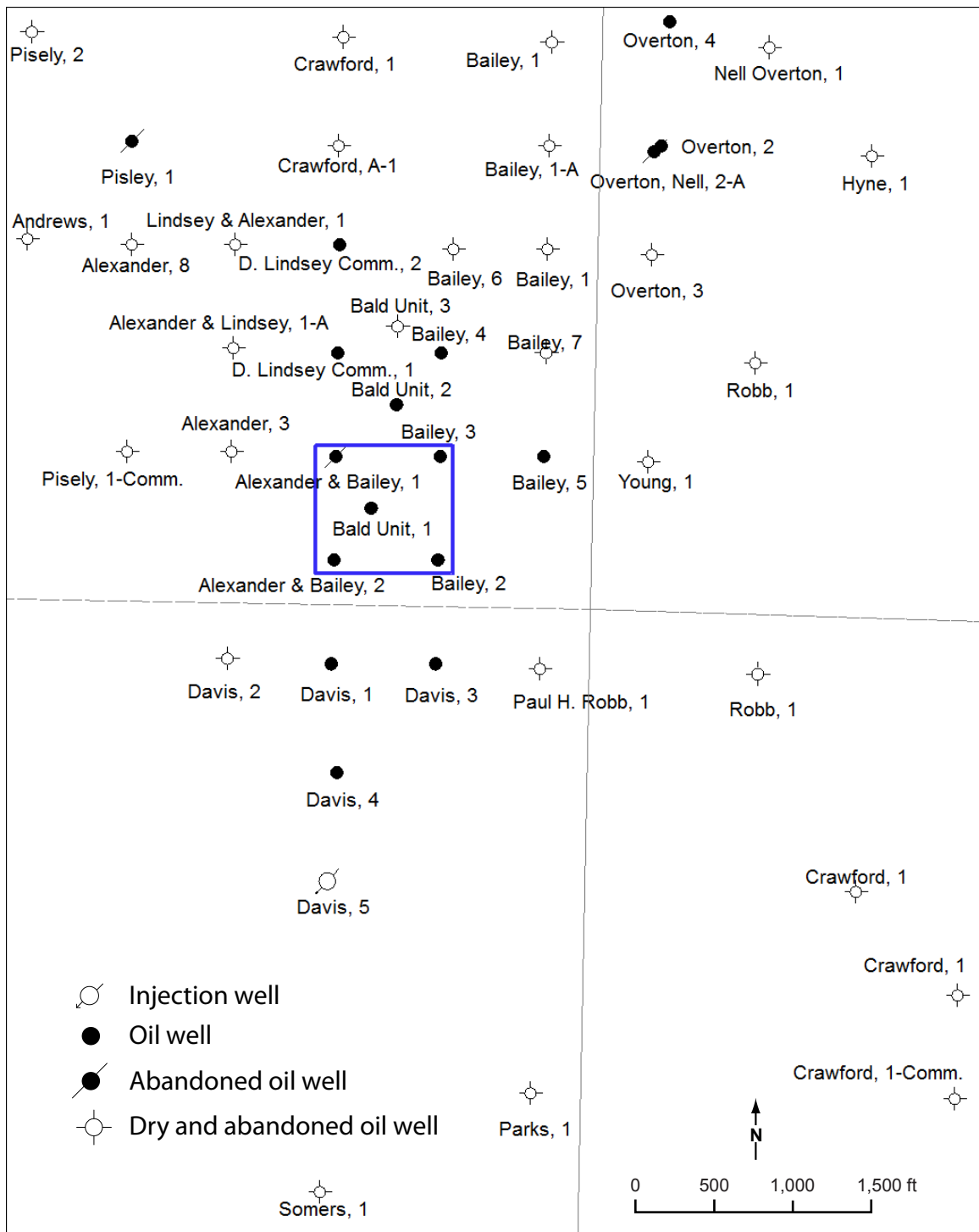


Figure 7 Map of well locations on the Bald Unit and the immediate vicinity.

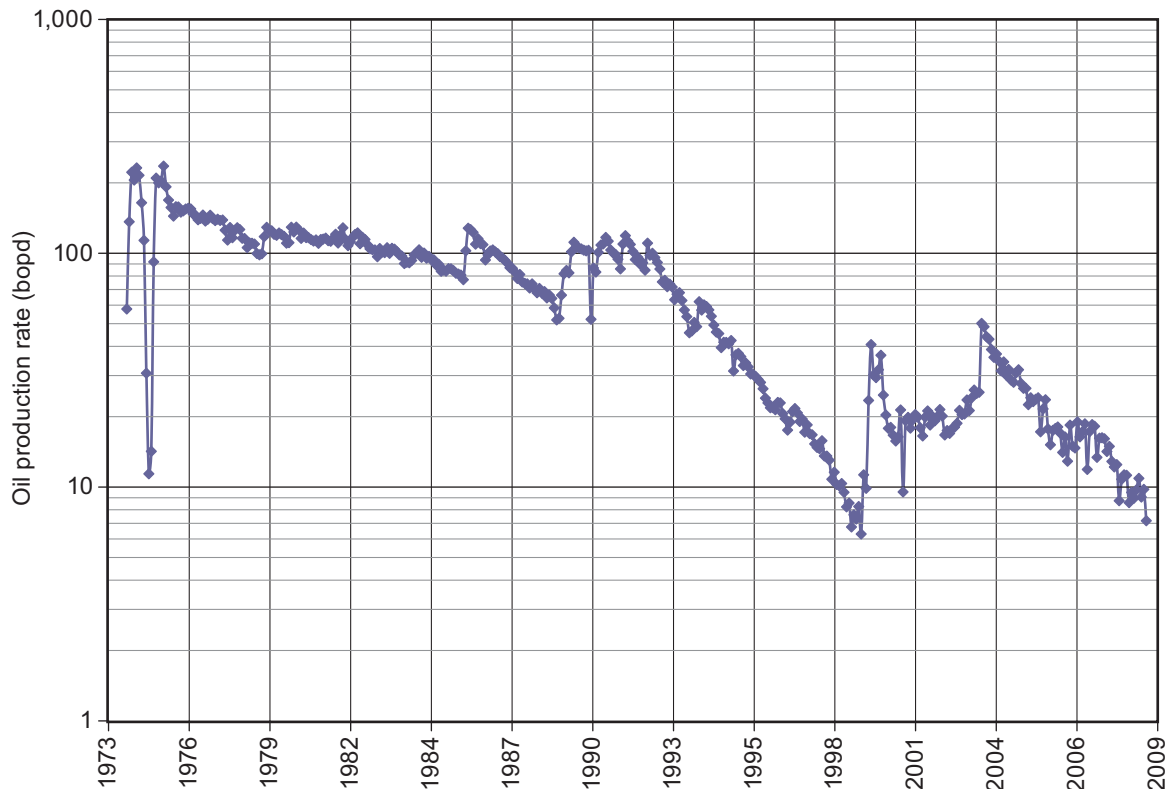


Figure 8 Bald Unit's average daily oil rate in barrels of oil per day (bopd) from the beginning of primary production through early 2009 (several months before commencement of CO₂ injection).

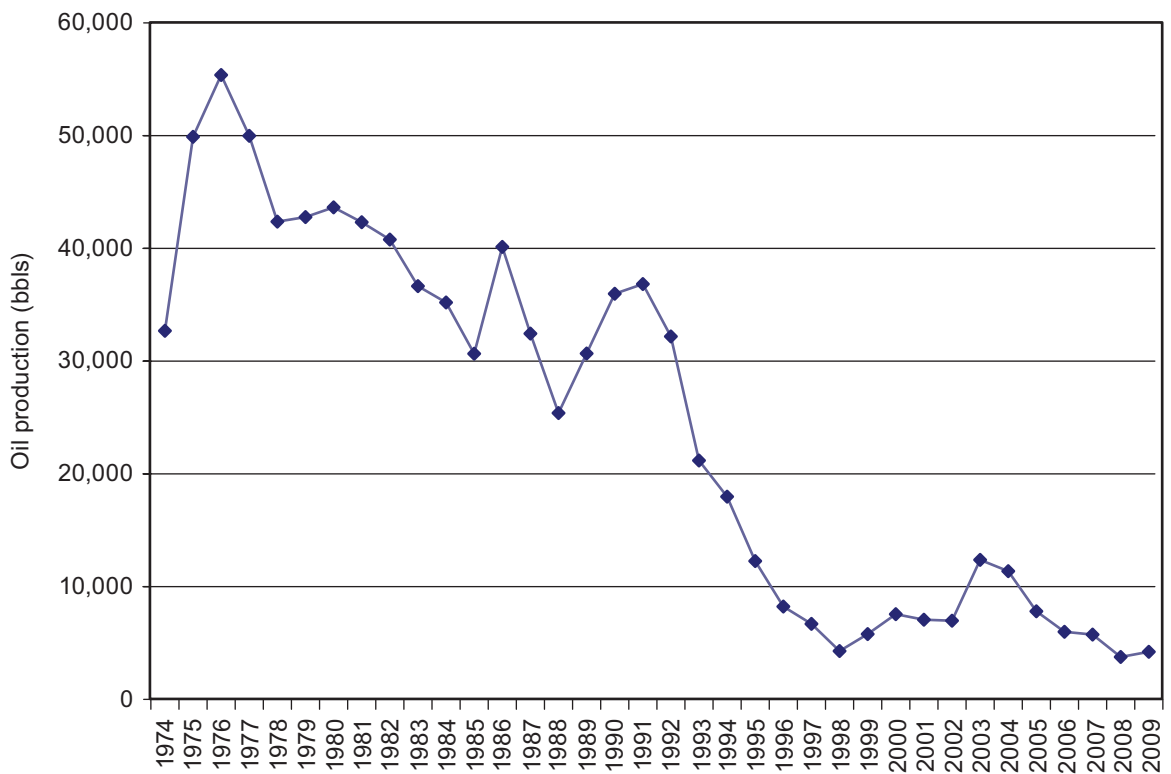


Figure 9 Annual oil production (bbls) from the beginning of primary production through 2009.

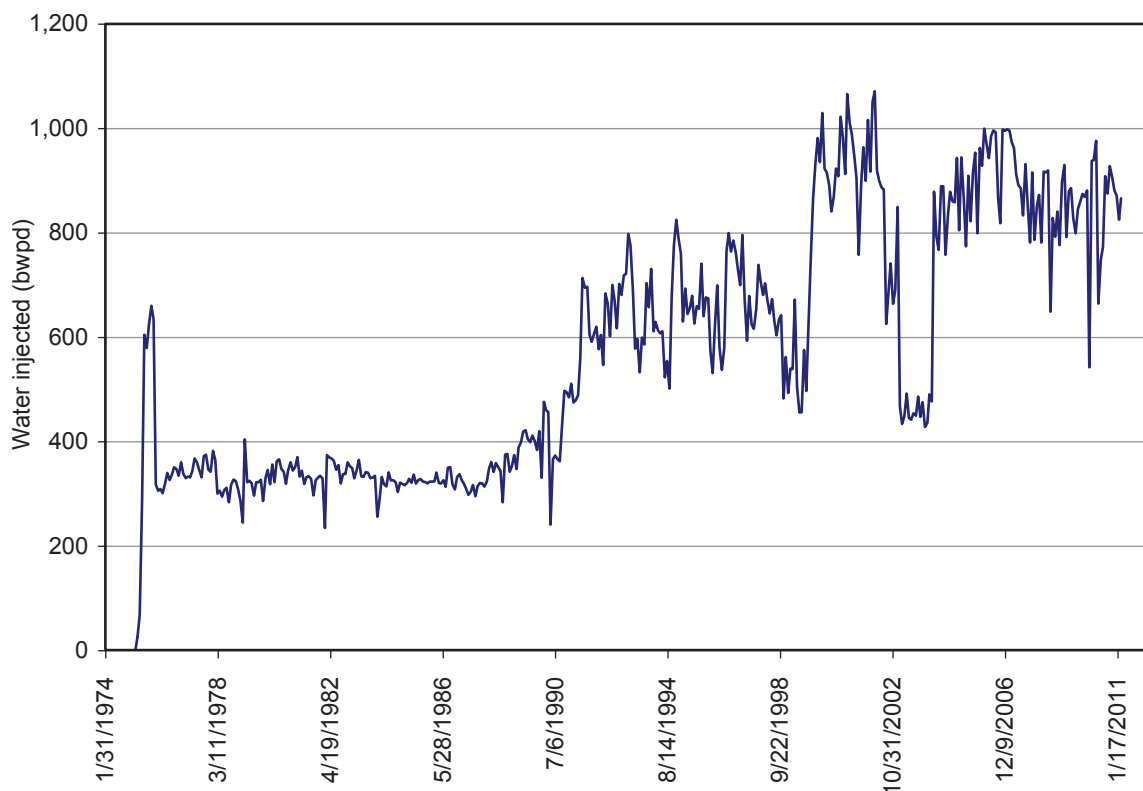


Figure 10 Average daily water injection rate in barrels of water per day (bwpd) from the beginning of primary production through early 2011.

Well Completion Data

Figure 12 is a diagram of a typical Bald Unit production well. However, there were significant design variations from well to well, particularly in parameters such as casing and tubing lengths and diameters, depth of perforations, and total well depth. Figure 12 and the following text should be taken as a generalized description of a Bald Unit production well rather than an exact description of any particular well.

The surface wellbore of a typical Bald Unit producer was drilled with a 30.5-cm (12-inch) diameter bit and cased with 22-cm (8 $\frac{5}{8}$ -inch) diameter surface casing to a depth of 21 m (68 ft). The surface and production casing were bonded with 100 sacks of cement. The production wellbore was drilled with a 20-cm (7.9-inch) diameter bit and cased with 14-cm (5.5-inch) diameter production casing. Casing grade for both production and surface casing was H-40; surface casing weighed about 30 kg/m (20 lb/ft) and production casing weighed about 21 kg/m (14 lb/ft).

Beneath the surface hole and wellbore was a 20-cm (7 $\frac{7}{8}$ -inch) diameter hole to around 610 m (2,000 ft), with 580–610 m (1,900–2,000 ft) of 14-cm (5 $\frac{1}{2}$ -inch) diameter casing and about 564 m (1,850 ft) of 7.3-cm (2 $\frac{7}{8}$ -inch) diameter tubing. The 20-cm (7 $\frac{7}{8}$ -inch) hole was cemented from immediately above the perforations to a depth of 286 m (940 ft) using 150 sacks of cement. Most of the reservoir pilot test configuration wells were cased-hole, although BU-2 was open-hole.

Perforations were in the oil-saturated portion (above the water-oil contact [WOC]) of the Clore sandstone at depths ranging from 576 to 591 m (1,890 to 1,940 ft); a typical perforated zone was 3 to 4.5 m (10 to 15 ft) in vertical extent.

All actively producing wells had pumping units, rods, and tubing installed. The injection well BD-5 had tubing and packer in place. A Baker AD-1 packer (60-durometer elastomer) was installed above the perforations. All temporarily abandoned wells had packers and tubing in place to protect the casing from elevated pressure from the reservoir.

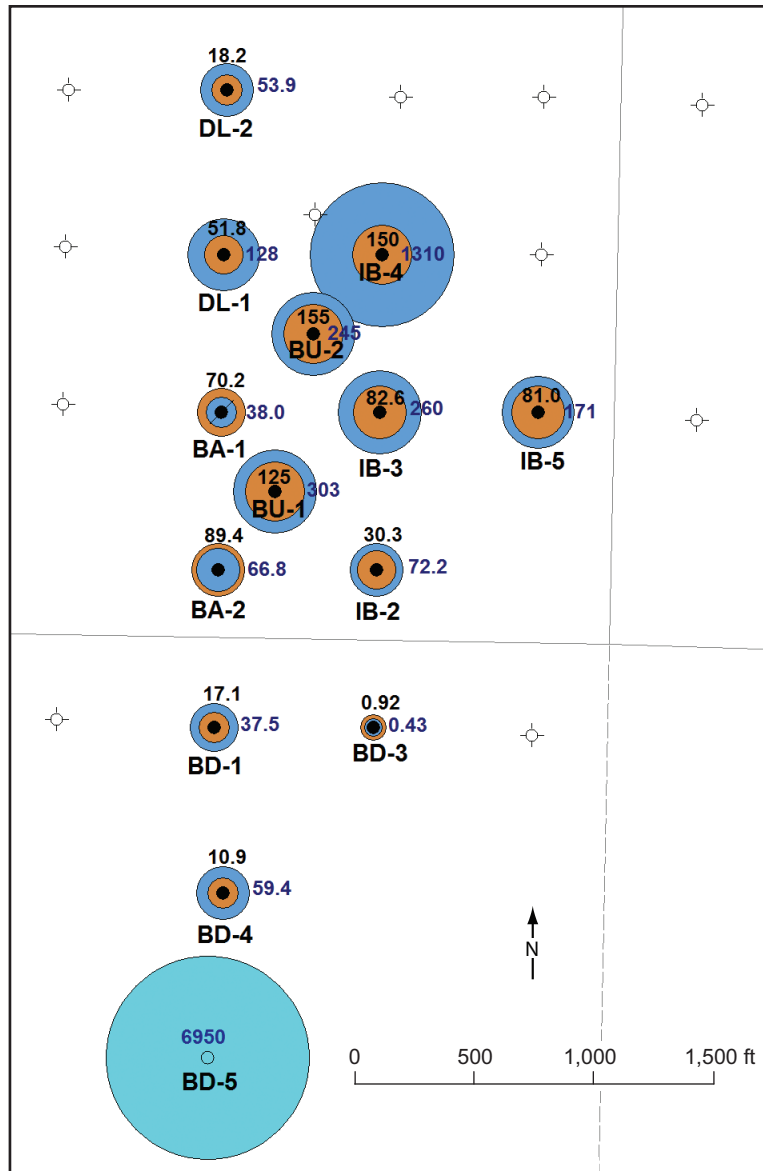


Figure 11 Bald Unit oil and water production and water injection bubble map for life of the Bald Unit prior to the pilot, by well. Brown circles around individual wells (with black numbers above the well symbol) represent cumulative oil production at each well from 1974 through the end of April 2009. Dark blue circles around producing wells (with dark blue numbers to the right of the well symbol) represent the cumulative water production for the same time period. Light blue circles around injection wells (with numbers in blue type) indicate cumulative water injection from March 1975 (the beginning of waterflooding) through the end of April 2009. Larger bubbles indicate higher total production or injection. Bubbles are overlapping circles, not concentric rings; each is measured from the center of the circle. Bubbles indicating injection volumes are at a different scale than production bubbles. All numbers are in thousands of barrels.

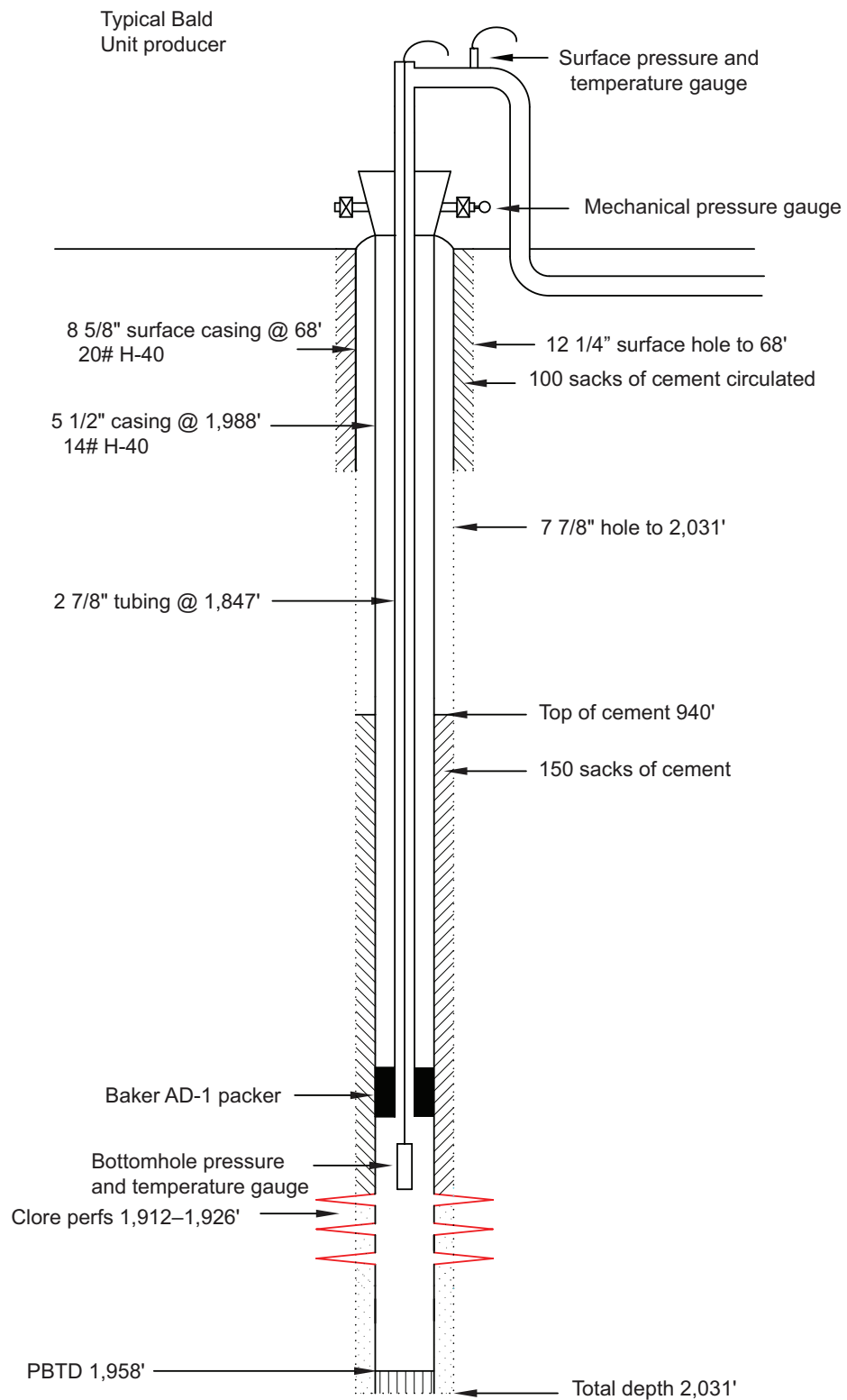


Figure 12 Wellbore schematic of a typical Bald Unit production well (courtesy of Gallagher Drilling, Inc.).

Cumulative Production and Injection Maps

A cumulative production map for the Bald Unit for the period prior to the pilot is shown in Figure 11. Production during the primary period is not distinguished from waterflooding production because the primary period was less than a year and represented less than 1% of the total production. The most productive well during waterflooding was BU-2, producing 24,600 m³ (155,000 bbl) of oil. Injection wells with cumulative injection totals are also shown in Figure 11.

BU-1, which had been one of the most prolific oil producers in the Bald Unit, was chosen as the CO₂ injection well.

Tank Battery and Flow Lines

Buried fiberglass production flow lines (same as injection line) from the individual production wells merged into a manifold (Figure 13), which was connected to a gas-liquid separator and a portable test separator.

Each production flow line emerged vertically out of the ground into a stainless steel tee, which had a mechanical pressure gauge on one end and, on the other, a Baker double disk choke (rated to 25.55 MPa or 3,705 psig). The choke was used to adjust individual wells' production flow rate by applying back-pressure. Downstream of each choke was an In-Val-Co model V-198-3 Mani-Flo (pressure rating of 4.1 MPa [600 psig]) with water, oil, and gas service), ductile-iron body, and -4 to 120°C (40 to 250°F) temperature limits. The Mani-Flo was a dual valve flow diverter that, in series with the other well's Mani-Flo devices, allowed all wells' produced fluids to commingle and pass to different production equipment. These four Mani-Flo devices with the four wells' chokes were collectively the production manifold. This manifold was designed to divert all wells' production to the gas-liquid separator or an individual well's production to a portable test separator.

The Natco three-phase separator was designed for rates up to 64 m³/day (400 bbl/day) and pressure up to 1.7 MPa (250 psig). It was about 3.7 m (12 ft) high and 1.8 m (6 ft) in diameter. The gas from this separator



Figure 13 Production manifold at Bald Unit tank battery. Four vertical production flow pipes are in the foreground at center. Mani-Flo dual valve flow diverters are painted blue. Baker chokes (brass with blue handle) are between the flow diverters and the stainless-steel tees. The tees are topped with mechanical pressure gauges (backs shown). The large gray line to left leads to the gas-liquid separator.

was metered using a Teledyne well tester and a Siemens pressure transducer. For this pilot, the Natco separator was used as a gas-liquid separator only. The portable test separator was a separate piece of equipment which is not discussed in this report.

Liquid flowed from the Natco separator into the “gun barrel” oil-water separator, a tall narrow tank (Figure 14). Oil segregated to the top of the gun barrel and flowed to one of two oil tanks; the denser brine at the bottom of the tank flowed to settling pits. The two pits hold about 60 m³ (2,000 bbls) of brine. The pits provide settling time for the brine so that solids settle out in the first pit, and clear water is stored in the second pit. A pump moves the fluid to the fiberglass suction tank for the injection pump. The netting is to keep out migratory birds.

The tank battery (Figures 4, 14) was located about 170 m (550 ft) from the injection well, BU-1. Squibb Tank Company, Inc. manufactured the tank battery, which consisted of two oil tanks, a lined pit, one brine tank, and a “gun barrel” oil-water separator. The steel oil tanks were 3 m (10 ft) in diameter and 4.6 m (15 ft) in height. The two brine tanks were of similar dimensions to the oil tank but were made of fiberglass. The nominal capacity of each oil and brine tank was 33.4 m³ (210 bbl). The fiberglass oil-water separator was 1.8 m (6 ft) in diameter and 6 m (20 ft) tall and had a nominal capacity of 15.9 m³ (100 bbl).



Figure 14 Bald Unit tank battery. The light-colored tank at left is the gas-liquid separator. The taller black tank behind the production manifold is the Natco “gun barrel” oil-water separator. The shorter black tanks behind the gun barrel are oil tanks. The second gun barrel at right was not used in the pilot project; BU-4 production was isolated from the pilot production and was sent to this gun barrel and to separate oil tanks.

A dike surrounded the tank battery. According to regulations, the dike volume must be 1.5 times the volume of the largest tank within the battery. The dike had approximate dimensions of 30 m (100 ft) × 11 m (35 ft); the longer sides of the rectangle ran parallel to the row of oil tanks. The height of the dike varied slightly along its length but exceeded the 46 cm (18 inch) minimum height implied by the dike volume requirements at all points along its length. The height of the dike ranged from a minimum of approximately 51 cm (20 in) to a maximum of approximately 86 cm (34 inch) above the adjacent level ground surface. Its average width was approximately 2 m (6 ft).

Brine Injection Equipment and Injection Lines

A pump house containing the water injection equipment was located immediately south of the oil tanks at the south end of the tank battery, near the driveway entering the tank battery area from Bald Unit road. Produced brine from the tanks was piped to the pump house for re-injection at BD-5 and BU-1. The brine was supplemented with water from water supply well BD-3 when the amount available from the brine tanks was insufficient.

Figure 15 shows water injection control panels. The instruments on the bottom row are OPLC series Switch-gage® pressure gauges and switches manufactured by FW Murphy. The boxes above the dials are TR-1760 electronic motor controllers. The gauges were used to monitor pressures and tank water levels. If the measured parameter exceeded an upper limit or dropped below a lower limit set by the operator, the controller was engaged and shut down the motor driving the pumps. The first and second gauges from the left both connected to the same TR-1760 assembly, which controlled the injection pump motor. The first gauge on the left shuts down the injection pump if the pressure exceeds or drops below a specified range; the second gauge from the left shut down the pump if the level of water in the water tank got too low.

The BD-5 water injection line was a 3.8-cm (1.5 inch) i.d. fiberglass pipe rated to 13.8 MPa (2,000 psi). The connections were threaded with double O-rings as part of the threaded end of each 9-m (30-ft) length of pipe. Between the pump house and BD-5, approximately 760 m (2,500 ft) of water injection line was in place.



Figure 15 Example of control panels for water injection equipment in the Bald Unit pump house. (The photograph is from Sugar Creek Field.)

The BU-1 water injection line was a Fibersystems fiberglass pipe (1.5-inch, EUE 10 Round with integral joint) rated to 13.8 MPa (2,000 psig) and buried directly between the pump house and BU-1.

The water injection pump was a type B-323, size 6.4 × 7.6 cm (2.5 × 3 in) triplex pump manufactured by Wilson-Snyder Works. The maximum plunger size and fixed stroke are 6.4 cm (2.5 inch) and 7.6 cm (3 inch), respectively; at the Bald Unit, the plungers were 4.45 cm (1.75 in), less than the maximum. Water entered the injection pump and exited through one of two filter lines. One line went to BD-5 and another to BU-1. These lines passed through medium-flow Nowata Filtration liquid filter housings, each containing one cartridge. Maximum working pressure on these housings was 9.93 MPa (1,440 psi). Pressure of the water immediately upstream of the inlet was measured by a mechanical pressure gauge, and pressure of the fluid downstream of the outlet was measured by an electronic MC-II flow analyzer from Halliburton Services and measured again by a mechanical gauge before entering the ground. There was a mechanical pressure gauge attached to the filter housing, a Halliburton MC-II flow analyzer downstream of the filter system, and a Lenz mechanical pressure gauge further downstream toward the injection wells.

PILOT SITE DESIGN AND WELL ARRANGEMENT

There was no waterflood pattern at the Bald Unit. A single water injection well in the southernmost edge of the Unit was used to maintain pressure. BU-1 and BU-2 were drilled as infill production wells. The conversion of either of these wells to an injection well made an inverted five-spot pattern, an injection well with four equally spaced production wells. Two wells to the north (BU-2) and northeast (IB-4) of the BU-1 CO₂ pilot area were instrumented with pressure monitoring equipment.

In preparation for liquid CO₂ in transit to the site and on location, emergency medical service providers in the area were contacted to discuss the project scope and operations. This contact provided information to local officials who could provide answers to questions from the community and increase their preparedness in the case of an emergency. Maps of the oil field and a summary of project operations were given to local first responders (e.g., fire and emergency medical services).

Returning Wells to Production

Prior to the startup of the CO₂ injection pilot, four of the wells in the five-spot pattern were temporarily shut-in with uncoated tubing (7.3025 cm, 9.67 kg/m, 6.200 cm i.d.; 2⅞ inch, 6.5 lb/ft EUE, 2.441 inch i.d.) and packers (AD-1, 80-durometer hard element elastomer) installed to protect the casing from higher pressure. BA-1 (northwest of the injector) had been plugged and abandoned a few years earlier and had to be re-entered and prepared for production.

To return BA-1 to production, the topmost section of the surface and production casing was found about 0.9 m (36 in) below surface by backhoe. A surface casing section 0.6 m (2 ft) in length and 0.9 m (3 ft) of production casing were welded to the top of the casing, and soil was backfilled to the surface. A workover rig with a power swivel was used to drill out one cement plug and one cast iron plug from surface to total depth (TD). A roller cone bit on tubing was used as the drilling assembly. Water was used as the drilling fluid; the wellbore fluid level was kept full. A wellhead was attached to the top of the casing. A packer and tubing were run into this well. The well was shut-in until the previously abandoned flow lines could be re-connected to this well.

A well permit application was submitted to and approved by the State of Indiana (Appendix 1).

Because of the relatively high injection rate and good reservoir communication between the wells, the average reservoir pressure was relatively high, and the wells could readily flow to surface without artificial lift (i.e., rod pumps). Therefore, no rods or downhole insert pumps were used. From a CO₂ EOR perspective, the higher pressure would result in reservoir conditions that would sustain a liquid CO₂ flood. From an oil field operator perspective, this eliminated one of the highest operating expenses, electrical costs to operate pumping units. Furthermore, operating without rods and pumps eliminated the possibility of losing production due to downtime associated with rod or pump failures and the expense of subsequent well workovers.

The wells were produced for about three months prior to starting CO₂ injection. The wells' average oil rates were 0.3 to 0.56 m³/day (0.2 to 3.5 bopd). For the pilot area, 0.8 m³/day (5 bopd) was considered the pre-CO₂ injection oil rate baseline.

Because packers were used to isolate reservoir fluids from the casing, all produced fluids (CO₂, oil, and brine) were commingled from the reservoir through the production tubing to the wellhead. The commingled fluids continued through the buried production flow lines to the production manifold. Gases separated from liquids in the gas-liquid separator, and liquids (oil and brine) separated in the gun-barrel style separator.

Observation Wells

The two observation wells were instrumented with surface pressure gauges only. IB-4 was an active producer on rod pump. Its pressure gauge measured the pressure of the casing-tubing annulus; there was no meter in place to measure produced gas rates. BU-2 had tubing and a packer in place and was liquid-filled to surface. Consequently, readings from the surface pressure gauge on BU-2 together with an estimate of brine density could be used to approximate the bottomhole pressure. The production of fluids from this well was isolated from the production from the four wells in the pilot pattern.

Well Preparation

The packer chosen was the same AD-1 type packer used for water injection; however, the 60-durometer elastomer used during water injection was replaced with a harder rubber element, 80-durometer. The packer was placed above the perforations, and a bottomhole pressure and temperature gauge was lowered below the packer to about 580 m (1,900 ft). No other special considerations were made on the production or injection wells for the CO₂ pilot project. As part of the re-entry, BA-1 was acidized. Prior to injection no other well was treated.

Tank Battery Site for Production and Separation

In the Illinois Basin, crude oil production has very little associated gas production, and most gas is vented to the atmosphere at the wellhead or the stock tanks. An important aspect of CO₂ sequestration and EOR is accurate accounting of the CO₂ produced from an oil field. The CO₂ that remained dissolved in the oil and water at bottomhole pressure and temperature was produced through the tubing and pumped through the production flow lines to the tank battery. A portion of the CO₂ would likely be in the vapor phase and would need to be metered at the tank battery.

To measure the CO₂ at the tank battery, a Natco gas-liquid separator was placed in series upstream of the gun-barrel style oil-water separator. The separator had a maximum allowable working pressure of 0.86 MPa (125 psi) at 54°C (130°F) and a minimum design metal temperature of -29°C (-20°F) at 0.86 MPa (125 psi). A U-bend of pipe was connected to the top of the separator. This pipe connected to a horizontal gas pipe, which allowed collection of gas samples, monitoring of gas pressure, and metering and venting of gas. A Kimray cast iron back-pressure gas regulator (red apparatus at center of pipe cluster in Figure 16) sets pressure at 138 kPa (20 psi), as measured by a mechanical gauge. If pressure exceeds this value, the gas regulator opens to vent gas through the well tester (aluminum colored device at the distal end of the pipe, Figure 17, right side of photo). The 0.64-cm (¼-inch) ball valve on the well tester was included for gas sampling and field measurements of gas composition. A Siemens electronic pressure transducer (left side of Figure 17, adjacent to gas regulator) was used to measure pressure at the distal end of the gas regulator and calculate the gas flow rate through the well tester at the gas-liquid separator.

No gas metering or detection equipment was placed on the oil or water stock tanks.

Chemical Corrosion Treatment Plan

Because the producing wells were produced through tubing with packer set downhole, there was no simple means of circulating corrosion inhibitor to the bottom of the hole to protect the tubing. The surface production flow line and tank battery were made of PVC and fiberglass, so there was no benefit to adding corro-



Figure 16 Kimray cast iron back-pressure gas regulator attached to gas separator at the Bald Unit tank battery. Well tester (see Figure 17) is visible immediately above and to the left of the gas regulator.



Figure 17 Teledyne Merla orifice well tester (aluminum pipe to right) attached to the liquid-gas separator at the Sugar Creek Field tank battery (a photograph of the well tester at the Bald Unit tank battery was not available). A Siemens electronic pressure transducer (blue cover) is shown on the left side of the figure.

sion inhibitor to protect the surface lines and equipment. Consequently, only a small chemical corrosion treatment was implemented at the Bald Unit CO₂ injection pilot to protect the production manifold and gas-liquid separator. Baker Hughes CRO195 was used as the corrosion inhibitor.

Pre-injection Reservoir Modeling

As part of the site selection process, a simple geologic model was used for reservoir modeling to provide general design specifications such as CO₂ injection rate; CO₂, oil, and water production rates; injection pressure; CO₂ distribution; and time to CO₂ breakthrough. The model covered 0.78 million m² (8.4 million ft²) or 194 acres. The top of the model was assigned a constant elevation of -435.9 m (-1430 ft) (i.e., 435.9 m [1,430 ft] below msl) and was based on average elevation of the top of the Clore taken from the geophysical well logs. The grid had 24 cells in the x-direction, 55 cells in the y-direction, and 7 cells in the z-direction. Each cell was 11 m × 11 m × 1.5 m (80 ft × 80 ft × 5 ft). Permeability and porosity values were based on core data and field performance. Porosity was set at a constant value of 21% throughout the model. For horizontal permeability, the model was divided into upper and lower zones to reflect the geological characteristics gathered from preliminary analysis of the geophysical logs. The upper zone was 4.6 m (15 ft) thick and assigned a horizontal permeability of 1.50×10^{-13} m² (150 mD). The lower zone was 6.1 m (20 ft) thick and assigned a horizontal permeability of 2.50×10^{-13} m² (250 mD). Based on general Mississippian reservoir trends, the vertical to horizontal permeability ratio (k_v/k_h) was set at 0.84.

The general MGSC Illinois Basin oil field reservoir model was used with the simple geologic model. CO₂ injection rates of at least 18 tonnes/day (20 tons/day) or 9.6 million scm/day (340 million scf/day) and 3–5 months until CO₂ breakthrough were projected. The reservoir model suggested that 5,000 to 7,000 tonnes (6,000 to 8,000 tons) of CO₂ followed by water injection would be required to cause a measureable oil production response in some of the offset wells. At peak oil production, an increase in oil production of 0.3 to 0.6 scm/day (10 to 20 stb/day) was projected based on model results.

CO₂ UIC II Injection Permit

Well BU-1 was not previously permitted for injection. For CO₂ injection, a permit was required from the Department of Natural Resources, Division of Oil and Gas, State of Indiana (Appendix 2). The State of Indiana issued a permit for CO₂ injection up to 10.3 MPag (1,500 psig) bottomhole pressure. Injection could commence only after a State-approved mechanical integrity test. The pressure requested by the operator was significantly lower than the 14.8 MPag (2,150 psig) water injection pressure designated on the permit.

GEOLOGIC CHARACTERIZATION

Area Geology

Surface Geology

The Bald Unit is located on a ridge of bedrock near the edge of the eastern bluffs overlooking the valley of the Wabash River. The ridge may have been shaped in part by glaciers during the Illinois glacial episode (300,000–130,000 years ago [ya]). The area is covered by a thin layer (<6.1 m or <20 ft) of aeolian deposits, primarily consisting of dune sand and loess (windblown silt), laid down during the Wisconsin glacial episode (110,000–13,000 ya) (Shaver, 1979; Gray, 1989). The nearby river valley is filled with alluvium deposited by the Wabash River, which carried large quantities of glacial outwash for extended periods of time during the Pleistocene glacial episodes (Shaver, 1979). The ancient alluvium is overlain by alluvium from the modern Wabash River (Shaver, 1979; Gray, 1989). The name Mumford Hills comes from a nearby bedrock bench in the middle of the lower Wabash River floodplain (Shaver, 1979).

Bedrock

The unit at the top of the bedrock at the site is the Pennsylvanian (Missourian Series) Bond Formation, which consists primarily of sandstone (Burger, 1986; Gray et al., 1987). The depth to the top of bedrock in the area ranges between 45 m (150 ft) and less than 3 m (10 ft) (Shaver, 1979).

The oil-producing horizon of the Bald Unit within Mumford Hills Field is a sandstone within the Mississippian (Chesterian Series) Clore Formation that is referred to informally in this report as the Clore sandstone. The Clore Formation consists of three members: a lower limestone/shale interval; a middle sandstone and shale interval called the Mount Pleasant Member in Indiana and the Tygett Sandstone Member in Illinois; and an upper shale and limestone interval (Droste and Keller, 1995; Atherton et al., 1975). Droste and Keller (1995) described the composition of the sandstone as “very fine grained to fine-grained white to light-gray to light-brown sandstone ... in beds of shaly sandstone a few feet thick to intervals of massive sandstone as much as 50 feet thick”. The Clore Formation was deposited in a shallow marine to coastal terrestrial environment. The clastic sediments that constitute the sandstone were transported by rivers from sources that lay to the north and northeast. The Clore sandstone, like many of the other oil-bearing formations of the Chesterian Series in the Illinois Basin, has a strong northeast to southwest trend and an elongate, lenticular geometry (Atherton et al., 1975; Droste and Keller, 1995).

General Site Hydrology and Hydrogeology

Posey County is bordered on the west by the Wabash River and on the south by the Ohio River. Robison (1977) described the hydrogeology and some groundwater chemistry for Posey County. Sand and gravel aquifers are present along the valleys of the major rivers and their tributaries (Figure 18). The alluvium along the Wabash and Ohio Rivers generally yields a few hundred to as much as 3,800 L/min (1,000 gallons per minute [gpm]) from single vertical wells. Alluvium in the tributaries of the major rivers generally is finer grained than the sand and gravel deposits of the major river valleys. The highest known yield from a well in the alluvium of the tributaries is 0.3 m³/min (80 gpm). Domestic water supplies can also be obtained from the Pennsylvanian bedrock, primarily from sandstone layers. Shallow wells in the alluvium typically produce soft water, whereas deep bedrock wells generally produce hard water (total dissolved solids greater than 500 mg/L).

Hydrologic data were obtained from the website of the Indiana District of the U.S. Geological Survey (<http://waterdata.usgs.gov/in/nwis/rt>). Specifically, streamflow data were downloaded for Big Creek (USGS station 03378550). The Big Creek gauge is located 15 km (9.4 miles) southeast of the study site, near Wadesville. Using daily mean streamflow data for the period July 1, 1975 through June 25, 2009, the median flow of Big Creek was determined to be 34,000 m³/day (1.56 million ft³/day), and the 25th percentile flow was 5,900 m³/day (207,000 ft³/day). This flow level, designated Q75, the flow that is exceeded 75 percent of the time, was used for calibration of the hydrogeologic model for the site.

Reservoir Geology

Core Analyses

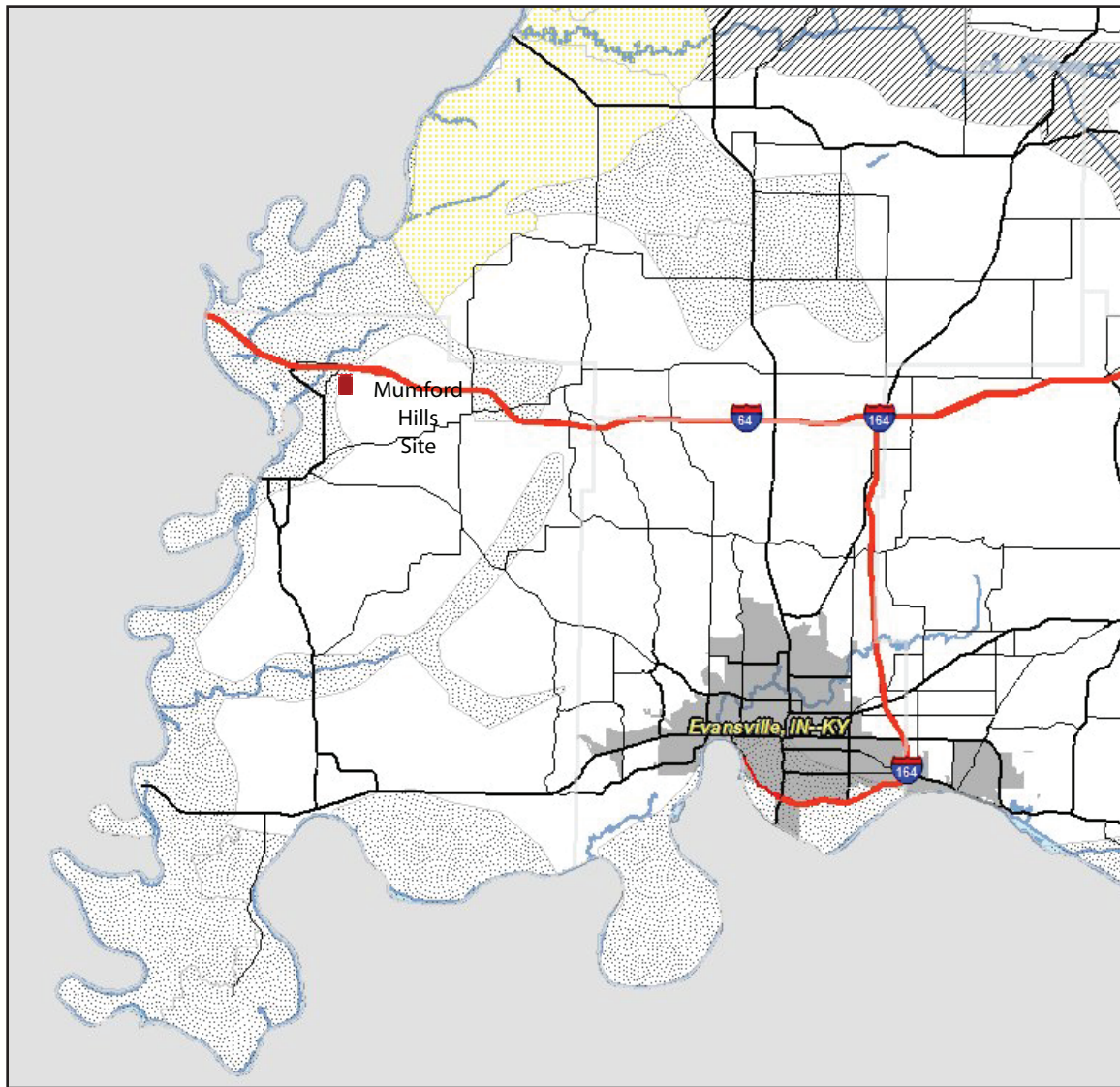
The Clore sandstone in this portion of the Mumford Hills Field was extensively cored with 15 complete core analyses (from 15 wells) provided by the operator for study. The mean porosity of the Clore sandstone was 19.0%, the mean horizontal permeability was 1.46×10^{-13} m² (148 mD), and the mean vertical permeability was 6.85×10^{-14} m² (69.4 mD). The average k_v/k_h ratio was found to be 0.685. Only one core from the BU-1 well was retained and available for study. An interval from this core is shown in Figure 19. Depositional characteristics of the sandstone in this core include tabular cross bedding to subhorizontal bedding, angular clay clasts, carbonaceous plant material and imprints, and mica along shaly bedding planes. These characteristics are commonly found in channel deposits.

Log Analyses






Geophysical logs from a total of 40 wells were available for analyses, and 20 of them were within the Bald Unit area. The majority of the wells were drilled in 1974–1975, and the logs consist of spontaneous potential and either a normal/lateral or a short normal/induction log package. There were also four neutron (gamma-ray) logs, one density log, and two density-neutron logs. The average TD of the wells was 670 m (2,197 ft) and all the wells pass through the entire Clore sandstone.

Conceptual Geological Model

In addition to the core and log data, the conceptual geologic model was based on mapping and cross sections digitally constructed using Landmark Corporation’s Geographix® software. Several cross sections



Aquifer type

-  Buried bedrock valley
-  Surficial sand and gravel aquifer
-  Discontinuous surficial sand and gravel aquifer
-  Buried sand and gravel aquifer
-  Discontinuous buried sand and gravel aquifer

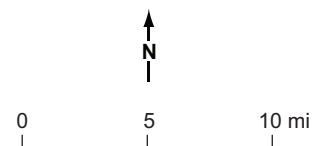


Figure 18 Map of the un lithified aquifers in the Mumford Hills area (data obtained from Indiana Map Service, <http://inmap.indiana.edu/viewer.htm>, March 12, 2012). Red square showing site location is not to scale, and its position is approximate.

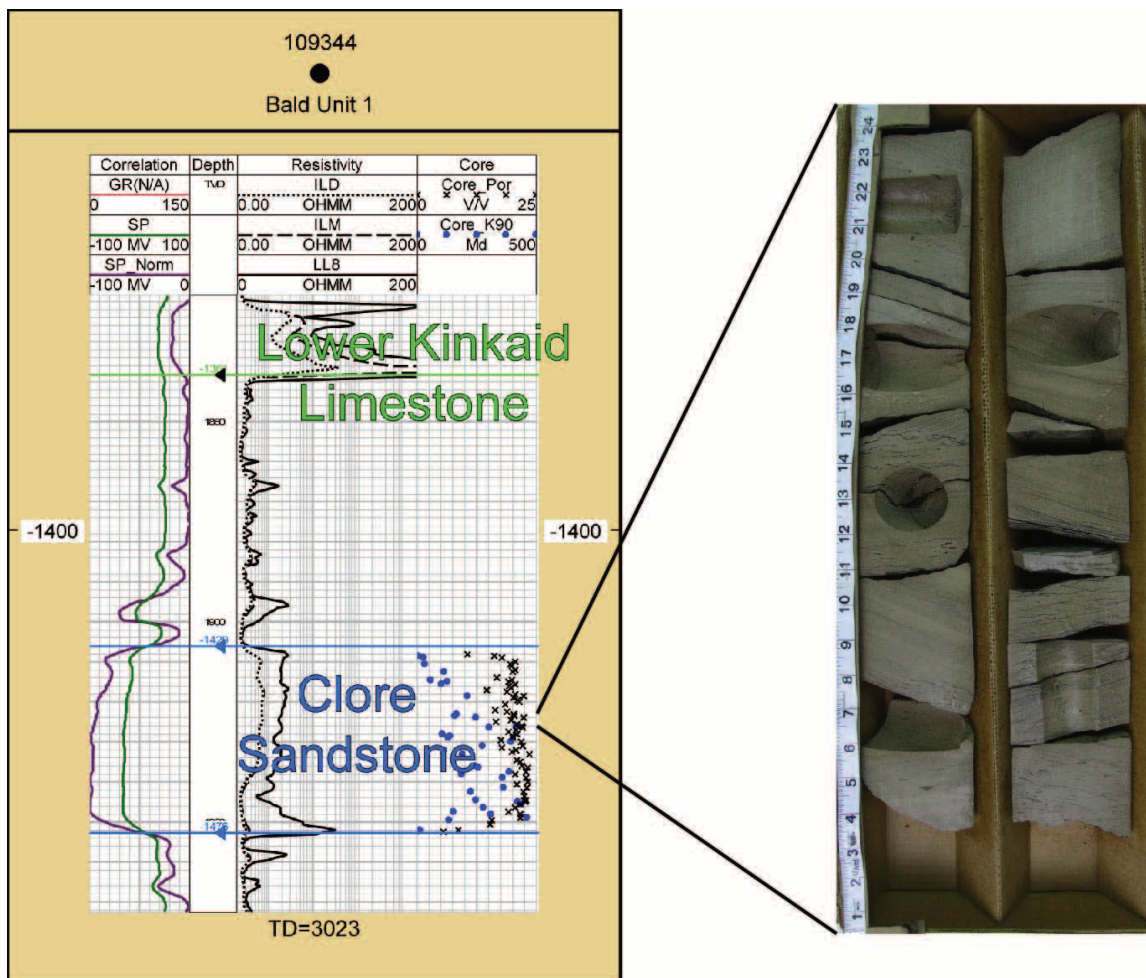


Figure 19 Photo of a sample of the core taken from the Bald Unit #1 well at a depth of 586–587 m (1,923–1,926 ft). The core contains characteristics of a channel depositional system including carbonaceous plant material and tabular cross-beds to subhorizontal bedding planes.

were constructed based on the geophysical logs, and the tops of relevant formations above and below the Clare sandstone were delineated (see Figures 20 and 21 for examples). The base of a continuous layer of limestone, the Lower Kinkaid Limestone, was used as the primary stratigraphic reference. Note that in Figure 21, the log signatures show that the Clare sandstone is completely absent in the westernmost Alexander #3 well but appears in the next well to the east as a thick package of reservoir-quality sandstone, which rapidly decreases in quality in the two easternmost wells in the cross-section. Contrast this with the continuity of the thick Clare sandstone shown in the north-south cross section in Figure 20. Additionally, the log signatures show that the thick, blocky sandstone has a sharp contact at the base, and the quality of the sandstone decreases slightly upward, all common features of active channel-fill sandstones.

Formation tops were picked, and structure contour (Figure 22) and isopach maps (Figure 23) were constructed for the Clare sandstone. The average depth of the Clare sandstone was 581 m (1,907 ft). The structure map (Figure 22) shows that the Field lies along a north-south-trending anticlinal ridge. The isopach map (Figure 23) shows that the reservoir consists of a thick wedge of sandstone with a strong north-south trend. The two cross-sections demonstrate a consistent trend of reservoir quality increasing with depth. In addition, there is a clear water-oil contact (WOC) in the reservoir at an elevation of –444.4 m (–1,458 ft) msl throughout the Bald Unit. Thus most of the oil in the reservoir is in the upper part of the reservoir.

The reservoir was most likely deposited in a channel environment. The elongate, thick sandstone geometry of the isopach map, the geophysical log character profiles, and the core characteristics all indicate the Clare sandstone was deposited in a fluvial or deltaic channel environment.

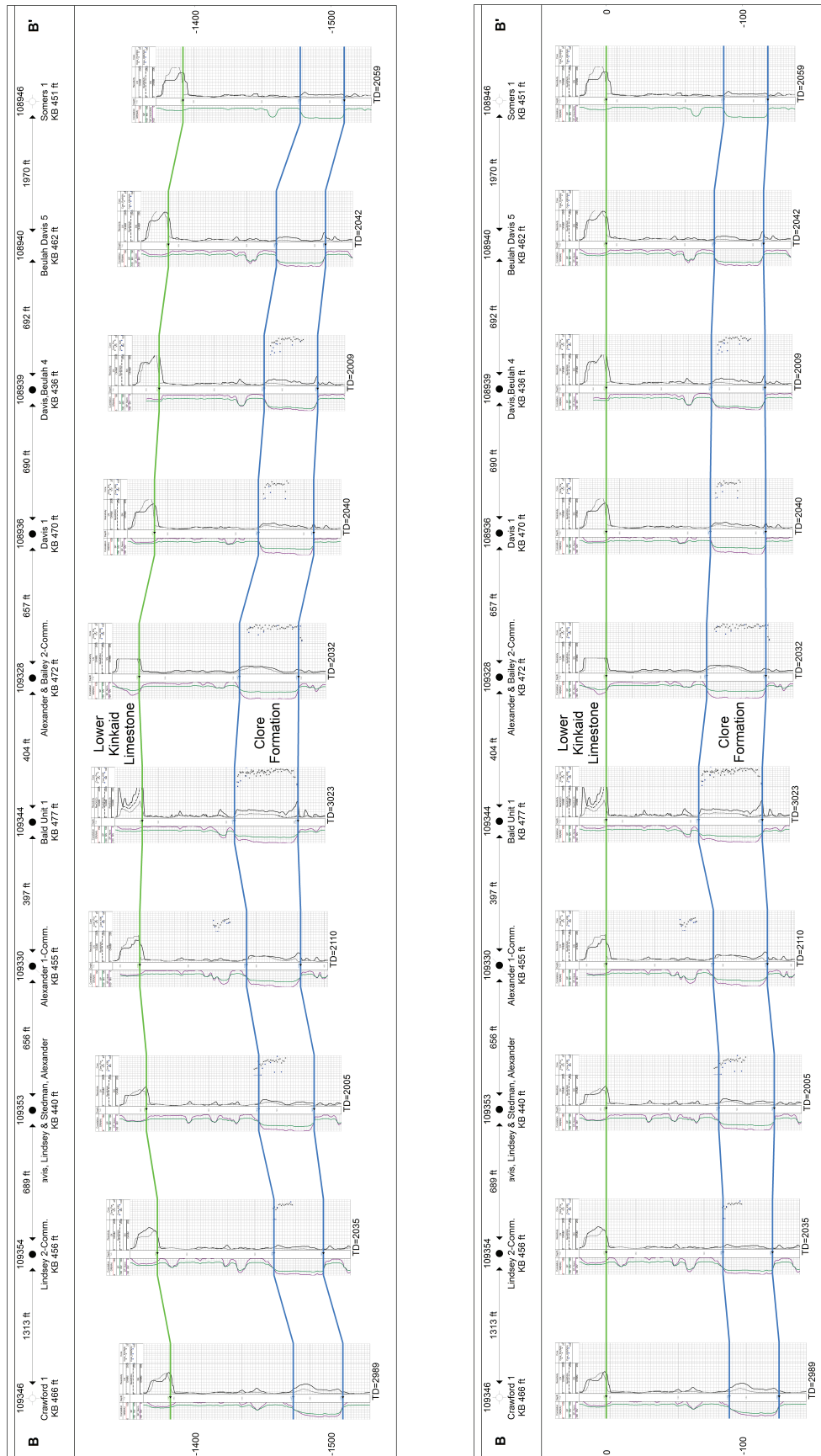


Figure 20 A north to south geophysical log cross section showing the unit of interest, the Clore Formation, and a reference unit, the lower Kinkaid Limestone. The upper figure is a stratigraphic view with the lower Kinkaid serving as the datum. The top and base of the Clore is marked by the blue lines, and the base of the lower Kinkaid is marked by the green line. See Figure 22 for location of the cross section.

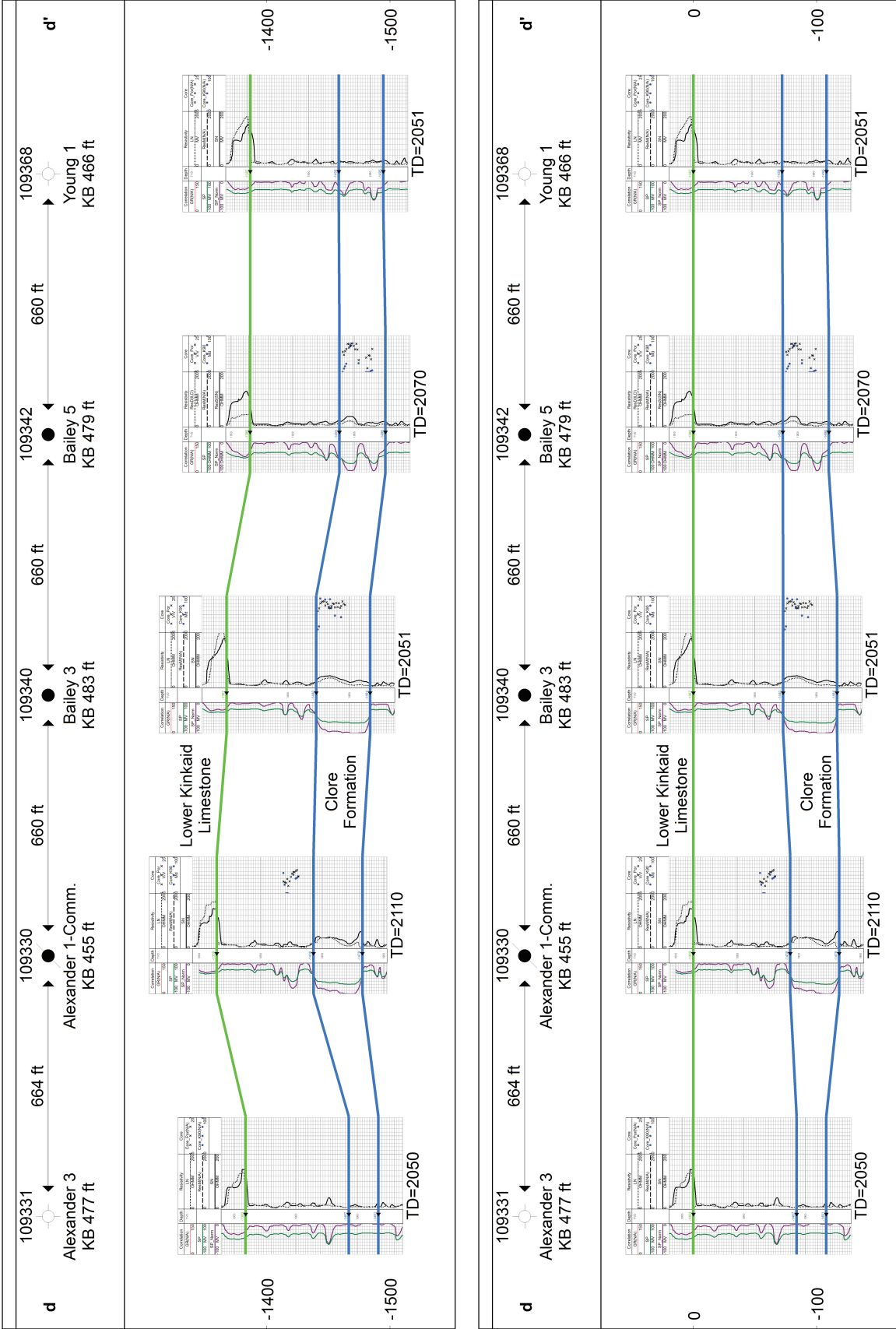


Figure 21 A west to east geophysical log cross section showing the unit of interest, the Clore Formation, and a reference unit, the Lower Kinkaid Limestone. The upper figure is a structural view while the lower figure is a stratigraphic view with the Lower Kinkaid serving as the datum. The top and base of the Clore is marked by the blue lines and the base of the Lower Kinkaid is marked by the green line. See Figure 22 for location of the cross section.

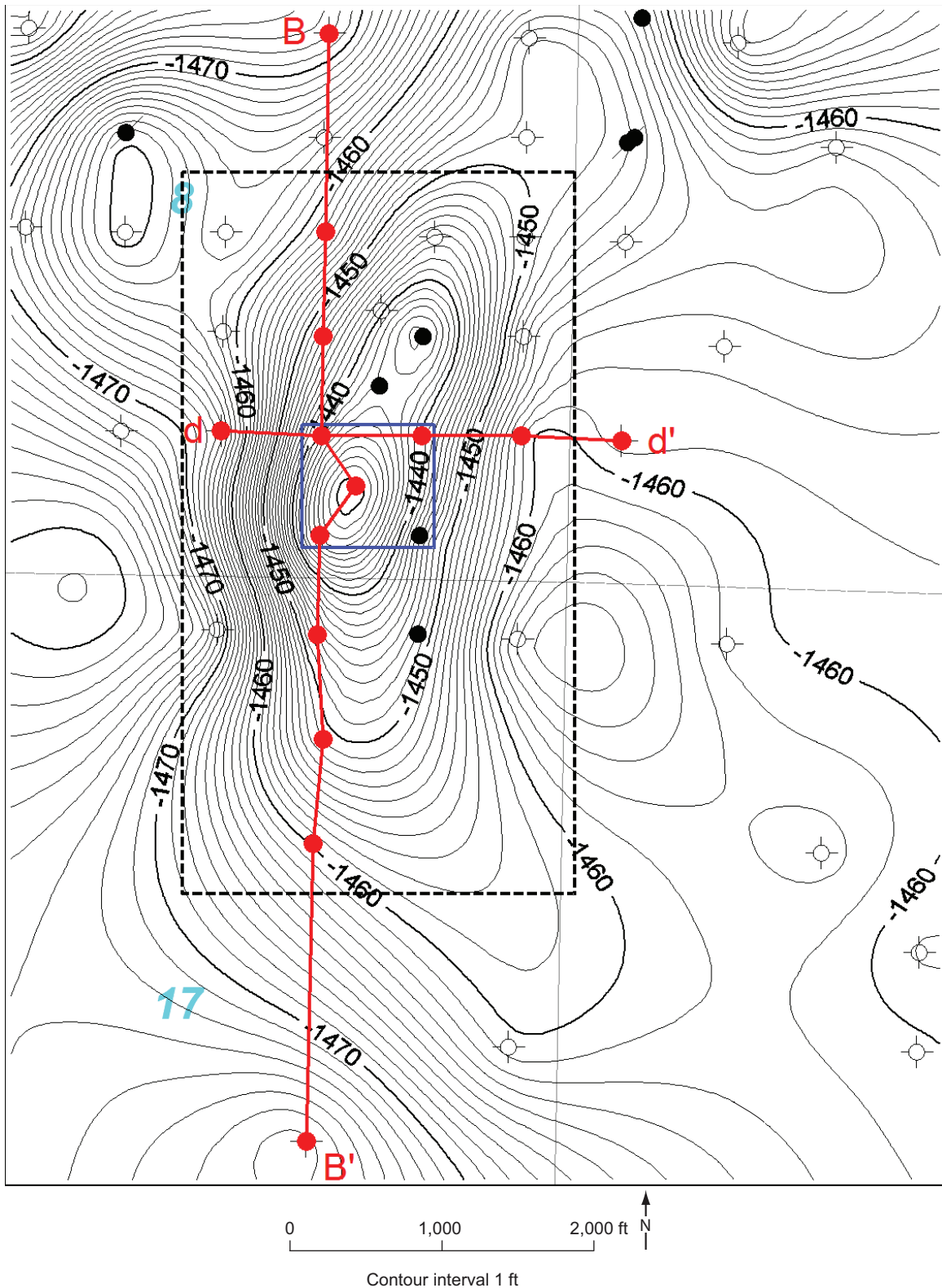


Figure 22 Structure map on the correlative top of the sandstone member of the Clore Formation. The dashed rectangle marks the boundaries of the geocellular model and the blue box contains the injection well and the four offset production wells. The red lines and letters mark the traces of the cross sections in Figures 20 and 21.

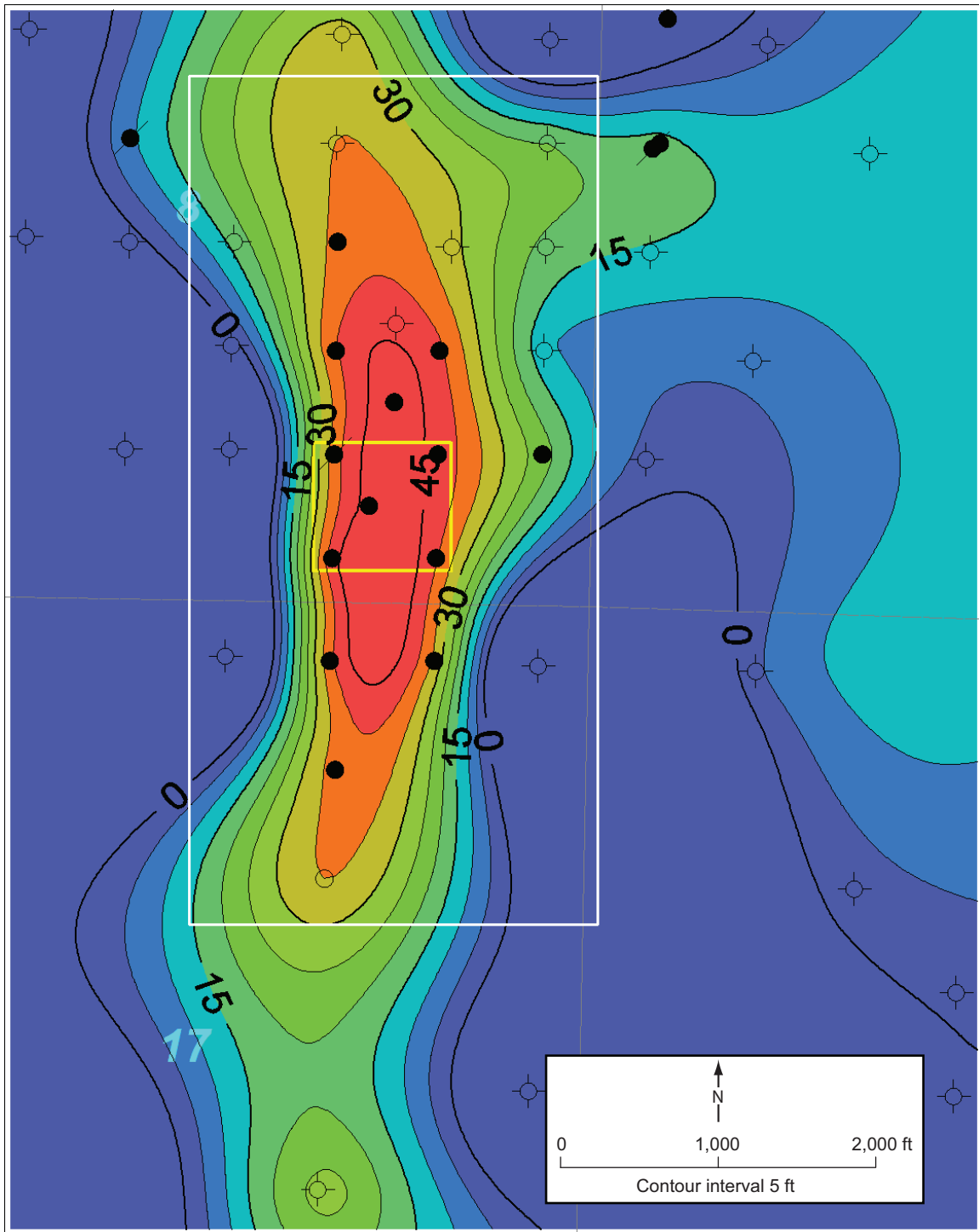


Figure 23 Isopach map of the net thickness of the sandstone member of the Clore Formation. The white rectangle marks the boundaries of the geocellular model, and the yellow box contains the injection well and the four offset wells.

Geocellular Model

The approach to building the geocellular model followed a workflow that utilizes geostatistical methods to describe the heterogeneity of the reservoir. The workflow was developed during the course of preparing models for other EOR fields within the Illinois Basin and employed the geostatistical geologic modeling software Isatis® by Geovariance Corporation. The Mumford Hills Field, like the majority of fields in the Illinois Basin, includes few if any wells with modern neutron-density or gamma-ray log packages. Since geostatistical modeling requires a larger data distribution than that offered by the available core analysis data or porosity logs, the spontaneous potential (SP) log was chosen as an indicator of reservoir quality because of its availability, its correlation with actual permeability, and its independence from fluid content.

First, the SP logs were normalized in order to produce a curve or value that was an approximate indicator of the percentage of sandstone relative to shale. The normalization process reduces well-to-well SP variation that results from fluid chemistry (electrical activity) and other borehole conditions. Geocellular models were built based on the normalized SP data and then the normalized SP values were converted into the desired petrophysical properties utilizing a transform equation relating permeability and porosity values to the normalized SP values.

The normalized SP values were used on a quantitative basis for the geostatistical analysis. After transforming the normalized SP data into a Gaussian distribution, the data set was used to create semivariogram maps and directional semivariograms, as shown in Figure 24. The semivariogram maps indicated a strong north-south trend of N 0°. The models fitted to the semivariograms, shown in Figure 24, had a range of 1,000 m (3,300 ft) in the north-south direction and 91 m (300 ft) in the west-east direction. The semivariogram models used an exponential structure with a sill of 0.752. For the geocellular model, a grid with a total volume of $16.9 \times 10^6 \text{ m}^3$ ($5.98 \times 10^8 \text{ ft}^3$) and covering a surface area of $1.16 \times 10^6 \text{ m}^2$ ($1.25 \times 10^7 \text{ ft}^2$) or 116 hectares (286 acres) was built. The grid initially had spacing of 12 m (40 ft) in the horizontal directions and 0.3048 m (1 ft) in the vertical direction. Later, the grid was up-scaled to a spacing of 24 m (80 ft) in the horizontal directions and 0.61 m (2 ft) vertically, with 33 nodes in the x direction, 59 nodes in the y direction, and 24 nodes in the z direction. The semivariogram models were used in simulations that utilized the turning band method, first proposed by Matheron (1973) and Journé (1974). The simulations produced 100 unique,

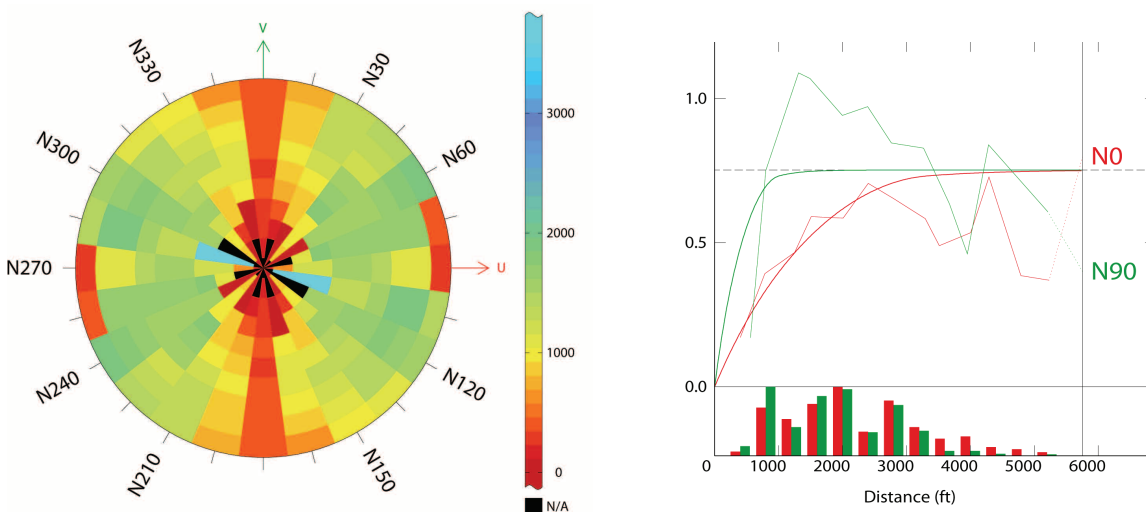


Figure 24 Variogram map, on the left, and variogram with the fitted models on the right. A very strong N-S anisotropy is present in the variogram map, as expected given the geometry of the target formation indicated by the structure and isopach maps of the sandstone, shown in Figures 22 and 23. In the figure on the right, the corresponding variograms calculated in the two directions are represented by the erratic, lighter lines while the models are the smoother, darker lines. The number of pairs of data at each lag is represented by the histogram in the lower part of the figure. The sill is the dashed horizontal line at 0.752. The range of the variogram model in the direction of maximum continuity (red line) was 1006 m (3300 ft), while the range of the variogram model in the direction of minimum continuity (green line) was 305 m (1000 ft). The variograms indicate a highly elongated body, which is typical in channel depositional environments.

equiprobable realizations. The median (P50) and the mean of the realizations were used as the most representative models of the reservoir.

After an acceptable geocellular model had been constructed using the normalized SP data, the model was populated with permeability and porosity values using a transform to convert the synthetic, normalized SP values. The transform was derived from regression analysis techniques: permeability values and corresponding normalized SP log data were plotted and a number of different curves fitted to the data spread. A large amount of scatter in the data made it difficult to fit a curve that had a high level of correlation; therefore, the chosen curve was based on the modelers' experience and expectations regarding the reservoir characteristics commonly found in other Illinois Basin reservoirs. The final transform curves and corresponding equations are shown in Figure 25.

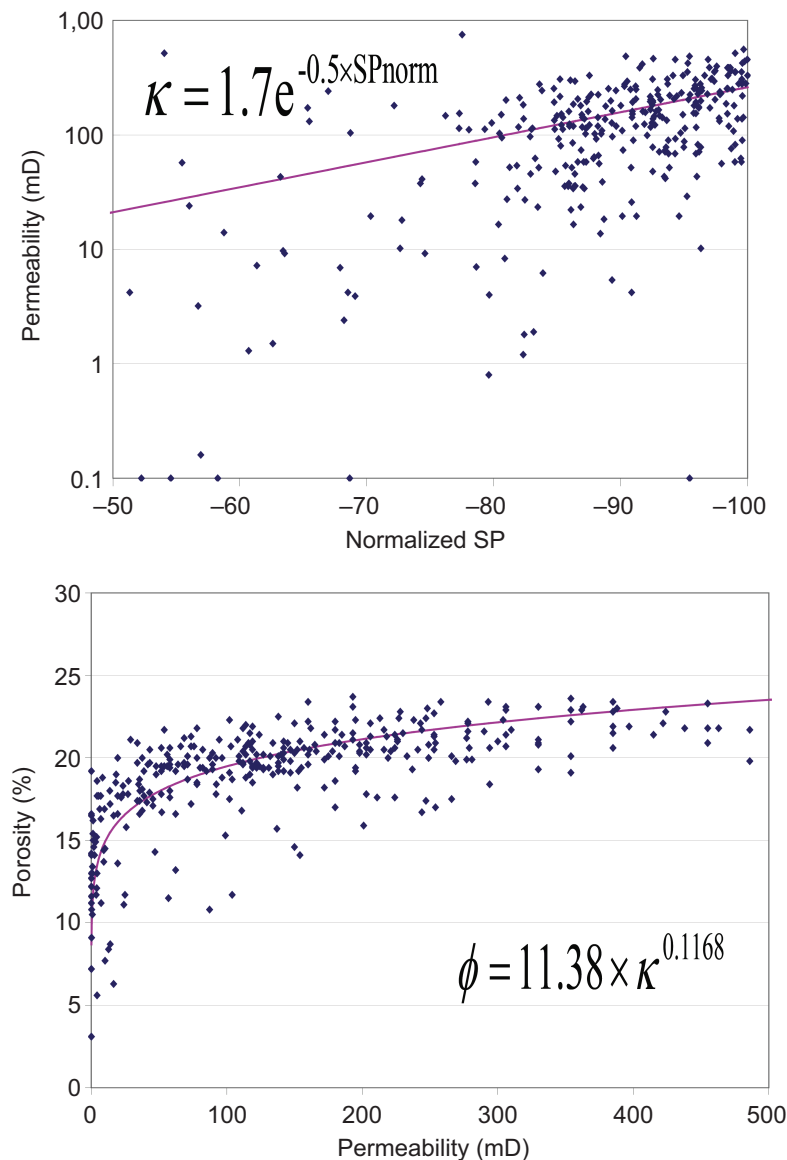


Figure 25 Graphs illustrating the transforms created to convert normalized SP data into permeability (left) and permeability into porosity (right). The data were derived from core analyses and geophysical log records. Data were first plotted on the graph then a curve was fitted to the data as best as possible using regression techniques.

Figures 26, 27, 28, and 29 show a selection of images from the final geocellular model. As expected, the model captured the elongate nature of the sandstone, shown in Figure 26 through 28, as well as the change in reservoir quality in the vertical direction, as shown by Figure 29. The average porosity of the model was 18.9%, and the average permeability was $9.40 \times 10^{-14} \text{ m}^2$ (95.2 mD), which compares favorably with the 19% and $1.46 \times 10^{-13} \text{ m}^2$ (148 mD) averages determined for the reservoir from the core analyses. The difference between the core and the model average permeability can possibly be attributed to oversampling of the best quality reservoir in the core data. The geocellular model was able to reasonably approximate the boundaries of the Field, as represented in the isopach map shown in Figure 26.

The geocellular model was then used for reservoir simulation. As new data were acquired or different reservoir simulations projections were made, the geocellular model was modified to support the data or test hypotheses based on field observations or reservoir simulations.

STRATEGIES AND METHODS FOR THE MONITORING, VERIFICATION, AND ACCOUNTING PROGRAM

Objectives

The techniques used for the monitoring, verification, and accounting (MVA) program at the Bald Unit pilot site were selected based on the results of the MVA programs at the three previous MGSC Phase II pilots. The MVA program's techniques were chosen based on each method's effectiveness in detecting possible CO₂ leakage events based on the relatively small size of the injection volume and the duration of the pilot's planned monitoring period. For example, aerial monitoring of changes to vegetation with infrared imagery for very short injection periods of up to one year and one year of post-injection monitoring are not likely to be effective in detecting small leaks over short periods of time. While these methods were concluded to be less effective for the MGSC short-term pilot injection projects, their effectiveness in longer-term projects with larger injection volumes are considered important.

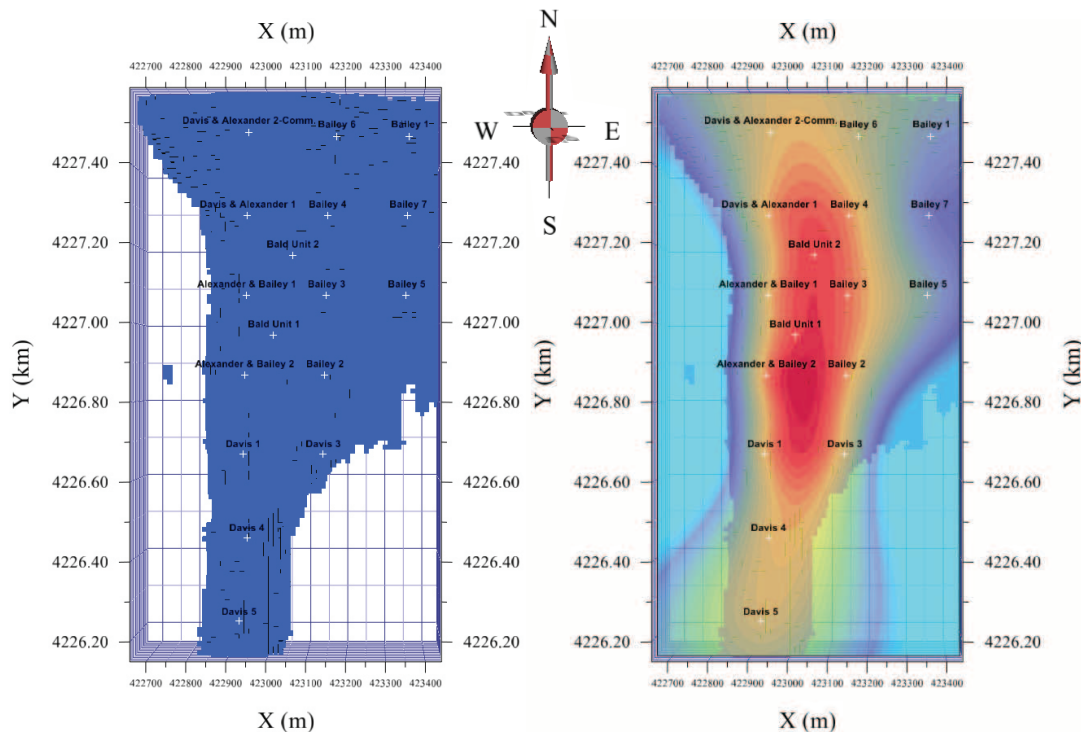


Figure 26 Left: boundary of the 3D geocellular model with a porosity cutoff applied, which shows the extent of the reservoir in the model. Right: the isopach map from Figure 23 is overlain on the model to show the agreement of the conceptual model and the geocellular model.

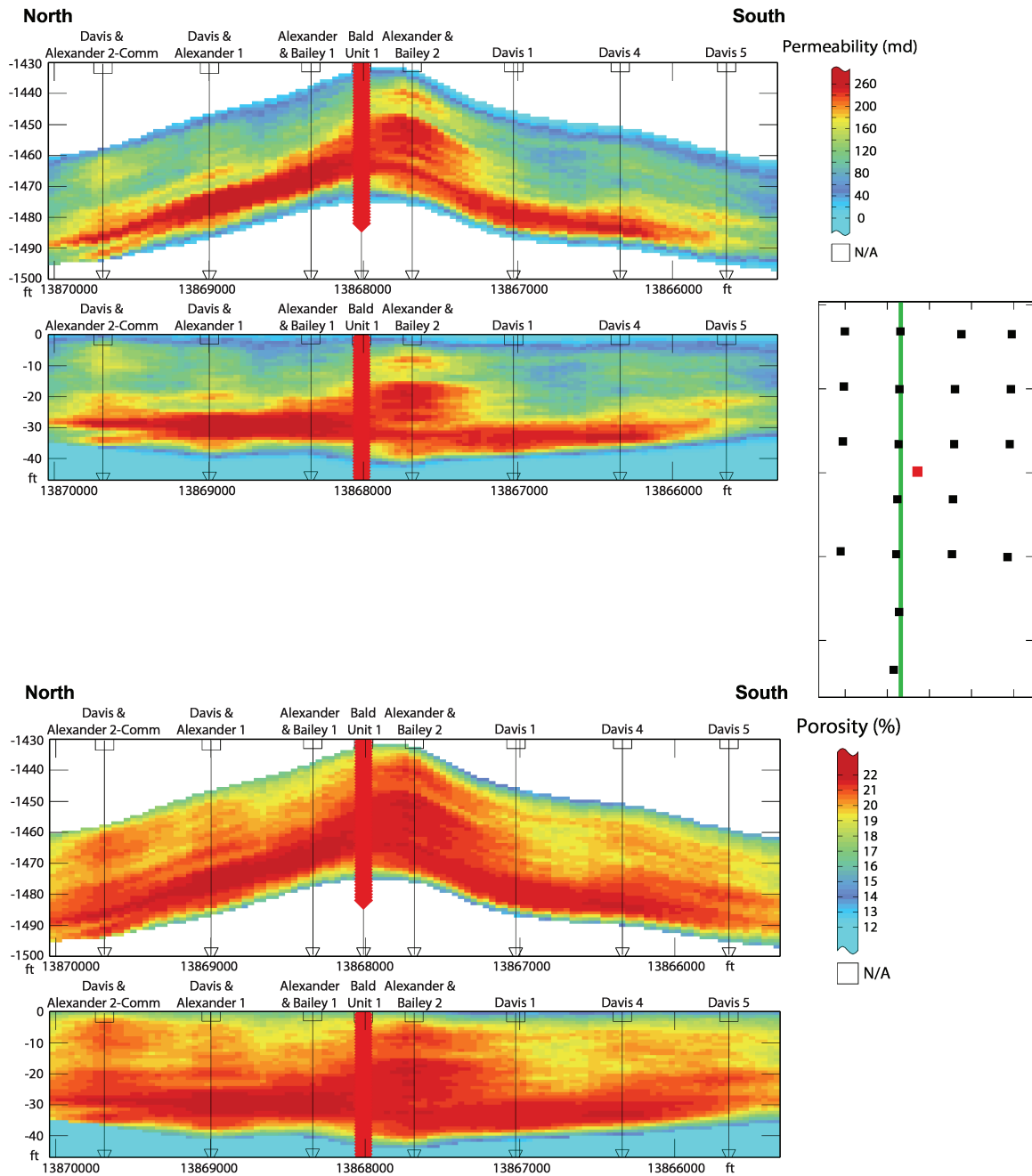


Figure 27 North-to-south cross sections showing the distribution of permeability (top two figures) and porosity (bottom two). The cross sections are in structural space and stratigraphic space with the correlative top of the Clore sandstone serving as the datum. The injection well (BU-1) is marked with a thick, red vertical line. The location of the cross section is shown on the map to the right.

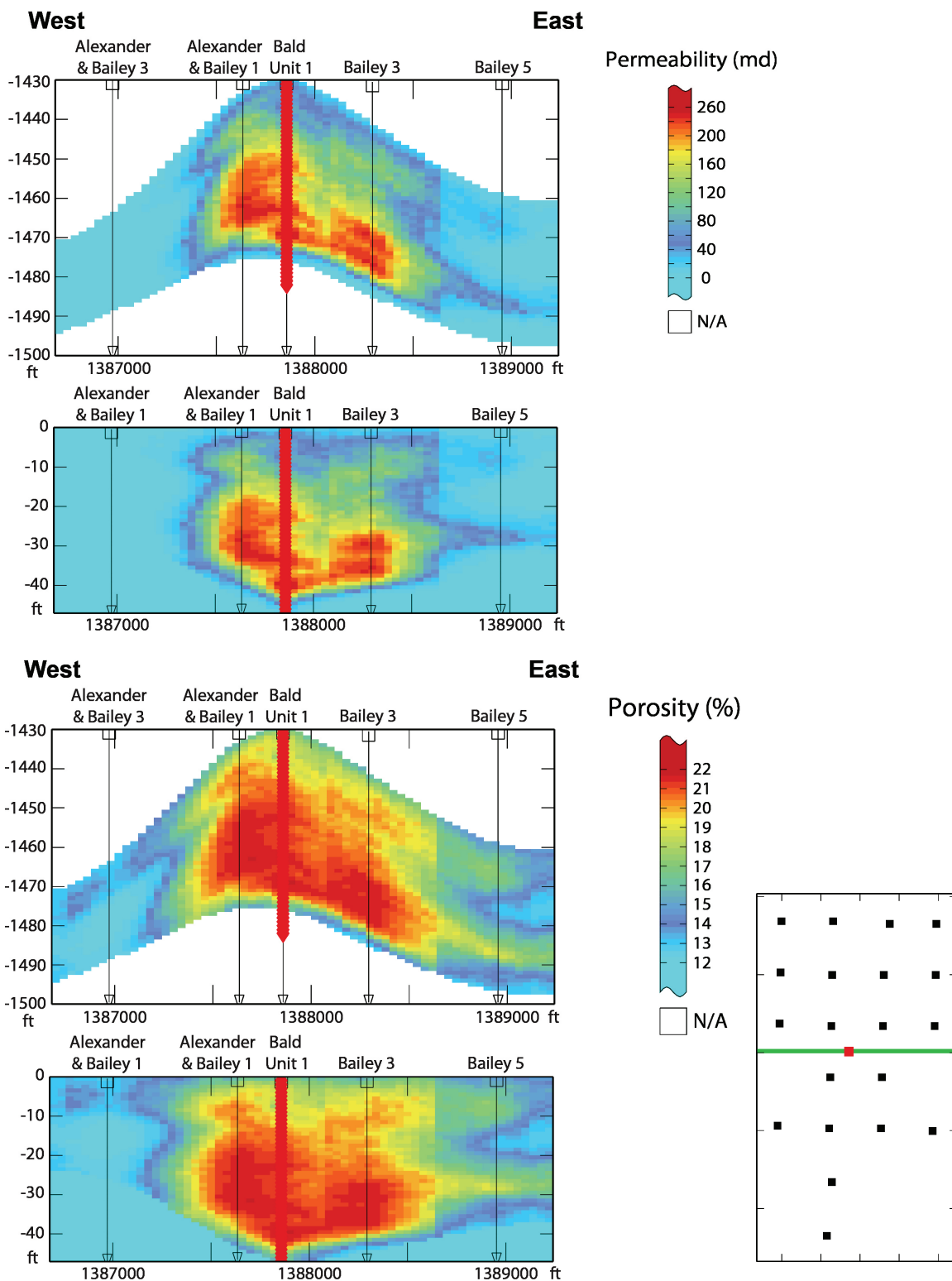


Figure 28 West to east cross sections showing the distribution of permeability (top two figures) and porosity (bottom two). The cross sections are in structural space and stratigraphic space with the correlative top of the Clore sandstone serving as the datum. The injection well (BU-1) is marked with a thick, red vertical line. The location of the cross section is shown on the map to the right.

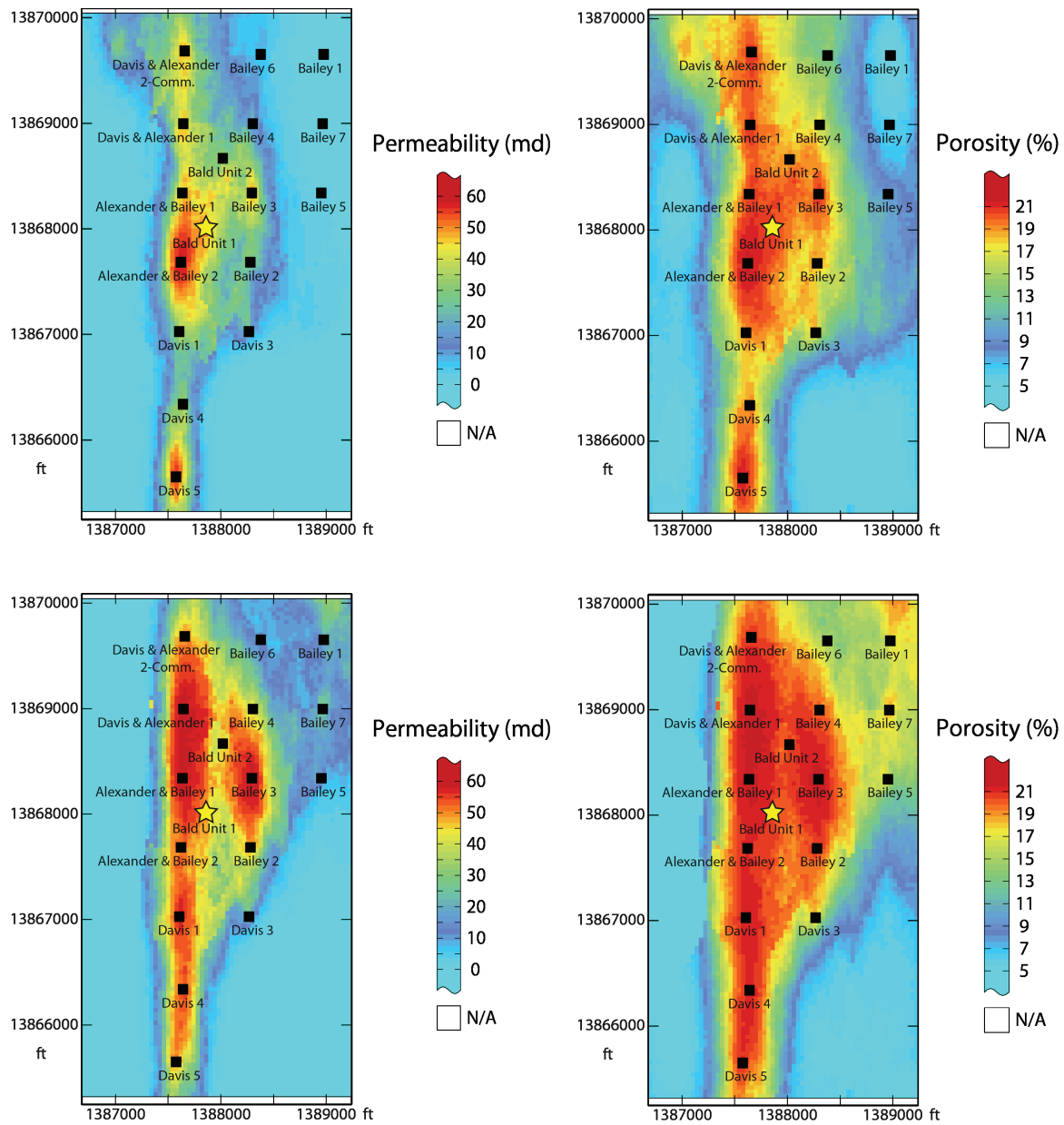


Figure 29 Planar slices through the geocellular model. The upper and lower two images are taken at depths of 6 and 9 meters (20 and 30 feet) below the top of the Clore Formation, respectively. Images on the left show the distribution of permeability; images on the right show the distribution of porosity. The injection well, Bald 1, is marked by a gold star. All images are taken from the geocellular model projected stratigraphically using the top of the Clore Formation as the origin.

Sampling Priorities

The MVA techniques used at the site consisted of the following:

1. preliminary modeling of groundwater flow and particle tracking;
2. inorganic and isotopic compositional analysis of brine from the oil reservoir;
3. inorganic and isotopic compositional analysis of shallow groundwater;
4. compositional and isotopic analysis of gas samples from the four oil production wells; and
5. continuous monitoring of atmospheric concentrations of CO₂ to ensure the safety of project personnel.

To cover the project life cycle, MVA measurements were conducted in three stages corresponding to time periods before, during, and after CO₂ injection. Pre-injection MVA work focused on characterizing ambient aqueous fluid chemistry and developing a baseline data set against which changes due to CO₂ interactions could be documented. The MVA work during injection provided the basis for documenting types of CO₂-water-rock interactions, the magnitudes of the reactions, and their spatial distribution in the field. Post-injection MVA work focused on documenting the extent to which fluid chemistry in the oil reservoir returned to pre-injection values and ensuring that CO₂ and brine did not migrate into the shallower groundwater.

Health and Human Safety

The MGSC had a health and safety plan (HASP) addressing the activities related to the Bald Unit pilot. The purpose of the HASP was to assign staff responsibilities, establish safety standards and procedures, and address contingencies that might arise during operation. The HASP contained the emergency telephone numbers for the local first responders (fire, law enforcement, and ambulance services). A map was provided showing the route to the nearest clinic and the nearest major hospital. The HASP also included information on occupational hazards (e.g., CO₂ exposure, high pressures) and field hazards (e.g., heat and cold exposure, Lyme disease, snakebites, tornadoes, lightning, and poison ivy).

All employees from the MGSC who visited or worked at the EOR site were required to attend a HASP training session. A printed copy of the HASP was kept on-site during injection activities. Level D personal protective equipment—which includes safety glasses, hard hats, gloves, steel-toed boots, and hearing protection where appropriate—was required for all workers. In the immediate area of the injection equipment, air sampling was conducted to monitor CO₂ levels in the atmosphere.

Sampling Strategies

A short summary of the major MVA procedures is provided here, and further details are given in Appendix 3. Additional operational activities included in the MVA program, such as monitoring of CO₂ injection rates and volumes and reservoir temperatures and pressures, are discussed elsewhere in this report.

Design of the Groundwater Monitoring System for the Injection Site

Preliminary modeling of the near-surface groundwater system was required to design a monitoring system capable of detecting CO₂ leaked to shallow groundwater from a point source such as an injection well and its annulus. The modeling provided estimates of the likely flow rate and transport direction of any CO₂ leakage from the injection point into the groundwater for use in assessing risks to the environment and human health.

The software used for the model was GFLOW v2.1.0 (Haitjema, 2005). The model for this site was developed by expanding the GFLOW model developed for the MGSC's Tanquary coal bed methane pilot site, located in Wabash County, Illinois, across the Wabash River from the Mumfords Hills Field (Frailey et al 2012a). The revised model included a thicker aquifer and lower hydraulic conductivity. The model was calibrated using streamflow data from two streams—Bonpas Creek in Wabash County and Big Creek in Posey County, Indiana. If a leak occurred at the injection well or the well's annulus, it was assumed that the CO₂ would enter the surficial aquifer as a point source.

The particle tracking option of GFLOW was used to determine the direction and travel time for a hypothetical CO₂ leak at the Bald Unit project site. The model assumed a non-reactive particle that is not subject to

any retardation processes such as sorption or chemical or biological reactions with groundwater constituents, aquifer materials, or microbes. Thus, the model was predicated on conservative parameters and likely to predict the greatest distances the particle would travel from the source via dispersive and advective flow. Model results indicated that under natural groundwater flow conditions, CO₂ (modeled as a non-reactive particle) that leaked into the shallow groundwater would be transported very slowly to the west or north-west. Particle tracking results suggested that the leading edge of a CO₂ plume in the groundwater would travel between 20 and 200 m (66 and 660 ft) in 100 years. Thus, for the scenarios modeled, CO₂ leakage would not pose a significant risk to groundwater resources in the vicinity of the injection site. Details of the development of the model and its results are presented in Appendix 3.

Groundwater Monitoring Well Description

Groundwater monitoring wells were drilled and completed in July, 2009. Three boreholes were drilled by Illinois State Geological Survey staff members using the Survey's CME-75 rig. Two of the boreholes (MH-1 and MH-2) were drilled using wireline coring tools. The third borehole (MH-3) was drilled by the mud rotary method. Cores were collected from the MH-1 and MH-2 boreholes. Descriptions of the cores and additional information regarding drilling details and well construction can be found in Appendix 4. Figure 5 shows the locations of the groundwater monitoring wells and oil field production wells at the Bald Unit site.

Geophysical logs were run in all boreholes prior to well construction. A natural gamma log was run in each borehole using an MGX II console and 2PGA-1000 downhole tool from Mt. Sopris Instrument Company (Golden, CO, <http://www.mountsopris.com/index.php/products>). The natural gamma logs of the wells are presented in Appendix 4.

Most residential wells located near the study site were completed in an interlayered sandstone and shale bedrock aquifer. The monitoring wells installed at the test site were screened at depths and in bedrock materials similar to the nearby residential wells. The elevations at the tops of the groundwater monitoring well casing were 139.026 m (456.125 ft) msl, 144.827 m (475.156 ft) msl, and 139.857 m (458.850 ft) msl for wells MH-1, MH-2, and MH-3, respectively. The total depths of each well were 53.3 m (175 ft), 51.8 m (170 ft), and 54.2 m (177.7 ft) for wells MH-1, MH-2, and MH-3, respectively. Each monitoring well's uppermost casing was enclosed in a metal well protector (painted yellow) with a hinged, lockable lid. The protectors were anchored in the concrete surrounding the well pipe. Complete well construction details are given in Appendix 4.

After installation, the wells were developed using a Geotech 1.66 Reclaimer™ pump. Each well was instrumented with a dedicated Geotech Bladder Pump™ and a Solinst F65 Levelogger™ pressure transducer. A Solinst Barologger™ was placed inside the well protector at well MH-2 for continuous barometric logging (Figure 30). Additional details can be found in Appendix 3.

Frequency of Sampling

Table 3 summarizes the sampling locations, types of samples collected, and frequency of sample collection in relation to the various operational activities during the process of testing CO₂ EOR and performing MVA at the Bald Unit site.

Due to the short amount of time available between the completion of monitoring wells, the installation of sampling ports in the manifold at the tank battery for collecting reservoir fluids, and the start-up of CO₂ injection at BU-1, only two sampling events were conducted to collect background samples of water from the shallow groundwater monitoring wells and brine from the oil production wells prior to starting CO₂ injection. Difficulties in developing monitoring well MH-3 precluded collecting any pre-CO₂ injection background samples from this well. Background samples were collected at the other two groundwater monitoring wells in order to determine the pre-injection water composition. These analyses provided a very limited baseline for subsequent samples that could be used to compare and monitor changes that might result from migration of injected CO₂ at BU-1 through the oil reservoir and into the local groundwater aquifer.

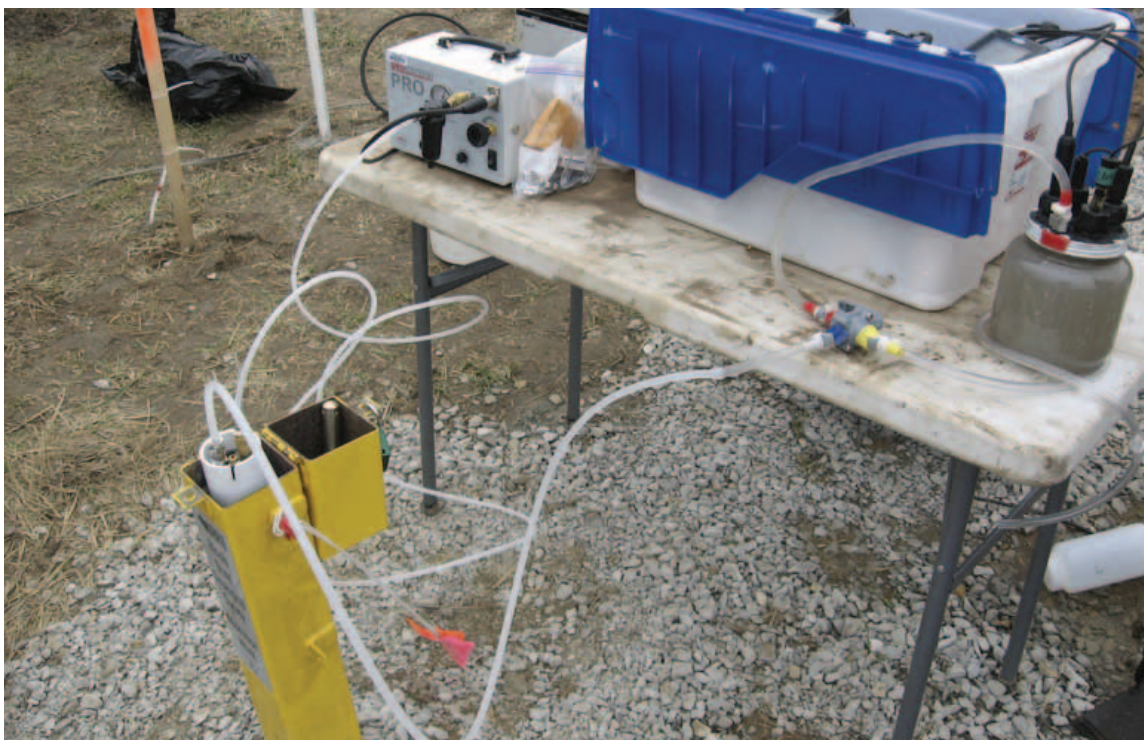


Figure 30 Metal well protector (yellow) of monitoring well, with Solinst Barologger™ resting in open lid. The box on the left side of the table is a geocontrol PRO™ low flow sampler which controls the pumping speed of the bladder pump. The jar at the right side of the table holds a water sample, and the lid of the jar contains sensors which measure water quality parameters. The plastic tub in the middle of the table contains the equipment which reads the signals from the sensors and displays values for water quality parameters. (This picture was taken at the MGSC Loudon pilot site, but similar equipment was used at Mumford Hills.)

Table 3 Summary of sampling locations, number of sampling events, and types of samples collected in relation to operational activities at the Bald Unit CO₂ pilot.

Sampling location	Number of sampling events per operational activity (Injection activity is specific to injection at BU-1)					Total sampling events
	Pre-injection 8/11/09–9/3/09	First CO ₂ injection 9/3/09–1/22/10	First water injection 1/27/10–4/29/10	Second CO ₂ injection 5/3/10– 12/14/10	Second water injection 12/21/10–12/8/11	
Brine						
BA-1	2	4	2	3	5	16
BA-2	2	4	2	3	5	16
IB-2	2	4	2	3	6	17
IB-3	2	4	2	3	6	17
BD-3	2	1	2	2	4	11
Tank battery	2	4	2	3	3	14
Groundwater						
MH-1	2	4	2	3	6	17
MH-2	2	4	2	3	5	16
MH-3	0	4	2	3	4	13
Gas						
BA-1	0	0	2	3	4	9
BA-2	0	0	1	3	4	8
BD-2	0	0	1	2	4	7
BD-3	0	0	2	3	4	9
Tank battery	0	0	2	2	3	7
BD-3	0	0	0	1	0	1
Gas separator	0	0	0	2	1	3

Sample Types

Groundwater Samples

A low-flow sampling technique (ASTM Standards, 2002) was used to collect groundwater samples from the three groundwater monitoring wells. Additional details on sample collection, preservation, and analysis can be found in Table 4 and Appendix 3.

Oil-Reservoir Brine and Gas Samples

Samples of reservoir brines and gases were collected from the four oil-producing wells: BA-1, BA-2, IB-2, and IB-3. Prior to CO₂ injection, the flow line for each oil-producing well was connected to a manifold near the tank battery (Figure 13). The manifold allowed for the fluids from all four oil-producing wells to flow through a test separator into the tank battery. A separate valve for each oil well was installed on the manifold for the purpose of fluid sampling, and pressure gauges were also installed to ensure that over-pressuring would not occur. A barrel containing de-emulsifier and a barrel containing corrosion inhibitor chemicals were connected into the manifold to prohibit CO₂-related corrosion. At the start of each brine-sampling event, this corrosion inhibitor pipe was detached, and the sampling line was purged of all corrosion-inhibitor fluid before samples were collected.

Sampling ports were installed in the production manifold to allow samples to be collected from each oil well. The oil, gas, and brine mixture flowed continuously through the manifold from the oil-producing wells to the tank battery, providing continuous flushing of all pipes. The sampling ports were accessed using quick-connect fittings and purged prior to sampling to reduce the potential of cross-contamination between wells. The tube from the sampling port was attached to a 13.25-L (3.5-gallon) plastic sampling carboy, which allowed the oil to separate from the oil and brine mixture and allowed gases dissolved in the mixture to be vented through the lid (Figure 31). The lid of the carboy contained an entry and exit valve, which allowed continuous flow through the carboy while the fluids segregated. The carboy also included a spigot with a two-way valve at the base, allowing simultaneous measurement of field parameters and collection of samples. After the carboy was filled, the flow rate into the carboy was adjusted to allow the oil to separate from the brine. After an equilibrated state was established in the carboy to maintain brine-oil separation, brine was allowed to flow through a flow-through cell attached to a Hydrolab MS5 MiniSonde™. Specific conductance (EC), pH, oxidation-reduction potential (Eh), dissolved oxygen (DO), and temperature were measured every three minutes. Once these parameters became stable, samples were collected. Stabilization criteria, based on three successive measurements of each parameter (Yeskis and Zavala, 2002), were as follows: pH ±0.1 pH units; EC ±3% of previous reading; Eh ±10 mV; and DO ±0.3 mg/L. A portable Cole-Parmer Masterflex® peristaltic pump was connected to the bottom of the carboy and pumped brine through a 0.45-µm capsule filter. Brine samples followed the same preservation routine, bottle type, analyses, and holding times as groundwater samples (Table 4).

Table 4 Sample preservation, containers, and methods.¹

Analyte	Preservation	Holding time	HDPE Bottle	Method
Alkalinity	Filtration, 4°C	In field, 14 days	60 mL	EPA 310.1 APHA 2320
Dissolved anions	Filtration, 4°C	28 days	60 mL	EPA 300.0 APHA 4110B
Dissolved cations	Filtration, 4°C, HNO ₃ < pH 2	6 months	30 mL	EPA 200.8 APHA 3120B
Total CO ₂	Filtration, 4°C	14 days	60 mL	ASTM D513-06 B
Ammonia	4°C H ₂ SO ₄ < pH 2	1 day	125 mL	Orion, 1990, APHA 4500-NH ₃ D
Isotopes	Filtration, 4°C			
Total dissolved solids	Filtration, 4°C	7 days	250 mL	APHA 2540 C

¹ Abbreviations: HDPE, high-density polyethylene; EPA, Environmental Protection Agency; APHA, American Public Health Association.

Gas samples were collected from a valve located at the top of the sampling carboy. A tube was connected from the production manifold to one of the two valves located at the top of the carboy. Both valves were opened as the carboy began filling with the oil and brine mixture from a specific oil production well. When gas was present in the oil-brine fluid, the change in pressure from the manifold to the carboy caused rapid degassing to occur inside the carboy as the fluid flowed into the carboy. A Landtec GA200™ non-dispersive infrared gas analyzer (NDIR) was attached to the other valve located on the top of the carboy. The gas was pumped into the NDIR using the internal pump of the instrument, and concentrations of carbon dioxide, oxygen, nitrogen, and total hydrocarbons as methane, were measured. Once all concentrations were constant, they were recorded, and an additional gas sample was collected in a Cali-5 Bond™ sample bag for compositional and isotopic analysis in the laboratory using a gas chromatograph and mass spectrometer. Gas concentrations were also measured in the headspace of the tank battery using the NDIR, and additional samples were collected for laboratory analysis. The tank battery was not completely isolated from the atmosphere, resulting in these samples being contaminated with air.

After each oil-producing well had been sampled separately from each well's outlet on the production manifold, a composite brine sample was collected from the tank battery. A PVC pipe carried the brine, which had segregated to the bottom of the separator, to a saltwater waste pit about 9.2 m (30 ft) from the tank battery. A sampling port with a valve was installed in this pipe for the purpose of collecting composite samples from the separator. A 5.1-cm (2-inch) reducing valve was used to adapt the sampling port to the quick-connect on the sampling tube. This sampling tube was attached to the MiniSonde, and field parameters were measured every three minutes. Once parameter values stabilized to meet sampling criteria, the brine samples were collected.

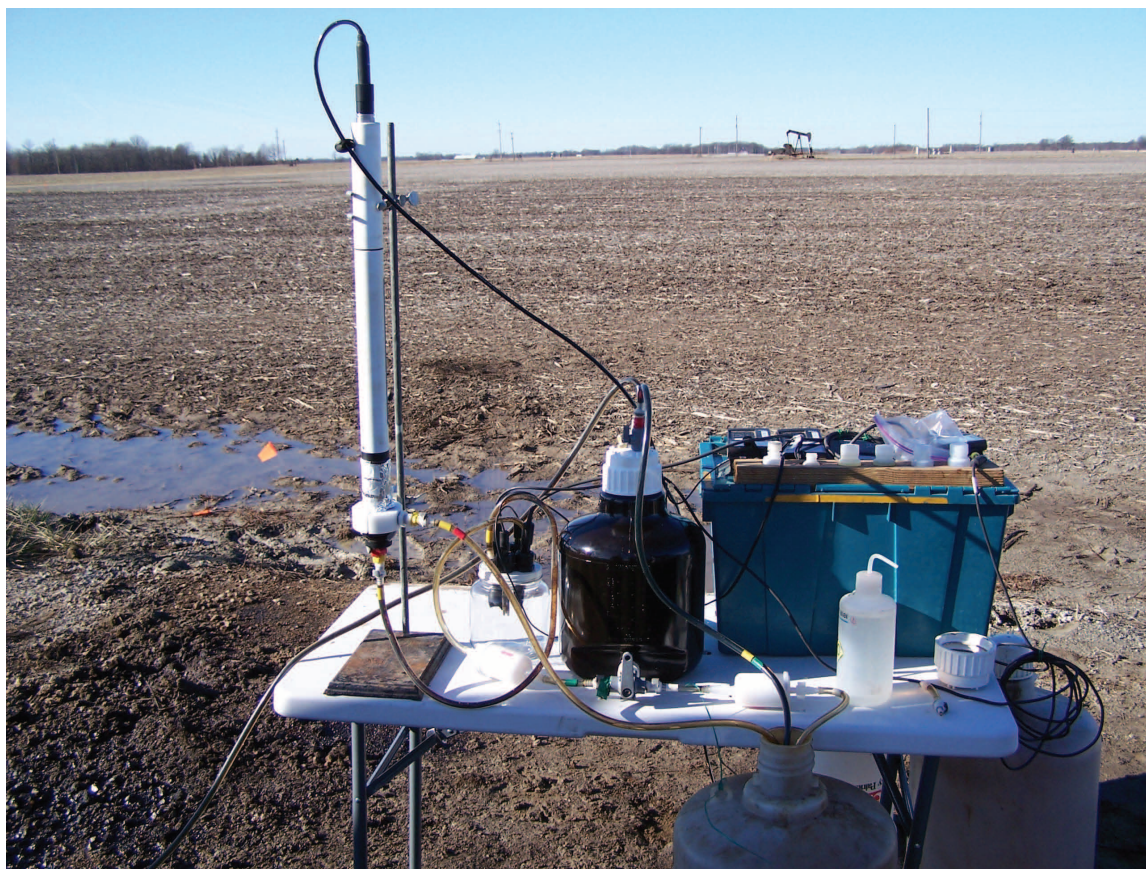


Figure 31 The carboy is the black container with white lid in the center of the table. The flow-through cell is the clear container to the left of the carboy used to monitor brine field parameters. The tall cylinder to the left is a MiniSonde with flow through cell, also used to monitor brine field parameters. (This picture was taken at the MGSC Loudon pilot, but similar equipment was used at Mumford Hills.)

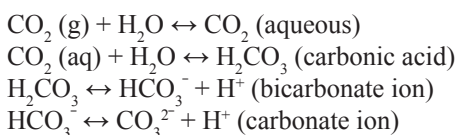
Measurements and Sample Analyses

If CO₂ with isotopically different carbon encounters water, much of the CO₂ can be expected to dissolve into the water and change the chemistry and the isotopic composition of the dissolved inorganic carbon (DIC).

The short duration of pre-CO₂ injection sampling and monitoring of the shallow aquifer and oil reservoir fluids prevented measurement of the natural variations in groundwater composition. Sources of naturally occurring fluctuations of groundwater chemistry include seasonal changes such as precipitation quantities, recharge, and anthropogenic disturbances other than the CO₂ injection. Fluctuations of the reservoir brine chemistry also could occur due to changes in oil field operational practices. Unfortunately, no gas samples were collected during aqueous sampling from either the groundwater monitoring wells or the oil production wells to provide baseline compositional and isotopic information before starting CO₂ injection.

Bulk Chemistry and Fluid Characterization

Reservoir Brine Chemistry Brine samples were collected from the four oil production wells, the tank battery (TB-1) where brines from all the production wells were commingled, and from the water supply well (BD-3). Water from BD-3 was mixed with producer water for injection into BU-1 and BD-5. Brine samples were collected twice prior to CO₂ injection and bimonthly during the project. The goal of monitoring the brine chemistry was to examine the response of the oil reservoir to CO₂ injection. A critical parameter in understanding how the brine chemistry changed as CO₂ dissolved into the brine is the pH of the fluid. Dissolution of CO₂ in water can result in the following reactions:



The production of H⁺ can result in a decrease in pH and subsequent dissolution of parts of the solid matrix of the reservoir. Therefore, analysis of the brine data focused on analytes involved in the carbonate chemistry of the brine and potential dissolution products of clay minerals.

Reservoir Brine Characterization The reservoir brine had a relatively large EC (38 to 50 mS/cm; Appendix 5) compared with that of the shallow groundwater in the study area (1.3 to 2.9 mS/cm; Appendix 6) but is more dilute than seawater (56 mS/cm). Predominant species in the brine include sodium and chloride; their concentrations gradually decreased in samples collected from most of the production wells during the project (Figure 32). The decrease in these constituents may be the result of injecting more dilute water (Figures 33 and 34) from well BD-3 into the reservoir during waterflood operations. Other minor constituents (Br, Ca, K, and Mg) also decreased or remained relatively constant during the project (Figure 35). Samples from BA-1 exhibited trends in analyte concentrations comparatively different from the other samples, and the concentrations were smaller than in the other wells (Figures 36 and 37). The concentrations of most major brine cations in well BA-1 generally were less variable, and Ca concentrations increased with time, which may be a result of dissolution of carbonate minerals in the reservoir rocks due to a CO₂-induced decrease in brine pH.

Reservoir Gas Chemistry Understanding oil production response and changes in reservoir fluid chemistry due to the injection of CO₂ requires examining the distribution of CO₂ in the oil reservoir. Unlike other CO₂-EOR projects the MGSC has conducted, where CO₂ concentrations could be monitored directly from the oil production well annulus space, the Bald Unit production wells contained packers that precluded collection of gas samples from the casing-tubing annulus. Instead gas samples were collected during reservoir fluid sampling. As fluid samples degassed in the sampling carboy, gas samples were analyzed in the field using the NDIR gas analyzer through a port in the top of the carboy and also were collected in gas bags for laboratory gas chromatographic analysis. Gas samples were analyzed with either an SRI 8610C or a Varian 3800 gas chromatograph equipped with thermal conductivity, flame ionization, and helium ionization detectors. See Appendix 3 for details on chromatograph operating conditions. The CO₂ concentrations determined by the two methods were similar (Figures 38 and 39), but the gas chromatograph analyses also provided data for particular hydrocarbons in the gas samples.

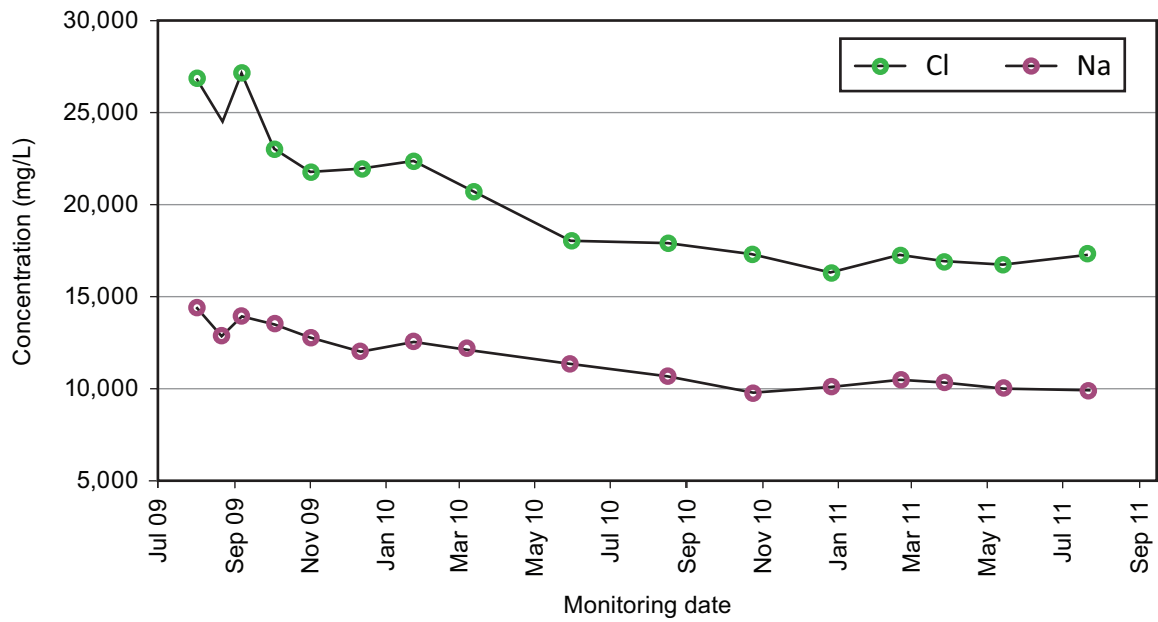


Figure 32 Typical concentrations of sodium and chloride in brine collected from the Mumford Hills oil reservoir. (IB-2 concentrations are shown in this figure.)

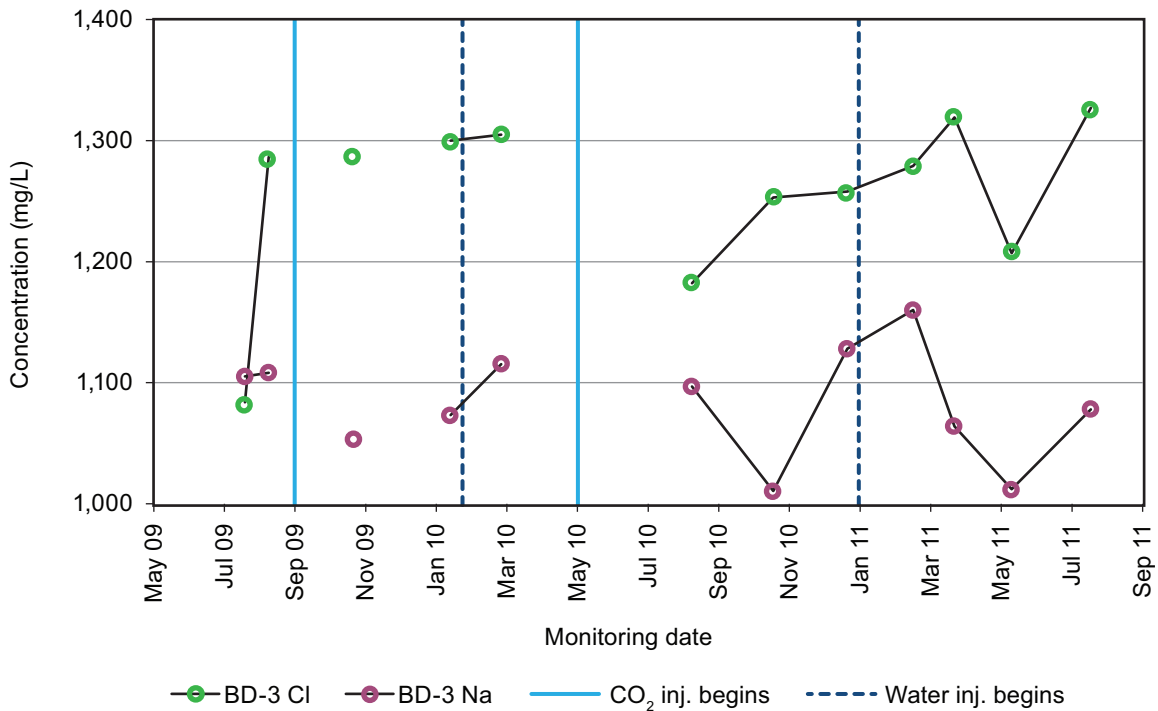


Figure 33 Concentration of sodium and chloride in water injected into oil reservoir at well BD-3 during water flood activities at Mumford Hills. Breaks in the line connecting data points are for sampling periods when the water well BD-3 was not pumping. Vertical lines indicate beginnings and endings of CO₂ injection periods.

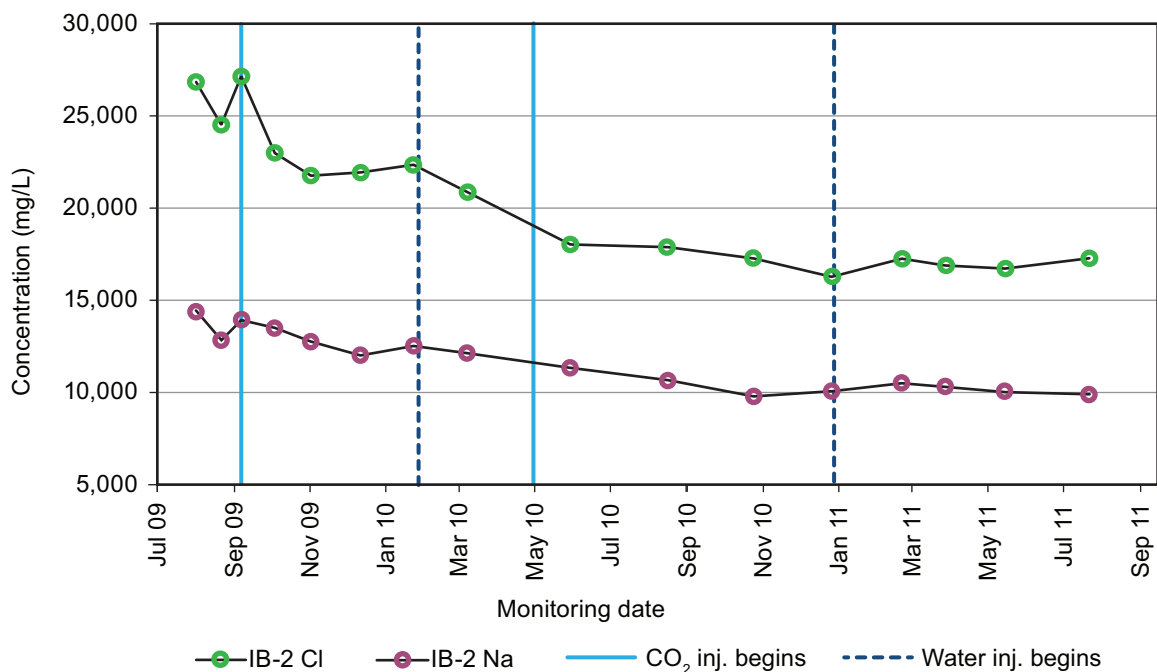


Figure 34 Concentrations of major analytes in water samples collected from well BD-3. Breaks in the lines connecting data points are for sampling periods when the water injection well BD-3 was not pumping. Concentrations of all analytes were higher when sampled in December 2011, but those data were collected after completion of the pilot project and are omitted from this figure. Vertical lines indicate beginnings and endings of CO₂ injection periods.

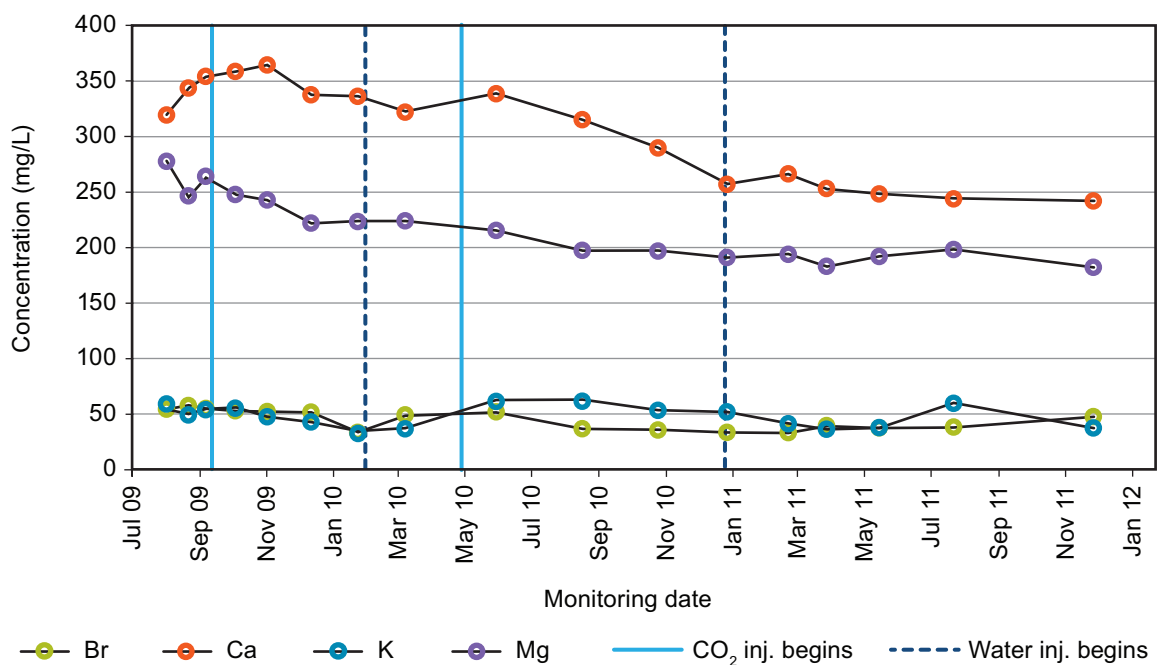


Figure 35 Typical concentrations of common constituents detected in brine samples from oil production wells. (IB-3 concentrations are shown in this figure.) Vertical lines indicate beginnings and endings of CO₂ injection periods.

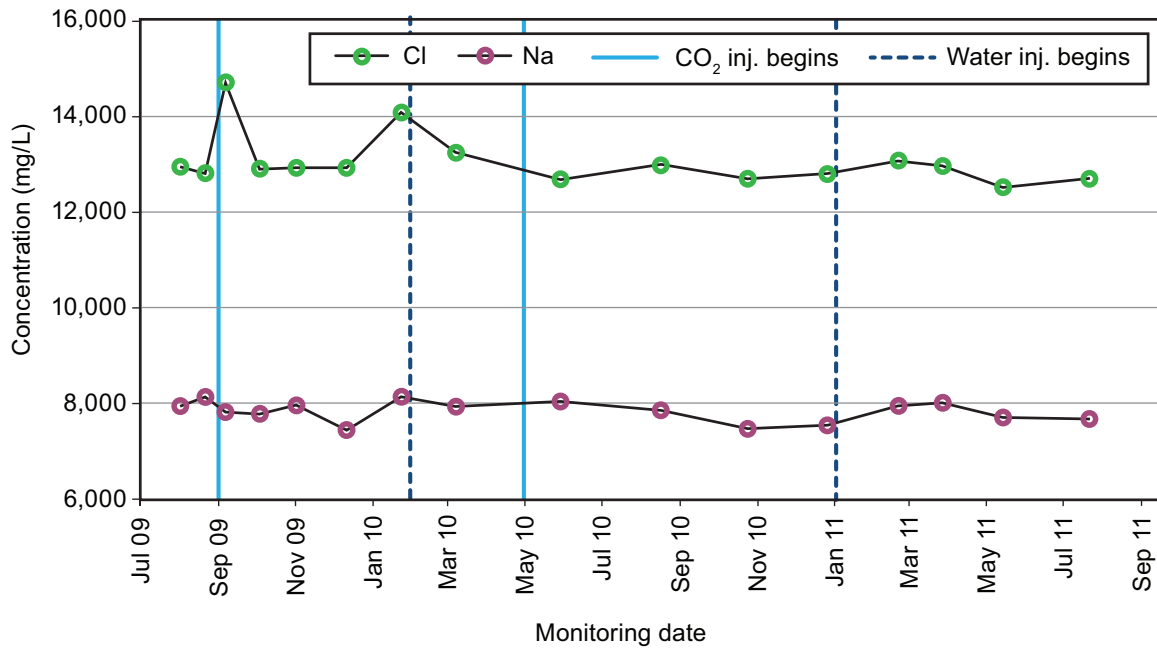


Figure 36 Concentrations of sodium and chloride in brine samples collected from oil production well BA-1 do not follow trend observed in other production wells. Vertical lines indicate beginnings and endings of CO₂ injection periods.

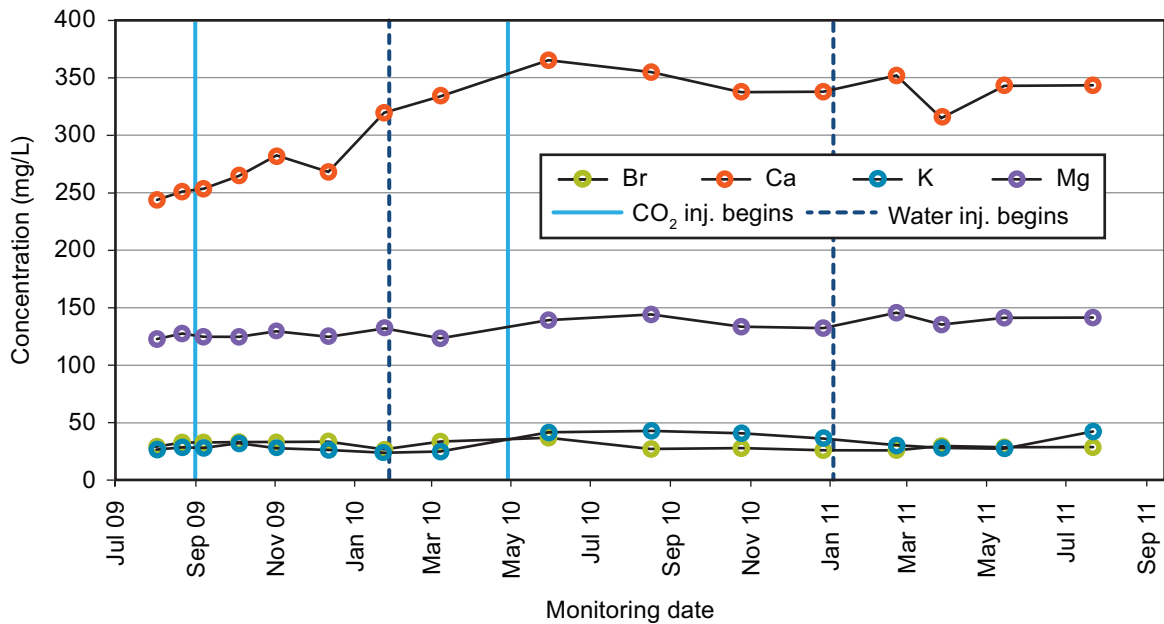


Figure 37 Concentrations of typical constituents detected in brine collected from oil production well BA-1. Vertical lines indicate beginnings and endings of CO₂ injection periods.

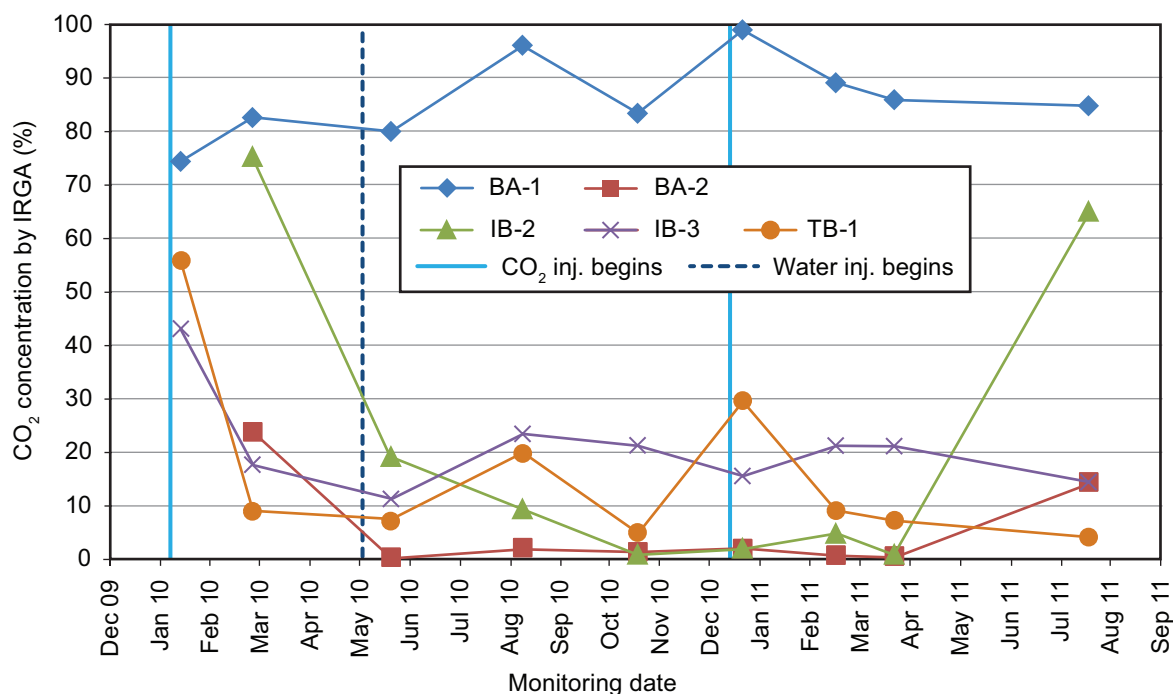


Figure 38 Carbon dioxide concentrations in gas samples collected from BA-1, BA-2, IB-2, and IB-3, and the tank battery (TB). Concentrations were determined by a non-dispersive infrared (NDIR) gas analyzer in the field. Vertical lines indicate beginnings and endings of CO₂ injection periods.

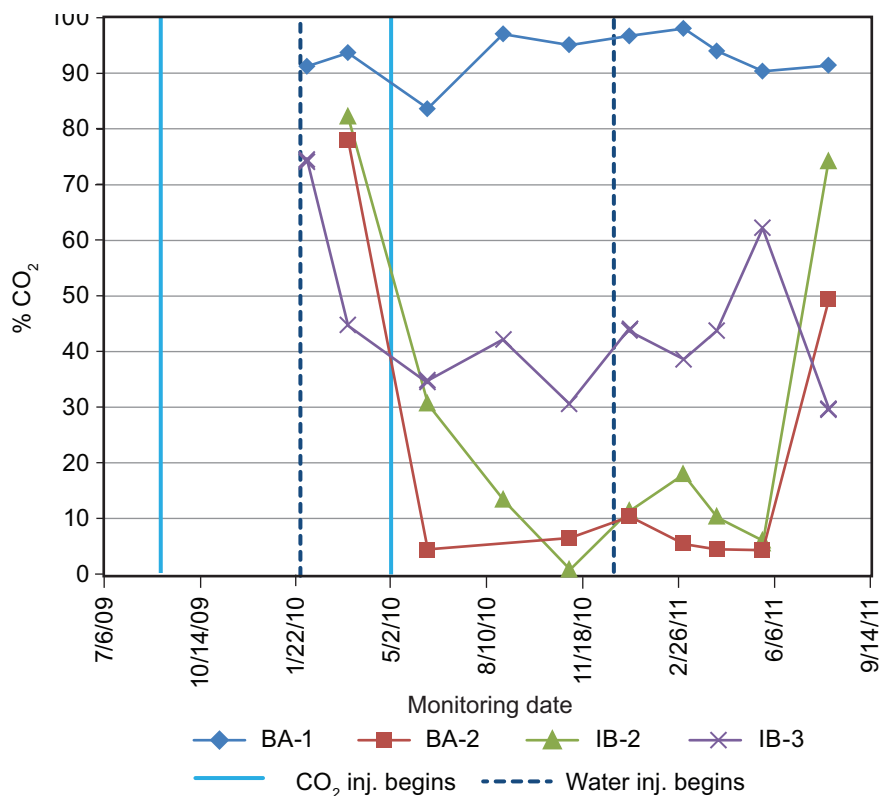


Figure 39 Carbon dioxide concentrations in gas samples collected from BA-1, BA-2, IB-2, and IB-3, and the tank battery (TB). Concentrations were determined by gas chromatography in the laboratory and corrected for air contamination in the samples.

Gas was not present during sampling prior to CO₂ injection; thus background compositional characterization of reservoir gas was not possible. Most gas samples collected from the reservoir contained oxygen and nitrogen, which in some samples were at concentrations similar to air (Figures 40 and 41), probably due to the method of collection. Actual CO₂ concentrations in the reservoir could have been greater than measured because dilution by air in the samples reduced the concentrations measured with our instruments. Calculations were made to correct for air dilution in the production gas samples for the laboratory gas chromatographic data and are included in the figures and in Appendix 7. The CO₂ injected at BU-1 came from an ethanol fermentation plant in Indiana and an oil refinery in Illinois. Approximately 30% of the CO₂ was from the oil refinery and 70% was from the ethanol plant. The carbon isotopic composition ($\delta^{13}\text{C}$) of the ethanol-derived CO₂, sampled prior to the beginning of injection, was -10.8‰ with a ¹⁴C activity of 104.4 percent modern carbon (pMC). A sample of the oil refinery-derived CO₂ was collected from the storage tank at the Bald Unit site and had an isotopic composition of -35.4‰ and a ¹⁴C activity of 0.98 pMC.

Groundwater Chemistry Three monitoring wells (MH-1, MH-2, and MH-3) were installed to monitor shallow (~52 m [-170 ft] below ground surface) groundwater quality on the project site. Difficulties in developing well MH-3 prevented groundwater samples from being collected at this well for three months, which was after CO₂ injection had begun. The pH values of the groundwater in all three wells ranged from 8.05 to 8.96 and followed similar temporal trends in all wells (Figure 42; Appendix 6). Generally pH values were greater in samples collected from well MH-2 and lower in samples from well MH-1. The pH values for samples collected at the beginning of the project for MH-1 (8.37) and MH-3 (8.57) were similar to the pH values in corresponding samples analyzed at the end of the project for these two wells (MH-1: 8.28 and MH-2: 8.59) suggesting that CO₂ was not leaking into the shallow groundwater. Initial pH values in well MH-2 were slightly greater (8.94) than final pH values (8.5), but alkalinity values actually decreased. The high pH values for all the wells suggest that carbonates likely are not buffering the groundwater system near the wells.

Pennsylvanian Sandstone Mineralogy Cores (Figure 43) were collected during well construction, and two samples from the screened interval of well MH-2 were submitted for mineralogical analysis by x-ray diffraction. The samples were from a gray laminated sandstone/siltstone. Sample 1 was collected from a mostly gray section of the core that contained areas of reddish brown color and visible pyrite. Sample 2 was taken from a relatively uniformly gray-colored section of the core. Both samples contained significant (20.7% and 8.3%) amounts of siderite (Table 5). Siderite equilibrium could buffer the pH of the ground-

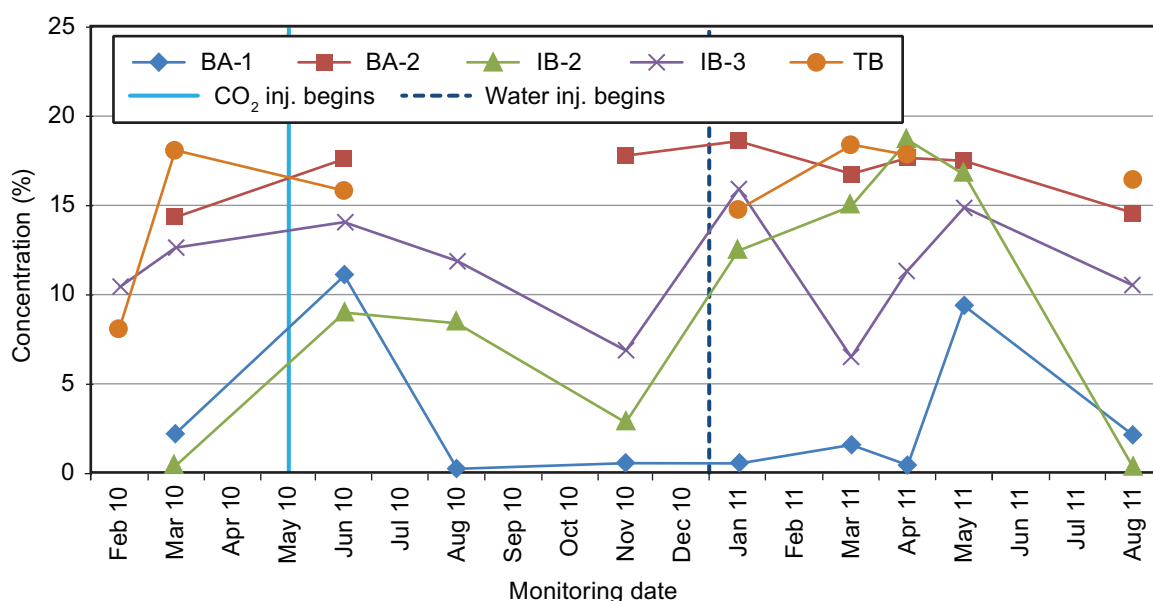


Figure 40 Oxygen concentrations determined by gas chromatograph in gas samples collected from oil production wells and the tank battery (TB). Vertical lines indicate beginning and end of second CO₂ injection period.

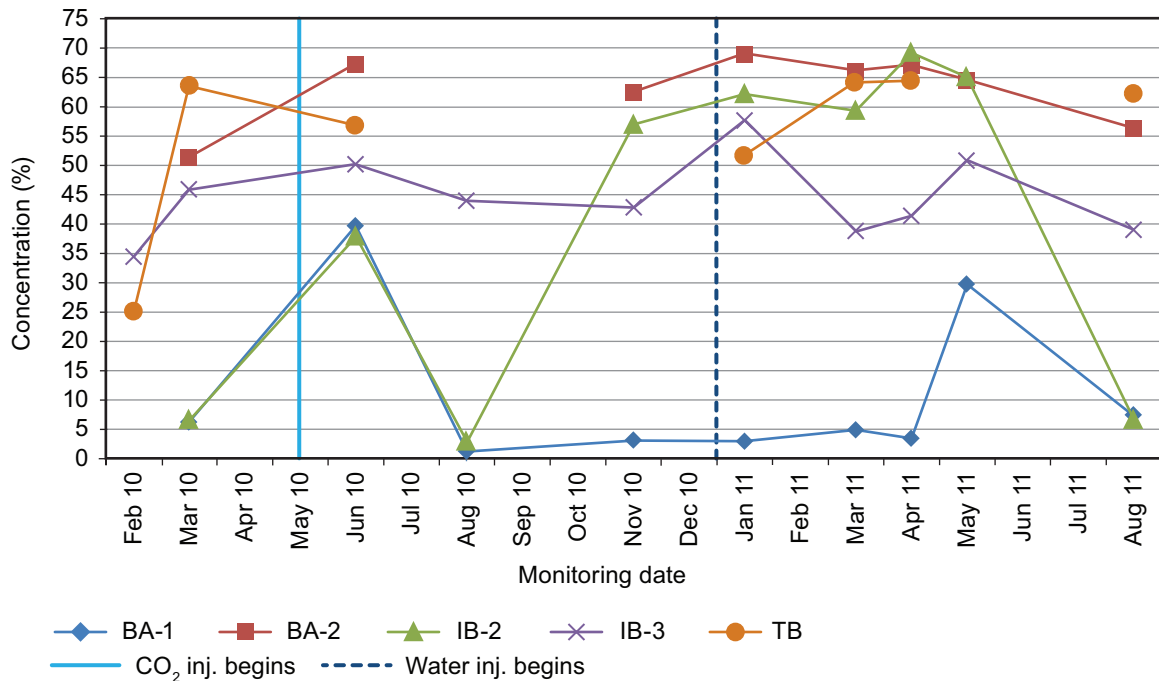


Figure 41 Nitrogen concentrations determined by gas chromatograph in gas samples collected from oil production wells and the tank battery (TB). Vertical lines indicate beginning and end of second CO₂ injection period.

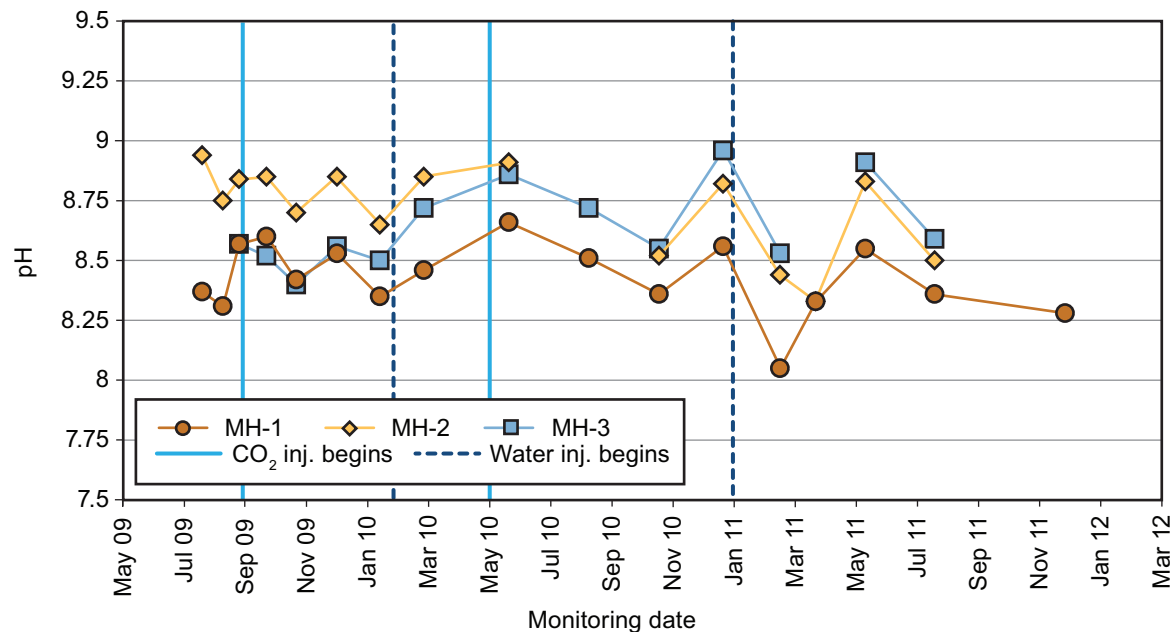


Figure 42 pH of shallow groundwater from the groundwater monitoring wells MH-1, MH-2 and MH-3. Vertical lines indicate beginning and ending of first and second CO₂ injection period.



Figure 43 Picture of core from MH-2. The core interval shown here does not encompass either of the depths sampled for x-ray diffraction, but it is representative of the general lithology of the sampled intervals.

water system and result in the pH values observed in our groundwater samples. Redox (Eh) values for the groundwater samples ranged from -0.07 to +0.4 volts, which, based on groundwater pH values, suggest the samples are near the siderite-hematite stability fields (Figure 44). Because siderite is a thermodynamically meta-stable mineral compared with hematite, and hematite was not detected in the mineralogical analysis, the high pH values suggest that siderite likely is controlling the pH in the groundwater.

Table 5 Mineralogy of two core samples taken from the screened interval of groundwater monitoring well MH-2.

Sample	Depth (ft)	%Illite-smectite	%Illite	%Kaolinite	%Chlorite	%Quartz
1	158.25	1.5	6.4	3.4	1.2	48.7
2	150.5	4.5	16.1	3.1	2.8	49.3
		%K-feldspar	%Plagioclase feldspar	%Calcite	%Dolomite	%Siderite
1	3.7	7.8	1.3	0.7	20.7	4.5
2	2.9	11.4	0.4	0.6	8.3	0.5

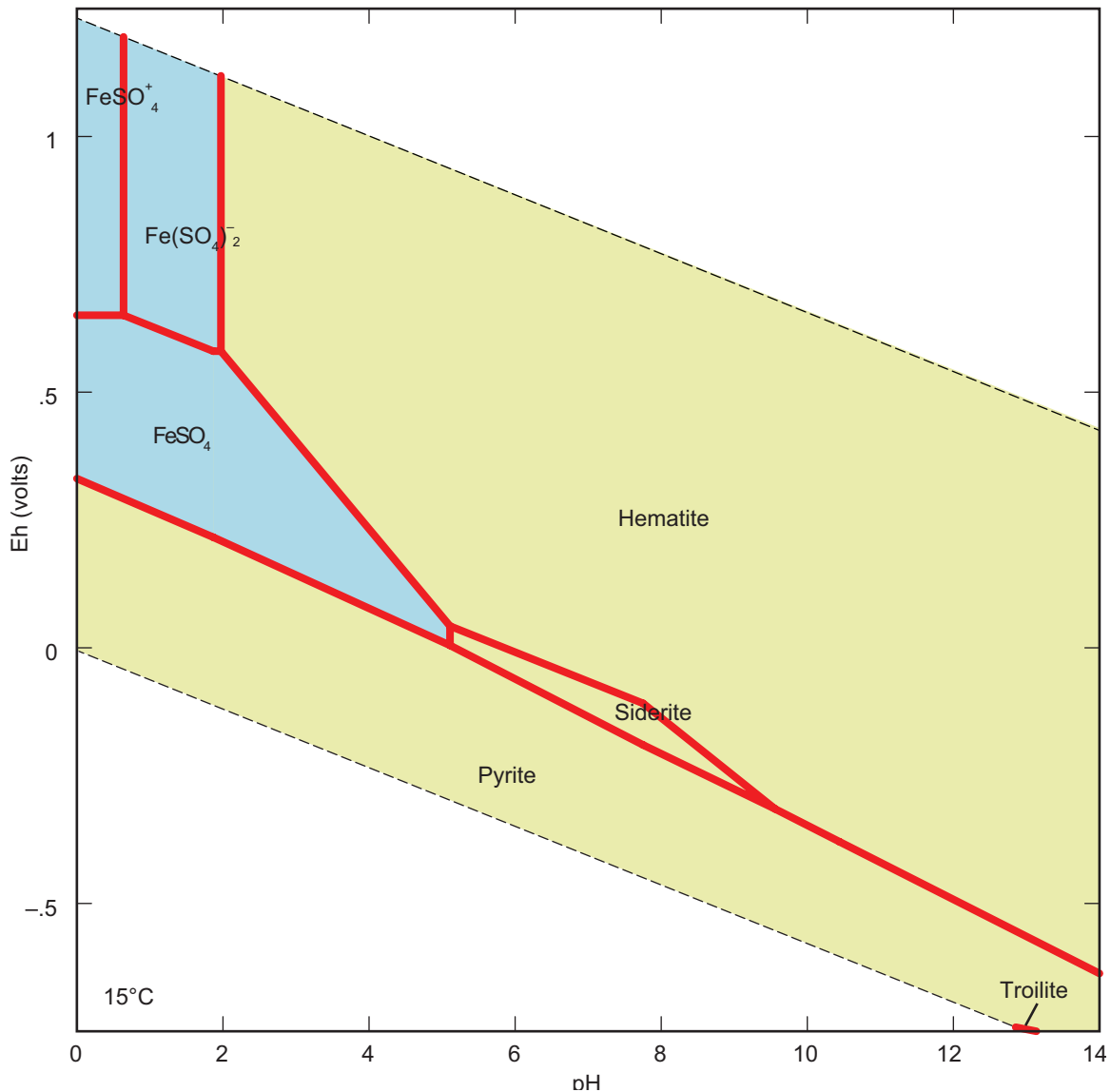


Figure 44 Eh-pH plot showing stability field for iron compounds.

Isotope Chemistry

Selected samples of the groundwater and the reservoir brines were analyzed for isotopic composition. Parameters analyzed in the groundwater and the brines included the $\delta^{13}\text{C}$ of DIC and the δD and $\delta^{18}\text{O}$ of the water molecules. These parameters are useful in identifying whether biological activity is affecting the composition of the water and the CO_2 and whether the near surface groundwater has been affected by leakage of the injected CO_2 .

Geochemical Modeling

Coupling geochemical modeling with the chemical and isotopic data is an essential technique for understanding the chemical fate of injected CO_2 and the potential changes in groundwater composition resulting from CO_2 escaping from the injection formation and migrating into drinking water supplies. In other modeling studies, the United States Geological Survey's geochemical model PHREEQC (Parkhurst and Appelo, 1999) has been used to predict the extent of mineral trapping of CO_2 and potential changes in porosity (Gaus et al., 2008) and the long-term fate of CO_2 in the Alberta Basin (Strazisar et al., 2006). Berger et al. (2009) applied kinetic and equilibrium models to an EOR project led by the MGSC using React 7.0.4 (Bethke and Yeakel, 2007) and PHREEQCi 2.13.2. In this study, the chemical compositions of groundwater samples collected from the MVA monitoring wells were entered in Bethke and Yeakel's geochemical model Geochemist's Workbench. The REACT module of the model was used with mineralogical data from cores collected during well construction to predict and interpret the significance of changes in the concentration of CO_2 in the groundwater.

Cased Hole Logging

Schlumberger Carbon Services provided the RST log runs for monitoring of wellbore integrity and near-wellbore changes to saturation in any zones above the injection zone. To monitor the possible movement of CO_2 into the zones above the injection zone, the RST was used. The RST is a wireline pulsed neutron logging tool; the primary measurements are the macroscopic capture cross section and the neutron porosity of the formation. Appendix 8 relates primarily to the analysis of the RST data collected on the five wells in the pilot. The RST is considered most accurate within a few feet from the wellbore and diminishes in relevance radially from the wellbore.

The cased hole logging program consisted of running two passes of the RST to evaluate the CO_2 containment. The first logging runs (base pass) of the RST were made in late July 2009, prior to CO_2 injection. In early October 2011, after injection of CO_2 and about 10 months of water injection, the post- CO_2 injection run of the RST log was made in each well.

FIELD OPERATIONS DURING CO_2 INJECTION

CO_2 Pumping Equipment

Overview

The pump skid used at the Bald Unit site was designed to inject CO_2 at surface pressures up to 14 MPa (2,000 psig). A rotary vane booster pump was used to reduce or prevent vapor locking in the main triplex plunger pump by increasing the pressure of the feed to the plunger pump to approximately 140 kPa (20 psi) above the inlet pressure from the storage tanks. A triplex plunger pump specifically designed for liquid CO_2 was installed downstream of the booster pump. There was a CO_2 return line to the storage tanks on the discharge lines of both the booster pump and the main triplex pumps. The two CO_2 storage tanks were connected with vapor and liquid pressure equalization lines connecting the two storage tanks.

The pump skid was equipped with a liquid turbine flow meter used to measure the injection flow rate and a transmitter to send a 4–20 mA signal, proportional to the flow rate, to a data recorder. Temperature and pressure gauges were provided for manual recording of the triplex pump suction and discharge temperatures and pressures.

An automated pressure control valve (PCV) on the recycle line of the triplex pump discharge was connected to a pressure transmitter on the outlet of the line heater. If the discharge/injection set pressure was

not exceeded, all of the CO₂ flowed out into the discharge line and to the injection well. If the discharge set pressure was exceeded, a portion of the CO₂ was diverted back to the storage tank through the PCV in order to meet the surface injection pressure set point on the main discharge line. The set point was typically around 4.5 MPa (650 psi), but was periodically adjusted up or down by a few psi in order to inject approximately one truckload of CO₂ per day and in order to keep the storage tanks approximately half full. (Later in the injection period, about 1½ truckloads per day were injected.)

A propane-fired line heater downstream of the liquid turbine flow meter heated the liquid CO₂ prior to delivery to the injection well. Temperature and pressure gauges were installed between the line heater and the wellhead so that the temperature and pressure of the CO₂ injected into the wellhead could be manually recorded.

The surface facilities at the Bald Unit provided for automatic measurement and recording of the following parameters:

- booster pump inlet temperature and pressure;
- booster pump outlet temperature and pressure;
- main pump outlet temperature and pressure;
- CO₂ injection rate;
- line heater outlet temperature; and
- wellhead (surface tubing) temperature and pressure.

Typical operations at the EOR II pilot test site, as indicated by field temperature, pressure, and flow meter readings, were as follows:

CO₂ injection rates ranged from 18 to 32 tonnes/day (20 to 35 U.S. tons/day) (17.4–31.1 m³/day [3.2–5.7 gpm], 111–195 bbl/day).

Typical CO₂ supply conditions to the booster pump inlet were –22 to –18°C (–8 to 0°F) and 1.7 to 2.0 MPa (250 to 290 psig).

- The booster pump raised the pressure by about 170 kPa (25 psig).
- Typical CO₂ discharge conditions from the main (triplex) pump were –21 to –17°C (–6 to 2°F) and 4.3 to 4.6 MPa (630 psig to 670 psig).
- CO₂ leaving the line heater was heated to about 4°C (40°F).

These values are representative of typical operations and are presented here to provide an understanding of the operational requirements of the CO₂ storage, pumping, and heating equipment during CO₂ injection at this site.

Figure 45 shows the piping and instrument diagram for the EOR II test site.

Portable Storage Tanks

At the Bald Unit site, CO₂ was provided to the pump skid from two unrefrigerated, insulated 54-tonne (60-ton) capacity storage tanks leased from Air Liquide. One tank served as the primary feed tank, and the second storage tank held a reserve supply in case of CO₂ delivery problems. Each tank had two 10-cm (4-inch) liquid CO₂ connections and three 5-cm (2-inch) vapor CO₂ connections. The tanks were each approximately 14.9 m (49 ft) long, 2.4 m (8 ft) in diameter, and 4.0 m (13 ft) high and weighed 27,000 kg (60,000 pounds) at 0 kPa (0 psi) (i.e., when empty). Figures 46 and 47 show the portable storage tanks at the Bald Unit site.

Booster Pump

A booster pump was used to improve the reliability of the main triplex plunger pump by increasing the pressure of the feed to the main pump to approximately 138 kPa (20 psi) above the pressure of the liquid CO₂ in the storage tanks. (Because CO₂ vapor is in equilibrium with CO₂ liquid in the storage tank, the



Figure 46 Portable Air Liquide CO₂ storage tanks. Tank capacity is 55 tonnes (60 tons) of CO₂. Photo courtesy of Trimeric Corp.



Figure 47 Connection line between CO₂ storage tank and injection equipment. Photo courtesy of Trimeric Corp.

pressure at the vapor-liquid interface is the vapor pressure of CO₂.) This reduced the possibility of vapor locking the main plunger pumps. The pump, which is shown in Figure 48, was a model CRL1.25 rotary vane pump manufactured by Blackmer. The booster pump was driven by a 0.75-kW (1 hp) motor equipped with a 0.75-kW variable frequency drive (VFD) made by Toshiba. The motor was manually set to maintain an approximately 138 kPa (20 psi) differential between the suction and discharge pressure on the booster pump.

The booster pump was rated for 71 m³/day (13 gpm) at a differential pressure of 138 kPa (20 psi), requiring 1.1 kW (1.5 hp) of power at an impeller speed of 1,150 rpm. The maximum capacity of the booster pump was approximately 82 m³/day (15 gpm) at 34 kPa (5 psi) of differential pressure. Because the motor used on the booster pump was rated for only 0.75 kW (1 hp), the maximum capacity and/or the discharge pressure of the pump was less than the value listed in the specification sheet for the pump.

Main Pump Skid

The main CO₂ pump at the site was a model 3521 triplex plunger pump manufactured and supplied by CAT Pumps® and driven by an 11.2-kW (15-hp) motor equipped with an 11-kW (14.8-hp) VFD made by Toshiba. The VFD speed settings were manually adjusted to achieve the desired CO₂ injection rate. The triplex plunger pump was capable of delivering liquid CO₂ at a rate of 125 m³/day (33,120 gpd) and discharge pressure up to 13.8 MPa (2,000 psi) with a power requirement of 23.6 kW (31.6 hp). Because the motor used on the EOR II pump skid was rated for only 11.2 kW (15 hp), the maximum capacity and/or discharge pressure of the pump was significantly less than the maximum values listed in the specification sheets for the CAT pump. Figures 49 through 51 show pictures of the skid, the CAT pump, and the pump control panel, respectively.

Automated Injection-Pressure Control System

The automatic injection-pressure control system was designed to return a portion of the CO₂ discharged from the main pump back to the storage tanks in order to maintain a constant discharge pressure on the line going to the injection well. A pressure transmitter measured the pressure of the CO₂ on the line going to the injection well and sent a signal to a controller that adjusted the pressure control valve, which regulated the amount of CO₂ returned to the storage tank as needed to maintain the pressure set point in the injection line. At the Bald Unit site, the pressure transmitter was located on the outlet of the line heater. Placing the pressure transmitter near the line heater separated it from the pump skid's vibrations.

The pressure control valve (Figure 52) was a 2.5-cm (1-in) Type 1711 Globe Cast Control Valve manufactured by BadgerMeter, Inc. The valve has an EVA-200 electric actuator, a 4–20 mA input signal, and linear size “G” trim with a flow coefficient of 0.2. In case of a loss of signal, the control valve fails in the open position, which ensured that CO₂ was diverted back to the storage tank if it could not continue to the injection line. For example, if the wellhead inlet valve was closed due to a mistake or failure, then the automated pressure control valve would divert the CO₂ back to the storage tank instead of forcing mechanical pressure relief valves to open. If the site lost power, then the valve remained in its position prior to the loss of electricity. The pressure transmitter connected to the pressure control valve is a Siemens Model Sitrans P 7MF4033-1EA10-1AC1-Z with flush-mounted process connections (Figure 53).

The Model # CNi3253-C24 Omega Controller (Figure 54) compared the actual pressure relayed from the pressure transmitter against the pressure set point and provided an output to the pressure control valve.

Flow Meter

A Cameron NuFlo™ 1.3-cm (0.5-inch) liquid turbine flow meter was installed to measure the CO₂ injection rate (Figure 55). This flow meter can accurately measure flow between 4 to 41 m³/day (0.75 to 7.5 gpm or 25 to 250 bbl/day) of liquid CO₂. This particular type of flow meter is a volumetric measuring turbine type; the flowing CO₂ fluid engages the vaned rotor, causing it to rotate at an angular velocity that is proportional to the fluid flow rate. The angular velocity of the rotor results in the generation of an electrical signal (AC sine wave type) in the pickup. The summation of the pulsing electrical signal is directly related to the total flow. The frequency of the signal relates directly to the flow rate.



Figure 48 Booster pump (frosted over) and motor. The circular dial at the upper center of the photo (labeled Tel-Tru) is a manual temperature gauge. A Siemens pressure gauge (green-blue back, partially out of frame at upper right of photo) is located to the right of the manual gauge. Lines are covered with neoprene pipe insulation. The storage tanks are to the right; the main pump is to the left. Photo courtesy of Trimeric Corp.



Figure 49 Injection pump skid at the Bald Unit tank battery. Frosted-over booster pump and motor seen in Figure 48 are visible at center. CO₂ tank supports are visible in background. Photo courtesy of Trimeric Corp.

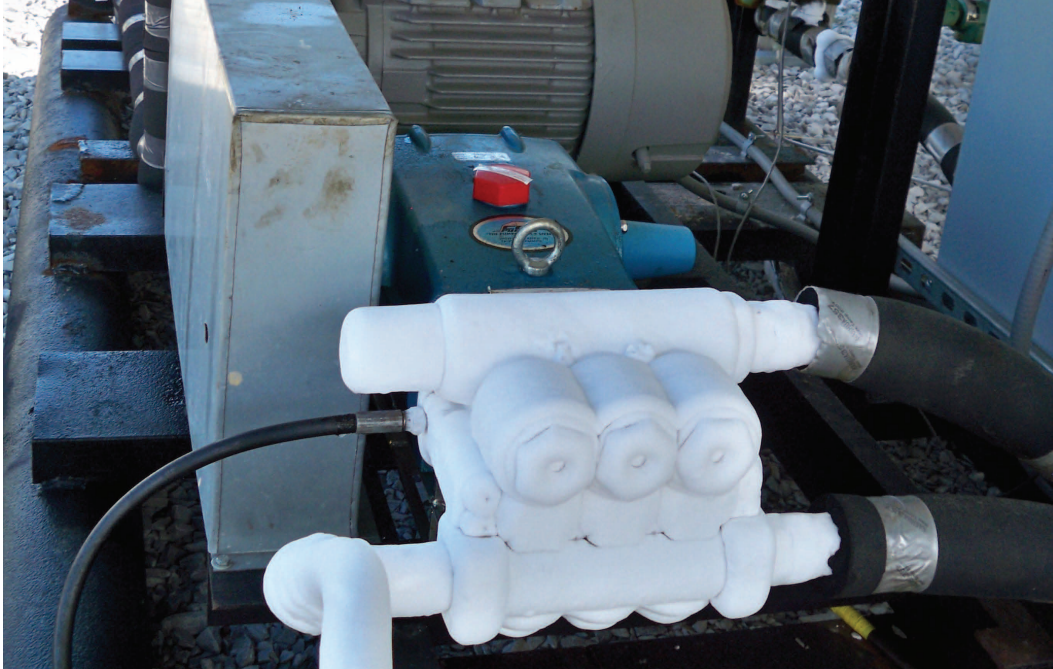


Figure 50 CAT triplex pump in operation at Bald Unit tank battery. Input and output lines and valves (frosted over) are in foreground. The gray motor (center) is behind the pump's crankcase (blue). The storage tank is out of the picture to the right. Rectangular aluminum housing covers the belt and pulleys between the motor and pump crankcase. Photo courtesy of Trimeric Corp.

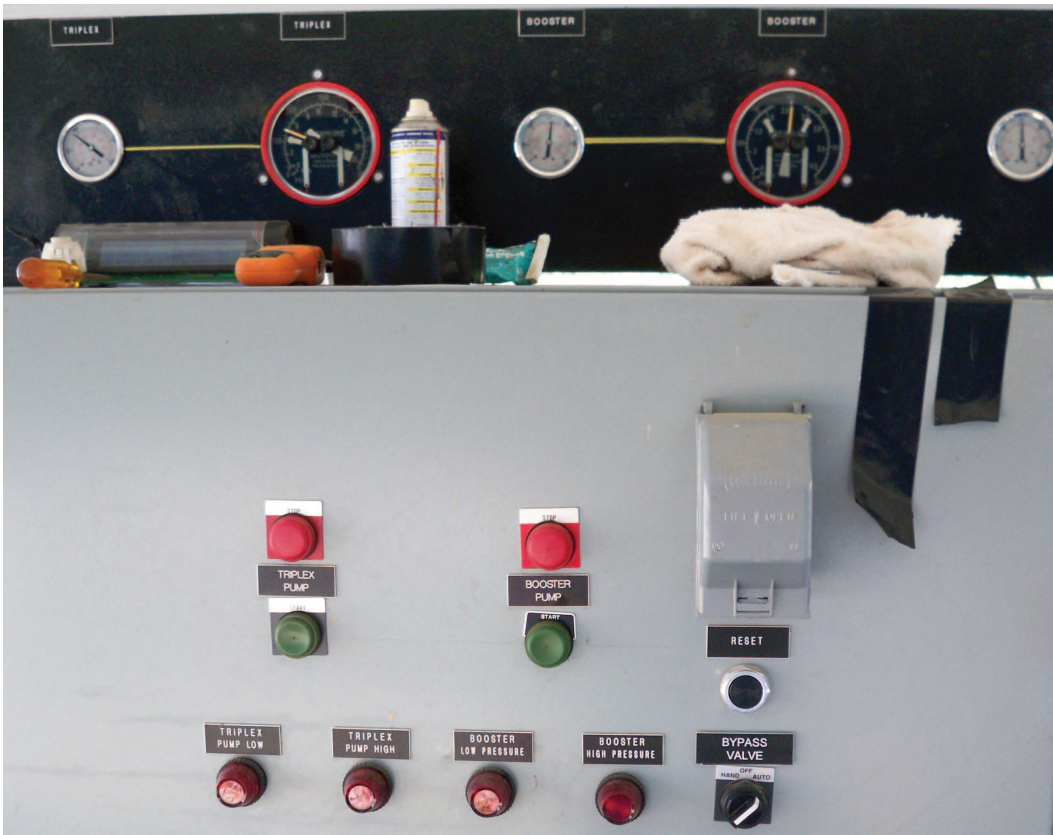


Figure 51 Injection system control panel. Photo courtesy of Trimeric Corp.



Figure 52 Globe Cast (BadgerMeter, Inc.) pressure control valve (red object at upper center) on return line between discharge of main pump and storage tank. The red casing conceals an electric actuator. The valve is below the actuator and is covered with black neoprene and gray duct tape. Photo courtesy of Trimeric Corp.

In-line Heater

The liquid CO₂ discharged from the flow meter passed through a reconditioned 263,800 kJ/hr (250,000 Btu/hr) line heater (Figure 53) supplied by Natco. The line heater was 0.6 m (24 in) in diameter and 2.4 m (8 ft) long and was equipped with a heat exchanger coil made from 5-cm (2-in) diameter schedule 80 tubing configured for eight horizontal tube passes, each 2.1 m (7 ft) long, with 180-degree elbows connecting each pass. The heater was equipped with a standard fuel gas manifold with a thermostat, thermometer, regulators, and a fuel gas drip scrubber. A skid and lifting lugs were added to the heater for increased portability.

The shell side of the line heater was partially filled with a 50/50 (by volume) mixture of propylene glycol and water. Propane fuel gas was burned in a burner that discharged hot flue gas into a horizontal U-shaped fire tube immersed in the lower portion of the solution. Heat released by the burning fuel gas was transmitted through the fire tube wall to the solution of propylene glycol and water. The desired propylene glycol/water bath temperature was maintained within upper and lower dead band limits by turning on and off the fuel gas flow to the burner based on thermostatic control of the solution temperature. The CO₂ on its way to the injection well passed through the flow coil of the heater immersed in the upper portion of the solution. Heat was transmitted from the propylene glycol and water solution through the tube wall to the CO₂ inside the flow coil.



Figure 53 Natco 263,800 kJ/hr (250,000 Btu/hr) line heater. In-line heater's CO₂ inlet (right) frosted over; top of this line has Siemens pressure gauge/transmitter (small box with blue circle on casing) that is connected to the Globe Cast pressure control valve. In-line heater discharges to the injection line (blue line to right). Photo courtesy of Trimeric Corp.



Figure 54 Omega pressure controller panel cover and housing at Sugar Creek site with pressure reading shown. Photo courtesy of Trimeric Corp.



Figure 55 Cameron NuFlo liquid turbine meter (center, immediately behind "meter valve" sign) and Siemens pressure gauge (with blue cover, immediately behind NuFlo meter) in series on frosted line. In-line heater in upper left background. Tel-Tru mechanical temperature gauge at right is connected to pump discharge line. Photo courtesy of Trimeric Corp.

Data Acquisition Equipment

Pressure and Temperature Sensors

Surface and downhole pressures at the five-spot wells in the test site were measured using Geokon 4500-series vibrating wire pressure transducers. Based on the manufacturer's specifications, the resolution and accuracy of the pressure transducers was at least 0.025% full scale (F.S.), and the accuracy was $\pm 0.1\%$ F.S. with a maximum drift of 0.05% F.S. per year. Each of the pressure transducers also contained a thermistor with a temperature range of -20 to 80°C (-4 to 176°F) and thermal zero shift of $<0.05\%$ F.S./ $^{\circ}\text{C}$. Calibrated pressure ranges can be seen in Appendix 9.

Additionally, atmospheric pressure was measured at the IB-2 wellhead using a Geokon 4580-1 (barometer) vibrating wire pressure transducer, which was programmed for a range of 0 to 17 kPa (0 to 2.5 psi). Based on the manufacturer's specifications, the resolution of the barometer was at least 0.025% F.S., and the accuracy was $\pm 0.1\%$ F.S. with a maximum drift of 0.05% F.S. per year.

Data Acquisition System

All of the five-spot wells in the test site were outfitted with both a surface and a downhole pressure-temperature sensor. Each sensor was connected to a vibrating wire spectrum analyzer, housed within the data acquisition enclosure at the wellhead. The analyzer measured the wire's resonant frequency and resistivity, which were then transmitted to a datalogger and converted to digital pounds per square inch (psi) and degrees Fahrenheit. Figure 56 shows a typical data acquisition enclosure. Additionally, surface pressures of the two monitoring wells north of the five-spot pattern were measured using Siemens Sitrans P Pressure Transmitters. Schematics of the data acquisition equipment can be seen in Appendix 10.

Pressure and temperature of the CO_2 were measured upstream and downstream of the main CO_2 injection pumps using Siemens Sitrans P Pressure Transmitters and Siemens Sitrans TK-H Temperature Transmitters. Discharge temperature of the CO_2 leaving the line heater also was measured using a Siemens Sitrans TK-H Temperature Transmitter. The CO_2 injection flow rate was measured using a Cameron NuFlo Liquid Turbine Flowmeter installed downstream from the pumps. All pressure, temperature, and flow rate measurements at the pump skid and line heater were sent by 4–20 mA signal to the pump skid datalogger.

Radio transmitters connected to each datalogger sent pressure and temperature data to a common receiver, housed within the IB-3 enclosure. The data were then sent by cellular transmission every 5 minutes to the Illinois State Geological Survey. Removable flash cards within each datalogger served as a backup in case of interrupted transmission. Data were also transmitted by cable to a desktop computer located in the on-site office trailer. Each datalogger had an independent power supply (battery) that was continually recharged by a solar panel.

Wellhead Design

Very little was done at each individual wellhead. The tubing-casing annulus was isolated from the reservoir. All fluids produced through the tubing into the flowline. The only adaptations were for the cable passing through the cross and cable gland that suspend the downhole pressure and temperature gauges. Because only surface gauges were used at the monitoring wells, neither of these wells had special adaptations except an additional fitting for the pressure gauges. The surface wellhead at IB-2 is shown in Figure 57.

General Operations

Liquid CO_2 was delivered in road transport tanks that had capacities of about 18 tonnes (20 tons). On site, the CO_2 was transferred to the storage tanks and pumped through an inline heater to ensure that the liquid CO_2 temperature was at least 4°C (40°F) but stayed in the liquid phase from the pump storage tank to the bottom of the injection well, BU-1. There were concerns about contraction of flow line connections if CO_2 started through the flow line at -21 to -17°C (-6 to 2°F).

The CO_2 injection system was designed to minimize the need for a regular on-site operator of the equipment. The system was designed to shut down safely when operator-specified pressures and temperature thresholds were exceeded under various conditions. Gallagher Drilling, Inc., and Illinois State Geological

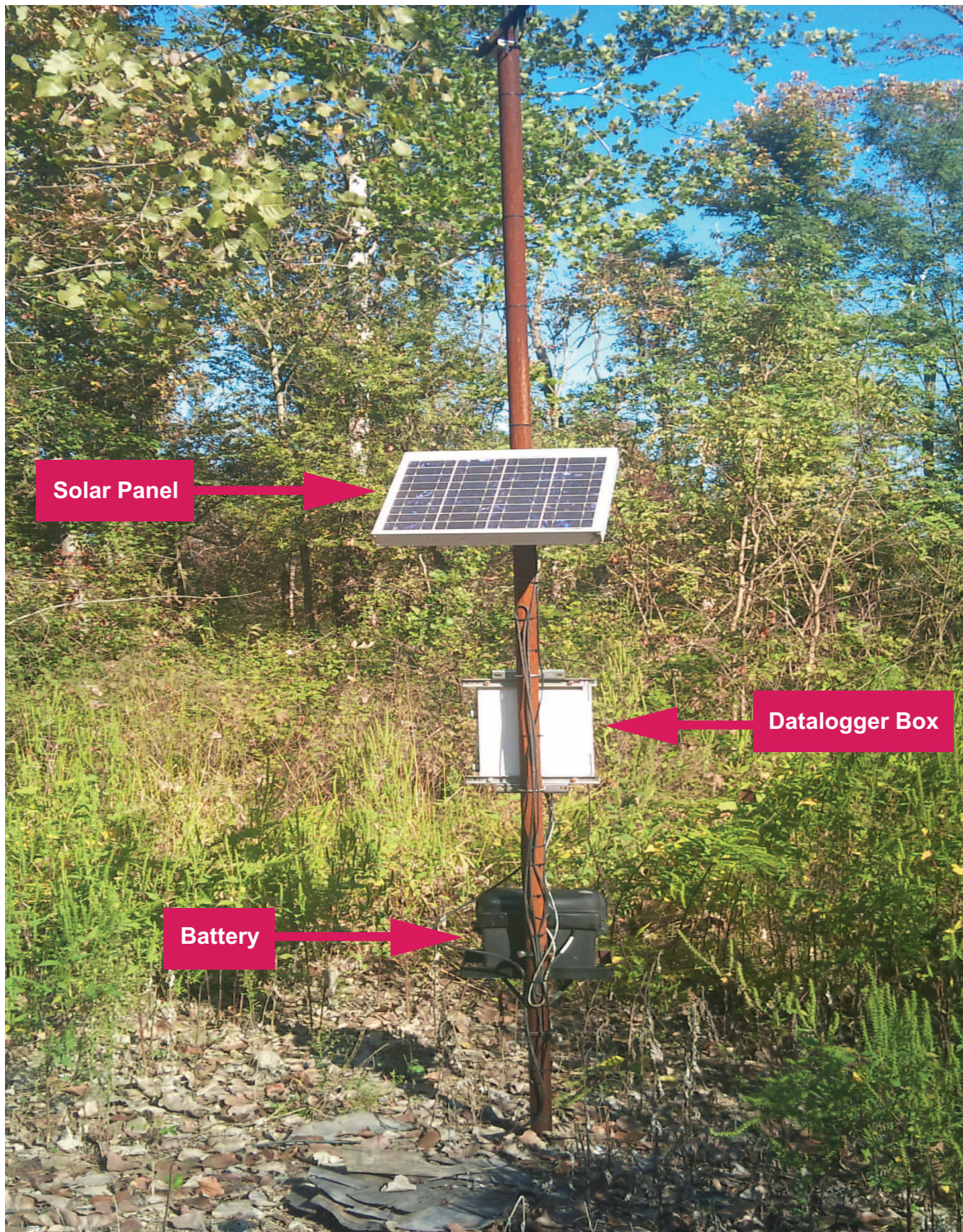


Figure 56 Data acquisition and transmission enclosure at a production well, showing the solar panel, datalogger box, and battery. The enclosure in this image was at Sugar Creek Field (where another MGSC EOR project took place), but the enclosures at the Bald Unit followed the same design.



Figure 57 A typical production wellhead (right), IB-2 (B2), at the Bald Unit. The Bald Unit tank battery and CO₂ storage tanks are visible in the background. The cables emerging from glands on the wellhead are for pressure (black cable) and temperature (blue cable) gauges. Production flow line is to the left.

Survey staff monitored the data remotely several times a day. The data acquisition system allowed an instantaneous download of data or monitoring of updated data every hour. A pumper made visual inspection of all pumping equipment, the tank battery, and the production and injection wellhead areas once per day. Monitoring the CO₂ tank levels was the most critical task, because continuous injection was only possible if adequate CO₂ volume was maintained in the tanks. If the tank levels were too low, operators communicated directly with the CO₂ supply company, Air Liquide, to obtain additional supply or make plans for a temporary, controlled shut down.

Operational Challenges

Scheduling CO₂ Delivery

In general, CO₂ was delivered when required. However, there was a period of about one month (August 11 to September 3, 2010) when delivery was less than requested and injection was at a lower rate or periodically shut-in. This period of fewer deliveries was attributed to lack of availability of CO₂ from the supplier.

Winter Road Restrictions

From January 15 through April 15, some township roads have load limit restrictions referred to as winter road restrictions. These are invoked to prevent destruction of roads during periods of thawing and freezing by heavy loads on semi-truck trailers. The township road commissioner can grant access to specific locations on a case-by-case basis. In the site screening process, sites with year-round access of semi-truck trailers were of most interest. Because oil was sold year-round at the Bald Unit, it was thought that there was at least one road to the Bald Unit without winter road restrictions. After the site was chosen and pre-injection site and well work had begun, it was learned that, although oil was sold year-round, during winter months it was through prior approval of the township road commissioner. Oil sales were one semi-truckload every one to two months. Unfortunately, delivery of one to two truckloads of CO₂ per day during the period of winter road restrictions was not allowed. Consequently, only water injection occurred during this period.

Scale Accumulation

Scale accumulated near the wellhead of the producing wells downstream of the surface pressure gauge. Scale was analyzed by a Baker-Hughes lab and determined to be 85% CaCO₃ and 15% FeS. Tubing pressure buildup at individual wells was indicative of the scale buildup, and periodically (approximately every two months) field staff would shut-in the well and remove the blockage.

Significant scale buildup was found in three wells (BA-2, IB-2, and IB-3) after the water injection period separating the two CO₂ injection periods. Most or all of this accumulation likely was present prior to the CO₂ injection. The scale developed again in these wells when they were prepared for the post-CO₂ cased hole logging survey. This type of scale precipitation was an operational problem at the Bald Unit prior to CO₂ injection, but may not have been as significant.

In general, scale buildup is a common problem in almost all waterfloods in many oil-producing basins around the world. A proactive treatment was recommended that required injection of acids and solvents (Appendix 11), but the treatment was considered relatively expensive and was not attempted. Once buildup occurs in the bottom of a wellbore, removal with a workover rig is the only reactive remedy.

Booster Pump Failure

Injection operations stopped for about eight days due to the failure of the booster pump. A metal burr was found on the side plate, and the pump would not turn. The burr was removed, and the pump was returned to service. The failure of the pump immediately followed a short period when the pump was suspected of operating while there was low CO₂ volume and it pumped dry.

Corrosion and Well Work

Placing tubing on packers in the producing wells prevented application of a chemical corrosion treatment of the tubing. As such there was no corrosion protection on the tubing. (Used tubing was tested and inspected prior to installation in the wells in the pilot; the tubing in the wells prior to the CO₂ project was reported “full of scale.”) After the first four months of CO₂ injection and the four months of water injection, the tubing was pulled in preparation for fracture stimulation of BA-2, IB-2, and IB-3. Visually, the tubing showed no indications of corrosion related to CO₂, but scale buildup was present. When the tubing and packers were pulled from the wellbores to prepare for the cased hole logging surveys in fall 2011 (after 10 months of post-CO₂ water injection), the packers and elastomers of all wells had no corrosion. The tubing of all wells except BA-1 had no indication of corrosion. BA-1 had noticeable holes in the tubing attributable to CO₂ corrosion. The operator described the corroded tubing as “small and randomly distributed” through the tubing string.

Because the wells were not pumped but flowed reservoir fluids to surface, there was no possibility for the rod or pump failures common to almost all oil field operations. There were no tubing or packer failures in the producers or injectors during the pilot period.

The only well treated prior to CO₂ injection was BA-1, which received treatment as part of the process of re-entering this well and returning it to production. The remaining producing wells in the pilot were not treated.

These wells had very low liquid production compared with BA-1. Pressure buildup tests were conducted on these wells to check for skin damage when BU-1 was returned to water production during a temporary suspension of CO₂ injection due to winter road restrictions. The results of the test were a modest positive skin, but the value of skin was not adequate to reduce the rate to the magnitude observed. The permeability from the buildup tests was very low compared with core data for the wells. Only a very low estimate of net thickness could reconcile the difference between the core and buildup test permeability estimates.

In May 2010, the tubing and packer of BA-2, IB-2, and IB-3 were pulled, and a workover rig was set up to find that nearly all of the perforations were covered with scale, which drilled out with a workover rig. Following this discovery, a relatively small fracture stimulation treatment was administered. The production of these wells increased about 200%. The increase in oil production due to the stimulation was estimated and excluded from that attributable to CO₂ EOR. The fracture stimulation treatment is described in Appendix 12.

FIELD OBSERVATIONS DURING ACTIVE CO₂ INJECTION

Overview

Appendix 13 contains a timeline of events at the injection and monitoring wells.

On September 3, 2009, CO₂ injection started at well BU-1. Injection rates were constrained by CO₂ availability rather than regulated pressure. CO₂ injection was temporarily suspended from January 23 to May 3, 2010, due to winter road restrictions; water was injected during this time. After this brief water injection period, CO₂ injection resumed and continued until December 14, 2010, when water injection was started again. Monitoring of all wells continued until September 2011, when the data acquisition equipment was removed in preparation for the post-CO₂ cased-hole logging runs.

The oil response from CO₂ occurred about three months after CO₂ injection started. The increased oil production was sustained until late January, about two weeks after CO₂ injection stopped due to winter road restrictions.

By mid-January 2010, when injection ceased, 2,600 tonnes (2,860 tons) of CO₂ had been injected. After a pressure falloff test of well BU-1, water injection was started near the end of January and continued through May 2010 when CO₂ injection started again. During this time, 2,080 m³ (13,100 bbl) of water were injected at BU-1 at about 25 m³/day (150 bwpd). After the second and final CO₂ injection period, an additional 3,700 tonnes (4,080 tons) of CO₂ was injected. Water injection resumed and continued through the end of the post-CO₂ monitoring period. Contrary to most observations of post-CO₂ water injection in West Texas fields (e.g., Henry and Metcalf, 1983; Chopra et al., 1990), water injection rates in well BU-1 were not adversely affected, and pre-CO₂ water injection rates were achieved immediately.

Through September 30, 2011¹, increased oil production due to pre-CO₂ injection wellwork was estimated as 87 m³ (545 bbl) and increased oil production due to CO₂ as 325 m³ (2,045 bbl). Project improved oil recovery (IOR) was estimated at 412 m³ (2,590 bbl). This includes variations in oil production due to cessation of CO₂ injection and booster pump failure and other operational problems and does not necessarily reflect the CO₂ enhanced oil recovery (EOR) completely. The pilot project data were used to calibrate a numerical model which was used to improve the CO₂ EOR estimate. Modeling is able to investigate scenarios with longer periods of uninterrupted CO₂ injection and multiple CO₂ injectors in the field.

The CO₂ produced and metered at the gas-liquid separator was about 27 tonnes (30 tons) or 0.5% of the injected CO₂. During the monitoring period, 99.5% of the injected CO₂ was estimated to have remained in the Clore sandstone.

¹Oil rates through January 31, 2011, are corrected for sales volumes. At the time of this report only the daily pumper measured rates via gauged oil tank levels were available from February 1 through September 31, 2011. Additionally, no individual well-allocated oil and water rates were available for this period.

BU-1 Injection Schedule

CO₂ Injection

Because of permit restrictions, pumping operations were constrained by the maximum bottomhole pressure of 10.3 MPag (1,500 psig). The downhole pressure gauge was placed at 583.7 m (1,915 ft) measured depth (MD) from 1.2 m (4 ft) above ground level (GL). This depth was the center of the BU-1 perforations, which was used as the datum for all datum-corrected pressures.

Injection of CO₂ began on September 3, 2009, and continued through December 14, 2010, with a single major and significant interruption of about three months when CO₂ injection stopped due to winter road restrictions such that CO₂ could not be delivered. During the first 1.5 months of CO₂ injection, the CO₂ injection rate was relatively constant at 18 to 23 tonnes/day (20 to 25 tons/day). There were four 1- to 2-day shut-in periods and one 8-day shut-in due to a failure in the booster pump. Following the longer shut-in period, the CO₂ delivery schedule was increased, and injection rates were increased to 27 to 32 tonnes/day (30 to 35 tons/day) for the month of November. In general, the rates during the second half of the first CO₂ injection period were highly variable (Figure 58). From September 3, 2009, to January 22, 2010, active injection occurred for 117 days out of the 142 days of operations at the test site, or 82.6% on-time injection. The average injection rate during active injection was 22.1 tonnes/day (24.4 tons/day).

During this time, bottomhole injection pressure (datum corrected) was relatively constant from 8.41 to 8.89 MPag (1,220 to 1,290 psig) during active injection and bottomhole shut-in pressure fell to 8.07 MPag (1,170 psig) during the period when the vane pump failed (Figure 59). Injection was not constrained by regulated pressure (10.3 MPag; 1,500 psig) or equipment ability, but by CO₂ delivery (initially limited to no more than one truckload per day) and the operator's need to gain familiarity with the pumping equipment and general operations. Because of the variability in rate, no general trend of injection pressure with time could be inferred.

After the three-month water injection period, the second CO₂ period started May 3, 2010, and continued through December 14, 2010. The CO₂ injection rate was relatively constant at 18 to 25 tonnes/day (20 to 28 tons/day). During this period, active injection occurred for 182 days out of the 226 days of operations at the test site, or 80.5% on-time injection. The average injection rate during active injection was 20.3 tonnes/day (22.4 tons/day).

At the beginning of this period following water injection, bottomhole CO₂ injection pressure (datum corrected) reached a maximum of 9.79 MPag (1,420 psig) during active injection and decreased and stabilized to about 9.0 MPag (1,300 psig) in three weeks (Figure 60). For the remainder of the CO₂ injection period, bottomhole injection pressure was between 8.6 to 9.0 MPag (1,250 to 1,300 psig). During the brief but numerous shut-in periods, bottomhole pressure decreased to no more than 8.34 MPag (1,210 psig).

The total mass and volume of CO₂ injected was 6,300 tonnes (6,950 tons) and 3.37 million scm (119 million scf), respectively.

Water Injection

BU-1 was an oil-producing well prior to being selected as the CO₂ injection well. At the request of the operator, during water injection the permitted bottomhole pressure was higher than that during CO₂ injection: 14.8 MPag (2,150 psig). Water was injected for 93 days between January 27 and April 29, 2010, when CO₂ injection was interrupted by road restrictions. Active water injection was 85 days or 91.4% of the entire period. The average water injection rate during active injection was 24.5 m³/day (154 bwpd) (Figure 61), and the total volume injected was 2,080 m³ (13,100 bbl). Bottomhole injection pressure started at about 8.62 MPag (1,250 psig) and increased to about 10.7 MPag (1,550 psig) after about two months of continuous injection (Figure 61). For the remainder of the period, injection pressures varied between 10.0 and 10.7 MPag (1,450 and 1,550 psig). At the end of this water injection period, a short falloff test was conducted and bottomhole shut-in pressure decreased to 8.69 MPag (1,260 psig).

During the water injection monitoring period following the final CO₂ injection period, 5,280 m³ (33,200 bbl) of water was injected. During this 267-day period, water was actively injected 250 days or 93% of the period. Average water injection rate during active injection was 21 m³/day (130 bwpd) with rates that ranged

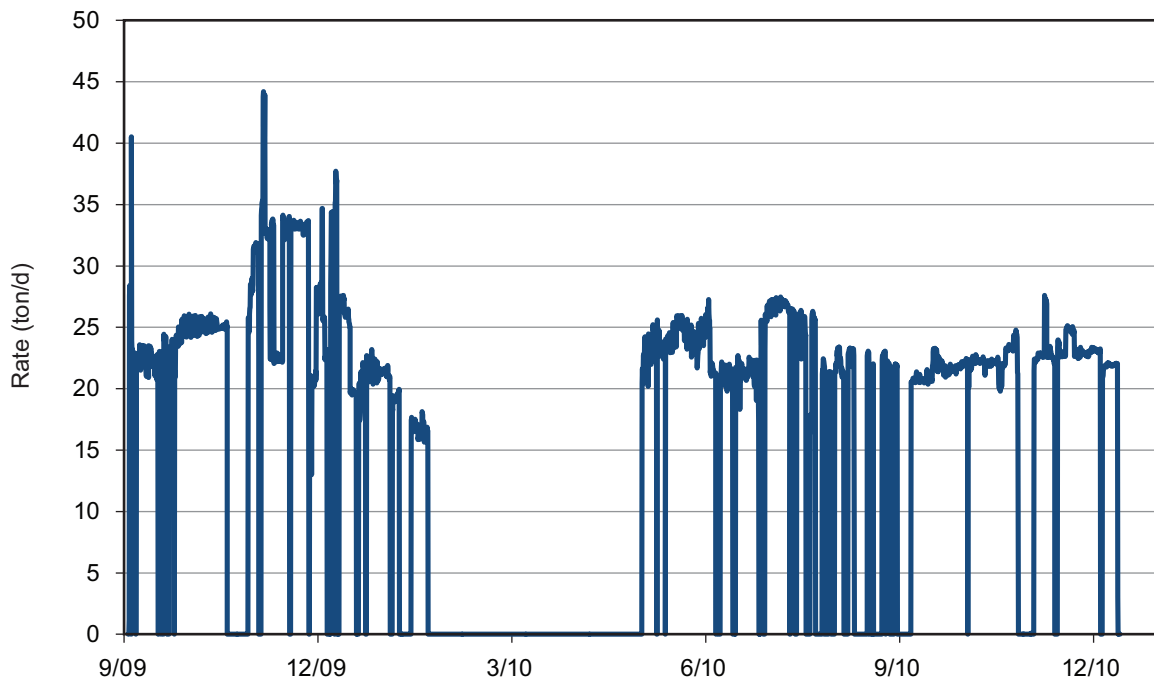


Figure 58 BU-1 daily CO₂ injection rates from September 3, 2009 to December 14, 2010.

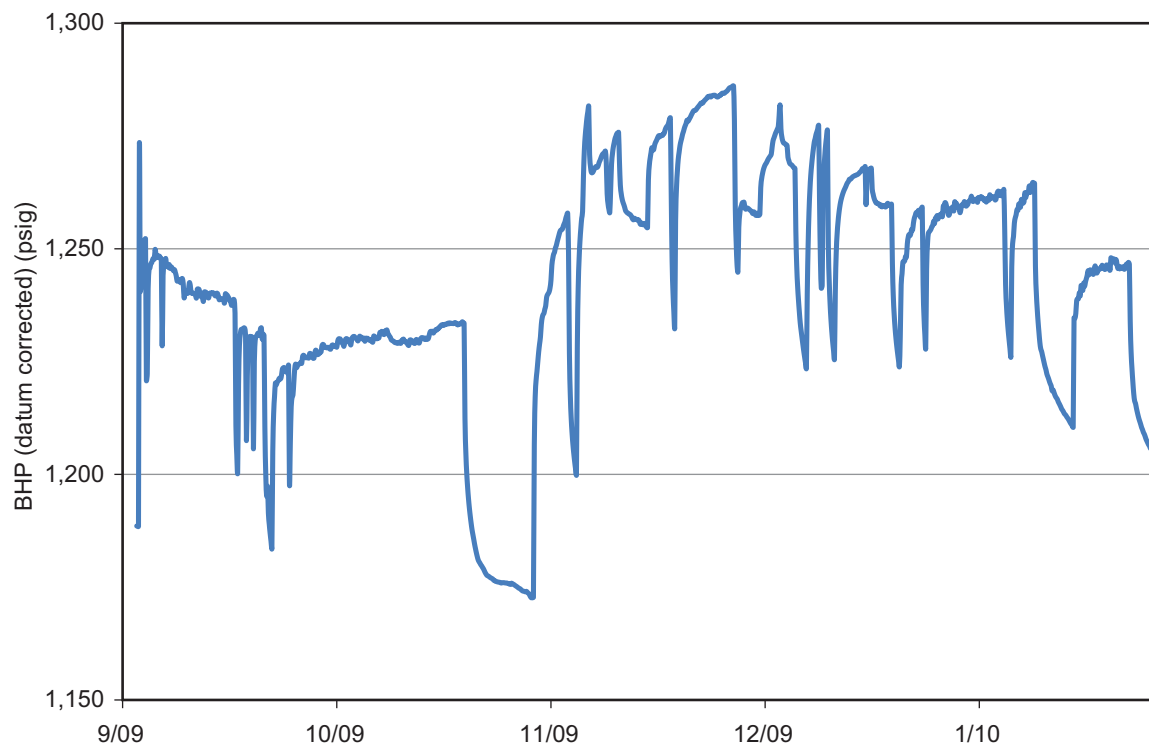


Figure 59 BU-1 bottomhole injection pressure (datum-corrected) during first CO₂ injection, September 3, 2009 to January 22, 2010.

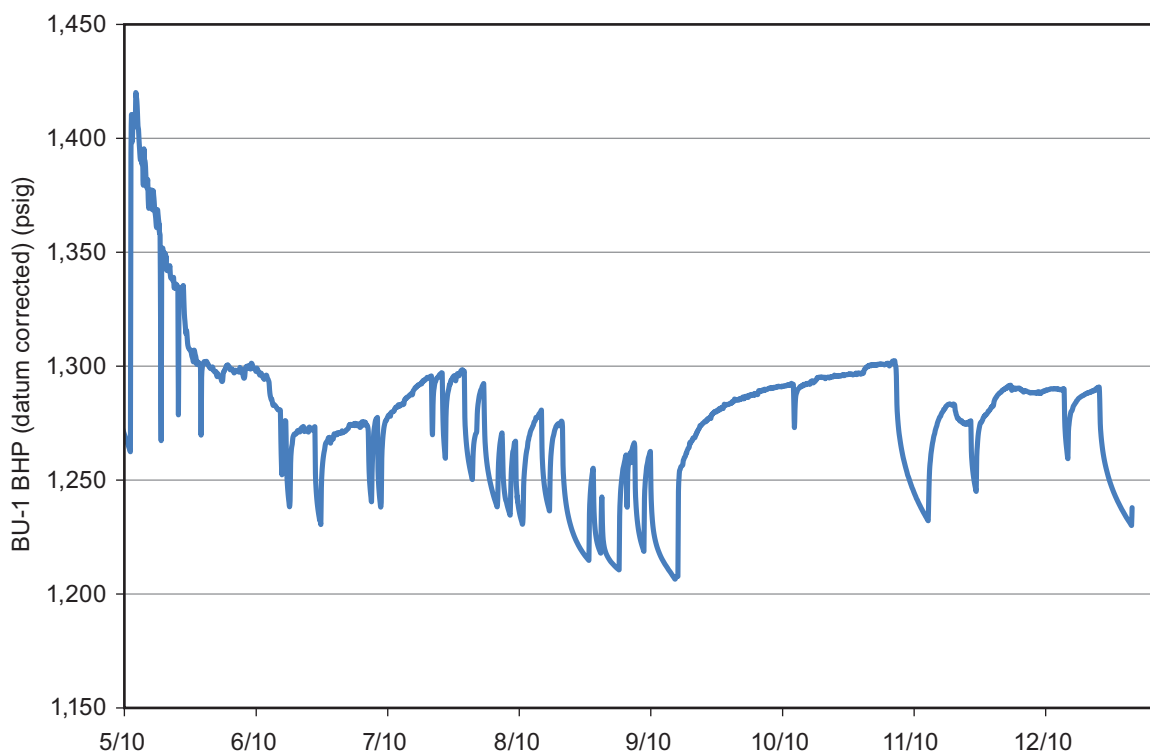


Figure 60 BU-1 bottomhole injection pressure (datum-corrected) period during second CO₂ injection, May 3, 2010 to December 14, 2010.

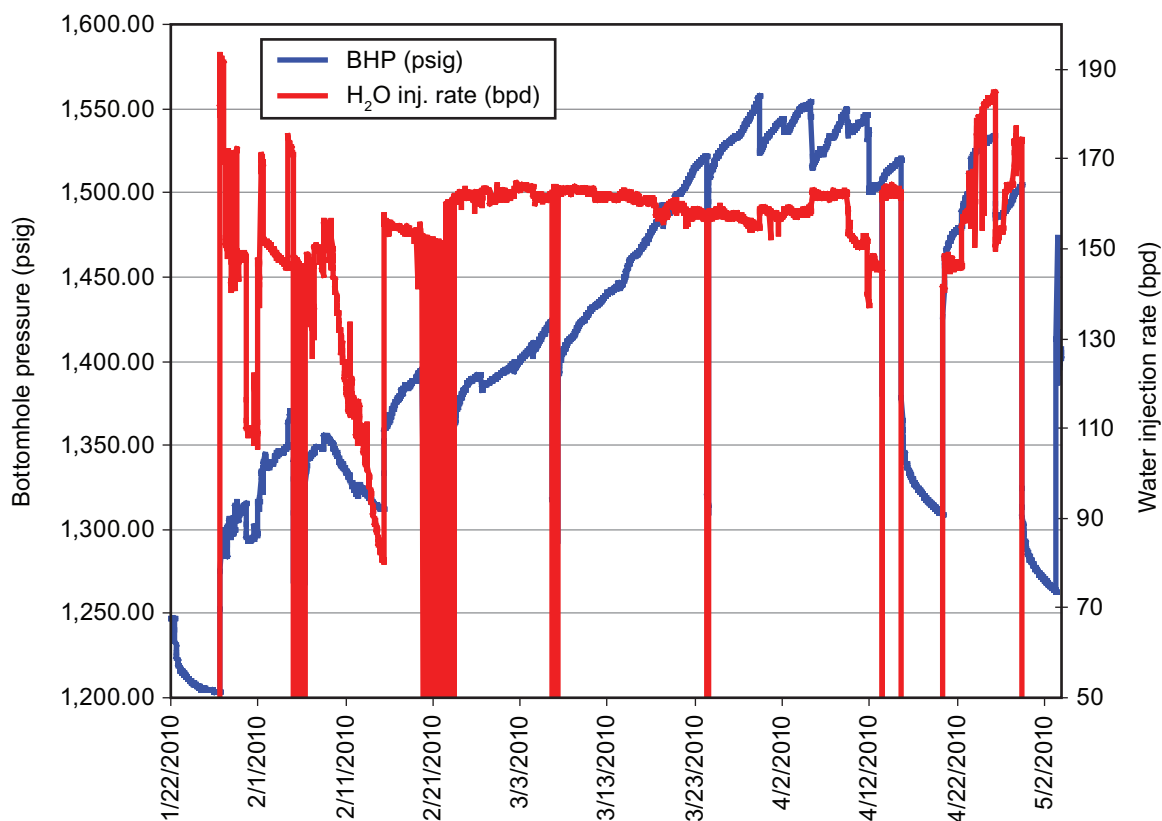


Figure 61 BU-1 bottomhole injection pressure (psig) and daily water injection rate (bwpd) between the two CO₂ injection periods, January 27, 2010 to April 29, 2010.

between 16 and 28 m³/day (100 and 175 bwpd) (Figure 62). Bottomhole injection pressure started at 9.31 MPag (1,350 psig) and reached 10.9 MPag (1,580 psig) after about three months of relatively continuous injection. Following this maximum bottomhole injection pressure, injection pressure was relatively stable between 10.0 and 10.7 MPag (1,450 and 1,550 psig), similar to the previous injection period (Figure 61).

Because the bottomhole injection pressure was not constant immediately after water injection startup, increasing 1.4 MPag (200 psig) over the first three months of injection, it is not readily apparent whether water injection decreased from the water rate of the previous water injection period. Lower rates during the latter part of the period were for operational reasons and not reservoir restrictions.

Pilot Area's Oil, Gas, and Water Production and Pressure Response

Fluid production from the four wells of the pilot was isolated from the remainder of the Bald Unit's production; direct oil, brine, and gas rates could be metered using an allocation methodology.

During periods of production, there was no discernible pressure response in the producing wells that could be attributed to the injection at BU-1. However, during planned shut-in periods of designed pressure transient tests, it was obvious that all wells were in communication. The shut-in monitoring well, BU-2, measured pressure that was attributable to injection changes at BU-1, demonstrating direct communication with at least one well location to the north. Moreover, when IB-4 was shut-in, the pressure recorded at BU-1 was directly affected. Consequently, through inference of direct pressure measurement, it was determined that all wells were in communication with the injector BU-1.

There was no significant breakthrough or production of CO₂ from any wells within the pilot area or the other producing well in the Bald Unit (IB-4).

Oil Production

A clear and definitive oil response from CO₂ started on December 14, 2009, about three months after CO₂ was injected (Figure 63). The increased oil production of 2.4 to 2.9 m³/day (15 to 18 bopd) was sustained until January 22, 2010, at which time oil rate linearly decreased to 0.95 to 1.3 m³/day (6 to 8 bopd) on

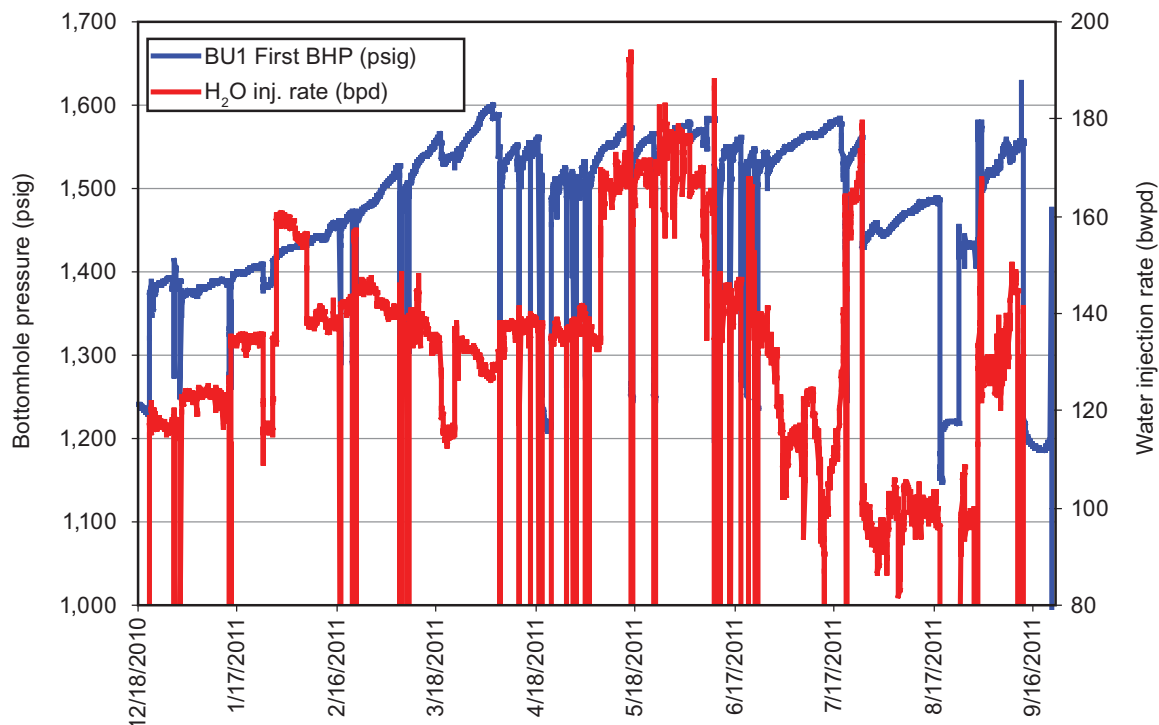


Figure 62 BU-1 bottomhole injection pressure (psig) and daily water injection rate (bwpd) following second (and final) CO₂ injection period, December 20, 2010 through September 11, 2011.

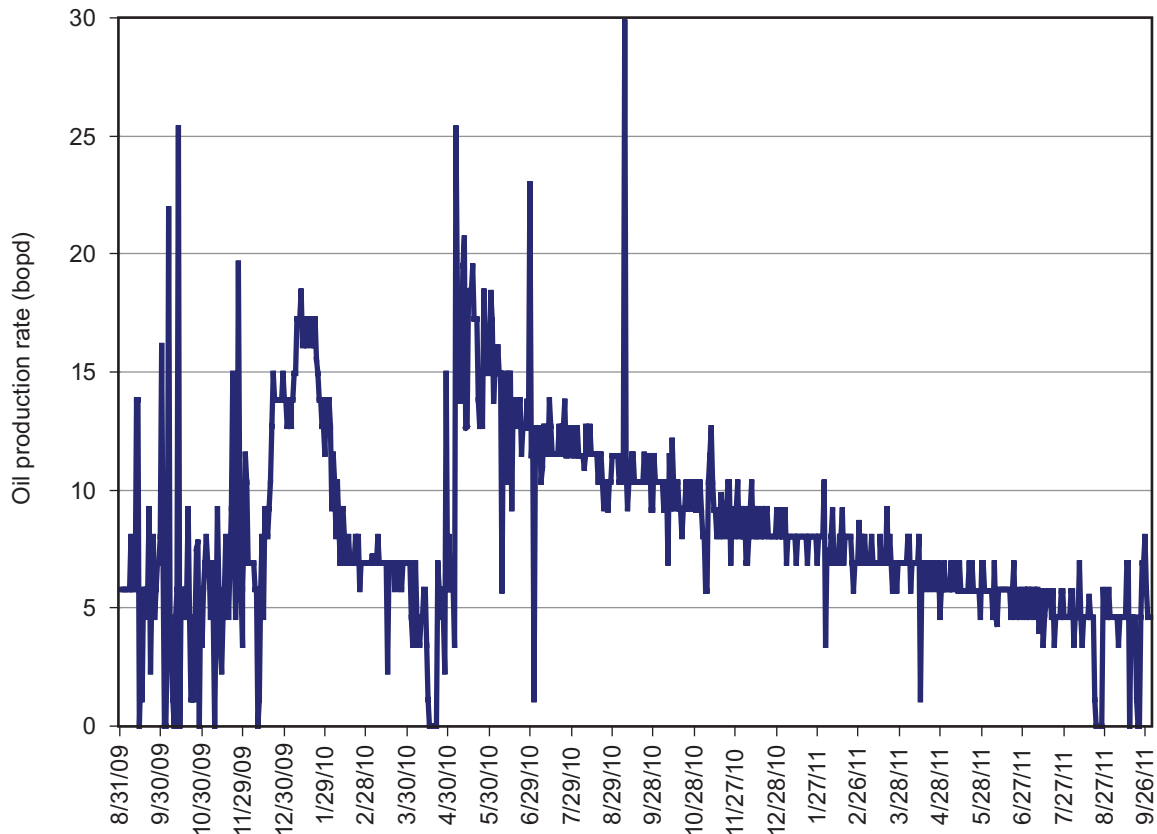


Figure 63 Five-spot daily oil rate (bopd) vs. time over entire monitoring period.

February 6, 2010. Except for shut-in periods for testing and well work, this oil rate continued until May 6, 2010. The beginning of the decline in oil production coincided with the temporary cessation of CO₂ injection during the winter months. The increase in oil production was primarily from BA-1 and IB-2.

Prior to CO₂ injection, BA-1 had nearly six times as much liquid production as the other wells combined, and near-wellbore impairment (positive skin) was suspected in the other wells. In April and May 2010, all the wells in the pilot were shut-in for individual pressure transient tests in order to estimate the skin, permeability, and average pressure. The results of the tests on the BA-2, IB-2, and IB-3 showed that there was modest skin, but the permeability calculated from the pressure transient tests was significantly less than that from core. Only the assumption of very low thickness of 0.30 to 1.2 m (1 to 4 ft) gave reasonable results; consequently, it was suspected that the bottoms of individual wells were filled with scale that was obstructing the perforations.

These wells were entered and fill was found to cover a large part of the perforated interval. The wellbores were cleaned up and a small fracture stimulation was made. When the BU-1 returned to CO₂ injection and all four wells returned to production on May 4, 2010, the initial daily oil rate was in excess of 4.0 m³/day (25 bopd), which was primarily from BA-2 (Figure 63). This was a substantial and instantaneous increase over the oil rate during the previous water injection period; the incremental oil production was attributable to the fracture stimulation on three of the four producing wells. Through decline curve analyses, the increase and subsequent decrease in oil production through mid-June was used to attribute 86.6 m³ (545 bbl) of oil production to the fracture stimulation.

In June 2010, a month after CO₂ injection re-started at BU-1, the oil rate from BA-1 (the only production well not fracture stimulated) increased three to four times from its oil rate during the water injection period, a very strong indication of the continued effect of CO₂ on the oil production compared with the fracture stimulation.

From mid-June through August 19, 2010, the oil rate was relatively stable between 3.4 and 4.3 m³/day (11 and 14 bopd), after which time the oil rate decreased relatively linearly through August 2011, when the oil rate reached the pre-pilot rate of 1.5 m³/day (5 bopd) (Figure 8-7).

The total oil production from the pilot area was 1,830 m³ (6,000 bbl). The stimulation was estimated to contribute 86.6 m³ (545 bbl) oil production. The baseline of 1.5 m³/day (5 bopd) was estimated to contribute 542 m³ (3,410 bbl) during this period. The oil production attributable to CO₂ is 325 m³ (2,045 bbl).

These direct measurements of oil production are used to calibrate the geologic model to project the CO₂ EOR for the pilot area if CO₂ had been injected at higher rates (at the regulated bottomhole injection pressure) and not interrupted by winter road restrictions. Full-field cases were studied to assess CO₂ EOR from multiple CO₂ injection patterns in the Bald Unit.

Water Production

Prior to CO₂ injection, the pilot water production was dominated by BA-1 production. The pilot water production was over 31.8 m³/day (200 bwpd), and BA-1 contributed 80 to 90%. Total water production decreased from the beginning of the pilot through April 2010, primarily because back-pressure was applied to BA-1 to reduce total fluid production to try to balance production from the entire pilot. After the well work of April and May 2010, BA-2 water production increased from 3.2 to 4.0 m³/day (20 to 25 bwpd) to about 16 m³/day (100 bwpd). IB-2 nearly doubled to 2.1 m³/day (13 bwpd). BA-1 decreased to about 12 m³/day (75 bwpd). These wells' water production remained nearly constant for the remainder of the monitoring period.

During active CO₂ injection the water rates of the non-pilot injection well (BD-5) were 24 to 48 m³/day (150 to 300 bwpd) with the lowest rates during the first 6 months of injection. After CO₂ injection with BU-1 returned to water injection, the field water injection rate was 44 to 56 m³/day (275 to 350 bwpd).

Gas Production

Prior to CO₂ injection and prior to the connection of the gas-liquid separator on June 6, 2010, the associated gas production was considered negligible. Gas rates began to increase slowly until back-pressure on the orifice tester was sufficient to record a reliable gas rate of 37 scm/day (1,300 scf/day) on July 23, 2010. Gas rates continued to increase slowly until they peaked at 130 scm/day (4,500 scf/day) in late August and early September, then slowly declined to roughly 60 scm/day (2,000 scf/day) by November. In early November, the gas separator experienced problems due to freezing of the flow lines and was bypassed on December 12, 2010. Although gas rate observations continued, no rate measurements were performed because rate appeared to decline.

Gas-to-oil ratio measurements were used to estimate gas rates after December 12, 2010. Cumulatively, between 27.2 and 33.9 tonnes (30.0 and 37.4 tons) or between 14,600 and 18,000 scm (514,000 and 641,000 scf) of CO₂ was produced, which is between 0.432 and 0.537% of the injected CO₂ mass.

Water Injection Outside of the CO₂ Injection Pilot Area

Prior to the CO₂ injection pilot, 1,120,000 m³ (7,060,000 bbl) of water was injected at BD-5 at an average rate of 89 m³/day (560 bwpd). For the 8 months immediately preceding CO₂ injection, the average water rate was 135 m³/day (850 bwpd). During the pilot period of September 2009 through September 2011, BD-5 injected 73,600 m³ (463,000 bbl) at an average rate of 135 m³/day (850 bwpd), which was identical to the water injection rate immediately preceding CO₂ injection startup.

MVA OBSERVATIONS AND INTERPRETATIONS

Brines and Gases from Oil Production Wells

Bulk Chemistry

pH and Alkalinity The pH of the brine prior to and in the early stages of CO₂ injection ranged from 7.08 to 7.65 (Figure 64). On November 12, 2009, the brine collected from well BA-2 was 0.8 pH units lower than for the previously collected sample (Appendix 5). The pH values for samples from the other three oil wells

also decreased approximately 1 pH unit (to between 5.65 and 6.5) between the samples collected on November 12 and December 22, 2009. The largest decrease in brine pH, which generally occurred between September 2009 and January 2010, followed the trend, based on subscripted well designations, of $pH_{BA-1} > pH_{IB-3} > pH_{IB-2} > pH_{BA-2}$, which exactly reflects the trend of the greatest to smallest CO_2 concentrations measured in

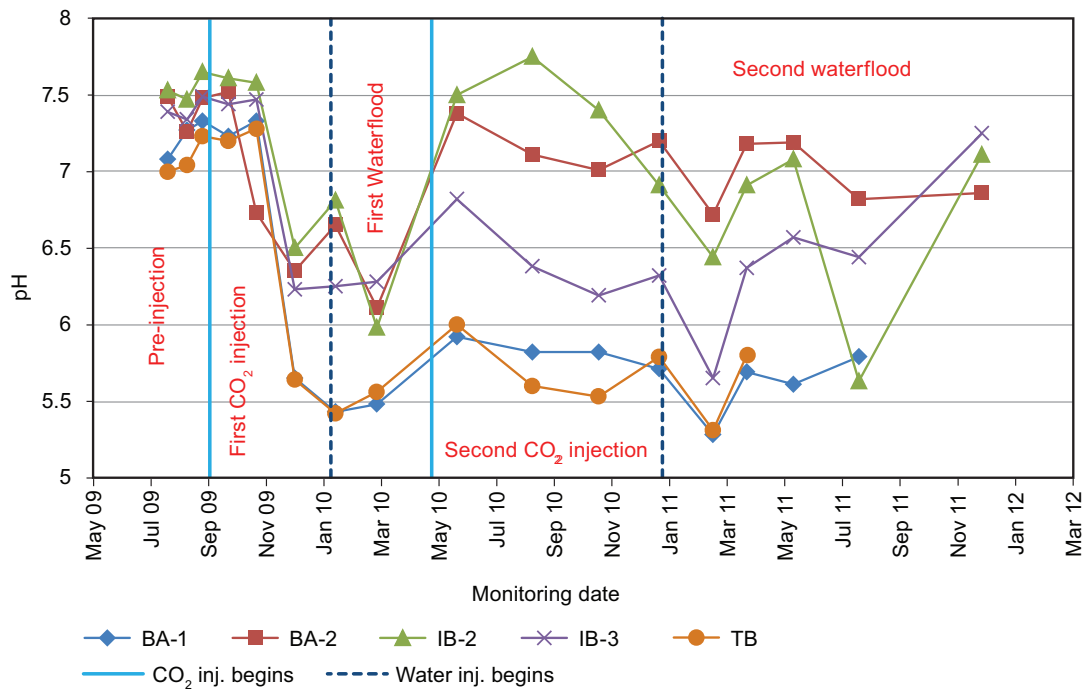


Figure 64 pH values in brine samples collected from BA-1, IB-2, IB-3, and the tank battery (TB) over entire monitoring period.

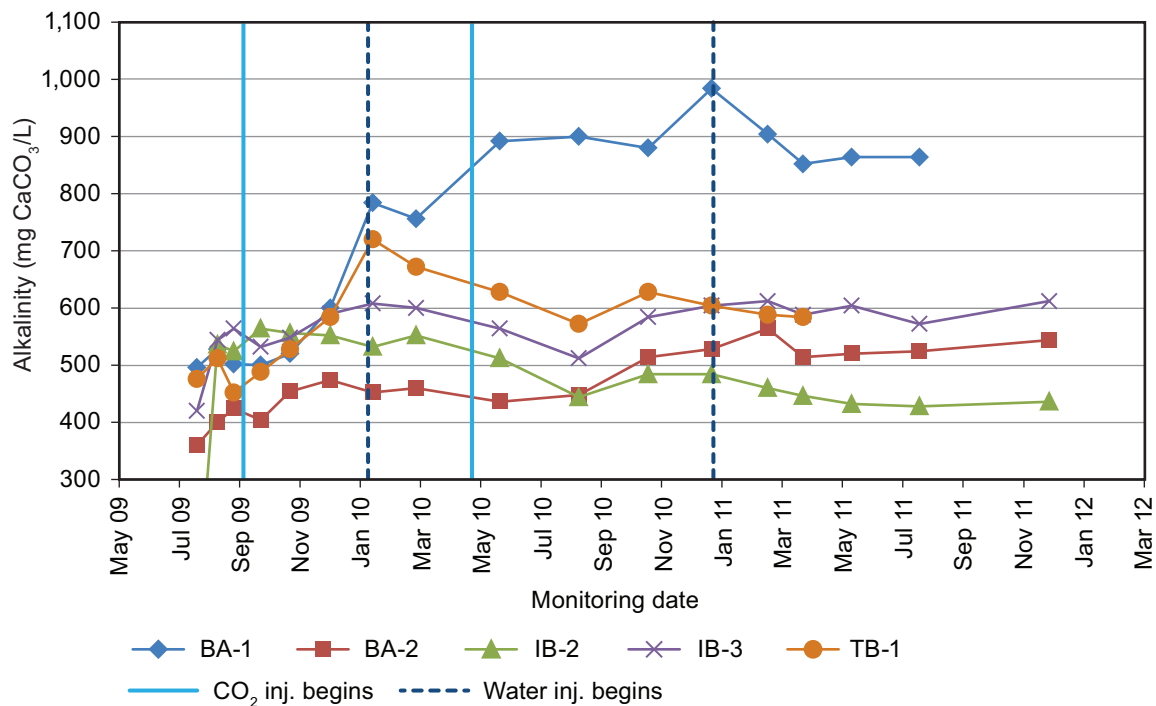


Figure 65 Alkalinity concentrations in brine collected from BA-1, IB-2, IB-3, and the tank battery (TB) over entire monitoring period.

the brines. The decrease in brine pH would suggest that CO₂-impacted brine had reached the wells approximately 45 days before any detectable gas phase CO₂ breakthrough, based on our sampling schedule. A more frequent sampling schedule might have detected CO₂ gas breakthrough earlier.

Brine pH values varied in response to field operations during the course of the project. Generally, pH values increased during and shortly after waterflood operations and decreased during and after CO₂ injection. Compared with the other oil-production wells, well BA-1 had the largest CO₂ concentrations in its gas samples and the largest decline in brine pH. The pH of brine from BA-2 varied the least, compared to samples from other wells.

Alkalinity of the brine, as expected, varied inversely to pH (Figure 65). Well BA-1 had the largest CO₂ concentrations, lowest brine pH, and largest alkalinity. The trend from largest to smallest alkalinity (TA) based on subscripted well names, like the brine pH, is $TA_{BA-1} > TA_{IB-3} > TA_{IB-2} \geq TA_{BA-2}$.

Common chemical parameters for brine samples over the course of the project are summarized in Table 6.

Table 6 Summary of common chemical parameters for brine samples.

Source	Parameter ¹	Samples (no.)	Range	Minimum	Maximum	Mean ²	Standard deviation
BA-1	DO, mg/L	15	2.72	0.08	2.80	0.51	0.76
BA-2	DO, mg/L	16	0.99	0.11	1.10	0.40	0.25
IB-2	DO, mg/L	16	1.52	0.06	1.58	0.35	0.42
IB-3	DO, mg/L	16	0.38	0.09	0.47	0.24	0.13
BD-3	DO, mg/L	15	0.15	0.10	0.25	0.18	0.05
Tank battery	DO, mg/L	13	1.65	0.09	1.74	0.38	0.46
BA-1	EC, mS/cm	16	24.89	27.80	52.69	38.37	7.46
BA-2	EC, mS/cm	17	26.93	26.23	53.16	41.08	7.71
IB-2	EC, mS/cm	17	24.58	31.96	56.54	44.63	7.74
IB-3	EC, mS/cm	17	35.77	29.17	64.94	49.76	9.72
BD-3	EC, mS/cm	15	40.35	4.14	44.49	11.74	13.10
Tank battery	EC, mS/cm	14	28.94	26.03	54.97	39.37	7.65
BA-1	Eh, mV	16	349	-187	162	83.50	111.02
BA-2	Eh, mV	17	255	-156	99	41.00	50.48
IB-2	Eh, mV	17	464	-191	273	95.00	119.42
IB-3	Eh, mV	17	304	-174	130	130.00	
BD-3	Eh, mV	16	598	-241	357	258.00	118.98
Tank battery	Eh, mV	14	159	-189	-30		
BA-1	pH	16	2.05	5.28	7.33	6.15	0.78
BA-2	pH	17	1.41	6.11	7.52	7.00	0.40
IB-2	pH	17	2.12	5.63	7.75	7.05	0.62
IB-3	pH	17	1.84	5.65	7.49	6.70	0.58
BD-3	pH	16	2.12	6.63	8.75	8.21	0.62
Tank battery	pH	14	1.97	5.31	7.28	6.17	0.78

¹Abbreviations: DO, dissolved oxygen; EC, specific conductance; and Eh, redox potential.

²Mean provided for comparative purposes and not intended to represent the entire period with a single, average value.

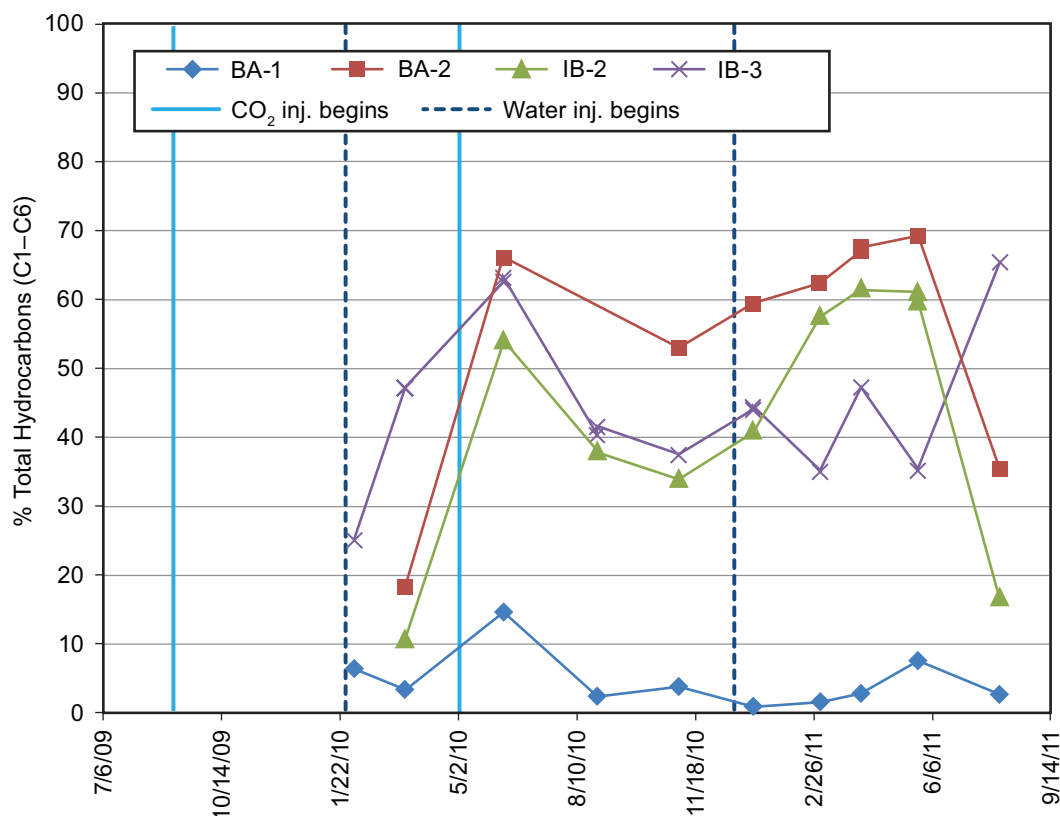


Figure 66 Total hydrocarbon concentrations (C_1 – C_6) (corrected for air contamination) in gas samples collected during brine sampling from BA-1, BA-2, IB-2, and IB-3 over entire monitoring period.

Hydrocarbons Total hydrocarbons (C_1 through C_6) also were measured in the reservoir gas samples. Generally, the gas from BA-1, which showed the greatest CO_2 concentration, contained the smallest concentrations of total hydrocarbons, and these concentrations decreased as EOR operations proceeded (Figure 66). Total hydrocarbons in the other wells (IB-2, IB-3, and BA-2) ranged from about 10% to nearly 70% (Figure 66). The most abundant components were propane and n-butane; the concentration of methane was relatively small, ranging from <0.1 to 4.9% by volume (Figures 67 and 68, Appendix 7). The variation in concentration of total hydrocarbons was basically the inverse of that observed for CO_2 concentration (compare Figures 39 and 66).

Isotope Chemistry

The isotopic composition of the brines varied significantly during the project (Appendix Table A14-1). The $\delta^{13}C$ of DIC of the brine samples ranged from -3.8 to -23.7‰ , excluding an outlier value of $+3.75\text{‰}$ for sample B2-01. Sample B2-01 also had anomalous chemical results, making the sample's integrity and representativeness suspect. The $\delta^{18}O$ and δD results of the brine samples ranged from -4.0 to -5.36‰ and from -24.9 to -35.4‰ , respectively. Table 7 summarizes the results of the isotopic analyses, and Appendix 14 presents the results of all the isotopic analyses available at the time this report was written.

Approximately four months after the start of CO_2 injection (December 22, 2009), brine collected from all of the oil production wells had a sharp positive shift in the $\delta^{13}C$ values of the DIC, reflective of the isotopic composition of CO_2 derived from ethanol production. Between September 2009 and January 2010 approximately 83% of the injected CO_2 originated from the ethanol plant, and about 17% originated from the refinery source. This change in $\delta^{13}C$ values of the brine samples was expected due to the influence of the isotopically heavier (more positive) $\delta^{13}C$ from the ethanol-derived CO_2 injected initially, which impacted the brine's composition as it migrated to the production wells (Appendix 14) (Figure 69). The greatest increase was observed in well BA-1, which also had the largest CO_2 concentrations in gas samples and the greatest

Table 7 Summary of stable isotope results from brine and gas samples.

Source	Parameter (‰)	Samples (no.)	Range	Minimum	Maximum	Mean	Standard deviation
BA-1	$\delta^{13}\text{C}_{\text{DIC-br}}$	16	8.5	-12.3	-3.8	-8.2	2.90
BA-2	$\delta^{13}\text{C}_{\text{DIC-br}}$	17	4.4	-15.2	-10.8	-13.8	1.14
IB-2	$\delta^{13}\text{C}_{\text{DIC-br}}$	17	11.1	-23.7	-12.6	-18.0	2.93
IB-3	$\delta^{13}\text{C}_{\text{DIC-br}}$	17	8.1	-20.3	-12.2	-16.5	2.63
BD-3	$\delta^{13}\text{C}_{\text{DIC-br}}$	16	16.1	-14.1	2.0	-5.5	3.96
TB	$\delta^{13}\text{C}_{\text{DIC-br}}$	14	7.9	-13.1	-5.2	-9.1	2.96
BA-1	$\delta^{18}\text{O}_{\text{H}_2\text{O-br}}$	16	0.7	-5.4	-4.6	-5.0	0.22
BA-2	$\delta^{18}\text{O}_{\text{H}_2\text{O-br}}$	17	1.2	-5.6	-4.4	-4.8	0.32
IB-2	$\delta^{18}\text{O}_{\text{H}_2\text{O-br}}$	17	1.3	-5.3	-4.0	-4.5	0.36
IB-3	$\delta^{18}\text{O}_{\text{H}_2\text{O-br}}$	17	0.9	-5.0	-4.1	-4.5	0.27
BD-3	$\delta^{18}\text{O}_{\text{H}_2\text{O-br}}$	16	2.3	-6.8	-4.6	-6.0	0.65
TB	$\delta^{18}\text{O}_{\text{H}_2\text{O-br}}$	14	0.5	-5.2	-4.8	-5.0	0.12
BA-1	$\delta\text{D}_{\text{H}_2\text{O-br}}$	16	3.7	-34.7	-31.0	-32.7	1.01
BA-2	$\delta\text{D}_{\text{H}_2\text{O-br}}$	17	7.6	-35.4	-27.8	-30.8	2.06
IB-2	$\delta\text{D}_{\text{H}_2\text{O-br}}$	17	9.5	-34.4	-24.9	-29.1	2.79
IB-3	$\delta\text{D}_{\text{H}_2\text{O-br}}$	17	6.8	-32.3	-25.5	-28.9	1.79
BD-3	$\delta\text{D}_{\text{H}_2\text{O-br}}$	16	11.3	-42.4	-31.1	-38.2	3.00
TB	$\delta\text{D}_{\text{H}_2\text{O-br}}$	14	1.9	-32.9	-31.0	-32.0	0.63
BA-1	$\delta^{13}\text{C}_{\text{CO}_2}$	10	4.9	-15.0	-10.1	-13.4	1.51
BA-2	$\delta^{13}\text{C}_{\text{CO}_2}$	9	5.7	-18.5	-12.8	-15.5	1.91
IB-2	$\delta^{13}\text{C}_{\text{CO}_2}$	9	8.7	-19.6	-10.9	-13.5	2.55
IB-3	$\delta^{13}\text{C}_{\text{CO}_2}$	9	3.2	-15.5	-12.3	-13.7	1.06
BD-3	$\delta^{13}\text{C}_{\text{CO}_2}$	1	na	na	na	na	na
TB	$\delta^{13}\text{C}_{\text{CO}_2}$	8	4.4	-16.0	-11.6	-13.9	1.74
Separator	$\delta^{13}\text{C}_{\text{CO}_2}$	2	0.7	-14.0	-13.3	-13.7	0.49
BA-1	$\delta^{13}\text{C}_{\text{CH}_4}$	0	na	na	na	na	na
BA-2	$\delta^{13}\text{C}_{\text{CH}_4}$	5	9.3	-56.8	-47.6	-51.2	3.89
IB-2	$\delta^{13}\text{C}_{\text{CH}_4}$	5	10.6	-58.0	-47.4	-51.4	4.08
IB-3	$\delta^{13}\text{C}_{\text{CH}_4}$	4	10.0	-58.8	-48.8	-51.8	4.68
BD-3	$\delta^{13}\text{C}_{\text{CH}_4}$	1	na	na	na	na	na
TB	$\delta^{13}\text{C}_{\text{CH}_4}$	0	na	na	na	na	na
Separator	$\delta^{13}\text{C}_{\text{CH}_4}$	0	na	na	na	na	na
BA-1	$\delta\text{D}_{\text{CH}_4}$	0	na	na	na	na	na
BA-2	$\delta\text{D}_{\text{CH}_4}$	4	28.0	-235	-207	-216	12.8
IB-2	$\delta\text{D}_{\text{CH}_4}$	5	72.0	-269	-197	-224	27.2
IB-3	$\delta\text{D}_{\text{CH}_4}$	3	16.0	-214	-198	-207	8.2
BD-3	$\delta\text{D}_{\text{CH}_4}$	1	na	na	na	na	na
TB	$\delta\text{D}_{\text{CH}_4}$	0	na	na	na	na	na
Separator	$\delta\text{D}_{\text{CH}_4}$	0	na	na	na	na	na

¹Abbreviations: DIC-br, dissolved inorganic carbon of brine samples; H₂O-br, water of brine samples; na, not applicable.

²Mean provided for comparative purposes and not intended to represent the entire period with a single, average value.

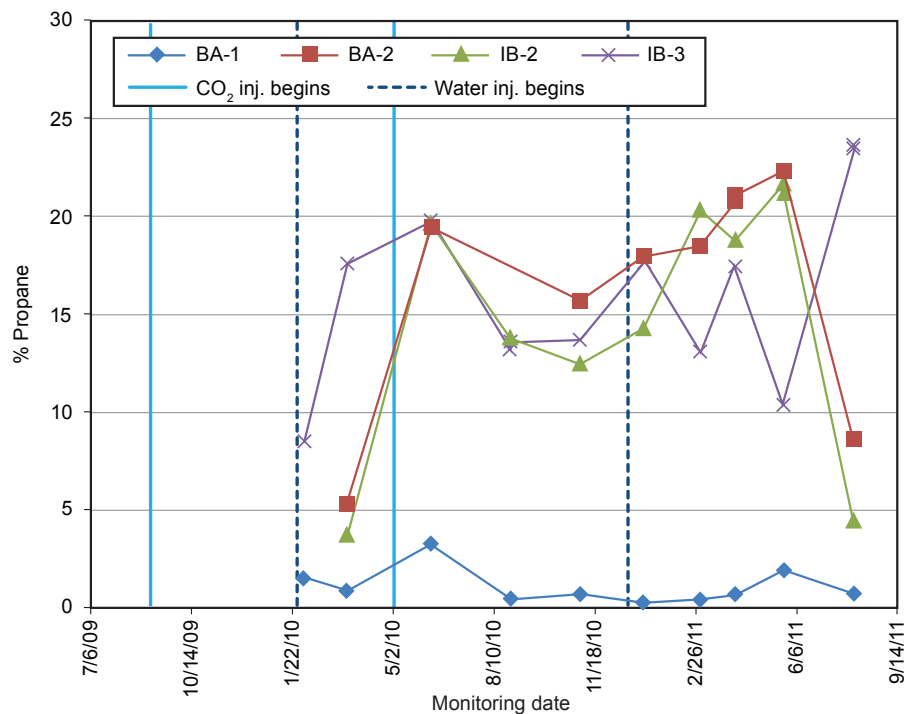


Figure 67 Concentrations of propane in gas samples collected during brine sampling from BA-1, BA-2, IB-2, and IB-3 over entire monitoring period.

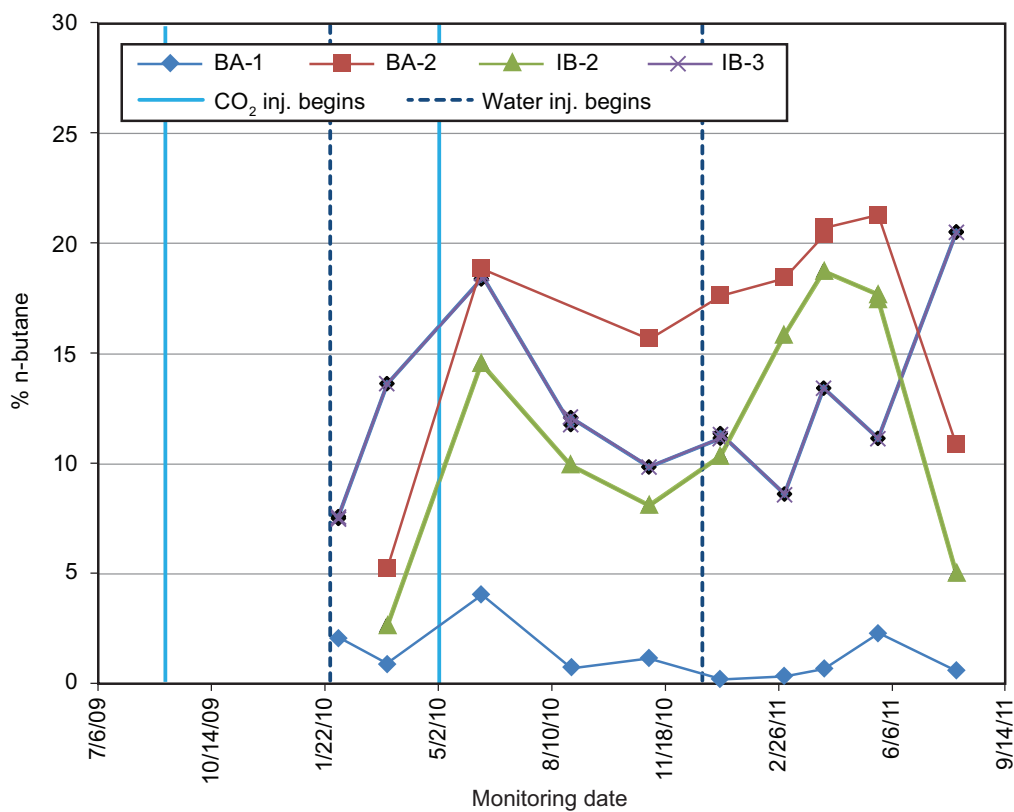


Figure 68 Concentrations of n-butane in gas samples collected during brine sampling from BA-1, BA-2, IB-2, and IB-3 over entire monitoring period.

pH change. The $\delta^{13}\text{C}_{\text{DIC}}$ values varied with pH and eventually stabilized at more positive values reflecting changes caused by both the injected CO_2 and the mixing of the DIC in the reservoir brine with DIC of the injection water from well BD-3. The impact of injected CO_2 on the brine, as measured by the decrease in pH from well BA-2 observed on November 12, 2009, was not reflected in the $\delta^{13}\text{C}_{\text{DIC}}$ of BA-2 until the next sampling event of December 22, 2009. The $\delta^{13}\text{C}_{\text{DIC}}$ for the rest of the production wells increased on December 22, 2009, correlating with the decrease in pH observed for those wells during the same sampling event. It is interesting to note that the parameters measured (pH, alkalinity, $\delta^{13}\text{C}_{\text{DIC}}$) on the brine samples at the production wells showed significant changes due to the injected CO_2 prior to actual gas phase CO_2 breakthrough at any of the wells.

The $\delta^{18}\text{O}$ and δD values of the brine samples from the oil production wells were significantly different from the values for the injection water samples from well BD-3 and the samples from the groundwater monitoring wells (Figure 70). The isotopic compositions of the aqueous samples showed evidence of mixing between the formation brines and the injected water. The effects of mixing were especially obvious for the brine samples from wells IB-2 and BA-2 (Figure 70). The gradual change in isotopic composition of the brines at the production wells due to mixing with injection water from well BD-3 over the course of the pilot study is better displayed in Figure 71, a graph plotting δD versus time. This mixing relationship is also shown using chloride concentrations and δD , both of which are considered conservative parameters in groundwater geochemistry (Figure 72).

The first sampling event in which gas-phase CO_2 breakthrough was detected at the oil production wells occurred on February 3, 2010, approximately five months after CO_2 injection began and shortly after the start of the first water injection period of BU-1. The CO_2 concentrations in oil production wells BA-1 and IB-3, located north of the CO_2 injection well, typically were greater than in wells BA-2 and IB-2, located south of the injection well (Figures 5 and 38). Generally, CO_2 concentrations (ϕ_{CO_2}) associated with each well followed the trend $\phi_{\text{BA-1}} > \phi_{\text{IB-3}} > \phi_{\text{IB-2}} > \phi_{\text{BA-2}}$ (Figure 38). The observed distribution of CO_2 breakthrough detections in the reservoir was expected because of the reservoir flow simulations and because the water injection well (BD-5) for the Field was to the south of the CO_2 injection well, driving reservoir fluids to

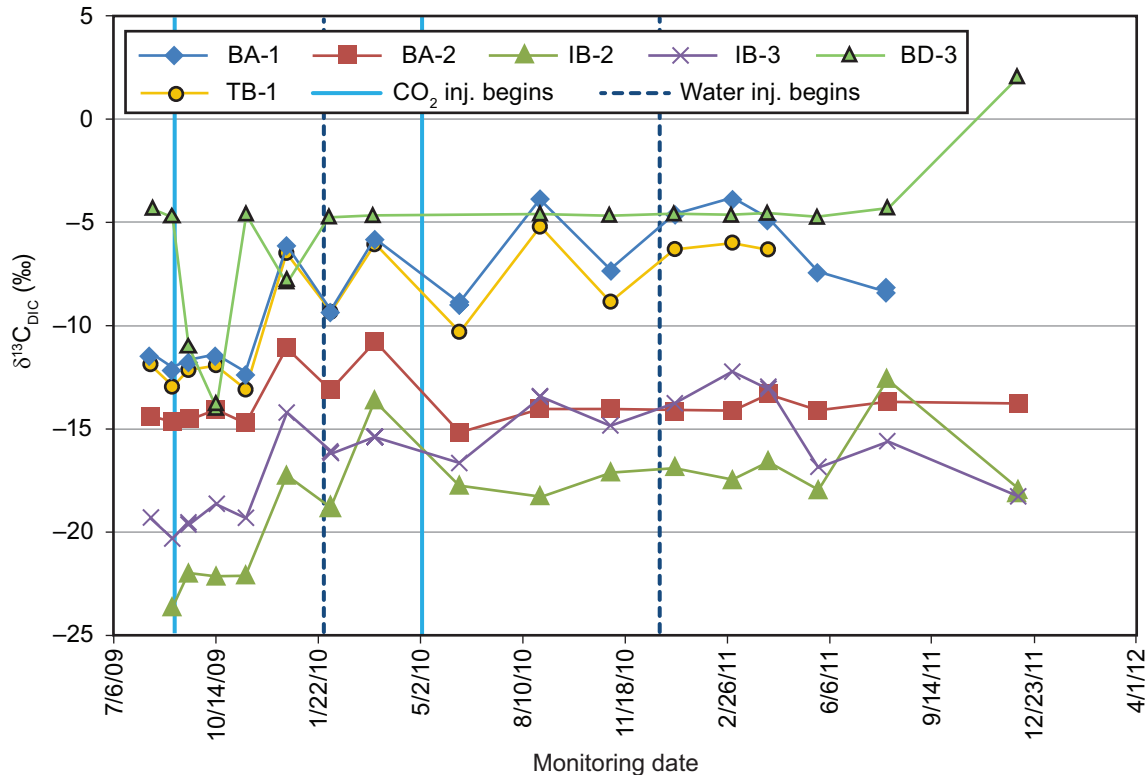


Figure 69 $\delta^{13}\text{C}$ of DIC in brine samples from BD-3, BA-1, BA-2, IB-2, and IB-3 over entire monitoring period.

the north. According to the gas chromatography analyses corrected for air contamination, the CO_2 concentrations in well BA-1 were greater than 80%, and increased to greater than 95% during the second CO_2 injection period (Figure 39). The CO_2 concentrations also were greater during the second waterflood period than in the first waterflood. Relatively large CO_2 concentrations were observed in wells IB-3, IB-2, and BA-2 after CO_2 breakthrough during the first water injection period, but the concentrations decreased significantly and remained lower during the second CO_2 injection period. Then, after some delay on August 2, 2011, the CO_2 concentrations in wells IB-2 and BA-2 increased sharply during the second water injection period (Figure 38). Brine samples from well BA-2 generally contained the smallest CO_2 concentrations (<10%).

Values of $\delta^{13}\text{C}$ of CO_2 from gas samples collected after CO_2 breakthrough was observed at the oil production wells ranged from -12 to -13‰ , similar to values of the ethanol-derived CO_2 that made up nearly 100% of the injected CO_2 during the first 2 months of CO_2 injection. The $\delta^{13}\text{C}$ composition for most of the production wells gradually changed to more negative values as the water injection continued and the second CO_2 injection began (Figure 73). This shift in $\delta^{13}\text{C}$ values was likely due to the influence of a greater percent of injected CO_2 from the refinery source as CO_2 injection progressed (Figure 73). The overall trend in $\delta^{13}\text{C}_{\text{CO}_2}$ toward more negative values continued for approximately nine months (February 3, 2010, to November 4, 2010), and then showed a strong trend toward more positive values. This positive trend in $\delta^{13}\text{C}$ values, beginning January 6, 2011, reflects the influence of a greater proportion of the ethanol-derived CO_2 impacting the production wells (Figure 73). The isotopic CO_2 composition becomes more negative beginning about 4 to 5 months after the start of the second waterflood, reflecting the influence of a greater amount of refinery-derived CO_2 being injected during the second CO_2 injection event. It should be noted that wells BA-2 and IB-2 both showed large increases in CO_2 concentrations in the gas samples during the final sampling event (August 2, 2011) (Figure 39). The positive shift of $\delta^{13}\text{C}_{\text{CO}_2}$ values from well BA-2 suggests an increased impact on isotopic composition from ethanol-derived CO_2 . However, the $\delta^{13}\text{C}$ of the CO_2 from well IB-2 actually decreased to a more negative composition relative to the previous sampling event when the well's CO_2 concentration was much less (Figure 73). The negative shift in $\delta^{13}\text{C}_{\text{CO}_2}$ values at well IB-2 most likely reflects an increase in refinery-derived CO_2 reaching this well. These results suggest that the two sources of injected CO_2 did not completely mix prior to migrating to the different production wells because they were injected at discrete time periods.

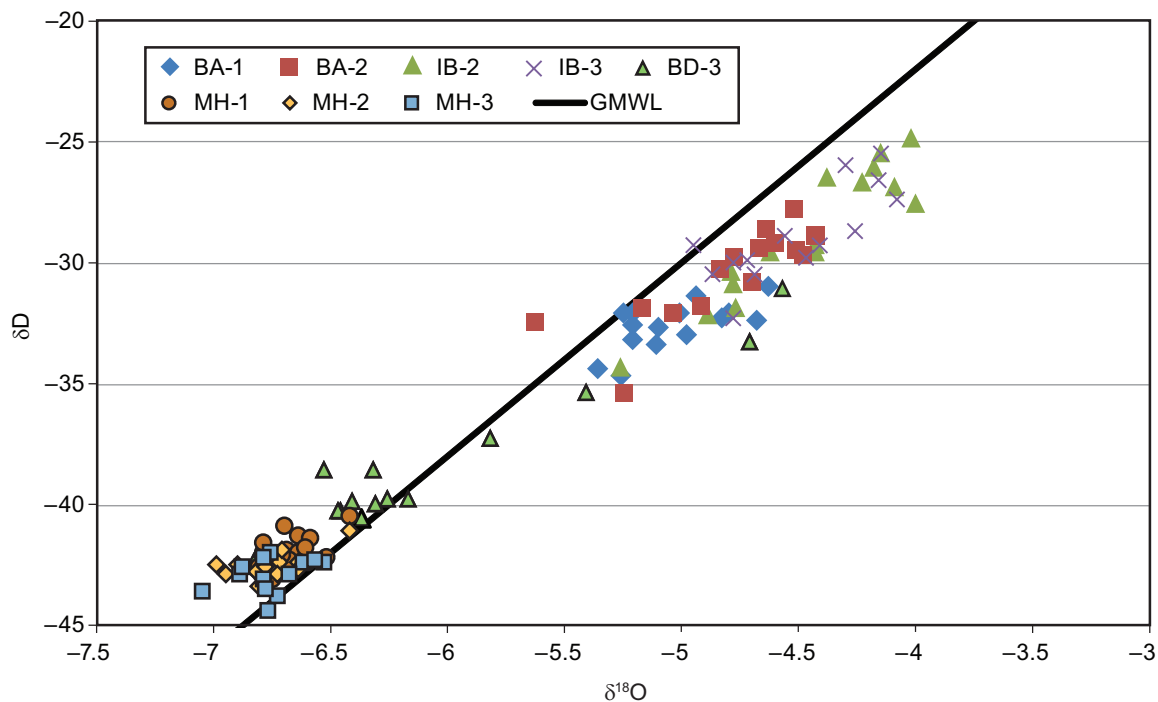


Figure 70 $\delta^{18}\text{O}$ and δD of all aqueous samples from the five-spot production wells (BA-1, BA-2, IB-2, and IB-3), water supply well (BD-3), and the monitoring wells (MH-1, MH-2, and MH-3).

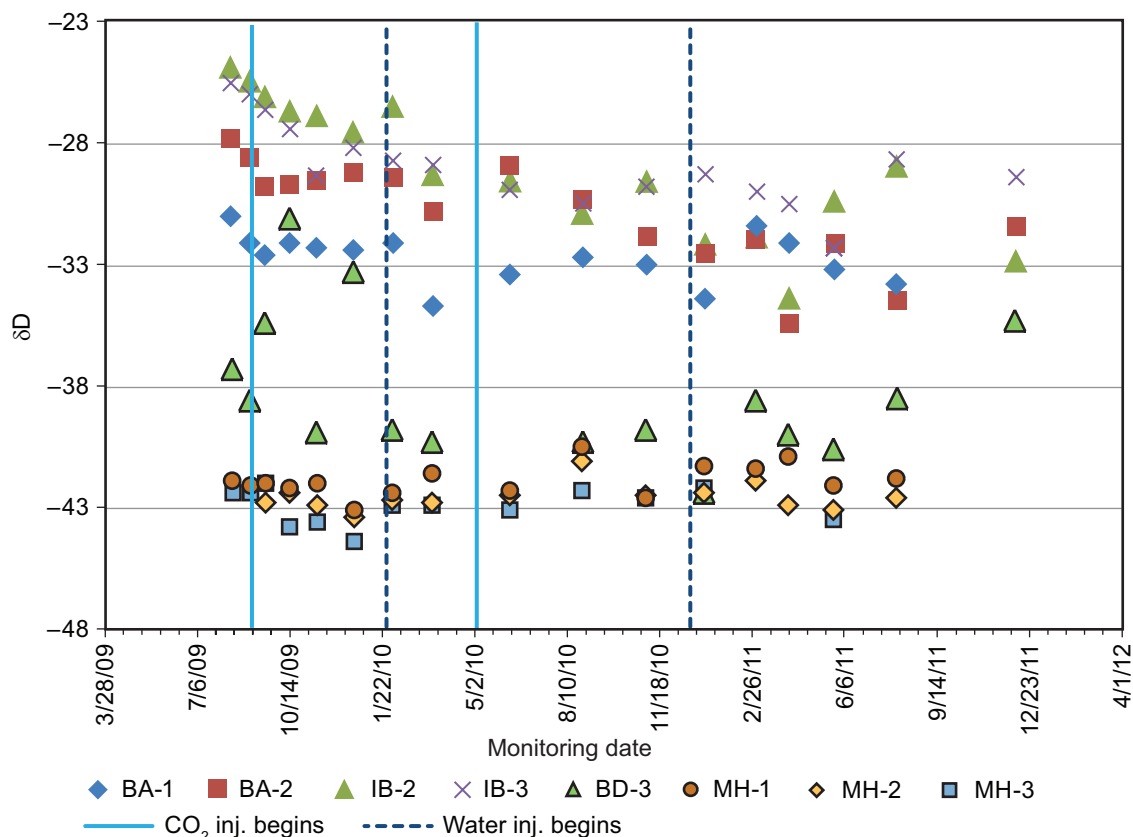


Figure 71 δD of aqueous samples from the five-spot production wells (BA-1, BA-2, IB-2, and IB-3), water supply well (BD-3), and the monitoring wells (MH-1, MH-2, and MH-3) over entire monitoring period.

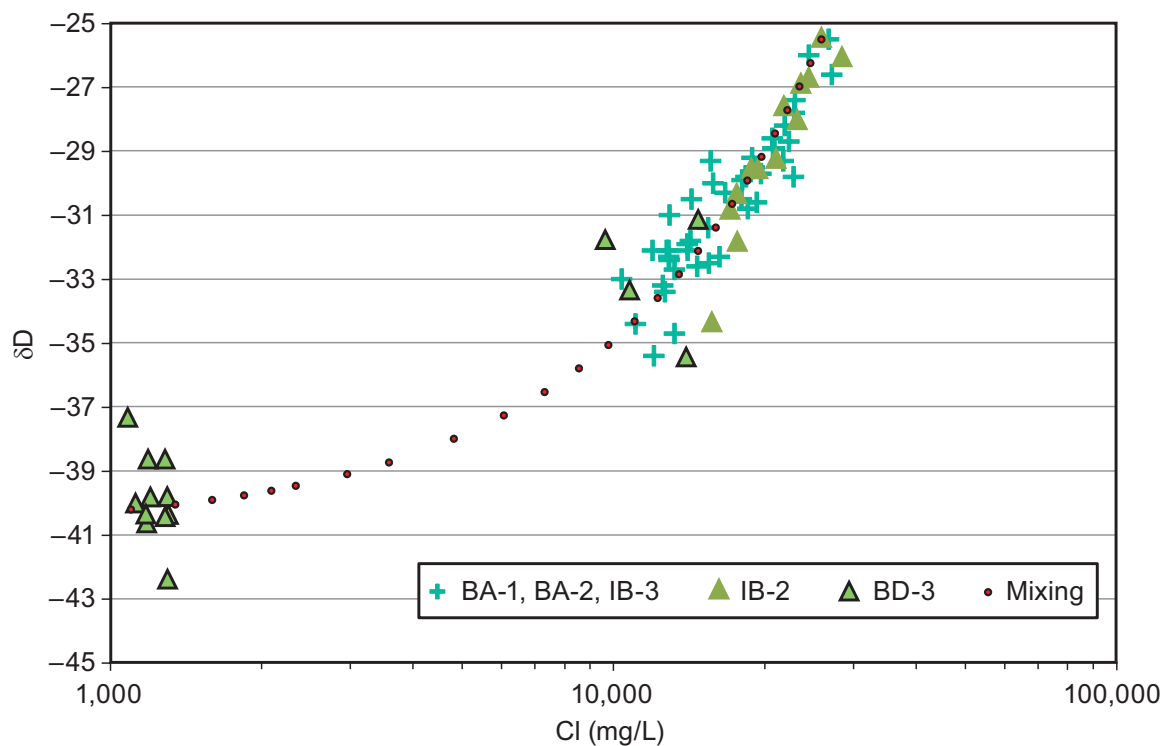


Figure 72 Chloride concentration versus δD of samples from BD-3, BA-1, BA-2, IB-2, and IB-3. The dotted line shows a calculated trend of mixing between the concentrated brine and BD-3 water.

The isotopic composition ($\delta^{13}\text{C}$ and δD) of methane from the production wells primarily indicates a thermogenic origin, which is typical for an oil field (Figure 74); however, some of the methane samples showed a shift to more negative $\delta^{13}\text{C}$ values, indicating microbial origin. Mixing with microbial methane from BD-3 was probably the cause for some of the isotopic shift, especially for two of the sampled wells, BA-2 and IB-3. However, toward the end of the pilot study there was evidence of some production of microbial methane within the oil field as shown by the negative shifts in both $\delta^{13}\text{C}$ and δD values of methane samples from IB-2 and possibly BA-2 (Figure 74 and 75). The most negative isotopic composition of methane was observed for IB-2, which plotted in the microbial gas domain on a delta-delta plot used to help determine the origin of methane (Figure 74). These results suggest that microbial degradation of organic matter within the formation began to occur with the production of microbial methane near the end of the pilot study at this site. This shift was observed in samples from IB-3, BA-2, and IB-2 (Figure 74).

Groundwater Monitoring Wells

Bulk Chemistry

Sodium and chloride or carbonate were the predominant species in the groundwater. Baseline (pre- CO_2 -injection) sodium concentrations were slightly greater in well MH-1 (414 and 411 mg/L) compared to MH-2 (329 and 348 mg/L), but chloride concentrations were significantly greater in MH-1 (244 and 291 mg/L) compared to MH-2 (11 and 10 mg/L) (see Appendix 6). Although baseline groundwater samples were not collected from well MH-3, concentrations of sodium and chloride in samples from well MH-3 collected after CO_2 injection began were similar to those measured in well MH-2. The reason for these initial differences in concentrations is unknown.

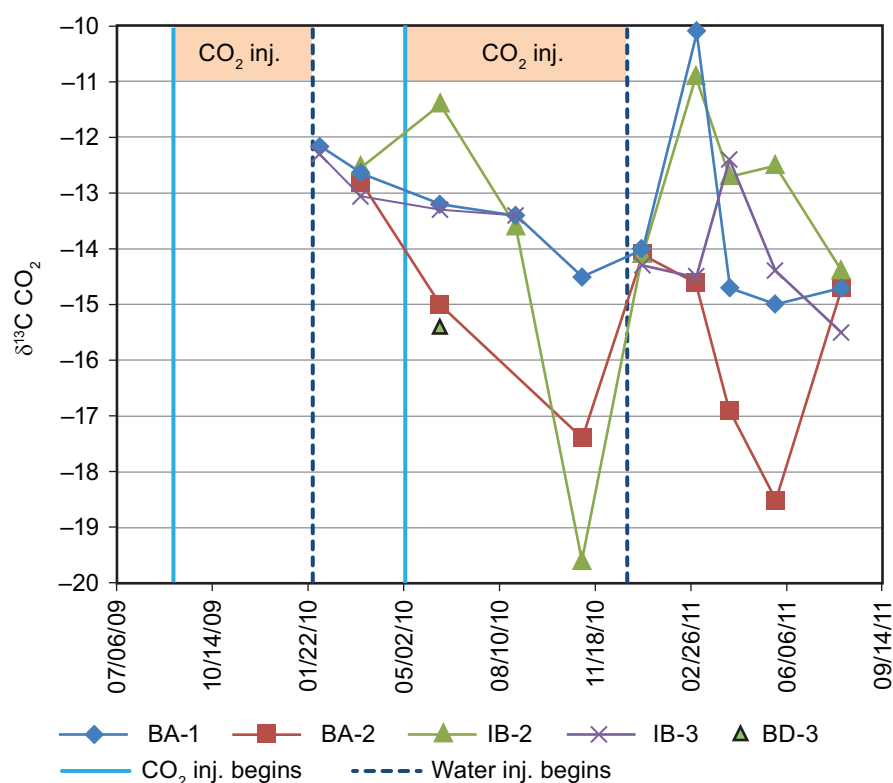


Figure 73 Carbon isotopic composition of CO_2 in gas samples acquired during brine sampling BD-3, BA-1, BA-2, IB-2, and IB-3 over entire monitoring period.

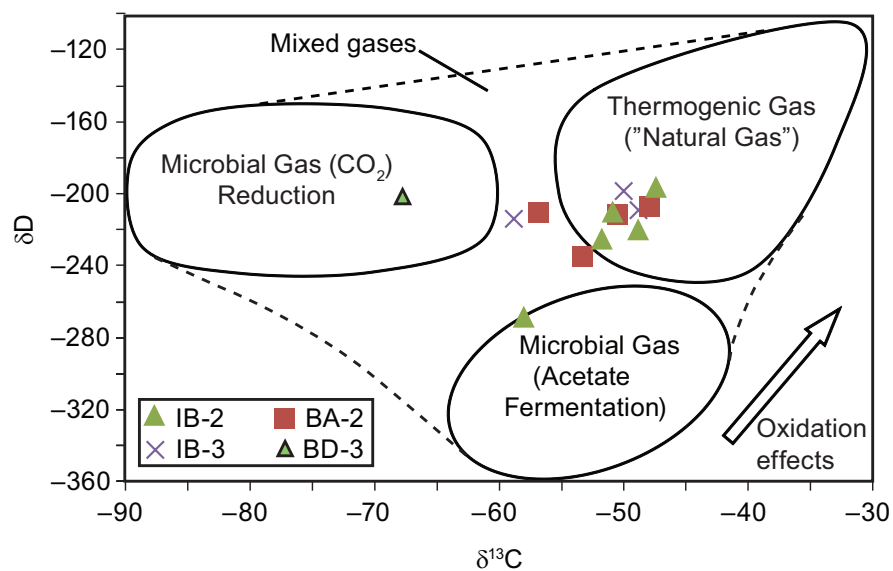


Figure 74 Isotopic composition of methane from gas samples acquired during brine sampling, showing typical compositions of different sources of methane at BD-3, BA-2, IB-2, and IB-3 over entire monitoring period.

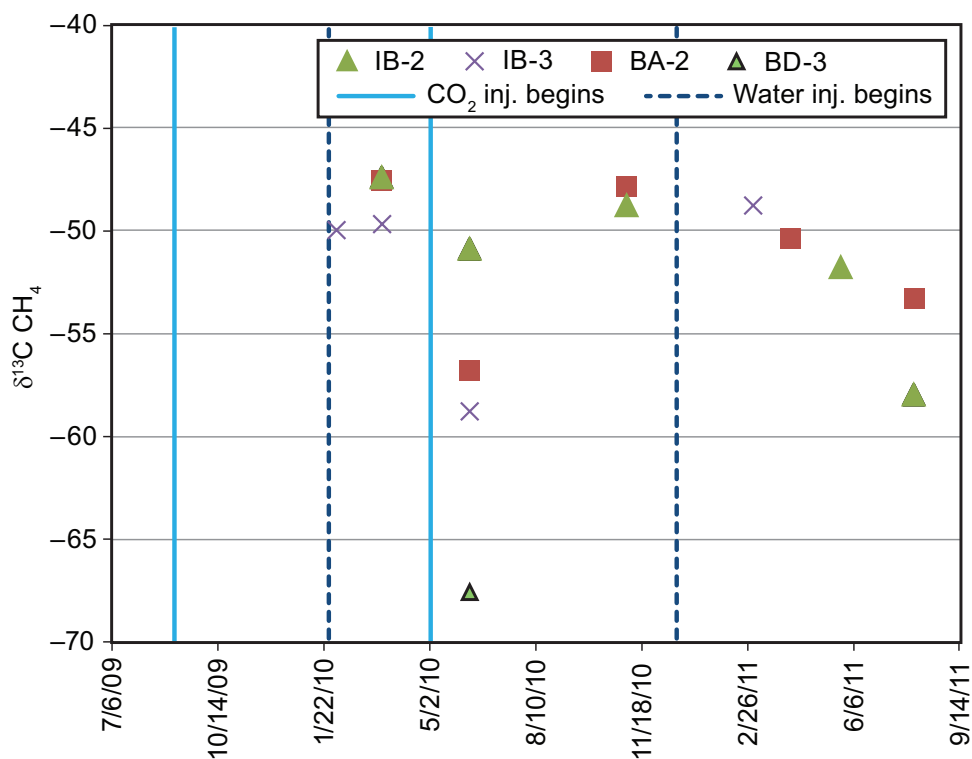


Figure 75 $\delta^{13}\text{C}$ composition of methane from BD-3, BA-2, IB-2, and IB-3 over entire monitoring period.

Sodium and chloride concentrations in groundwater from wells MH-2 and MH-3 remained relatively constant (Figure 76) throughout the project, but concentrations increased in MH-1 (Figure 77). Alkalinity was greater in wells MH-2 and MH-3 compared to MH-1 (Figure 78), and the very low chloride concentrations in wells MH-2 and MH-3 (Figure 76) indicate that carbonate was the counter ion for sodium in these wells, whereas chloride was the counter ion in MH-1. Bromide concentrations in groundwater samples from wells MH-2 and MH-3 were below detection limits, but were approximately 1 to 3 mg/L in the samples from MH-1. Bromide concentrations in brines from the Clore sandstone were approximately 50 mg/L or less (Figures 35 and 37) and 3 to 8 mg/L in source water used for waterflood operations (Figure 34). Barium concentrations in brine and source water were approximately 1.0 mg/L, with brine samples from well BA-1 having the largest concentrations (~2.4 mg/L), although these concentrations slowly decreased during the project. Similar to sodium and chloride, barium concentrations slowly increased in water samples collected from well MH-1 while remaining stable in water collected from the other two monitoring wells (Figure 79).

The alkalinity and pH values of the groundwater generally remained constant or decreased during the project, suggesting that there was no significant CO₂ leaking into the groundwater. The concentrations of sodium, chloride, bromide, and barium in the groundwater from well MH-1 are indicative of the presence of diluted brine. The exact cause of this is unknown. Isotopic analyses of the groundwater and the brines do not provide conclusive evidence of any impacts to groundwater from the CO₂-injection operations.

Common water quality parameters for groundwater samples across the course of the project are summarized in Table 8.

Table 8 Summary of common water quality parameters for groundwater samples.

Source	Parameter	Samples (no.)	Range	Minimum	Maximum	Mean ²	Standard deviation
MH-1	DO, mg/L	16	0.6	0.28	0.88	0.50	0.19
MH-2	DO, mg/L	15	0.88	0.15	1.03	0.43	0.26
MH-3	DO, mg/L	12	2.36	0.21	2.57	0.65	0.64
MH-1	EC, mS/cm	17	3.468	1.19	4.66	2.93	1.12
MH-2	EC, mS/cm	16	0.713	1.22	1.93	1.40	0.20
MH-3	EC, mS/cm	13	0.786	1.04	1.83	1.29	0.21
MH-1	Eh, mV	17	457	-74	383	170	119.32
MH-2	Eh, mV	16	462	-72	390	268	80.25
MH-3	Eh, mV	13	402	-47	355	210	94.15
MH-1	pH	17	0.61	8.05	8.66	8.43	0.15
MH-2	pH	16	0.61	8.33	8.94	8.71	0.19
MH-3	pH	13	0.56	8.40	8.96	8.65	0.17
MH-1	Temp, °C	17	5.24	13.07	18.31	14.98	1.33
MH-2	Temp, °C	16	8.87	12.29	21.16	15.75	2.28
MH-3	Temp, °C	13	6.5	11.70	18.20	14.58	2.05

¹Abbreviations: DO, dissolved oxygen; EC, specific conductance; and Eh, redox potential.

²Mean provided for comparative purposes and not intended to represent the entire period with a single, average value.

Isotope Chemistry

Stable isotope data from groundwater monitoring well samples is summarized in Table 9. The $\delta^{13}\text{C}_{\text{DIC}}$

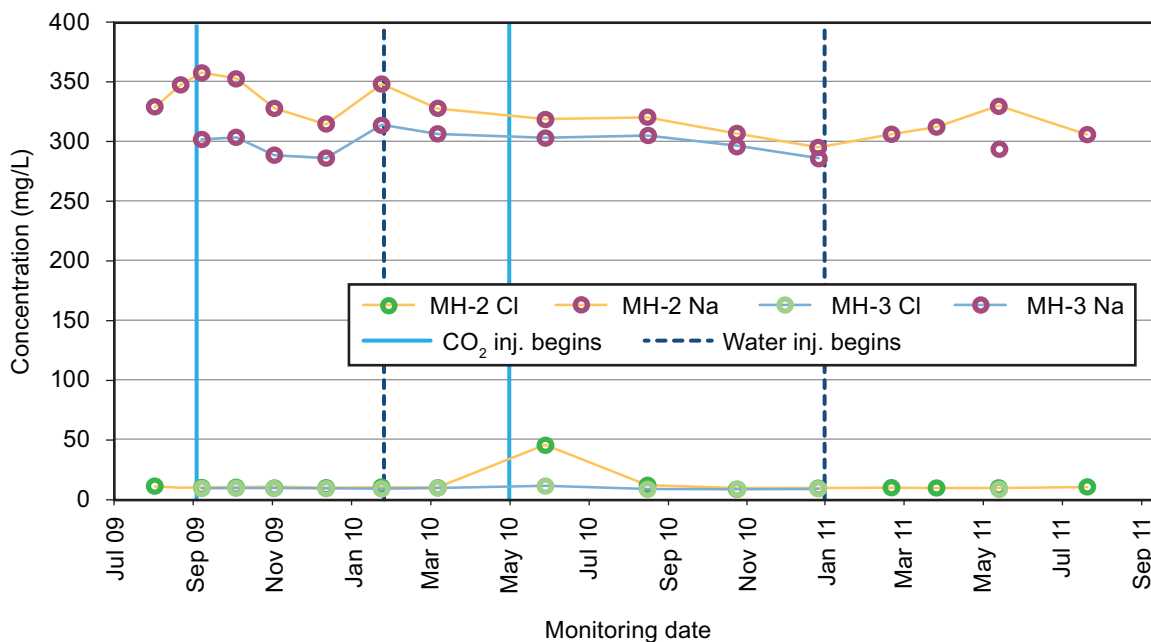


Figure 76 Sodium and chloride concentrations in groundwater samples collected from MH-2 and MH-3 over entire monitoring period.

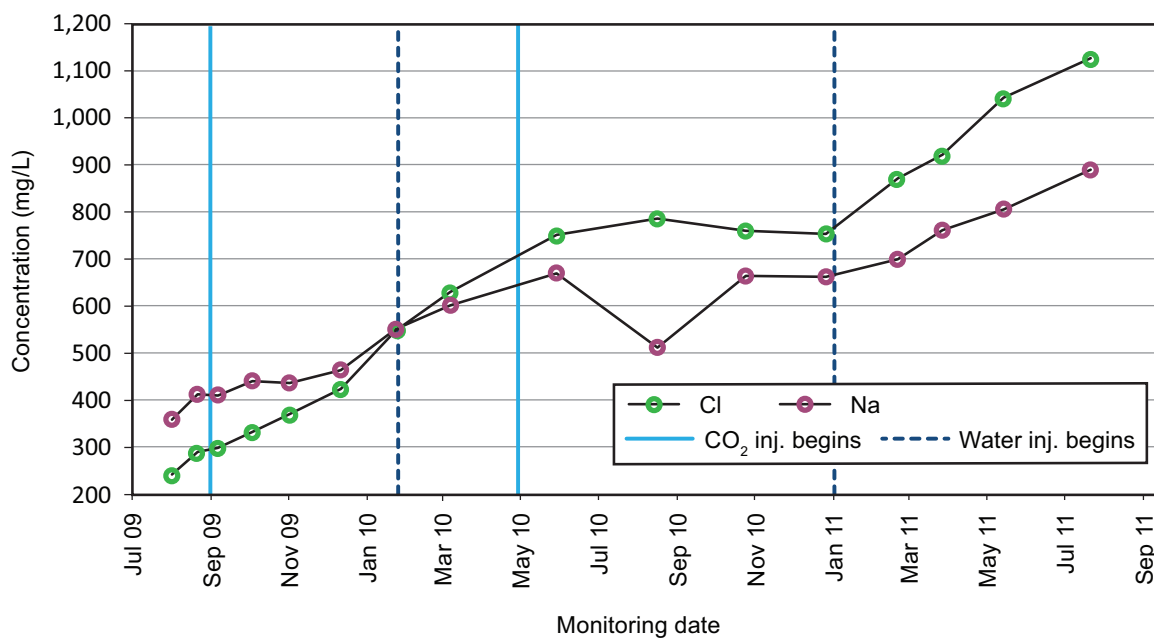


Figure 77 Sodium and chloride concentrations in groundwater samples collected from monitoring well MH-1 over entire monitoring period.

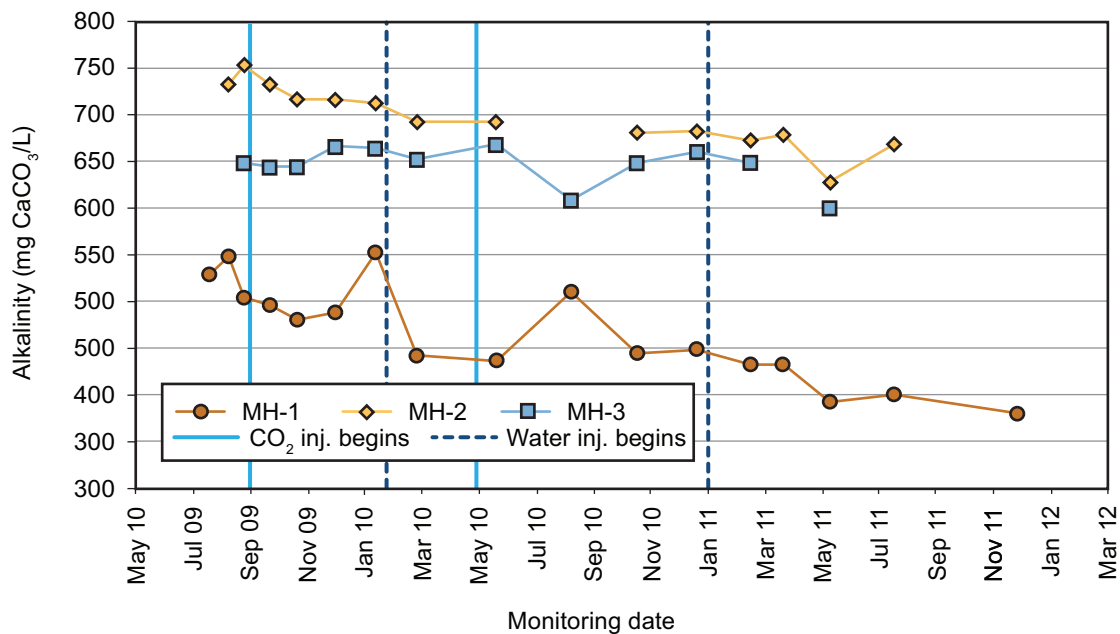


Figure 78 Alkalinity in groundwater samples collected from MH-1, MH-2, and MH-3 over entire monitoring period.

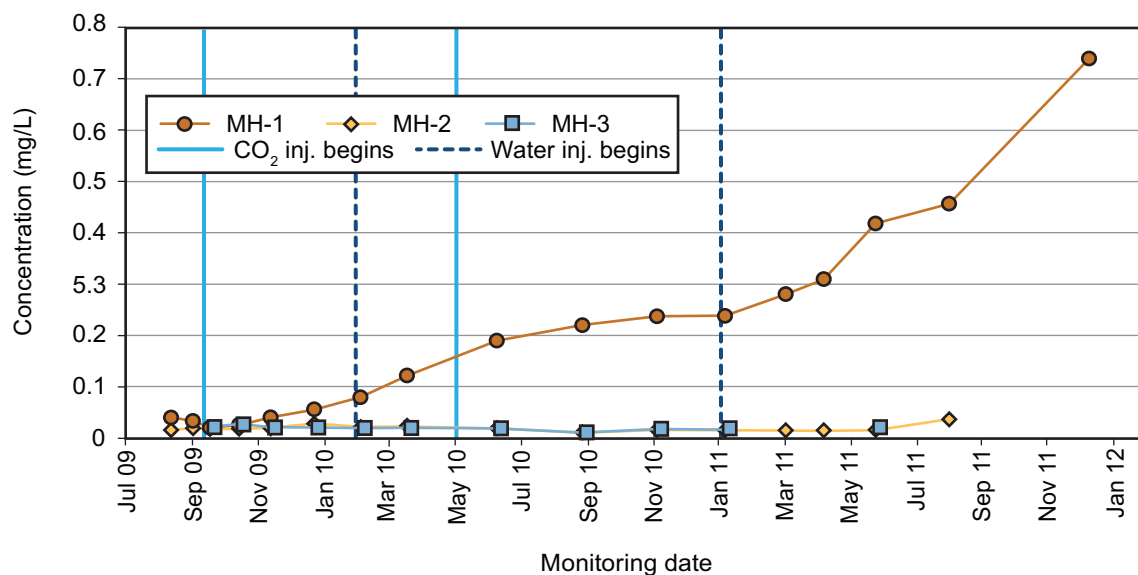


Figure 79 Barium concentrations in groundwater samples collected from MH-1, MH-2, and MH-3 over entire monitoring period.

values of the three monitoring wells were fairly similar, ranging from -5.1 to -6.5 ‰, and they generally showed an overall trend toward more negative values with time (Figure 80). The negative trend in the $\delta^{13}\text{C}_{\text{DIC}}$ values appears to be associated with sulfate concentrations (Figure 81). Samples with smaller sulfate concentrations tended to have more negative $\delta^{13}\text{C}_{\text{DIC}}$ values, and samples with greater sulfate generally had more positive $\delta^{13}\text{C}$ values. This trend was especially exhibited by the samples from well MH-2. Such a trend would be characteristic of sulfate reduction by organic compounds in the aquifer. Organic carbon is isotopically negative, typically in the range of -24 to -30 ‰ (Deines, 1980) and would be released as CO_2 during sulfate reduction reactions, causing a decrease in the $\delta^{13}\text{C}$ of the DIC. The $\delta^{13}\text{C}_{\text{DIC}}$ results from the monitoring wells showed no evidence of impacts to the groundwater from the CO_2 being injected into the deeper oil reservoir formation during this pilot study.

The results of the $\delta^{18}\text{O}$ and δD analyses of the monitoring well water samples clustered relatively tightly compared with results for the brines (Figure 70). Considering the standard deviations of these analyses (± 0.1 ‰ for $\delta^{18}\text{O}$ and ± 1 ‰ for δD), the isotopic composition of the water from the monitoring wells showed some variation but no consistent trends with time (Figure 82). The observed variations in $\delta^{18}\text{O}$ and δD could reflect seasonal precipitation inputs, but with some offset or lag time occurring, depending somewhat on the amount of precipitation. The isotopic analyses of the groundwater samples from the monitoring wells showed no discernible contribution from brines from the production wells due to CO_2 injection. According to mixing calculations, brine with a Cl concentration of 25,900 mg/L, if mixing with groundwater with a Cl concentration of 9.5 mg/L, would need only a 4% contribution from brine to yield the highest Cl concentration (1,045 mg/L) measured in the samples from the monitoring wells. A contribution of brine to the groundwater of this size would be too little to significantly impact the $\delta^{18}\text{O}$ and δD analyses of the groundwater.

Table 9 Summary table of stable isotope data from groundwater monitoring wells.

Source	Parameter ¹	Unit	Samples (no.)	Range	Minimum	Maximum	Mean ²	Standard deviation
MH-1	$\delta^{13}\text{C}_{\text{DIC}}$	‰	16	4.8	-6.5	-1.7	-5.6	1.07
MH-2	$\delta^{13}\text{C}_{\text{DIC}}$	‰	14	1.0	-6.2	-5.2	-5.7	0.37
MH-3	$\delta^{13}\text{C}_{\text{DIC}}$	‰	13	0.6	-5.7	-5.1	-5.5	0.17
MH-1	$\delta^{18}\text{O}_{\text{H}_2\text{O}}$	‰	16	0.39	-6.81	-6.42	-6.67	0.10
MH-2	$\delta^{18}\text{O}_{\text{H}_2\text{O}}$	‰	14	0.57	-6.99	-6.42	-6.77	0.14
MH-3	$\delta^{18}\text{O}_{\text{H}_2\text{O}}$	‰	13	0.52	-7.05	-6.53	-6.76	0.14
MH-1	$\delta\text{D}_{\text{H}_2\text{O}}$	‰	16	2.6	-43.1	-40.5	-41.9	0.6
MH-2	$\delta\text{D}_{\text{H}_2\text{O}}$	‰	14	2.3	-43.4	-41.1	-42.6	0.6
MH-3	$\delta\text{D}_{\text{H}_2\text{O}}$	‰	13	2.4	-44.4	-42.0	-42.9	0.7

¹Abbreviation: DIC, dissolved inorganic carbon.

²Mean provided for comparative purposes and not intended to represent the entire period with a single, average value.

Mineral-Fluid Equilibria

Alkalinity in the groundwater generally decreased during the project period (Figure 78). However, groundwater from MH-2 exhibited an increase in alkalinity and DIC during the pre- CO_2 and initial CO_2 injection operations. There was also an increase in the sulfur concentrations and a decrease in the iron concentrations during this period. However, no significant change in sodium and chloride occurred during this same period to suggest migration of brine into the groundwater. In addition, the CO_2 spike was brief and stabilized at background values before the end of CO_2 injection.

To investigate alternative explanations for the observations in MH-2, such as possible effects from oxygen entering the aquifer around the monitoring well during the well's construction and development, a geo-

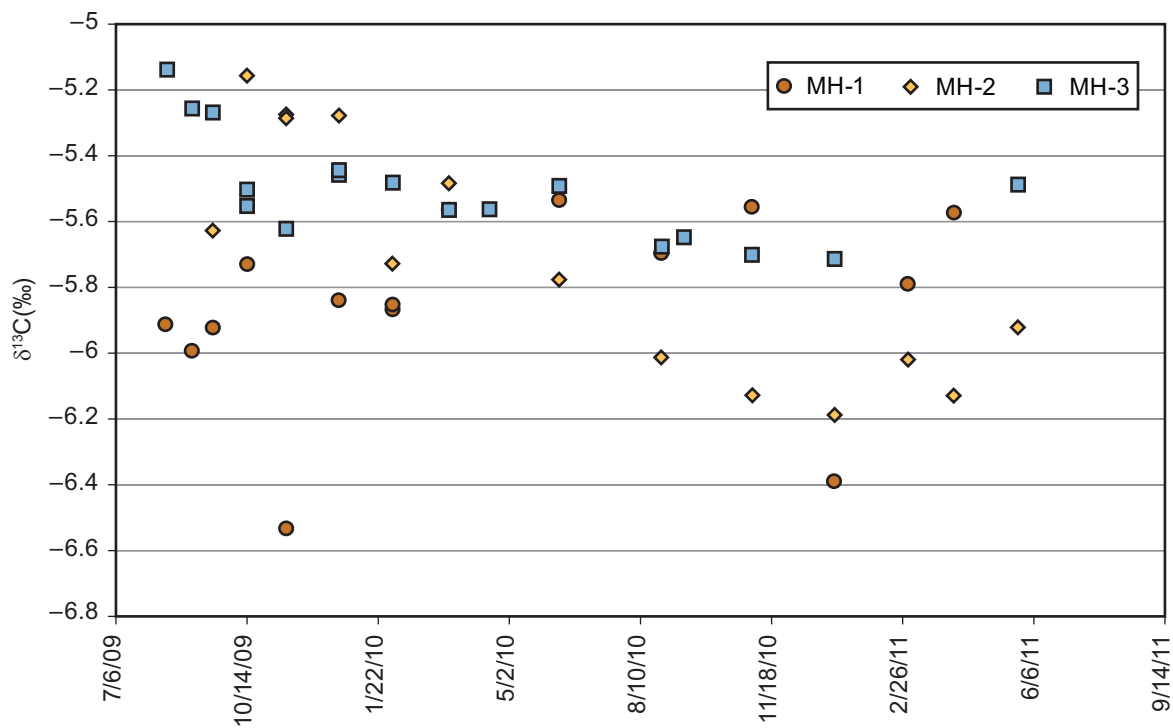


Figure 80 δ¹³C of DIC in groundwater samples collected from MH-1, MH-2, and MH-3 over entire monitoring period.

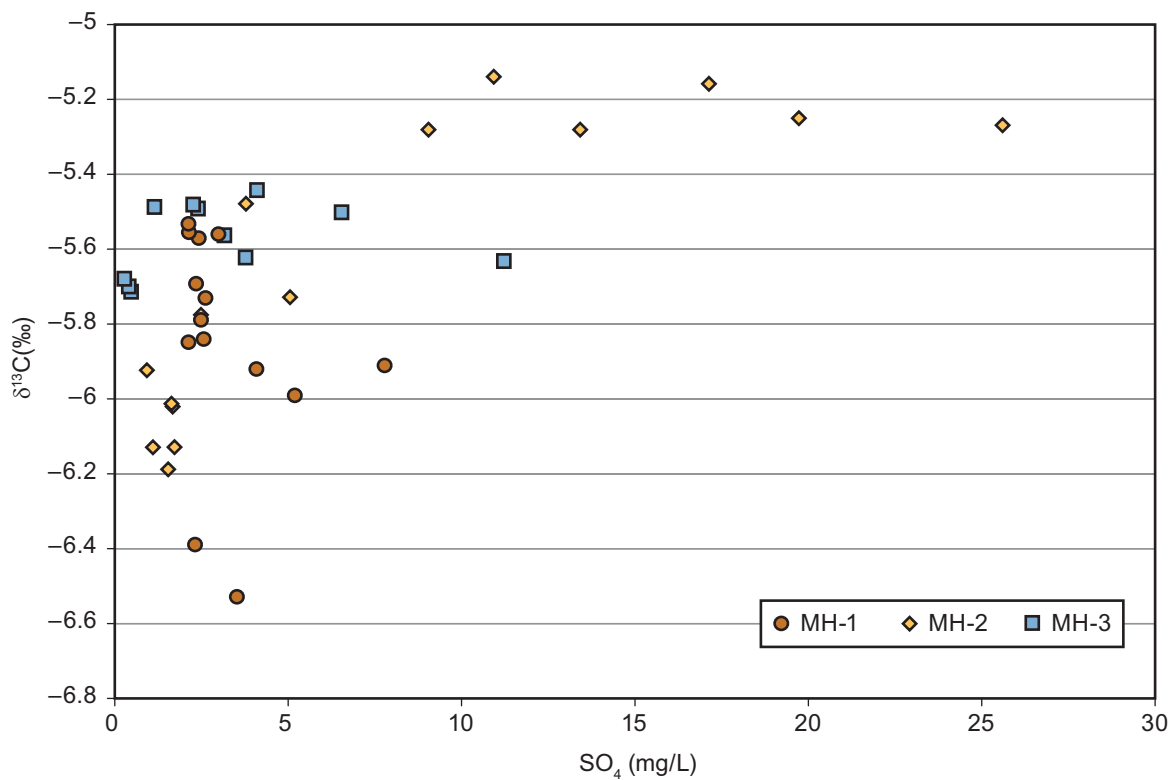


Figure 81 δ¹³C of DIC plotted versus sulfate concentration for MH-1, MH-2, and MH-3.

chemical modeling study was conducted. The hypothesis to be tested was that the introduction of O_2 into the aquifer could oxidize iron in the water, causing concentrations of both to decrease while also oxidizing pyrite, thus increasing sulfate concentrations and allowing for the potential for microbes within the aquifer to convert the remaining O_2 into CO_2 .

A batch geochemical model was built using the program React (Bethke and Yeakel, 2007) to test whether the observed changes were caused by leakage of CO_2 from the reservoir into the groundwater system or by the introduction of O_2 into the aquifer during construction of the monitoring wells. The model began with the introduction of the appropriate gas that then interacted with the groundwater and the aquifer minerals (Table 5). The program Ucode (Poeter et al., 2005) iteratively ran the models while adjusting the parameters to achieve closer fits to the data. Bicarbonate (HCO_3^-) was used as the surrogate for CO_2 leakage be-

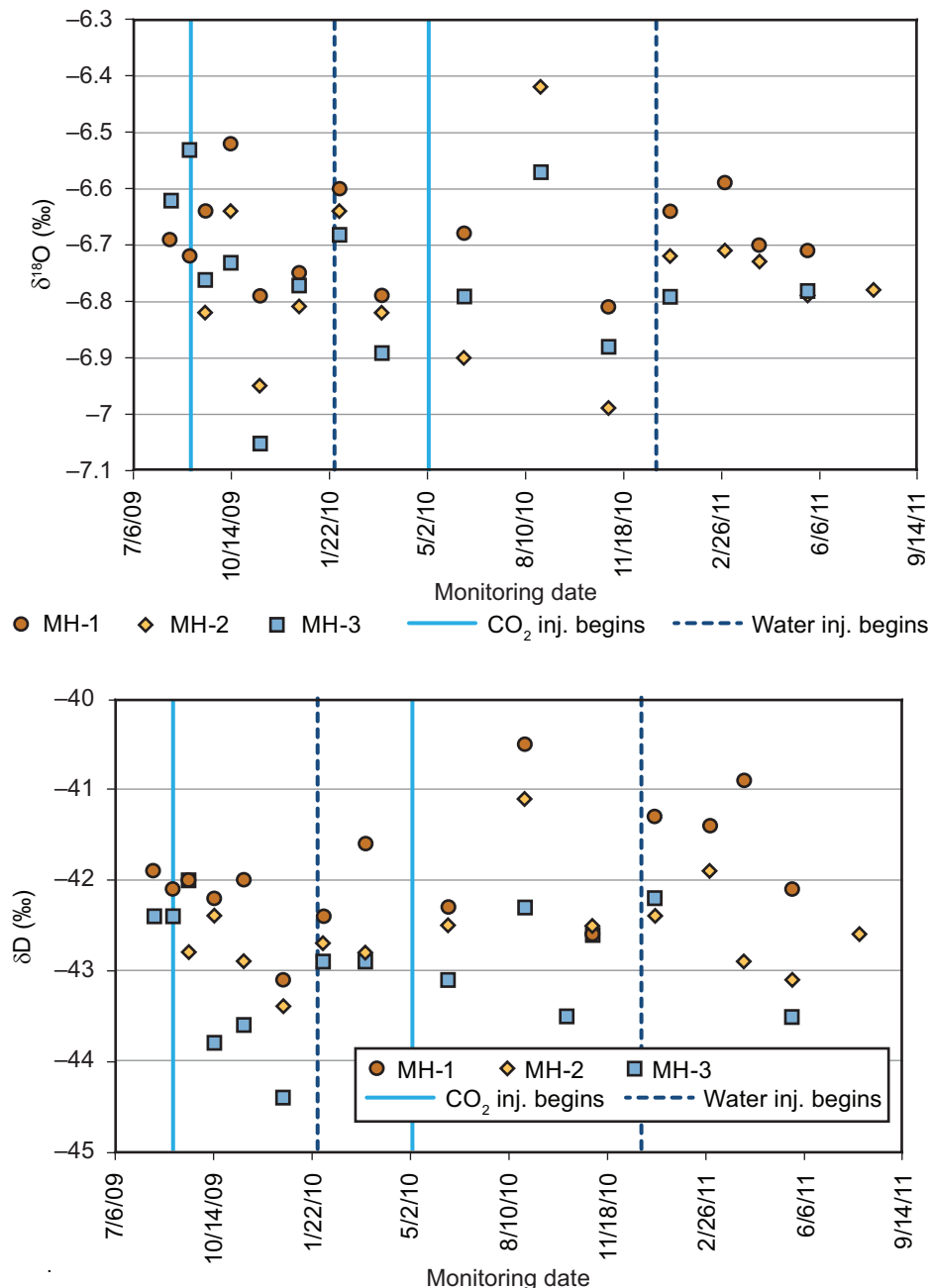


Figure 82 (top) $\delta^{18}O$ and (bottom) δD for MH-1, MH-2, and MH-3 over entire monitoring period.

cause HCO_3^- is the dominant form of inorganic carbon at the pH conditions observed for the groundwater.

The results of both models produced an HCO_3^- spike similar to the observed data (Figure 83). The delay in CO_2 production in the O_2 contamination model (Figure 83) was due to microbial kinetics and the growth time needed to build up an oxygen-reducing population (Figure 84). There was an offset in the start of the CO_2 model so that it coincided with the start of CO_2 injection.

In the CO_2 leakage model, there was little effect on the sulfur concentration in the groundwater, whereas the O_2 contamination model provided a reasonable fit to the data (Figure 85). The model indicated that an increase in pH or oxidation (via the introduction of O_2) could cause the dissolution of pyrite, but the addition of only CO_2 into the model caused neither of these effects. The introduction of O_2 , however, oxidized the pyrite that, in the model, then acted as an electron source to promote microbial growth, which subsequently increased CO_2 concentrations.

The addition of CO_2 caused siderite to precipitate, resulting in a minor decrease in iron concentrations. As the addition of CO_2 continued, the water became more acidic, and siderite began to dissolve. Iron oxides precipitate in the O_2 model, causing a significant decrease in iron concentrations. The occurrence of the iron spike in the O_2 model may not exactly match observed data because iron-sulfur redox reactions were not incorporated into the model.

Overall, the model simulating a CO_2 leak does not provide a good match to all of the measured data. There is reasonable certainty that O_2 was introduced into the zone near the wellbore of the monitoring well during well construction and development. Those data provided an excellent opportunity to test the ability of modeling to determine the source of CO_2 in the shallow subsurface. This modeling was only possible because the complete ion chemistry of the groundwater was analyzed. The O_2 model may be further refined in the future to improve the model's fit to observations and thereby gain a better understanding of the processes involved.

Cased Hole Logging

A comprehensive report comparing and interpreting the pre- and post- CO_2 cased hole logs is in Appendix 8. The interpretations show that there is no indication of CO_2 in the near-wellbore region of the wells logged. The RST sigma readings were considered identical and interpreted to indicate the presence of liquid only.

After the tubing and packer of BU-1 was removed, CO_2 started to return to the surface. Because of operational and safety concerns by the logging company and the operator, it was decided not to log this well during the post- CO_2 injection survey. It was possible to log these wells through tubing. However, after nine months of water injection, it was thought that CO_2 would no longer be around the wellbore of BU-1.

CO_2 SEQUESTRATION AND EOR: INTERPRETATION, ANALYSIS AND RESERVOIR MODELING

Bald Unit Pilot Area Reservoir Model Calibration

The pilot was designed to measure and record data that could be used to calibrate a reservoir simulation model of the Clore sandstone of the Bald Unit in order to estimate the CO_2 EOR and storage capacity. The field pilot data collected directly do not adequately quantify the CO_2 EOR or storage capacity. For example, it is not possible to eliminate the effect of the loss of CO_2 EOR directly from field data as a result of periods when CO_2 was not delivered to the site. A model calibrated to the measured field data can provide more representative CO_2 EOR and storage estimates. Through the use of a calibrated model, continuous CO_2 injection can be simulated and the resulting EOR estimated. Other examples of model scenarios to improve the EOR estimate are using injection rates at maximum regulated injection pressure, adding additional CO_2 injection wells, placing back-pressure on the producing wells to estimate a miscible flood, and employing infill drilling to achieve smaller CO_2 injection patterns.

The Bald Unit model calibration included less than a year of primary production and 34 years of

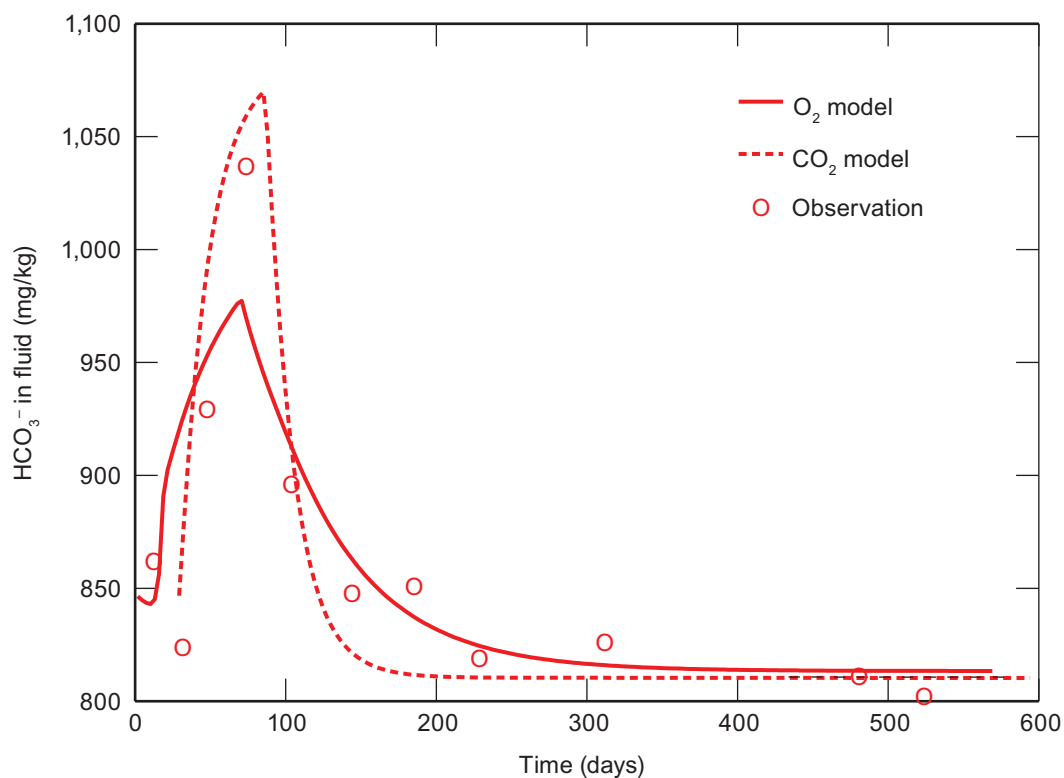


Figure 83 Observed and modeled concentrations of HCO_3^- in groundwater collected from MH-2. HCO_3^- is the dominant form of inorganic carbon at the observed pH levels. Time zero equals introduction of the appropriate gas into the groundwater.

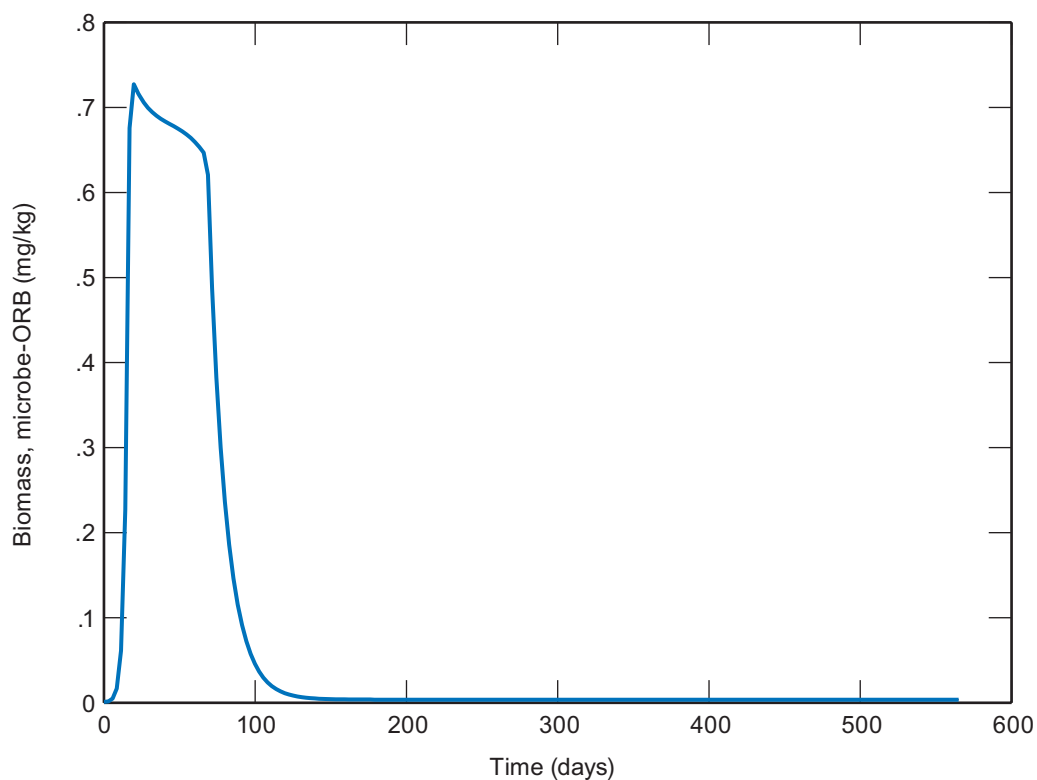


Figure 84 Mass of oxygen-reducing bacteria over time in the O_2 -driven model.

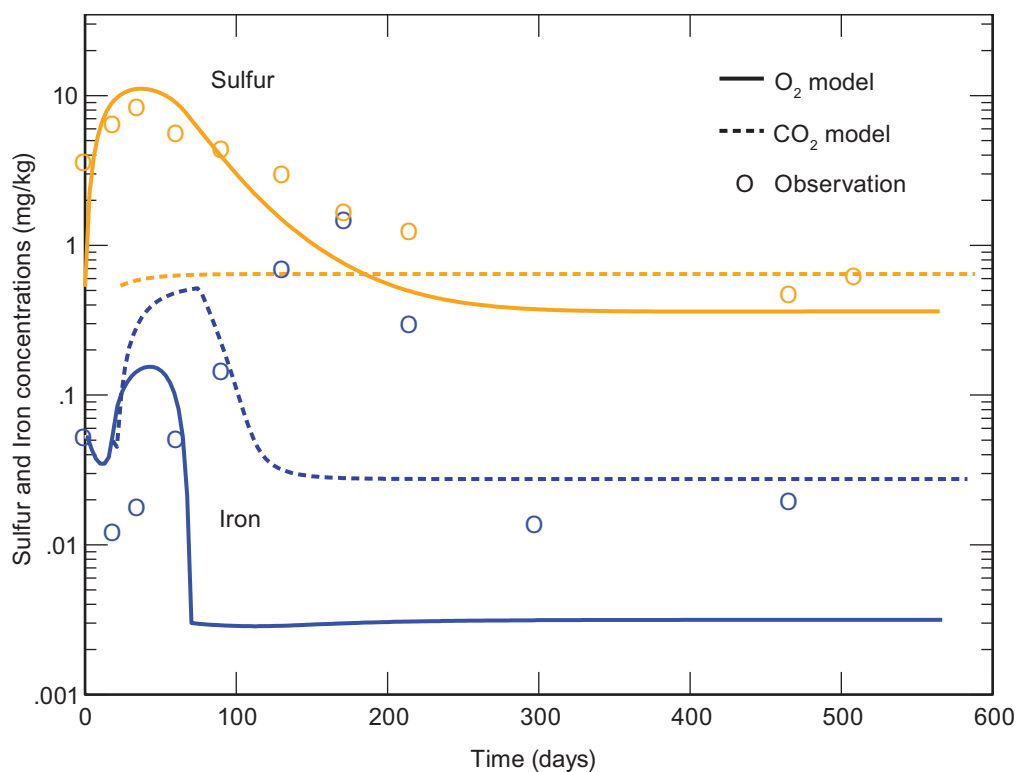


Figure 85 Measured and model-generated iron and sulfur concentrations in groundwater collected from well MH-2.

waterflooding, followed by about 4.5 months of CO₂ injection, 3.5 months of water injection, 8 months of CO₂ injection, and 10 months of water injection at BU-1. The calibration included changes to the geologic model, injection and production pressures, relative permeability, aquifer properties, and each well's skin factor.

Description of Geologic and Reservoir Models and Input Parameters

The reservoir model used to conduct reservoir simulations used a geostatistically generated geologic model (as described in the Geologic Characterization: Reservoir Geology section). The geological model was generated using the Isatis software package and then was input to the VIP Reservoir Simulation Suite for reservoir modeling. The permeability, porosity, reservoir thickness, well locations, and depth from the up-scaled geostatistical model were used as inputs in the reservoir model. The reservoir model consisted of 33 × 59 × 23 gridblocks in the x-, y-, and z-directions, respectively, i.e., 44,781 gridblocks (Figure 86). Each gridblock had dimensions of 24.4 m × 24.4 m × 0.610 m (80 ft × 80 ft × 2 ft).

To eliminate portions of the model considered non-reservoir, a porosity cut-off of 16%, which is equivalent to a permeability cut-off of approximately $1.83 \times 10^{-14} \text{ m}^2$ (18.5 mD), was applied to the model. The number of active gridblocks was 17,006.

The reservoir datum is located about 591.3 m (1,940 ft) below ground level and the water-oil contact is 591.4 m (1,940.4 ft) below ground level. Completion intervals of the wells were taken from well records and communication with Gallagher Drilling, Inc.

A five-component Peng-Robinson equation of state (EOS) was used to generate pressure-volume-temperature (PVT) properties of the crude oil. The five pseudo-components used to characterize the crude oil were CO₂, C₁, C₂, C₆, and C₂₅. The mole fractions of the pseudo-components (Table 10) were adjusted until the EOS-derived fluid properties matched the observed density and viscosity of the Mumford Hills fluids, which were 0.85 g/cm³ and 4.68 cP, respectively, at initial reservoir pressure (~940 psia) and temperature

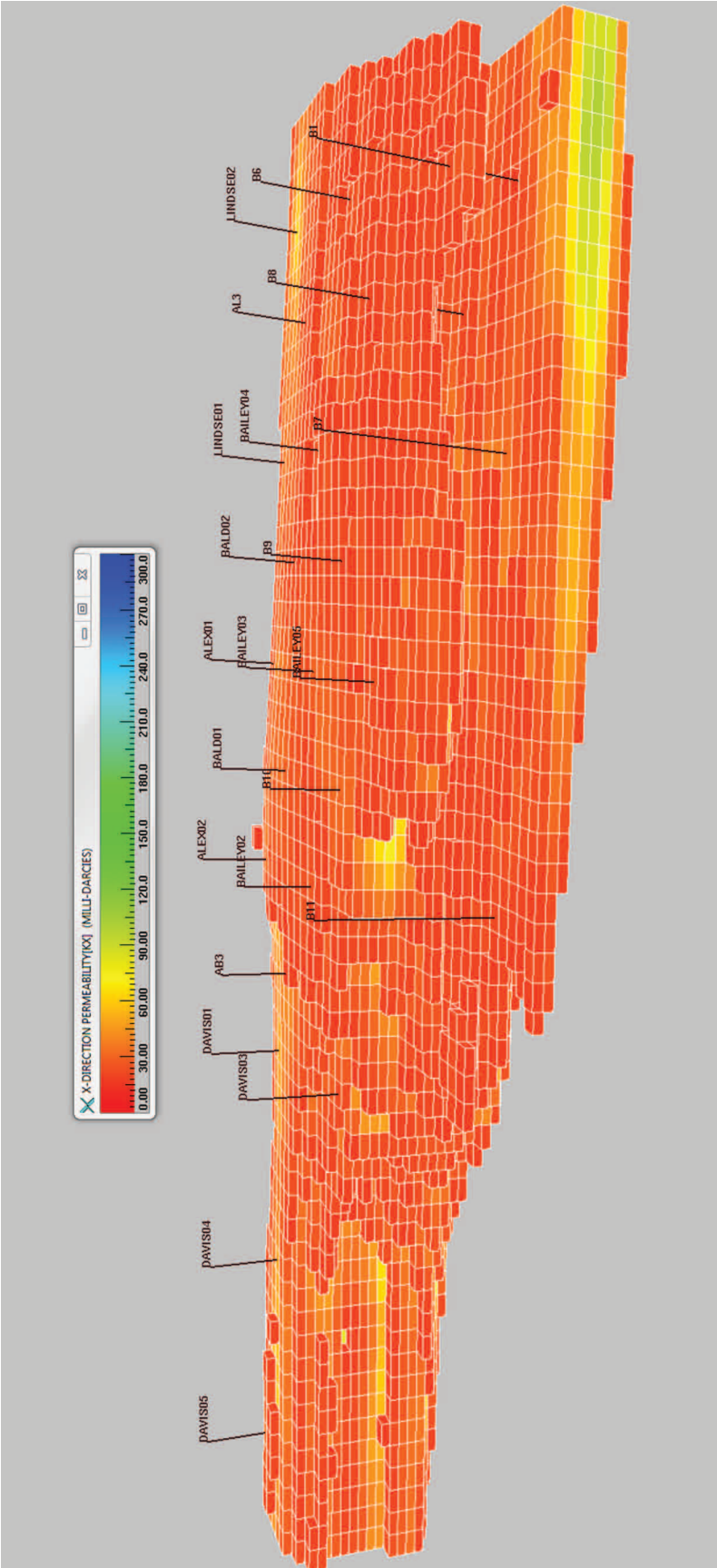


Figure 86 3-D geologic model of Mumford Hills depicting permeability distribution (South-North view).

($\sim 26.7^{\circ}\text{C}$ [$\sim 80^{\circ}\text{F}$]). Pederson's correlation was used to calculate the viscosity of the crude oil. Generalized water-oil and gas-oil relative permeability correlations were used in the simulations. Figure 87 shows the initial water-oil relative permeability curves. The irreducible water saturation employed was 0.35. Capillary pressure was assumed negligible; and, as a result, relative permeability hysteresis effect was assumed negligible. Table 11 shows the brine properties and rock compressibility.

Table 10 Mole fractions of the pseudo-components used in the five-component equation of state to match crude oil properties at Bald Unit.

Component	Mole fraction
CO ₂	0.01
C ₁	0.10
C ₂	0.16
C ₆	0.14
C ₂₅	0.59

Table 11 Reservoir brine and rock parameters.

Parameter ¹	Value
ρ_{wb}	1.1 g/cm ³ (69 lb/ft ³)
Bwi	1.01 rb/stb
μ_w	1.0 cP
cw	3.0×10^{-6} psi ⁻¹
cr	5.0×10^{-6} psi ⁻¹

¹Abbreviations: ρ_{wb} —stock tank water density; Bwi—water formation volume factor; μ_w —water viscosity; cw— water compressibility; cr—rock compressibility.

Based on generalities of Illinois Basin geology and oil field operations, the following assumptions were made in the simulations:

1. All wells were produced at a bottomhole pressure (BHP) of 3,280 kPa (475 psi) during the primary and early part of waterflooding. All production wells were pumped off as of January 1, 1986 (to present) at a BHP of 172 kPa (25 psi).
2. No-flow boundaries were imposed on the western and eastern edges of the geologic model. Aquifer support to the reservoir was from the southern and northern edges of the model.
3. Capillary pressures between oil and water and between gas and water were considered negligible. As such, the numerical model assumed that the thickness of the transition zone between oil and water was zero, i.e., there was a sharp interface between oil and water.
4. Pressure within the reservoir was hydrostatic, i.e., the reservoir was considered to be neither over-pressured nor under-pressured.
5. The crude oil in the reservoir was assumed to contain very small amounts or proportions of dissolved hydrocarbon gas.

Water-oil relative permeability data were available for the Clore sandstone reservoir. The values for S_{wr} , k_{rw} , $S_{g,max}$, $k_{rg,max}$, $k_{row,max}$, and $k_{rog,max}$ that are shown in Table 12 reflect the irreducible water saturation, relative permeability of water at residual oil saturation, maximum gas saturation, maximum relative permeability of gas, oil relative permeability at irreducible water saturation, and oil relative permeability at residual gas saturation in the reservoir, respectively. These were the initial values for the history match based on sandstones in general, and the final or calibrated relative permeability end points to the Mumford Hills history match.

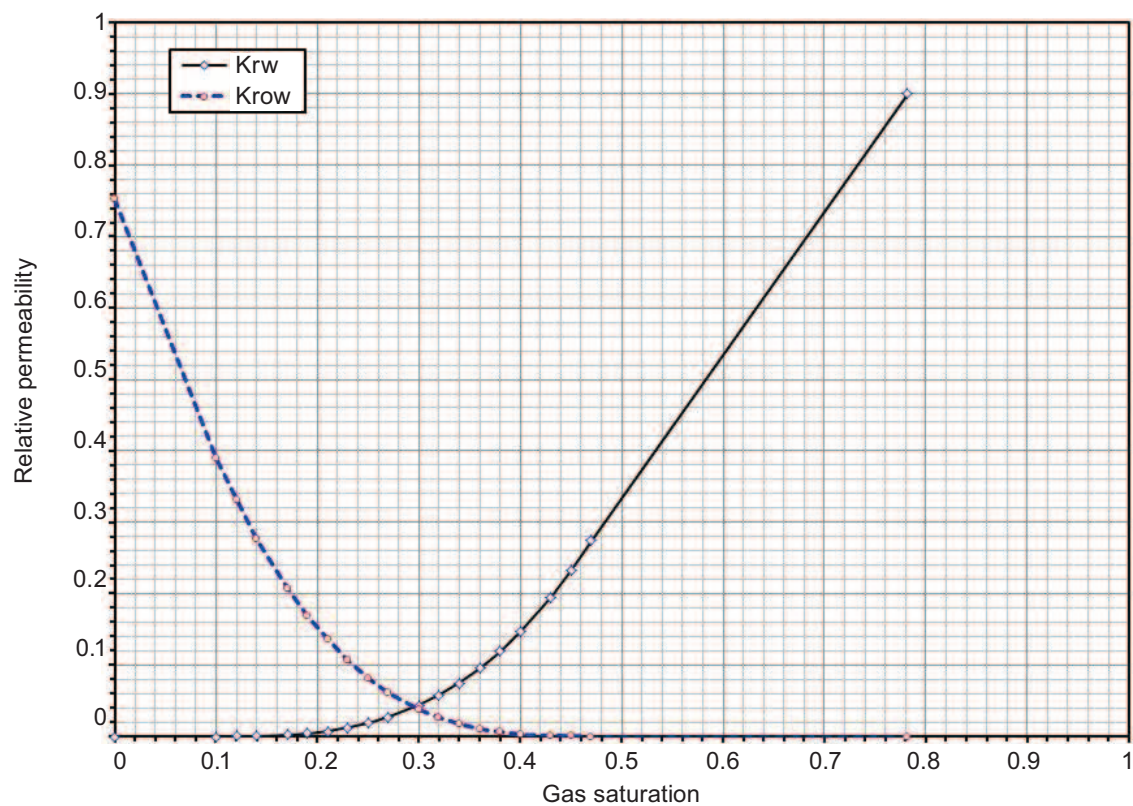
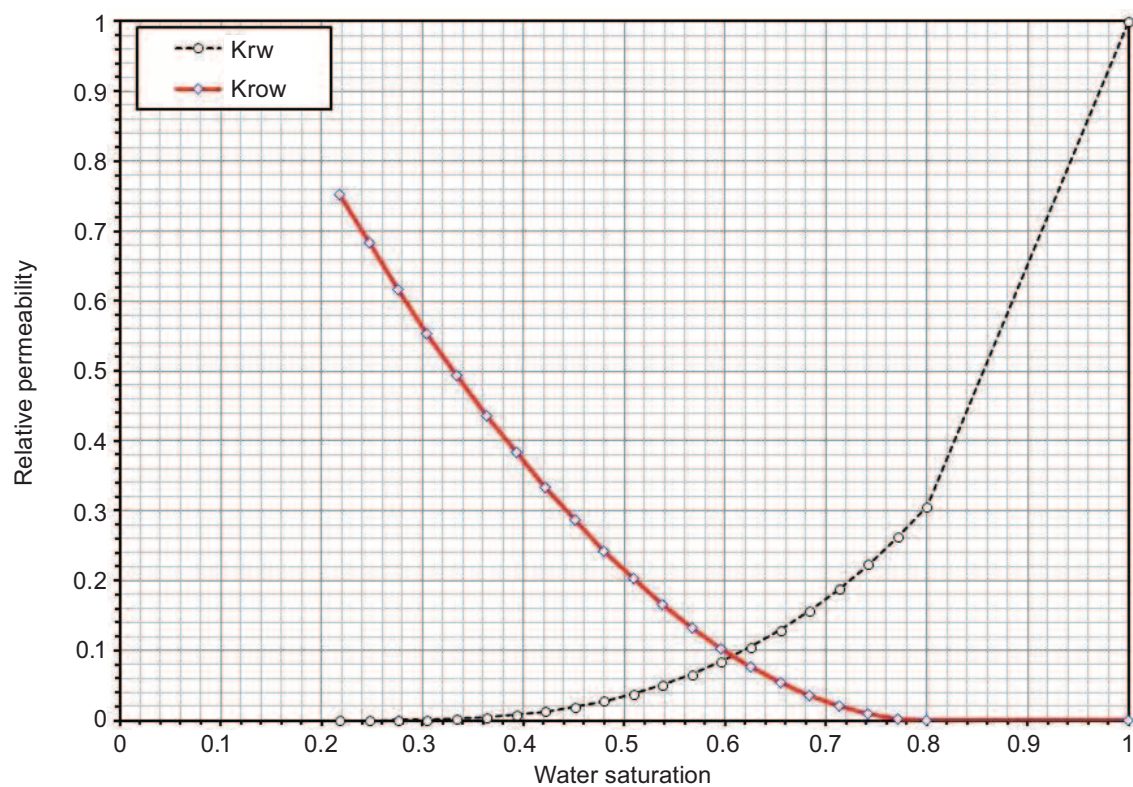


Figure 87 (top) Water–oil and (bottom) gas–oil relative permeability curves used in reservoir simulations.

Table 12 Saturation and relative permeability end points.

Parameter ¹	Initial value	Calibrated value
S_{wr}	0.22	0.22
$K_{rw@Sor}$	0.31	0.31
$S_{g,max}$	0.78	0.78
$K_{rg,max}$	0.90	0.9
$K_{row,max}$	0.75	0.75
$K_{rog,max}$	0.75	0.75

¹Abbreviations: S_{wr} , the irreducible water saturation; $K_{rw@Sor}$, relative permeability of water at residual oil saturation; $S_{g,max}$, maximum gas saturation; $K_{rg,max}$, maximum relative permeability of gas; $K_{row,max}$, oil relative permeability at irreducible water saturation; and $K_{rog,max}$, oil relative permeability at residual gas saturation in the reservoir.

Description of the Calibrated Model

The reservoir model was calibrated by specifying the total liquid production and matching historical oil production, historical water production, and water injection history data for all five leases in the Bald Unit. Even though field data were available by well, fluid production values were allocated based on periodic barrel tests. Fluid relative permeability values used in the simulations were iteratively adjusted to achieve a good match with oil and/or water production and water injection. The exact dates when wells became active or were shut-in were implemented in the simulations. In cases where precise dates were unavailable, the last day of the month was used.

Primary Recovery All of the wells except BD-4, BD-5, and DL-2 were simulated as production wells during primary recovery. BD-4 and BD-5 were drilled after February 1975, and DL-2 was drilled in 1974. Figure 88 shows column charts of simulated and field cumulative oil production by well at the end of primary recovery. The simulated values closely matched the field data.

Waterflood Recovery Wells BD-5 and BD-3 were converted to an injection well and Pennsylvanian water supply well, respectively, during waterflooding. Based on tubing head pressure (THP) data provided by the operator, the BHP for injection wells was set at 15.2 MPa (2,150 psi).

Adjustments to the oil-water relative permeability were made to match the waterflood history; the calibrated model's relative permeability curves are in Table 12. A comparison of simulated and field cumulative primary (oil and water) production by well (Figures 89 and 90) shows a reasonable match between the simulated and field cumulative oil production. However, a better match between the simulated and field cumulative water production was achieved (Figure 90). Figure 91 also shows a very good match between the simulated cumulative water injected during waterflooding and the field data (allocated water production).

After a few preliminary reservoir model simulations of produced water breakthrough time earlier than historically observed in the Bald Unit, a lower permeability interval was incorporated into the geocellular model in order to reduce the time at which water breakthrough occurred in the model from the underlying aquifer. The interval represented a thin layer of shaly sandstone or shale that occurred in the middle of the Clore sandstone. It was not included in the original model because it was deemed too small to be of significance and, while visually discernible, did not have a prominent response on the geophysical logs.

CO₂ Pilot CO₂ was injected into BU-1 for about one year, followed by water injection for 12 months. The simulated and field cumulative CO₂ injected were 6,334 tonnes (6,967 tons) and 6,307 tonnes (6,938 tons). The simulated post-CO₂ injection and field cumulative water injected were 6,036 m³ (50,547 bbls) and 6,432 m³ (53,850 barrels) from December 16, 2010, to February 28, 2011.

The modeled BU-1 CO₂ injection rates were matched to the field recorded rates (Figure 93). No CO₂ production occurred in the model during the simulated period of the pilot. The simulated and field oil rates did match well (Figure 92).

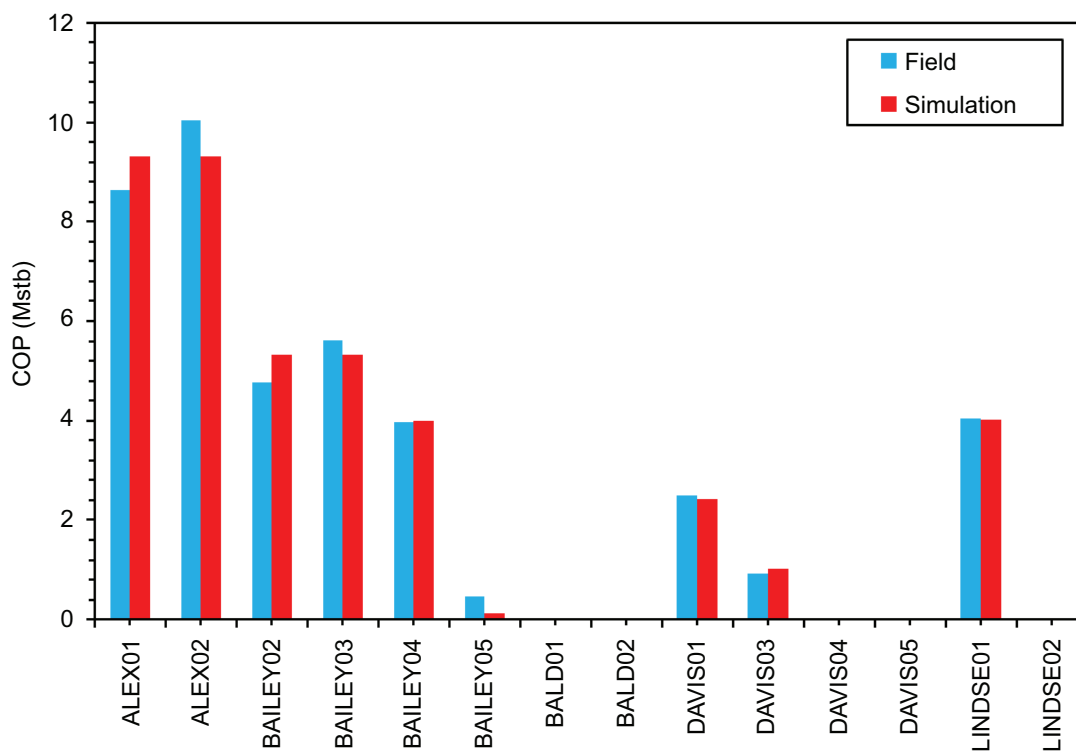


Figure 88 Comparison of simulation results and field data, by well, for cumulative oil production at the end of primary recovery. Alex01 and 02=BA-1 and BA-2; Bailey 02, 03, 04, 05=IB-2, IB-3, IB-4, IB-5; Bald 01 and 02=BU-1 and BU-2; Davis 01, 03, 04, 05=BD-1, BD-3, BD-4, and BD-5; Lindse01 and 02=DL-1 and DL-2.

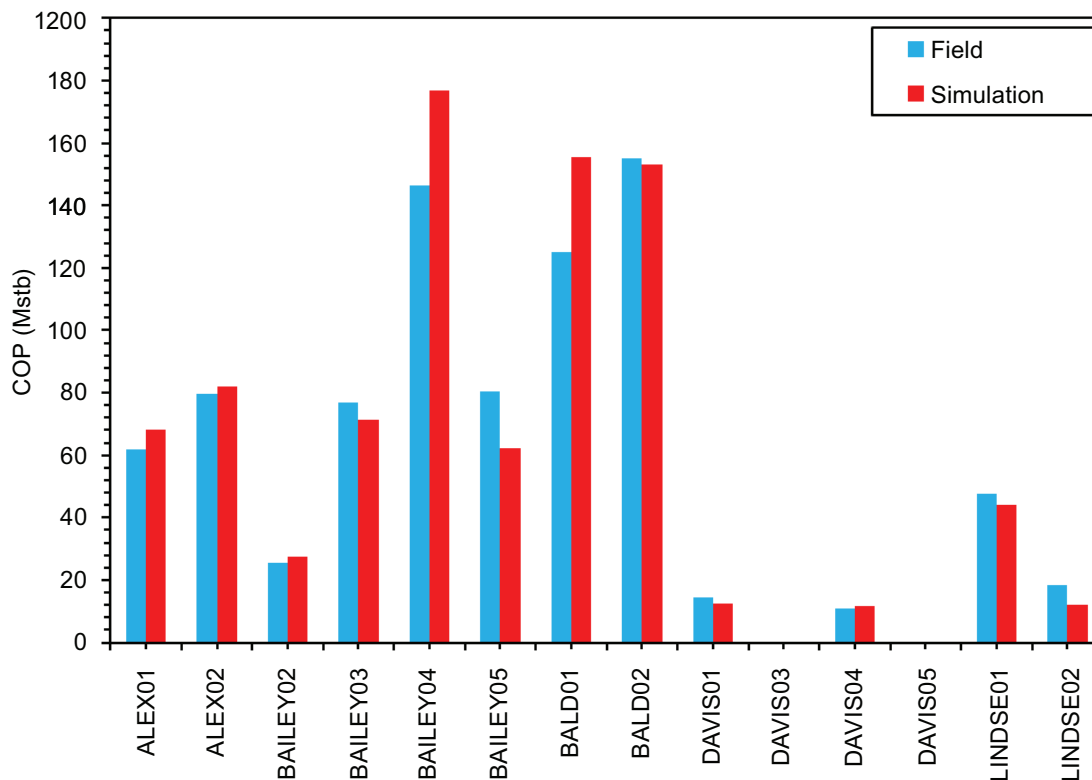


Figure 89 Comparison of simulated values and field data, by well, for oil production at the end of water-flooding (secondary recovery). See Figure 88 caption for explanation of well names.

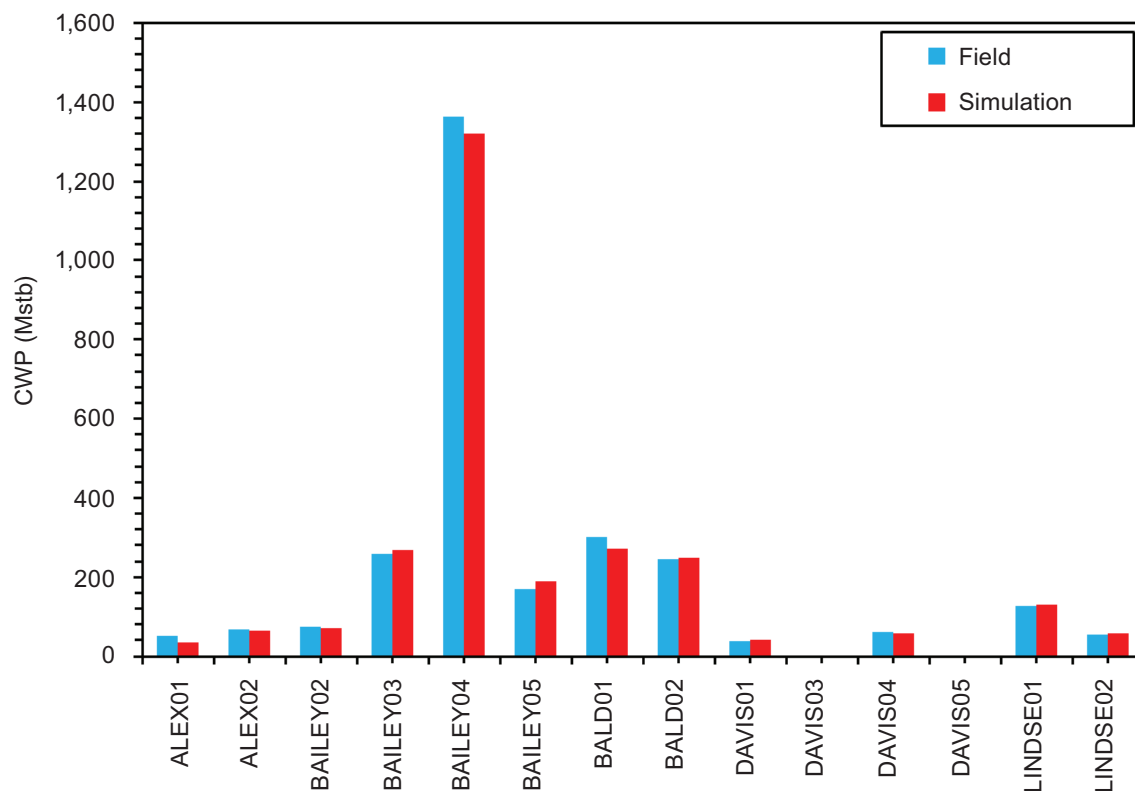


Figure 90 Comparison of simulated values and field data, by well, for water production at the end of water-flooding. See Figure 88 caption for explanation of well names.

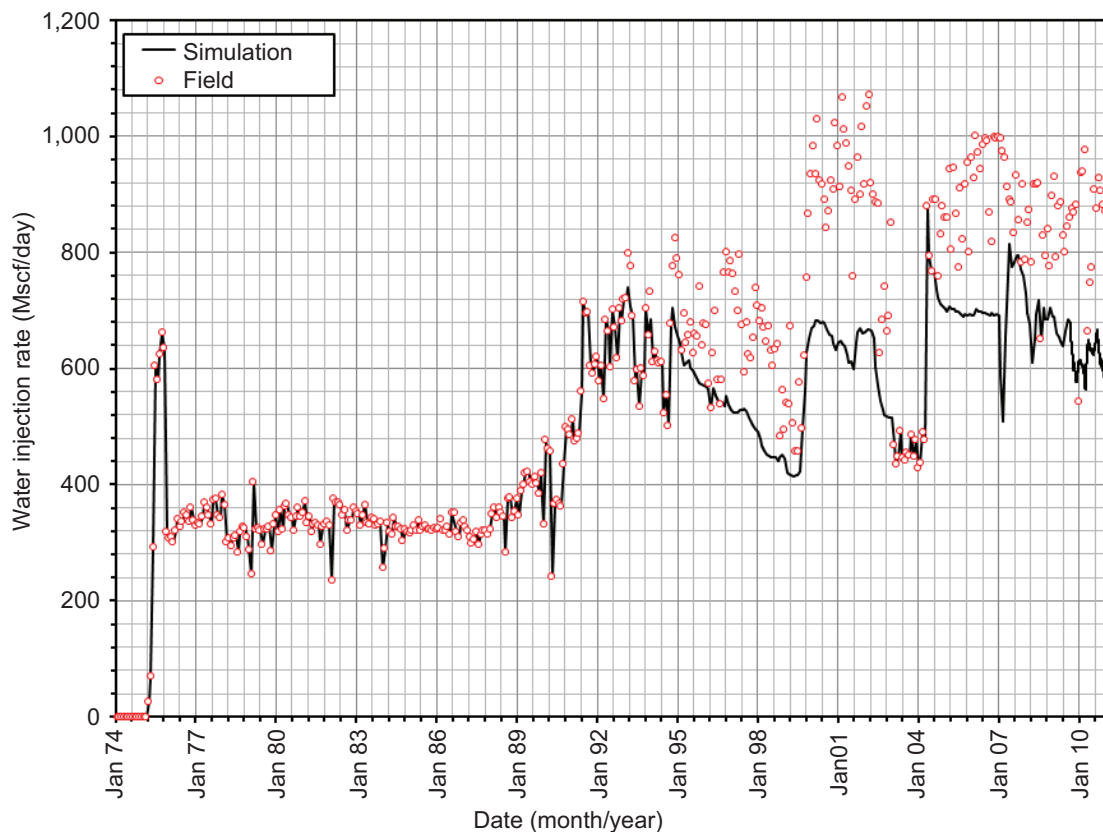


Figure 91 Cumulative water injected during waterflooding via BD-5.

The areal distribution (Figure 94) and cross-section (Figure 95) of the injected CO₂ at the end of the CO₂ injection and after one year of water injection is shown at its greatest extent in layer 17 and in an orthogonal cross section through BU-1.

Pilot Projections Using the Calibrated Model

In a pilot operation, oil rate increases and decreases occur for reasons other than the EOR processes. In the Bald Unit pilot, the oil rate increased due to well work immediately preceding the second CO₂ injection period. Very short term oil rate decreases occurred due to temporarily shutting-in wells and suspending injection. The oil loss from these problems needs to be quantified and excluded from an estimate of CO₂ EOR.

The most significant operational problems that occurred were the cessation of CO₂ injection due to winter road restrictions. Oil production began to increase about one month prior to stopping CO₂ injection and quickly decreased afterwards. If CO₂ had been injected continuously, the oil rate may have continued to climb and sustained higher oil production longer.

In addition to operational effects on oil production during this pilot, the daily delivery of CO₂ and budget constraints kept the field oil response to CO₂ from being maximized. BU-1 was injection rate constrained and not pressure constrained. Delivery of additional CO₂ each day would have allowed maximum injection rates. The logistics in planning truck delivery of CO₂ did not allow day-to-day changes in delivery, so a more regular plan was adopted (one truckload per day and a 2nd truckload every other day). Also, a larger CO₂ budget and injection period would have increased and sustained the field oil production rates.

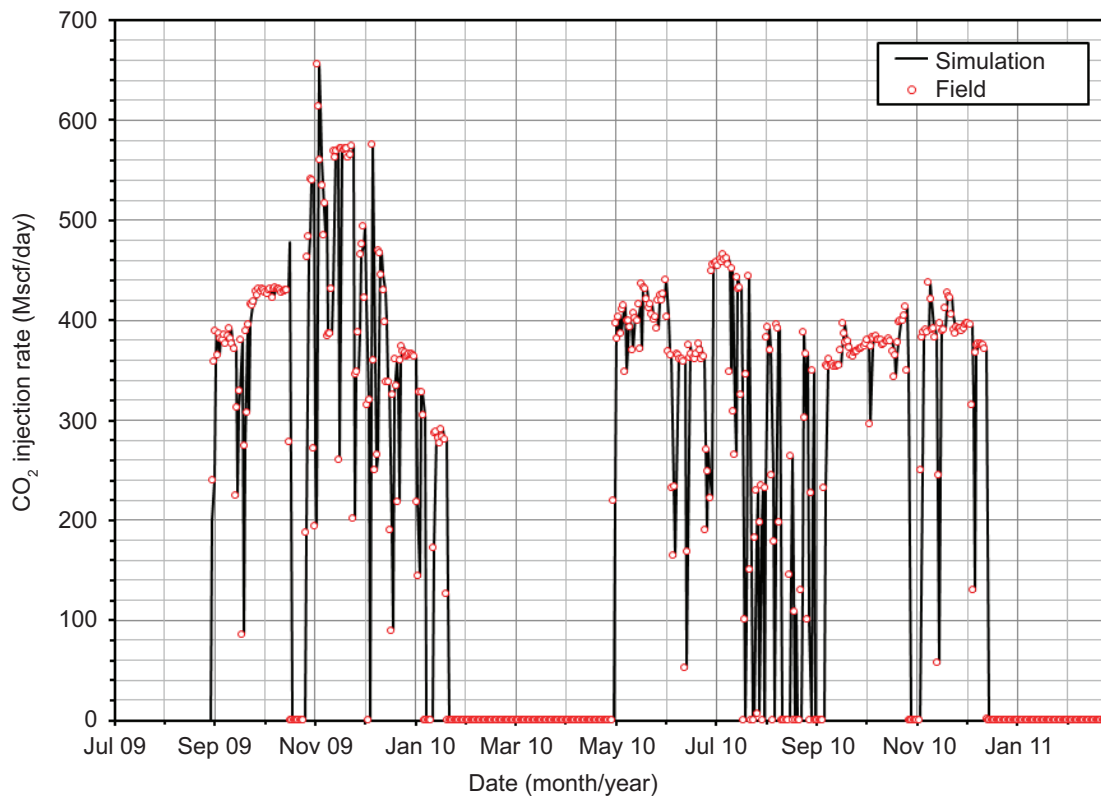


Figure 92 Simulated and field CO₂ injection rates during pilot project.

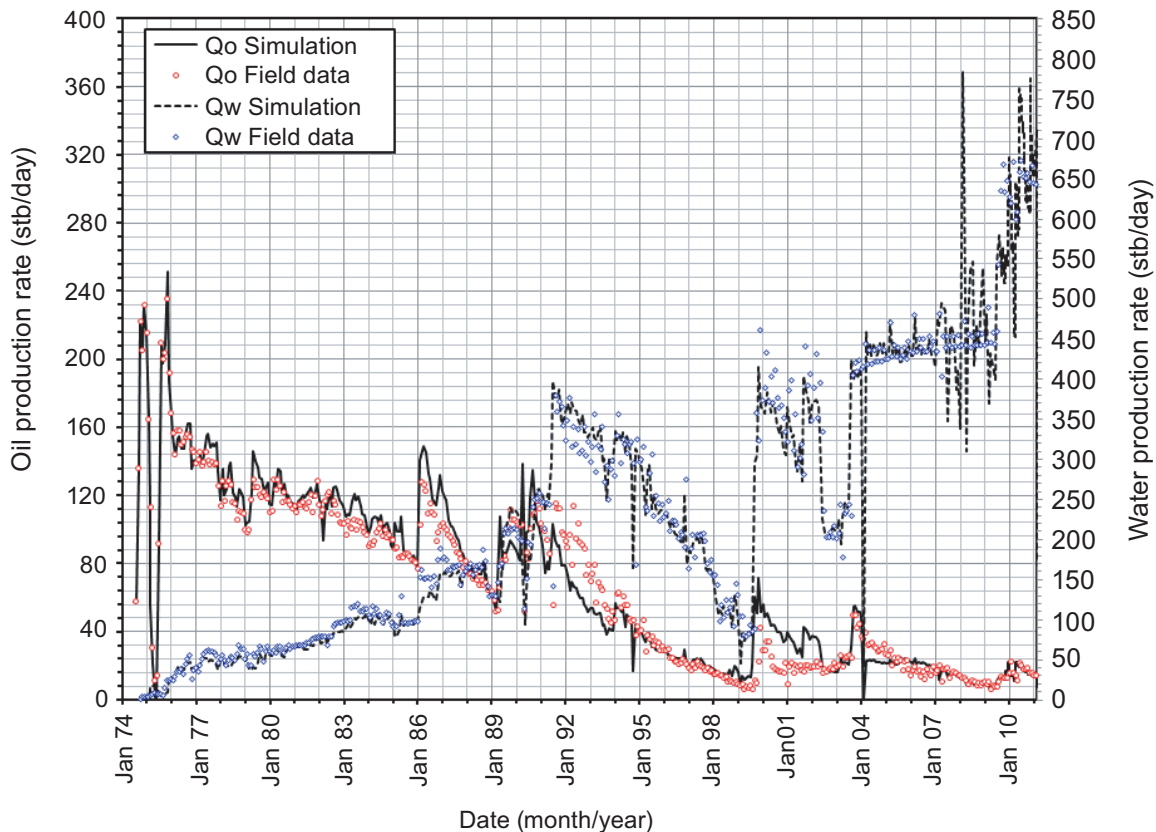


Figure 93 Field oil and water production rates during primary recovery, waterflooding, and CO₂ EOR.

To study the effect on oil recovery, CO₂ storage, and plume size and distribution on the pilot field results, the following scenarios were simulated in the two cases below:

- uninterrupted injection
- longer period of continuous CO₂ injection
- higher CO₂ injection rate
- increased injection pressure

A waterflood baseline case was run to reflect similar scenarios. The CO₂ EOR cases were compared against their respective waterflood baselines to determine the incremental oil production, which was added to the decline curve projection of the actual field oil production rates.

Pilot Case 1: Continuous Production and Injection at Maximum Pressure

In this case, BU-1 CO₂ injection is continuous, and its bottomhole pressure is constrained at the maximum waterflood bottomhole injection pressure, not that requested in the permit application for CO₂ injection for this pilot. CO₂ injection is for 12 months only. This approach eliminates effects of CO₂ delivery schedule and winter road restrictions.

For this scenario, the calibrated model results presented in Table 13 show CO₂ EOR estimates of 7,600 scm (48,000 stb) oil production, which is an oil recovery of 10.7% of OOIP and a CO₂ net utilization of 990 scm/scm (6,200 scf/stb).

Pilot Case 2: Continuous Injection of CO₂ for 5 years with Pilot Case 1 conditions

Using Pilot Case 1, CO₂ injection was continued for a total of 5 years, using bottomhole pressure constraints. This case eliminates the effects of the pilot duration and budget constraints.

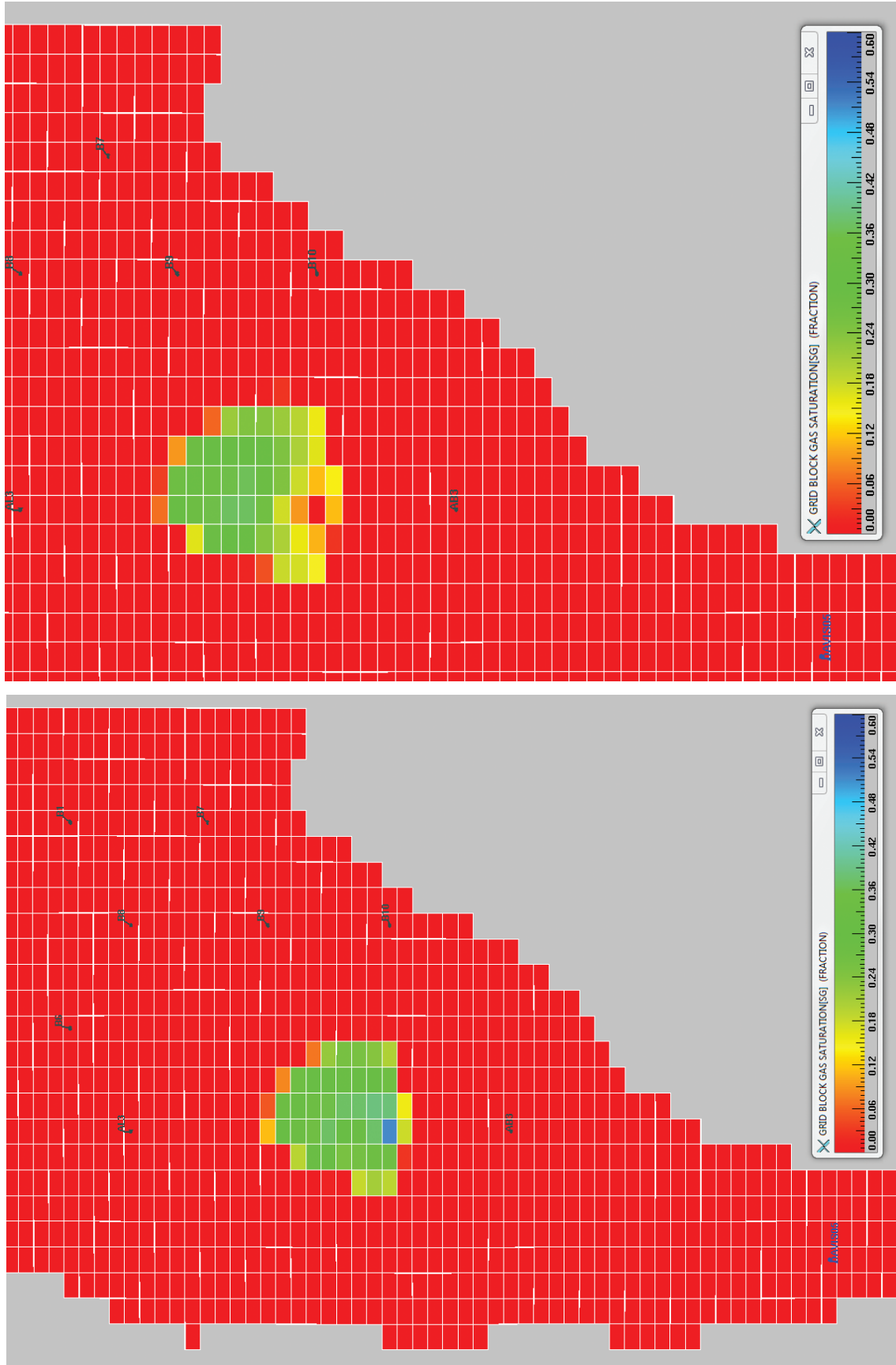


Figure 94 Areal distribution of gas (CO₂) saturation (left) at the end of CO₂ injection and (right) after one year of water injection (layer 17 in the model).

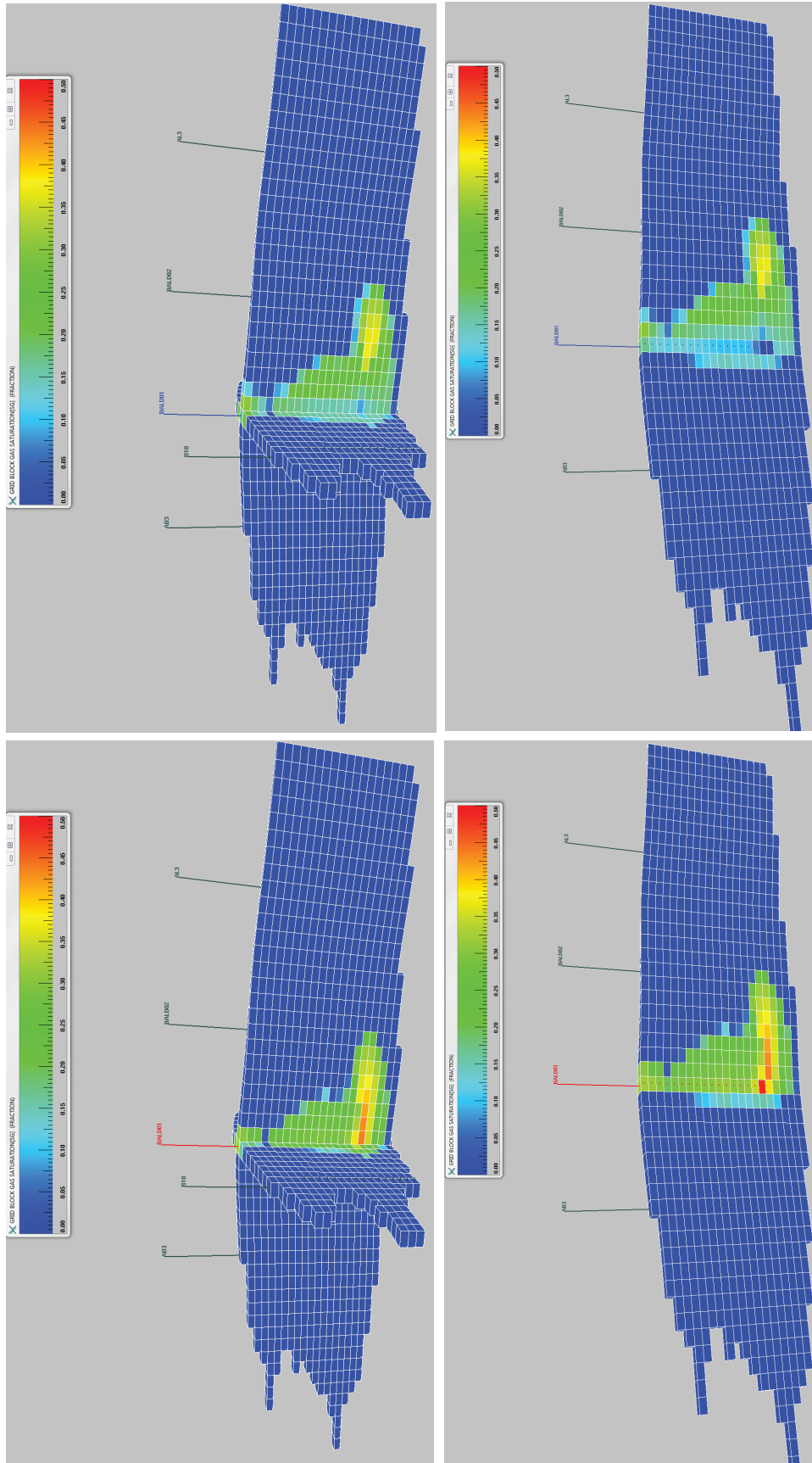


Figure 95 Cross-section of injected CO_2 distribution at the end of CO_2 injection viewed in (upper left) the x-y directions and (lower left) the x-direction, and cross-section of injected CO_2 distribution after one year of water injection viewed in (upper right) the x-y directions and (lower right) the x-direction. Note: All production wells in these figures are shut-in during CO_2 and chase water injection (pilot project).

For this scenario, the calibrated model results presented in Table 13 show CO₂ EOR estimates of 9,900 scm (62,000 stb) oil production, which is an oil recovery of 14% of OOIP and a CO₂ net utilization of 1,600 scm/scm (10,000 scf/stb).

Table 13 EOR and CO₂ utilization for optimized pilot cases.

	Pilot Case 1	Pilot Case 2
EOR (stb)	47,808	62,417
EOR, % OOIP	10.7%	13.9%
Net Utilization (scf/stb)	6,218	10,117
Gross Utilization (scf/stb)	7,861	30,093
CO ₂ Storage (tons)	17,345	36,841.4
CO ₂ Storage Factor (Mscf/stb-OOIP)	0.6634	1.40908
Storage Efficiency, % HCPV ¹	27.7%	59.1%

¹Hydrocarbon pore volume; the storage efficiency is relatively high due to additional storage in the pore space of the aquifer underlying the oil reservoir.

Full Field Projections Using Calibrated Model

Based on the pilot-calibrated model, estimates of full-field implementation of CO₂ injection were of interest. Two scenarios were simulated in which most of the existing oil-producing wells were converted to CO₂ injectors. This represents several regular five-spot patterns that included drilling new production and injection wells. Injection was for 20 years.

A waterflood baseline case was run to reflect similar scenarios. The CO₂ EOR cases were compared with their respective waterflood oil production forecast baselines to determine the incremental oil production, which was added to the decline curve projection of the actual field oil production rates (Figure 96).

The scenarios considered are as follows:

Field Case 1: Full Field CO₂ Injection

In this case, four regular five-spot patterns go through the center-west of the field. Wells DL-1, DL-2, BA-1, BA-2, IB-2, IB-3, IB-4, BD-1, and BD-3 are CO₂ injection wells. BU-1 and BU-2 remain oil producers. Two additional oil production wells and one CO₂ injection well were added to the model to complete the four five-spots (Figure 97a).

Results presented in Table 14 suggest that expansion of simultaneous injection of CO₂ at all Bald Unit wells would increase oil recovery by 17,000 scm (106,000 stb) after 20 years of CO₂ injection, which is an oil recovery of 10% of OOIP and a CO₂ net utilization of 5,500 scm/scm (34,000 scf/stb). The potential CO₂ storage is estimated to be 193,600 tonnes (213,000 tons). Because of the relatively high perm or fault zones, sweep efficiency is lower in parts of the field. Also, a longer injection period would increase oil production.

Field Case 2: Expanded Full Field CO₂ Injection

Field Case 2 is similar to Field Case 1 except that three additional regular five-spot patterns were added to the northeast. At least two of the CO₂ injection wells are very near the water-oil contact. A total of four CO₂ injectors and five oil-producing wells were added to the Field Case 2 model to complete seven five-spot patterns (Figure 97b).

Results presented in Table 14 suggest that expansion of simultaneous injection of CO₂ at all Bald Unit water injection wells and some of the oil-producing wells would increase oil recovery by 27,000 scm (170,000 stb) after 20 years of CO₂ injection. This is an oil recovery of 12% of OOIP and a CO₂ net utilization of 4,900 scm/scm (31,000 scf/stb). The potential CO₂ storage is estimated to be 277,450 tonnes (305, 200 tons).

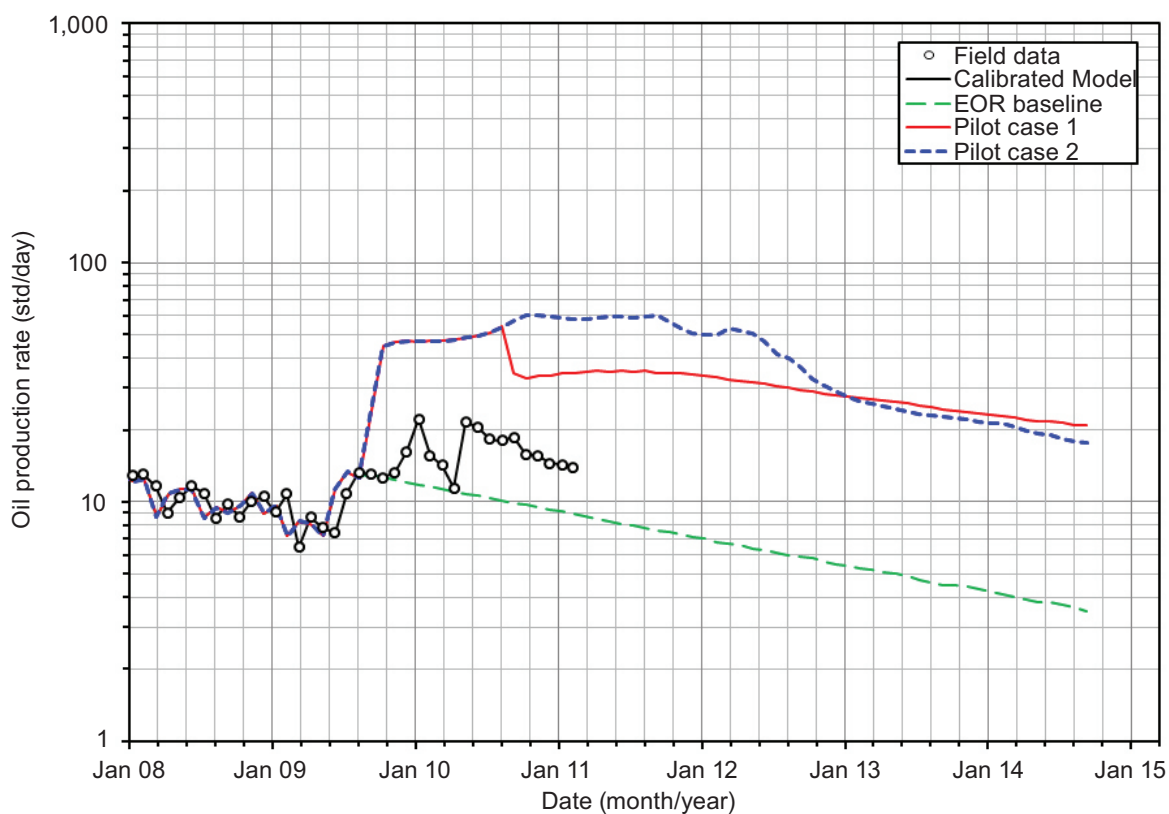


Figure 96 (top) Comparison of simulated oil production rates of Pilot Case 1 and Pilot Case 2 to that of the calibrated model; (bottom) comparison of simulated oil production rates of Field Case 1 and Field Case 2 to that of the calibrated model.

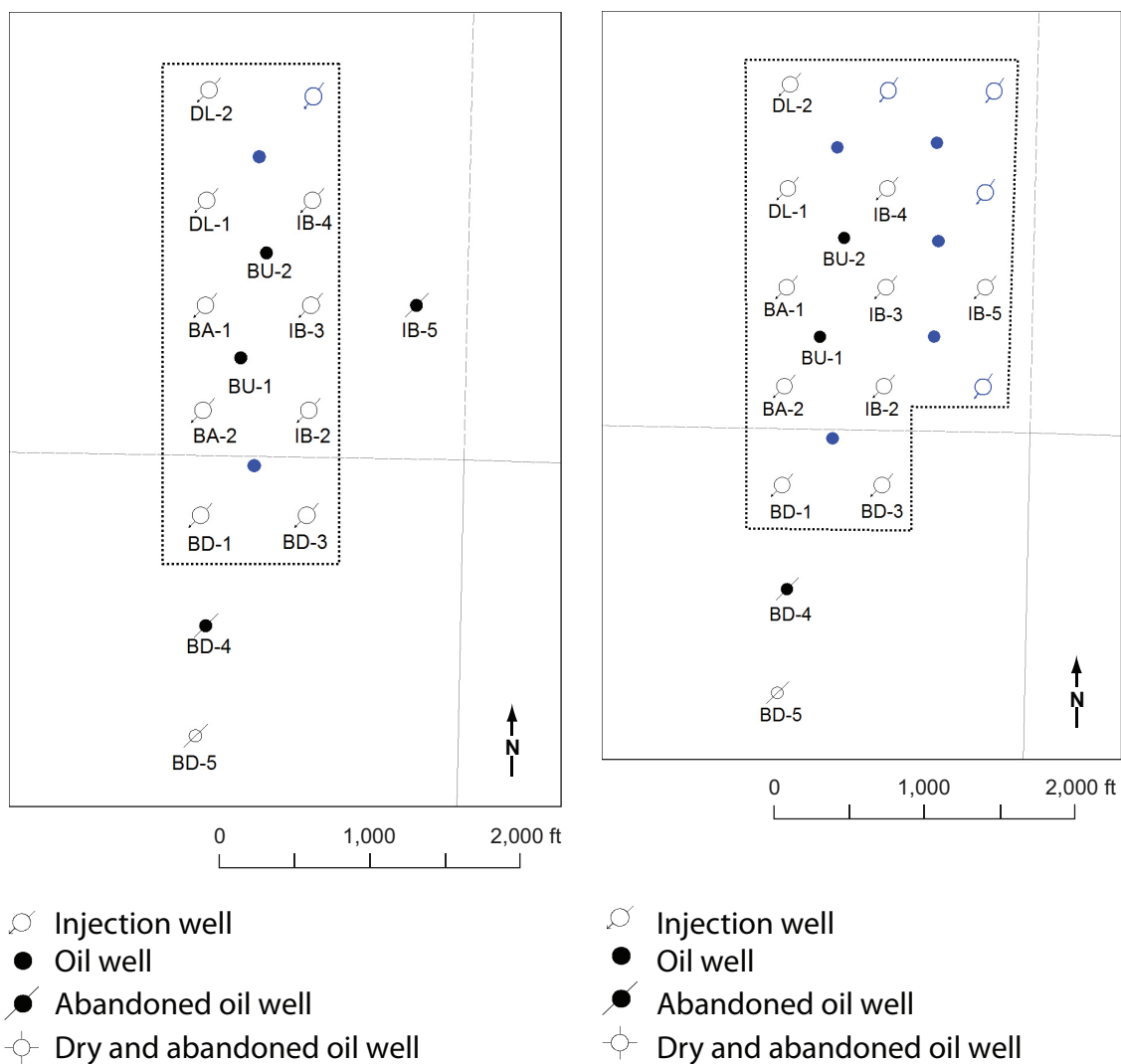


Figure 97 Map of the wells showing the proposed changes to the well pattern according to (left) the first simulation case and (right) the second simulation case. The area enclosed by the dotted line corresponds to the area that was evaluated in each case. Existing wells are shown in black while proposed additional wells are shown in blue.

Table 14 EOR and CO₂ utilization for optimized field-wide cases.

	Field Case 1	Field Case 2
EOR, stb	106,309	169,263
EOR, % OOIP	9.8%	11.8%
Net utilization, scf/stb	34,352	30,907
Gross utilization, scf/stb	203,324	162,250
CO ₂ storage, tons	213,065	305,213
CO ₂ storage factor, Mscf/stb OOIP	3.3605	3.6345
Storage efficiency, % HCPV ¹	131.6%	150.3%

¹Hydrocarbon pore volume; the storage efficiency is relatively high due to additional storage in the pore space of the aquifer underlying the oil reservoir.

Modeling Summary

Because of the continued water injection at BD-5, the wells in the pilot flowed to surface without artificial lift. The reservoir pressure was relatively high, and conditions were such that a miscible flood was present. The high CO₂ storage and oil recovery values in Table 13 show this. Similar to conclusions from the MGSC Phase I modeling, the net utilization of CO₂ is also significantly higher. High CO₂ storage efficiency is related to the definition of storage efficiency with respect to the hydrocarbon pore volume and because the aquifer underlying the oil reservoir was effective in storing CO₂.

The field case oil recovery was similar to that of the pilot area. The CO₂ EOR and storage were higher because of the larger flooded area. The normalized values of utilization and storage factor were higher. Average pressure for the field cases was slightly higher at 9.6 to 13 MPa (1,400 to 1,900 psia). Field Case 2 had a higher CO₂ storage efficiency than did Field Case 1, primarily due to the addition of more injection wells and injected CO₂ volume.

The oil recovery estimated from the Bald Unit Case 2 compares well to the MGSC Phase I estimates of 4.5 to 11%. The CO₂ net utilization is high relative to MGSC Phase I results (820 to 1,600 scm/scm; 4,600 to 9,000 scf/bbl). Low net utilization means that it takes less CO₂ to recover oil than with a higher net utilization.

PILOT CLOSURE

BU-1 continued water injection after completion of the CO₂ injection pilot, so relatively little in the way of site reclamation was required. Pilot closure consisted primarily of plugging and abandoning the groundwater monitoring wells, removing data acquisition equipment from the injection and production wells, and relocating injection equipment from the site.

Plugging and Abandonment of Groundwater Monitoring Wells

Groundwater monitoring wells were plugged and abandoned in October 2011. As required by Indiana Department of Natural Resources regulations, an Indiana Certified water well driller did the plugging and abandonment of the monitoring wells. Each monitoring well was plugged using 0.9525 cm (3/8 inch) Pel-Plug coated bentonite pellets and 0.9525 cm (3/8 in) Baroid Hole Plug from the bottom to the top using the gravity method. The protective casings and the top 1.5 m (5 ft) of pipe were removed as per the Indiana Administrative Code (Article 13, Water Well Drillers).

Removal of Data Acquisition Equipment

Surface and downhole pressure and temperature gauges were removed from the wells in late September and early October 2011. The gauges' calibration was checked to confirm that accurate pressure data were recorded.

Relocation of Injection Equipment

After CO₂ injection was completed, the injection pump skid and line heater were removed from the Bald Unit tank battery area.

CONCLUSIONS

CO₂ Storage Estimate

Assuming 100% recycling of produced CO₂, the CO₂ storage efficiency factor of the Clore sandstone of the Bald Unit oil field is 130 to 150% of HCPV, which is much higher than the MGSC RCSP Phase I results and is attributed to the aquifer underlying the oil reservoir and the completion in the aquifer of some of the injection wells on the eastern part of the model. An estimated 27 tonnes (30 tons) of CO₂ were produced at the surface representing 0.5% of the injected CO₂. Consequently, 99.5% of the injected CO₂ was stored at the Bald Unit Field after nine months of post-CO₂ injection monitoring. The potential CO₂ storage is esti-

mated to be 193,600 to 277,450 tonnes (213,000 to 305,200 tons). Test results showed that a portion of the injected CO₂ is moving into the water-saturated portion of the Clore immediately below the oil reservoir, likely because relative and absolute permeability to CO₂ were shown to increase with depth in the Clore at the Bald Unit. This increased net CO₂ utilization because some of the CO₂ is effectively being trapped below the oil reservoir where it cannot interact with the oil. The net CO₂ utilization was 4,900 scm/scm (31,000 scf/stb).

EOR Estimate

Based on reservoir and geologic modeling, the implementation of full-field CO₂ EOR at Bald Unit, Mumford Hills Field would be 10 to 12% of OOIP or 17,000 to 27,000 scm (106,000 to 107,000 stb); a CO₂ net utilization would be 4,900 to 5,500 scm/scm (31,000 to 34,000 scf/bbl). This oil recovery is within range of the 8 to 16% based on West Texas rules-of-thumb and slightly higher than the 8.6 to 11% miscible-Cypress results from MGSC Phase I (MGSC, 2005). The net utilization is significantly higher than the West Texas rules-of-thumb (900 to 1,800 scm/scm; 5,000 to 10,000 scf/bbl) and MGSC Phase I results (820 to 1,600 scm/scm; 4,600 to 9,000 scf/bbl) (Brock and Bryan, 1990; MGSC, 2005).

General Observations

Oil production directly from the Field was immediately affected by all shut-in periods of CO₂ injection, primarily the three to four winter months when delivery of CO₂ via semi-truck tanks was prohibited on the township roads leading to the Bald Unit. When CO₂ injection resumed, the oil rate did not reach the pre-shut-in level. The reason for the reduction in oil rate is not certain, but it is likely a result of an oil bank created by the CO₂, which was compromised. The oil bank was not achieved again after CO₂ injection resumed.

A simple, regular chemical corrosion treatment plan was not possible because the wells were produced using downhole packers. Consequently, corrosion was observed in one of the four producing wells. A CO₂-resistant, lined tubing option should be considered for wells that cannot be treated chemically. Alternatively, the batch treatment recommended by Baker-Hughes could be attempted.

Establishing a CO₂ EOR oil production baseline is difficult when pre-CO₂ injection well work is required to prepare wells for the pilot. Optimally, the well work would occur several months before start-up so that the baseline could more clearly be identified.

Effectiveness of Operations

Overall the operations were effective at meeting the objectives of the project with the given budget and project duration constraints. In general, pilots that have multiple injectors and patterns can give better representation of actual full-field deployment of CO₂ injection compared to a single injection well pilot.

An injection skid was designed and built that worked similarly to Illinois Basin waterflood operations. Consequently, an oil field operator familiar with waterflooding technology may find this design similar to currently used water injection equipment. The data acquisition system allowed for remote monitoring of operations such that a 24-hr operator was not required.

Real operational problems were encountered, which improved the general understanding of CO₂ EOR field deployment challenges. Problems are unavoidable but could have had lower impact on oil production if more wells and patterns were involved in the pilot.

Effectiveness of MVA Techniques

Measurements of groundwater chemistry before, during, and after CO₂ injection confirm that shallow Pennsylvanian aquifers at the Bald Unit pilot site were not affected by CO₂ injection. Measurements of brine and

gas chemistry in the Clore sandstone oil reservoir over the same period were successful in tracking the path of CO₂ migration. Moreover, the measurements provided sufficient data from which to infer the potential trapping of CO₂ through solubility trapping and geochemical reactions among CO₂, brine, and rock forming minerals.

Pre-injection brine characterization had an important role in reservoir characterization. pH measurements in the field are relatively simple and reliable for early indication of CO₂ breakthrough.

RECOMMENDATIONS

In the CO₂ EOR process the volume of CO₂ stored will always be less than the volume injected even when produced CO₂ is recycled. It is unreasonable to expect that all injected CO₂ can be accounted for in an active oil field operation. Leaks around producing and injection wellheads and related plumbing, injection line leaks, well workovers, and cased hole logging procedures all allow minor CO₂ to leave the CO₂ EOR system of reservoir, wells, and surface facilities. Some type of general and reasonable accounting guidelines for various types of CO₂ releases must be developed to account for the released CO₂ but not necessarily exactly quantify it for a specific event. For example, a producing well may be assigned a specific value of released CO₂ via a leaky wellhead based on its CO₂ production rate. Similarly, well workovers may be assigned a certain mass of CO₂ release instead of attempting to devise some means of measuring CO₂ that would be nearly impossible to meter and quantify during a well workover. Organizations and societies that deal with auditing (e.g., American Institute of Certified Public Accountants) have general guidelines for other industries that can likely be adapted to CO₂ sequestration in general and specifically to oil field EOR projects.

More single-well production tests would improve the rate allocation at each well. The method for allocating the oil and water rates to each well was suspect and introduced an unquantifiable amount of uncertainty into the analysis of the pilot performance. A better constraint on the amount of oil and water produced at each well would greatly improve the reservoir model calibration as well as the assessment of the overall pilot performance.

More regular delivery of CO₂ would have maintained the injection at the regulated bottomhole pressure, which would have increased oil production attributable to CO₂ directly. However, CO₂ availability, impracticality of two to three truckload deliveries per day, and winter road weight restrictions were unavoidable and adversely affected direct measurements of CO₂ EOR. Additional injection wells with dedicated injection lines could eliminate these operations-related problems.

Because a chemical corrosion inhibitor could not be administered to the oil-producing wells, lined tubing options should be investigated. If scheduling and budget allows, the well clean-ups and stimulations should be completed prior to CO₂ injection.

Post-CO₂ injection logging of the injection well or any well with tubing-packer completion should be logged through tubing to avoid a scenario in which the logging procedure is considered too risky to log by the service company.

REFERENCES

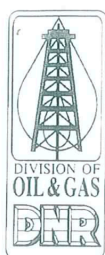
- ASTM Standards. 2002. Standard Practice for Low-Flow Purging and Sampling for Wells and Devices Used for Ground-Water Quality Investigation, in A.E. Greenberg, L.S. Clesceri, A.D. Eaton, eds., *Standard Method for the Examination of Water and Waste Water*: West Conshohocken, PA, ASTM International D 6771-02, vol. 18, pp. 2–25.
- American Public Health Association. 1992. *Standard Methods for the Examination of Water and Wastewater*, 18th ed.: Washington, DC, American Public Health Association, 1325 pp.
- Atherton, E., C. Collinson, and J.A. Lineback. 1975. Mississippian System, in *Handbook of Illinois Stratigraphy*: Champaign, IL, Illinois State Geological Survey, Bulletin 95, pp. 123–163.
- Berger, P. M., W. R. Roy, and E. Mehnert. 2009. Geochemical modeling of carbon sequestration, MMV, and EOR in the Illinois Basin: *Energy Procedia*, vol. 1, no. 1, pp. 3437–3444.
- Bethke, C.M., and S. Yeakel. 2007. *The Geochemist's Workbench Release 7.0: Reaction Modeling Guide*: Urbana, University of Illinois Urbana-Champaign, 84 pp.

- Brock, W.R. and L.A. Bryan. 1990. Summary Results of CO₂ EOR Field Tests, 1972–1987: 1990 SPE/DOE Symposium on Enhanced Oil Recovery, April 22–25, Tulsa, OK, paper 18977.
- Burger, A. M. 1986. Bond Formation, *in* Shaver, R. H., et al., Compendium of Paleozoic Rock-Unit Stratigraphy in Indiana—A Revision: Bloomington, IN, Indiana Geological Survey, Bulletin 59, p. 17.
- Coleman, M.L., T.J. Shepard, J.J. Durham, J.E. Rouse, and G.R. Moore. 1982. Reduction of water with zinc for hydrogen isotope analysis: *Analytical Chemistry*, vol. 54, pp. 993–995.
- Deines, P. 1980. The isotopic composition of reduced organic carbon, *in* P. Fritz and J. Fontes, eds., *Handbook of Environmental Isotope Geochemistry*, vol. 1: Elsevier Science Ltd., New York, pp. 329–406.
- Droste, J.B., and S.J. Keller. 1995. Subsurface Stratigraphy and Distribution of Oil Fields of the Buffalo Wallow Group: Bloomington, IN, Indiana Geological Survey, Bulletin 63.
- Epstein, S., and T. Mayeda. 1953. Variation of ¹⁸O content of waters from natural sources: *Geochimica et Cosmochimica Acta*, vol. 4, pp. 213–224.
- Frailey, S.M., D.G. Morse, I.G. Krapac, and R.W. McKaskle. 2012a. Sequestration and Enhanced Coal Bed Methane: Tanquary Farms Test Site, Wabash County, Illinois, C.C. Monson (ed.), Illinois State Geological Survey, Open File Series 2012-2, 182 pp.
- Frailey, S.M., T.M. Parris, J.R. Damico, R.T. Okwen, and R.W. McKaskle. 2012b. CO₂ Storage and Enhanced Oil Recovery: Sugar Creek Oil Field Test Site, Hopkins County, Kentucky, C.C. Monson and J. H. Goodwin (eds.): Illinois State Geological Survey, Open File Series 2012-4, 234 pp.
- Gaus, I., P. Audigane, L. Andre, J. Lions, N. Jacquement, P. Durst, I. Czernichowski-Lauriol, and M. Azaroual. 2008. Geochemical and solute transport modeling for CO₂ storage, what to expect from it?: *International Journal of Greenhouse Gas Control*, vol. 2, no. 4, pp. 605–625.
- Gray, H.H. 1989. Quaternary Geologic Map of Indiana: Bloomington, IN, Indiana Geological Survey, Miscellaneous Map 49, 1:500,000.
- Gray, H.H., C.H. Ault, and S.J. Keller. 1987. Bedrock Geologic Map of Indiana: Bloomington, IN, Indiana Geological Survey, Miscellaneous Map 48, 1:500,000.
- Hackley, K.C., C.L. Liu, and D. Trainor. 1999. Isotopic identification of the source of methane in subsurface sediments of an area surrounded by waste disposal facilities: *Applied Geochemistry*, vol. 14, pp. 119–131.
- Haitjema, H.M. 1985. Modeling three-dimensional flow in confined aquifers by superposition of both two- and three-dimensional analytic functions: *Water Resources Research*, vol. 21, no. 10, pp. 1557–1566.
- Haitjema, H.M. 2005. GFLOW version 2.1.0: Bloomington, IN, Haitjema Software.
- Journel, A.G. 1974. Geostatistics for conditional simulation of ore bodies: *Economic Geology*, vol. 69, no. 5, pp. 673–687.
- Matheron, G. 1973. The intrinsic random functions and their applications: *Advances in Applied Probability*, vol. 5, no. 3, pp. 439–468.
- Midwest Geological Sequestration Consortium. 2005. An Assessment of Geological Carbon Sequestration Options in the Illinois Basin. DOE Report, DE-FC26-03NT41994, 581 pp. (Issued December 31, 2005.)
- O'Dell, J.W., J.D. Pfaff, M.E. Gales, and G.D. McKee. 1984. Test Method—The Determination of Inorganic Anions in Water by Ion Chromatography—Method 300: Washington, DC, U.S. Environmental Protection Agency, EPA-600/4-84-017.
- Orion Research Incorporated. 1990. Ammonia Electrode Instruction Manual: Boston, MA, Orion Research Incorporated, 36 pp.
- Orion Research Incorporated. 2003. Carbon Dioxide Electrode Instruction Manual: Beverly, MA, Orion Research Incorporated, 37 pp.
- Ostlund, H.G., and H.G. Dorsey. 1977. Rapid electrolytic enrichment and hydrogen gas proportional counting of tritium, *in* Low-Radioactivity Measurements and Applications: Proceedings of the International Conference on Low-Radioactivity Measurements and Applications, October 6–10, 1975, The High Tatras, Czechoslovakia, Slovenske Pedagogicke Nakladatel'stvo, Bratislava, pp. 55–60.
- Parkhurst, D.L. and C.A. J. Appelo. 1999. User's Guide to PHREEQC (Version 2)—A Computer Program for Speciation, Batch-Reaction, One-Dimensional Transport, and Inverse Geochemical Calculations: U.S. Geological Survey Water-Resources Investigations Report 99-4259, 310 pp.
- Poeter, E.P., M.C. Hill, E.R. Banta, S. Mehl, and S. Christensen. 2005. UCODE_2005 and Six Other Computer Codes for Universal Sensitivity Analysis, Calibration, and Uncertainty Evaluation: U.S. Geological Survey Techniques and Methods 6-A11, 283 pp.
- Puls, R.W. and M.J. Barcelona. 1996. Low Flow (Minimal Drawdown) Ground-Water Sampling Procedure: EPA Ground Water Issue #EPA/540/S-95/504.
- Robison, T.M. 1977. Ground-water resources of Posey County, Indiana: Indianapolis, IN, Indiana Department of Natural Resources, Bulletin 39, 27 pp.
- Sara, M., and R.D. Gibbons. 1991. Organization and Analysis of Water Quality Data, *in* D.M. Neilsen, ed., *Practical Handbook of Ground Water Monitoring*: Chelsea, MI, Lewis Publishers, Inc., pp. 557–583.
- Shaver, R.H. 1979. Geologic Story of the Lower Wabash Valley with New Emphasis on the New Harmony Area: Indianapolis, IN, Indiana Department of Natural Resources, Occasional Paper 27, 14 pp.

- Strack, O.D.L., and H.M. Haitjema. 1981. Modeling double aquifer flow using a comprehensive potential and distributed singularities 1. Solution for homogeneous permeabilities: *Water Resources Research*, vol. 17, no. 5, pp. 1535–1549.
- Strazisar, B.R., C. Zhu and S.W. Hedges. 2006. Preliminary modeling of the long-term fate of CO₂ following injection into deep geological formations: *Environmental Geology*, vol. 13, pp. 1–15.
- United States Department of Energy Office of Fossil Energy, National Energy Technology Laboratory. November 2010. Carbon Sequestration Atlas of the United States and Canada, 3rd ed. 162 pp.
- United States Environmental Protection Agency. 1974. Methods for Chemical Analysis of Water and Wastes. EPA-625-/6-74-003a, pp.vi–xii.
- United States Environmental Protection Agency. 1989. Statistical Analysis of Ground-Water Monitoring Data at RCRA Facilities—Interim Final Guidance.
- Vennemann, T.W., and J.R. O’Neil. 1993. A simple and inexpensive method of hydrogen isotope and water analyses of minerals and rocks based on zinc reagent: *Chemical Geology*, vol. 103, pp. 227–234.
- Wood, W.W. 1976. Guidelines for collection and field analysis of groundwater samples for selected unstable constituents, *in* *Techniques for Water Resources Investigations*, Chapter D-2: Reston, VA, U.S. Geological Survey, 24 pp.
- Yeskis, D., and B. Zavala. 2002. Ground-Water Sampling Guidances for Superfund and RCRA Project Managers. EPA 542-S-02-001, Washington, DC, 53 pp.

APPENDICES

Appendix 1 Well permit application.



APPLICATION FOR WELL PERMIT

Form No. A1
Revised on 1/4/2006

INDIANA DEPARTMENT OF NATURAL RESOURCES
Division of Oil and Gas
402 W. Washington St., Rm. 293
Indianapolis, IN 46204
Phone (317) 232-4055
FAX (317) 232-1550
Internet: <http://www.in.gov/dnr/dnroil>

FOR STATE USE ONLY

Application number	Permit number
Date received	Date approved
IGS ID No.	Approved by
IGS Samples <input type="checkbox"/> Yes <input type="checkbox"/> No	IGS Pool Name

PART I GENERAL INFORMATION		
Name of operator <i>GALLAGHER DRILLING, INC.</i>	Telephone number <i>(317) 425-8250</i>	FAX number <i>(317) 425-0933</i>
Address of operator (Street or PO Box) (<input type="checkbox"/> Check here if this is a new address) <i>P.O. Box 3046</i>		
City <i>EVANSVILLE</i>	State <i>IN</i>	Zip code <i>47730</i>
Send permit to (Enter name and address) <i>Gallagher Drilling, Inc., P.O. Box 3046, Evansville, IN 47730</i>	Telephone number <i>(317) 425-8250</i>	FAX number <i>(317) 425-0933</i>
<input checked="" type="checkbox"/> Check here if you would like to have the permit sent via FAX		
<input type="checkbox"/> Expedite: Please check here and submit a total permit fee of \$750 to request 2 day processing NOTE: Expediting not available for Class II and Non commercial gas applications		
Applicant is (Check one only) <input type="checkbox"/> Individual <input type="checkbox"/> Partnership <input type="checkbox"/> Public corporation <input type="checkbox"/> Limited liability company <input checked="" type="checkbox"/> Corporation <input type="checkbox"/> Limited partnership		
NOTE: Corporations, limited partnerships and limited liability companies must register with the Secretary of State. For further information about registration contact the Corporations Division, Secretary of State at (317) 232-6576		
Type of bond (Check one only) <input type="checkbox"/> Surety bond <input type="checkbox"/> Check <input type="checkbox"/> Blanket bond <input type="checkbox"/> Personal surety bond (Valid for Non-commercial gas wells only) <input type="checkbox"/> Certificate of deposit <input checked="" type="checkbox"/> Bond not required per IC 14-37-6-1		
NOTES: A bond must accompany this application unless the operator has a valid blanket bond on file with the division or is exempt from bonding under IC 14-37-6-1. All bonds must be originals and an original Verification of Certificate of Deposit form must accompany CD's. Checks must be certified. The bond amount for individual wells is \$2,500 and for blanket bonds is \$45,000.		
Well type (Check one only) <input checked="" type="checkbox"/> Oil (Complete PARTS I thru IVa, VI and VII) <input type="checkbox"/> Gas (Complete PARTS I thru IVa, VI and VII) <input type="checkbox"/> Class II Enhanced Recovery (Complete PARTS I, II, IVb, V, VI, and VII) <input type="checkbox"/> Class II Saltwater Disposal (Complete PARTS I, II, IVb, V, VI, and VII) <input type="checkbox"/> Non-commercial gas (Complete PARTS I thru IVa, VI and VII) <input type="checkbox"/> Geologic/ Structure test (Complete PARTS I, II, IVa, VI, and VII) <input type="checkbox"/> Gas storage or observation (Complete PARTS I thru IVa, IVc, VI, and VII) <input type="checkbox"/> Non potable water supply (Complete PARTS I thru IVa, IVd, VI, and VII) <input type="checkbox"/> Dual completion for Oil and Class II injection only (Complete PARTS I thru IVb, V, VI, and VII) <input type="checkbox"/> Dual completion for Gas and Class II injection only (Complete PARTS I thru IVb, V, VI, and VII)		
Application type (Check no more than two) <input type="checkbox"/> New well <input type="checkbox"/> Change of operator (Complete PARTS I, II and VI only unless another application type is also checked) <input checked="" type="checkbox"/> Old well workover <input type="checkbox"/> Permit renewal (Complete PARTS I, II and VI only unless another application type is also checked) <input type="checkbox"/> Old well deepening <input type="checkbox"/> Horizontal well sidetracking <input type="checkbox"/> Conversion <input type="checkbox"/> Change of location Note: A \$250 permit fee is required except for expedited permits, which require a \$750 fee.		
Former operator (if applicable) <i>GALLAGHER DRILLING, INC.</i>		Former Permit number (if applicable) <i>34783</i>

Continued on next page

PART VI AFFIRMATION	
I affirm under penalty of perjury that the information provided in this application is true to the best of my knowledge and belief.	
Signature of operator or authorized agent <i>Daniel G. Gallagher</i>	Date signed <i>June 10th, 2009</i>

SPECIAL REQUIREMENTS

1. Only those individuals whose signatures appear in PARTS V and VI of the Organizational Report may sign this form
2. The name of the operator on this application and the name of the principal on the bond **must** be identical
3. If you are applying for a Change of Operator permit you are certifying that you have conducted a good faith search for the current operator and said operator could not be located.

APPLICATION REMINDERS

PART I:

- Enter the name of the operator exactly as it appears on the Organizational Report
- If you want to have a copy of the permit certificate faxed to you please check the appropriate box
- If you want to request an expedited permit please check the appropriate box and attach a \$750 permit fee
- Don't forget to register with the Indiana Secretary of State if you will operate as a Corporation, Limited Liability Company or Limited Partnership
- Don't forget to attach the \$250 permit fee or \$750 permit fee for expedited permits.
- If a Certificate of Deposit is selected as the Bond Type, don't forget to attach the original CD and original Verification of Certificate form

PART II

- If the well will be an oil or gas well be sure to indicate the distance to the nearest well capable of production from the same formation for which this permit is to be issued and make sure you check the rule requirements on well spacing to avoid placing the well an insufficient distance from an existing well.
- If you check the communitized box you must attach a copy of the pooling agreement or specify the permit number for the well under which the pooling agreement was previously submitted.
- If you check the Other box under the Drilling Unit section make sure to attach a copy of the exception

PART III

- This part is used by the division to determine if your proposed well construction will meet the rule requirements. Please be sure to enter all information about the proposed construction so that it can be evaluated accurately.

PART IV

- For all wells make sure to specify a Proposed total vertical depth, deepest formation name and pool name.
- For horizontal wells make sure to specify a Proposed measured length
- For Class II wells you must provide a proposed maximum allowable injection pressure and injection rate and attach all documentation needed to evaluate your request.

PART V

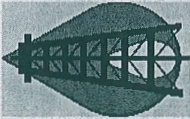
- The well diagram must be completed for all Class II well applications

PART VI

- Applications that do not contain an original signature cannot be processed
- The signature **must** match a signature shown in Parts VI or VII of the Organizational Report
- If this application is for a Change of Operator your signature in PART VI certifies that you could not obtain this permit through the permit transfer process **ONLY** because the former operator could not be located.

Important: A permit issued as a result of this application is a license to conduct an activity and does not convey any property rights to the permittee. Consequently, the permittee is solely responsible for acquiring any and all property rights necessary to use the permit for its stated purpose.

Appendix 2 CO₂ injection permit.



State of Indiana

Department of Natural Resources

Division of Oil and Gas

DRILLING AND CONSTRUCTION PERMIT

Gallagher Drilling, Inc.
P.O. BOX 3046
Evansville IN 47730-

Permit # **35202**
App. Type(s) Conversion

Issued On 6/29/2009
Effective On 7/17/2009
Surf. Elev. 465 feet

Pursuant to IC 14-37, the operator listed above is authorized to drill and construct a Class II Enhanced Recovery well as follows:

WELL #	LEASE NAME	COUNTY	TWP	RGE	Section	QUARTERS	FOOTAGE	FORMATION(S)	INTERVAL(S)
1	BALD UNIT	Posey	4 S	13 W	8	SW SE	660 S 1220 W	Clore	1905 to 1925


OPERATOR MUST OBTAIN INJECTION AUTHORIZATION PRIOR TO OPERATING THIS WELL

Important: The Field Inspector must be notified by the permittee

1. Before drilling commences
2. In the event of an emergency
3. Forty-eight (48) hours prior to plugging
4. When coal seam protection is required

Norm Tullis
Field Inspector

(812)459-4874
Phone Number



Mona Nemecek, Tech. Services Mgr.

A COPY OF THIS PERMIT MUST BE POSTED AT THE WELL SITE BEFORE DRILLING COMMENCES

109344

**INDIANA DIVISION OF OIL AND GAS
CLASS II
UNDERGROUND INJECTION CONTROL PROGRAM**

Permit Number: 35202

Facility Name: Bald Unit #1

Date Issued: June 29, 2009

Authorized By:



Pursuant to the provisions of the Underground Injection Control Program authorized under IC 14-37 and in accordance with the provisions of 312 IAC 16,

GALLAGHER DRILLING, INC.

is hereby authorized to convert the #1 Bald Unit well located in Posey County, Section 8, Twp. 4S, Rng. 13W, to an enhanced recovery well in the Lower Clore sandstone. After construction of the well has been completed, it will be necessary to submit Division of Oil and Gas Report R4, "Well Completion or Recompletion Report". This report must be received at the Division's central office within thirty (30) days after construction has been completed.

The purpose of the above mentioned well is limited to enhanced recovery for production wells owned or operated by Gallagher Drilling, Inc. in the immediate area. However, it should be noted that the following conditions and requirements must be completed prior to receiving injection authorization.

PERMIT CONDITIONS AND REQUIREMENTS

I. Construction

A. Casing and Cementing

1. General Requirements

- Injection wells shall be cased and cemented to prevent the movement of fluids into underground sources of drinking water, pursuant to 312 IAC 16-5-9, subsection (a) and (b).

2. Specific Requirements

- a) The operating well had 8 5/8 inch surface casing set at 86 feet and 100 sacks (106 cubic feet) of cement were used to bring the cement top to surface. 1980 feet of 5 1/2 inch long string were set and 100 sacks (118 cubic feet) of cement were used to bring the cement top to 1300 feet. The original drilled depth of 3023 feet was plugged back to a depth of 1975 feet.

B. Tubing and Packer

1. General Requirements

- The injection of permitted fluids must be through tubing separated from the innermost casing with a corrosion inhibiting fluid that meets or exceeds API standards. The tubing shall be installed with a packer which must be set inside casing within two hundred (200) feet above the injection zone. (312 IAC 16-5-14).

2. Specific Requirements

- The operator will run 1850 feet of 2 3/8 inch tubing with a tension packer set at 1850 feet. Injection will be from 1905 feet to 1925 feet into the Lower Clore sandstone.

C. Wellhead

• Specific Requirements

For every injection well, the operator shall install 1/4 inch female threaded NPT fittings with shutoff valves to the tubing and casing/tubing annulus. All piping, valves and facilities must meet or exceed design standards for the maximum allowable injection pressure. These fittings and valves must be accessible to the field inspector at all times.

II. Corrective Action

- Specific Requirements
 - There is no corrective action required at this time. However, should any upward fluid migration occur through the well bore of any previously unknown, improperly plugged or unplugged well in the area of review due to injection of fluids, injection will be shut-in until plugging can be accomplished. Should any problem develop in the casing of the injection well, injection will be shut-in until such time that repairs can be made to remedy the situation.

III. Mechanical Integrity

All mechanical integrity tests must be conducted in accordance with 312 IAC 16-5-15 and in the presence of a field inspector.

IMPORTANT: Authorization to inject will not be granted until the results of all MIT's have been reviewed and approved by the technical section of the Division of Oil and Gas.

Two types of integrity must be demonstrated:

A. Casing, Tubing and Packer

1. General Requirements

- A demonstration that there is no significant leak in the casing, tubing or packer.

2. Specific Requirements

- a) Pressure testing at a minimum of 300 psi with no more than a 3% pressure difference over a 30 minute period.

B. Injection Fluid Movement

1. General Requirements

- A demonstration that there is no significant injection fluid movement into an underground source of drinking water.

2.

Specific Requirements

- a) Proof that there is no injection fluid movement based on the results of a temperature survey, noise log, oxygen activation log or sonic cement bond/variable density log; or
- b) Records demonstrating adequate cementing, including but not limited to sonic cement bond/variable density log.

IV. Operating

A. Injection Rate and Pressure

1. General Requirements

- a) Well must be operated in accordance with 312 IAC 16-5-14.
- b) The division must be notified in advance of a permit change which may require the alteration of an approved condition. A permit change cannot be effected by the operator until the change is approved by the division.
- c) The division director may require additional testing or special equipment if appropriate to the protection of an underground source of drinking water.

2.

Specific Requirements

- a) Injection rate and volume - The maximum injection rate is to be **500** barrels of water per day as requested by the operator.
- b) Injection pressure - The injection pressure may not exceed **1500 psi** as requested by the operator and based on a step rate test in the Clore sandstone on a

INDIANA

nearby well. The maximum pressure of 2150 psi during the test was the formation breakover. The USEPA recommends 90% of this value less 14.7 pounds as the maximum allowable injection pressure.

- c) Source of injection fluid - Food grade liquid CO₂ and fresh water.

V. Monitoring and Reporting

- All records pertaining to this permit must be retained by the operator for a minimum period of three (3) years.
- The United States Environmental Protection Agency reserves the right to examine all records including those classified as confidential.

A. Quarterly Monitoring Report

- | |
|-----------------------|
| Specific Requirements |
|-----------------------|

 - The operator shall file with the division a quarterly monitoring report on a division form not later than thirty (30) days following the quarter reported. The operator shall monitor maximum and average injection pressures and injection rate for each Class II well on a weekly basis with the results reported and summarized monthly, and filed quarterly.

B. Injecting Fluid Reporting

- | |
|-----------------------|
| Specific Requirements |
|-----------------------|

 - The injection fluid must be analyzed on an annual basis. The analysis must be conducted during the third calendar quarter of the year and the laboratory report submitted with that period's Quarterly Monitoring Report. The analysis must include: 1) specific gravity, 2) pH, 3) total dissolved solids, 4) water resistivity and 5) water temperature.

Appendix 3 MVA methods.

Groundwater Modeling for the Site

Prior to deployment of a groundwater monitoring network at the Bald Unit site, groundwater modeling was conducted to (1) design a groundwater monitoring system able to detect any CO₂ leaked to shallow groundwater; and (2) determine the flow rate and transport direction of any CO₂ leakage from the injection point.

Analytic element modeling (AEM) was used for this project because shallow groundwater and surface water flow can be modeled simultaneously using a relatively simple data set. A disadvantage of the AEM method is that transient flow and three-dimensional flow can only be partially represented in the model, and gradually varying aquifer properties cannot be represented at all. However, these issues were not significant at this site.

The AEM method was developed at the end of the 1970s by Otto Strack at the University of Minnesota (Strack and Haitjema, 1981). In this method, instead of discretizing the entire groundwater flow domain, only the surface water features are discretized, entered into the model as input, and represented by closed form analytical solutions or analytic elements. The solution to a complex, regional groundwater flow model is derived from the superposition of hundreds of analytic elements.

Analytic elements were chosen to best represent certain hydrologic features. For instance, stream sections and lake boundaries were represented by line sinks, and small lakes or wetlands were represented by areal sink distributions. Areal recharge was modeled by an areal sink with a negative strength. Streams and lakes that were not fully connected to the aquifer were modeled by line sinks or area sinks with a bottom resistance. Discontinuities in aquifer thickness or hydraulic conductivity were modeled by use of line doublets (double layers). Specialized analytic elements were used for special features such as drains or slurry walls. Locally, three-dimensional solutions may be added, such as a partially penetrating well (Haitjema, 1985).

Model Description

A simple conceptual model was adopted for the local hydrogeology. A single surficial aquifer extends from ground surface to a thickness of 70 m (230 ft) and has a base elevation of 70 m (230 ft). This surficial aquifer is a combination of alluvial materials in the valleys and Quaternary deposits and bedrock in the uplands. Locally, the aquifer is the source of domestic and commercial water supplies (Figure 18). The aquifer is assumed to have uniform properties (hydraulic conductivity, porosity, etc.).

The software used for the AEM was GFLOW v2.1.0. Input parameters were either estimated from available information or calibrated in the modeling process (Table A3-1). The model for this site was developed by expanding the GFLOW model developed for the enhanced coal bed methane site, which is located in Wabash County, IL. The revised model included a thicker aquifer and lower hydraulic conductivity. The model was calibrated using streamflow data from two streams—Bonpas Creek in Wabash County (IL) and Big Creek in Posey County. The model was calibrated using two values of streamflow and two values of groundwater head. Because groundwater discharge is more significant to streamflow at low flows, Q_{75} (flow is exceeded 75% of the time) was adopted as the calibration target for streamflow. For the preliminary modeling of the Bald Unit, no groundwater head data were available, so the groundwater was assumed to be 9.1 m (30 ft) below ground surface or at an elevation of 134 m (440 ft).

Table A3-1 Input parameters for GFLOW.

Aquifer parameters	Value		Source
Base elevation	70 m (230 ft)		Field data
Thickness	70 m (230 ft)		Estimate
Porosity	0.2		Estimate
Hydraulic conductivity	0.24 m/day (0.79 ft/day)		Model calibration
Recharge	3.1e-05 m/day (0.45 inch/yr)		Model calibration
Stream parameters	Bonpas Creek	Big Creek	Source
Streamflow	13.9 cfs	2.4 cfs	USGS website
Width	33 ft	16.4 ft	Field data
Depth	16 ft	3.3 ft	Field data
Resistance	0	0	Estimate

Techniques for Drilling and Monitoring Well Installation

Monitoring wells were drilled and completed in July 2009. Three boreholes were drilled by Illinois State Geological Survey staff members using the Survey's CME-75 rig. Two of the boreholes (MH-1 and MH-2) were drilled using wireline coring tools, which require the use of bentonite-based drilling mud for unconsolidated materials. The wireline coring tool provides core with a diameter of 6 cm (2.4 inches). The cored hole was then reamed to a diameter of 11.4 cm (4.5 inches) to allow the installation of 5-cm (2-inch)-diameter PVC casing and screen to construct the monitoring wells. The other borehole (MH-3) was drilled by the mud rotary method, which produced an 11.4-cm (4.5-in)-diameter borehole. No samples were collected from this borehole.

Geophysical logs were run in all the boreholes prior to monitoring well construction. The natural gamma log was run in each borehole using an MGX II console and 2PGA-1000 downhole tool from Mt. Sopris Instrument Company (<http://www.mountsopris.com/products.htm>), Golden, CO, in a borehole filled with drilling mud or water. The natural gamma log provides data on the amount of gamma-emitting clays, primarily from the presence in the clays of naturally occurring isotopes of potassium, thorium, and uranium, which are used to identify the lithology of the geologic materials beyond the borehole.

All monitoring wells were constructed with 5-cm (2-inch)-diameter PVC casing with threaded connections. Slotted screens with 0.025-cm (0.010-inch) slots were used for the four monitoring wells. The elevations of the monitoring wells were determined by level surveying, based on the known elevation of a local benchmark. Level surveying was conducted with an automatic level (Wild Model NA2) and a micrometer or similar instrument. The micrometer allows elevations to be measured to the fourth decimal place. The elevations of all wells were determined to the nearest 0.003 m (0.01 ft). The elevations of the tops of the PVC casing are 139.026 m (456.125 ft) for MH-1, 144.827 m (475.156 ft) for MH-2, and 139.857 m (458.850 ft) for MH-3.

After well installation, the well was developed by overpumping with a Geotech 1.66 Reclaimer™ pump. Further details on monitoring well construction are given in Appendix 4.

Hydrogeologic Data from the Drilling and Monitoring Well Installation

Pressure transducers were installed in the four monitoring wells. Solinst Levelloggers™ (www.solinst.com) were installed in the three groundwater monitoring wells and were programmed to record water levels at 6-minute intervals. Because these loggers record absolute pressure, atmospheric pressure was also recorded at the site using a Solinst Barologger™. These instruments allowed water levels in the wells to be monitored over time. The atmospheric pressure data were processed according to the procedure in the Solinst user's manual and were used to correct the Levellogger data.

Collection and Analysis of Groundwater Samples

Once all the monitoring wells had been drilled and developed, bladder sampling pumps were installed into each well. The bladder pumps minimize sample disturbance and exposure to the atmosphere, which is criti-

cal when evaluating water quality in relation to CO₂ effects. Water levels in the site monitoring wells were determined using continuous recording pressure transducers and an electronic water level indicator prior to and during sample collection. A low flow sampling technique was used to collect groundwater samples (ASTM Standards, 2002). This method minimizes water disturbance and drawdown while optimizing water purge volumes to ensure that a representative water sample is collected from the formation (Puls and Barcelona, 1996). During the sampling process, water quality parameters such as pH, EC, Eh, and DO content were continuously measured using a flow-through cell. Once these parameters became stable, samples were collected. Stabilization criteria, based on three successive measurements of each parameter (Yeskis and Zavala, 2002), were as follows: pH \pm 0.1 pH unit; EC \pm 3% of previous reading; Eh \pm 10 mV; and DO \pm 0.3 mg/L.

The sample preservation techniques used were those outlined in publications by the U.S. Environmental Protection Agency (1974) and the American Public Health Association (1992). Unfiltered samples were used to determine ammonia and dissolved CO₂ concentrations. Samples to be analyzed for alkalinity, anions, cations, tritium, and carbon and oxygen isotopes were filtered through 0.45- μ m (1.77×10^{-5} in) pore size filters. All samples were kept on ice in the field and refrigerated at 4°C (39°F) in the laboratory until analyzed. Anion concentrations were determined by ion chromatography (O'Dell et al., 1984), and cation concentrations were determined by inductively coupled argon plasma spectrophotometry (ICP) (American Public Health Association, 1992). Detection limits were 0.01 mg/L for chloride, nitrate-N, and sulfate and 0.05 mg/L for phosphate-P. Detection limits for the ICP analyses were in the range of 0.00037 mg/L for constituents such as Sr (strontium) to 0.217 mg/L for S (sulfur). Ammonia-N concentrations were determined by electrode and had a detection limit of 0.1 mg/L (Orion Research Incorporated, 1990; American Public Health Association, 1992). Concentrations of total DIC (as CO₂) were determined by electrode and had a detection limit of 4.4 mg/L (Orion Research Incorporated, 2003). A titration method with a detection limit of 2 mg/L was used to measure alkalinity (American Public Health Association, 1992). Electrical conductivity, pH, Eh potential, and temperature were determined in the field using electrodes according to standard methods (American Public Health Association, 1992). The Eh potentials are reported relative to a standard ZoBell solution (Wood, 1976).

Statistical Analysis of Groundwater Quality Data

The time between the groundwater monitoring well development and the beginning of CO₂ injection was 2 months; during this time sampling occurred monthly. This sampling period was too brief to collect enough background water quality data to apply rigorous statistical techniques to determine changes in groundwater quality. For example, relatively simple techniques, such as the use of control charts, require 6 to 8 months of background data (U.S. Environmental Protection Agency, 1989). For all statistical methods employing the use of pooled background data, the background data set should be large enough to reflect naturally occurring changes in hydrogeology. For moving background data sets, Sara and Gibbons (1991) recommend that only data from the eight most recent sampling events be used. This approach helps to minimize temporal variability (Sara and Gibbons, 1991). Simple time series charts were constructed for intra-well and inter-well comparisons of groundwater quality analytes. Intra-well comparison provided a historic data review for a single well. Pre- and post-CO₂ injection water quality data were compared by this technique.

Isotopic Analysis of Gas and Water Samples

Gas samples were taken from the headspace in the sampling carboy caused by degassing of the oil-brine mixture during brine sampling events. The samples were collected in 1-L (61-inch³) Cali-5-Bond™ gas sampling bags produced by Calibrated Instruments, Inc., fitted with luer valves. The gas samples were analyzed using either a SRI 8610C or Varian 3800 gas chromatograph. The Varian 3800 gas chromatograph was equipped with a thermal conductivity detector (TCD) for fixed gases (CO₂, N₂, O₂, and CH₄) and flame ionization detector (FID) for hydrocarbons from CH₄ through hexane (C₆H₁₄). The SRI 8610C gas chromatograph (MG #1 Multi-gas configuration) was equipped with a thermal conductivity detector (TCD) and a helium ionization detector (HID) and sampling valves with a 1 cc sample loop. The fixed gases (H₂, O₂, N₂, CH₄, and CO₂) and hydrocarbons from CH₄ through hexane (C₆H₁₄) were separated through a 1.8-m (6-ft)-long, 3.175-mm (1/8-inch) diameter stainless steel column packed with either silica gel or molecular

sieve 13X. The initial column temperature was set at 40°C (104° F) and held for 4 minutes and then ramped from 20 to 220°C (68 to 428° F) and held for 17 minutes. The column and detectors' make-up flows were set at 40 and 20 mL (2 and 1 inch³), respectively. Before each injection, the sampling loop was flushed with helium for 2 minutes to remove air, and then 10 mL (0.6 inch³) of gas was injected into the gas chromatograph using a gas-tight syringe and the sample was analyzed using the detectors connected in tandem. Standard gas samples with four known concentrations were used to calibrate the gas chromatograph and to periodically check for instrument drift.

Gas samples with sufficient CO₂ were analyzed for stable carbon isotopes ($\delta^{13}\text{C}$). Selected samples containing sufficient CH₄ were analyzed for $\delta^{13}\text{C}$ and hydrogen isotopes (δD). The aqueous samples were analyzed for stable carbon ($\delta^{13}\text{C}$), oxygen ($\delta^{18}\text{O}$), and hydrogen (δD) isotopes as well as tritium (^3H). The CO₂ from a few gas samples was also analyzed for radiocarbon (^{14}C) concentrations.

The gas samples were extracted from the sample bags by passing a syringe through a septum fitted onto the luer valve. For those gas samples containing very little to no hydrocarbons heavier than CH₄, the extracted gas sample was then injected into a vacuum line, and the CO₂ was cryogenically purified and sealed in a 6-mL (0.37-inch³) Pyrex tube for isotopic measurement. For those gas samples that contained heavier hydrocarbons, the samples were sent to a laboratory equipped with a gas chromatograph separation method connected to a vacuum line for $\delta^{13}\text{C}$ analysis of the CO₂. Due to the number of aqueous samples, some of the samples were also sent to an outside laboratory for $\delta^{18}\text{O}$ and δD isotopic analysis. For those samples analyzed at the Illinois State Geological Survey, the $\delta^{18}\text{O}$ value was analyzed using a modified CO₂-H₂O equilibration method as originally described by Epstein and Mayeda (1953) with the modifications described by Hackley et al. (1999). The δD values of selected water samples were determined using the Zn reduction method described in Coleman et al. (1982) and Vennemann and O'Neil (1993), with the modifications described by Hackley et al. (1999). The $\delta^{13}\text{C}$ value of DIC was determined using a gas evolution technique. Approximately 10 mL (0.6 inch³) of water was injected into an evacuated vial containing crystalline phosphoric acid and a stir bar. The CO₂ evolved from the water sample in the vial was cryogenically purified on a vacuum system and sealed into a Pyrex break tube for isotopic analysis.

The isotopic compositions of the samples ($\delta^{13}\text{C}$, $\delta^{18}\text{O}$, and δD) were determined on a dual inlet ratio mass spectrometer. Each sample was directly compared against an internal standard calibrated versus an international reference standard. The final results are reported versus the international reference standards. The $\delta^{13}\text{C}$ results are reported versus the PeeDee Belemnite (PDB) reference standard. The $\delta^{18}\text{O}$ and δD results are reported versus the international Vienna-Standard Mean Ocean Water (V-SMOW) standard. Analytical reproducibilities were as follows: for $\delta^{13}\text{C}$, $\leq \pm 0.15\%$; for $\delta^{18}\text{O}$, $\leq \pm 0.1\%$; and for δD , $\leq \pm 1.0\%$.

The ^3H analyses were done by the electrolytic enrichment process (Ostlund and Dorsey, 1977) and the liquid scintillation counting method. The electrolytic enrichment process consists of distillation, electrolysis, and purification of the ^3H -enriched samples. The results are reported in tritium units (TU), and the precision for the tritium analyses reported in this study is ± 0.25 TU.

The ^{14}C activity of the DIC was analyzed using acceleration mass spectrometry (AMS). The DIC was extracted from the water samples by acidification; the released CO₂ was quantitatively collected on a vacuum line. The ^{14}C concentrations are reported as percent modern carbon (pMC) relative to the NBS reference material (oxalic acid #1) which is, by convention, defined as 100 pMC.

Appendix 4 Well construction details.

Geologic logs, natural gamma logs, and well construction details of groundwater monitoring wells.

Table A4-1 Detailed geologic log for Mumford 1 (MH-1) groundwater monitoring well.

Well name: Mumford1 Date: 7-14-2009		API: 131290000100
Location: Posey County, IN SE/4, Section 8, T4S, R13W Personnel: Wimmer, Mehnert, Aud, Padilla, Bryant Drilling rig (rig type and driller): CME 75 ISGS		
Core	Depth (ft)	Sample description (recovery [R], texture, color, structure)
1	0–4	R = 3.4 ft
		0–0.4 ft; silt, topsoil, roots, and gravel
		0–2.5 ft; silt, oxidized, mottled, roots; 7.5 YR 4/6
		2.5–3.4 ft; silt, no structure; 7.5 YR 4/2; “loess”
2	4–9	R = 2.9 ft
		0–0.8 ft; silt, no structure, very soft; 7.5 YR 4/2; “loess”
		0.8–2.9 ft; silt, some fine sand, harder than 0–0.8 ft
		7.5 YR 4/2; “loess”
3	9–14	R = 0 ft
		No recovery in this interval due to soft material.
4	14–19	R = 4.9 ft
		0–0.5 ft; silt and fine sand, very soft, reworked by drill bit; “lacustrine”
		0.5–4.2 ft; silt, some fine sand, some fractures and oxidation along fractures; 7.5 YR 5/4
		4.2–4.9 ft; silt, clayey, mottled matrix—10 YR 5/4 mottle—7.5 YR 5/1; “lacustrine”
5	19–24	R = 4.6 ft
		0–0.5 ft; silt, with some gravel, roots, very soft; “lacustrine”
		0.5–4.6 ft; silt, with sand and gravel, massive, gradational color change from gray to light brown; top: 2.5Y 6/2; bottom: 2.5Y5/6; “till” *Switched from auger to wireline coring
6	24–30	R = 5.5 ft
		0–3.4 ft; silt, with sand and gravel, some fractures with oxidation; “lacustrine”
		3.4–5.0 ft; silt, with sand and gravel, fine sand, softer than 0–3.4 ft, sharp transition at 3.4 ft, dark organic matter at 5.0 ft
		5.0–5.5 ft; silt, with sand and gravel, very soft; “lacustrine”
7	30–34.5	R = 4.1 ft
		0–0.6 ft; sand, silty, no bedding, no roots, no structure; “alluvial or weathered bedrock”
		0.6–3.7 ft; silt, with sand and gravel, no structure
		3.7–4.1 ft; sand, bedded, possible shell fragments
8	34.5–35.3	R = 1.0 ft
		0–1.0 ft; sand, silty, fine grained, no structure, mica throughout; gley 2 5/5 B
9	35.3–45	R = 8.4 ft
		0–8.4 ft; sandstone, silty, fine sand, mica throughout, oxidation throughout, thinly bedded, very friable
10	45–55	R = 9.2 ft
		0–2.6 ft; sandstone, thinly bedded, firm, fine sand
		2.6–2.8 ft; shale, very soft
		2.8–9.0 ft; sandstone, medium grained, thinly bedded, oxidized
		9.0–9.2 ft; sand, with silt, shale(?), very oxidized, very soft
11	55–60	R = 5.8 ft; highly broken by drill bit
		0–0.2 ft; sandstone, silty, fine sand
		0.2–0.4 ft; siltstone, laminated, thinly bedded, very soft
		0.4–5.8 ft; siltstone with interbedded shale, very friable, broken into small pieces

Core	Depth (ft)	Sample description (recovery [R], texture, color, structure)
12	60–70	R = 8.3 ft
		0–5.6 ft; siltstone, some layers of shale, very broken up
		5.6–6.6 ft; sandstone, few layers of shale, fine sand thinly bedded
		6.6–8.3 ft; siltstone, some layers of shale, very broken up
13	70–75	R = 5.1 ft; core got stuck in barrel; used water pressure
		0–0.8 ft; siltstone, with interbedded shale, thinly bedded, gray in color
		0.8–5.1 ft; claystone, very fine grained, plant fragments (?); no visible bedding, coal fragments throughout, gray color, coal seam from 74.5–74.9 ft
14	75–81.7	R = 6.5 ft; core is very broken up and disturbed
		0–6.5 ft; shale, very broken up from 0–0.2 ft and 6.3–6.5 ft, very thinly bedded, slicken-sides in 6.3–6.5 ft, shale is gray
15	81.7–90	R = 4.7 ft
		0–1.0 ft; shale, soft, thinly bedded
		1.0–1.1 ft; shale, laminated, harder than 0–1.0 ft, coal fragment at top, gray
		1.1–2.1 ft; shale, gray, soft
		2.1–2.6 ft; limestone, very hard, fossils present, slight reaction to HCl, white to gray
		2.6–4.7 ft; shale, thinly bedded, soft, gray
16	90–95	R = 3.4 ft
		0–3.4 ft; shale, thinly laminated, gradational color change from gray at top to dark gray at bottom
	90–95	*Driller recovered lost core from last two intervals.
		R = 3.7 ft
		0–3.7 ft; shale, thin horizontal bedding, dark gray color, no visible fossils or plant fragments
17	95–105	R = 6.2 ft; some core fell out of core barrel, will recover with next core run
		0–6.2 ft; shale, thinly bedded, fairly hard, gray, fossils throughout
18	105–110	R = 8.4 ft; continued from core 17
		0–6.4 ft; shale, thinly bedded, gray and fairly hard, some fossils present
		6.4–8.4 ft; limestone, fractured (horizontal fracture at 7.6 ft), fossils throughout, fairly dense
19	110–120	R = 9.7 ft
		0–4.0 ft; limestone, fractured (horizontal fracture at 1.2 ft), fossils throughout, fairly dense, 3.8–4.0 ft transition into black shale
		4.0–5.0 ft; shale, black, has tarry smell, organic-rich, very thinly bedded
		5.0–5.2 ft; coal, black, very blocky
		5.2–9.7 ft; siltstone, thinly laminated, deformed bedding, gray
20	120–130	R = 10.1 ft
		0–10.1 ft; siltstone, thinly bedded, organic material throughout, cross-bedding ~6 ft, deformed bedding ~7–8 ft, possibly some fine sand throughout, color gray, bottom gravelly and chewed up, most likely from drill bit
21	130–140	R = 9.9 ft
		0–6.4 ft; siltstone, thinly bedded, fossils throughout, few sand pockets
		6.4–9.9 ft; shale, sandy, very fine-grained sand, deformed beds throughout, organic material present, fairly nice sand pocket at 138 ft
22	140–150	R = 9.4 ft
		0–9.4 ft; sandstone, fine with silt interbeds, fossils and plant fragments around 4–4.5 ft, fine to coarse sand from 5–6.5 ft, deformed bedding beneath 6.5 ft
23	150–155	R = 5.0 ft
		0–5.0 ft; sandstone, with interbedded silt, sandstone is fine grained, plant fragments visible, fine to coarse sand at 3–4 ft; siltier sand toward bottom
24	155–165	R = 8.9 ft
		0–8.9 ft; sandstone with interbedded silt, sandstone is fine grained to medium grained and relatively clean at 2.6–3.0 ft; micaceous
25	165–174.7	R = 10.0 ft
		0–5.0 ft; interbedded sandstone and siltstone, fine-grained sand
		5.0–10.0 ft; sandstone with some siltstone, interbedded sand is fine-grained, vertical fracture at 6.5 ft, lower silt content on this interval

Table A4-2 Detailed geologic log for Mumford 2 (MH-2) groundwater monitoring well.

Well Name: Mumford2		API: 131290000200
Date: 7-16-2009		
Location: Posey County, IN SE/4, Section 8, T4S, R13W		
Personnel: Wimmer, Mehnert, Aud, Padilla, Bryant		
Drilling rig (rig type and driller): CME 75 ISGS		
Core	Depth (ft)	Sample description (recovery, texture, color, structure)
1	0–4.5	R = 2.3 ft
		0–2.3 ft; silt, some roots, no structure, very soft; 10YR 4/3
2	4.5–9.5	R = 3.4 ft
		0–2.1 ft; silt, mottled, black along a horizontal fracture at 1 ft; 10YR 5/6 “loess”
		2.1–3.1 ft; sand, fine to medium gley; 2 4/10B
		3.1–3.4 ft; silt, mottled, lacustrine (?); matrix: 7.5YR 3/3; mottle: gley2 6/5 PB
3	9.5–14.5	R = 3.8 ft
		0–3.8 ft; silt, mottled, lacustrine (?)
4	14.5–19.5	R = 2.0 ft
		0–2.0 ft; silt, mottled (same as core 2); top 1 ft is softer and more moist; very bottom of core is highly oxidized
5	19.5–25	R = 3.7 ft
		0–3.7 ft; silt, very soft and moist, little bit of oxidation ~2.5 ft
6	25–35	R = 6.7 ft
		0–6.7 ft; silt, very soft, lacustrine; gley2 5/5PB
7	35–45	R = 2.5 ft
		0–1.8 ft; silt with sand and gravel, fairly dense, no structure, not too much gravel
		1.8–2.5 ft; sand with some silt, fine to medium sand, black material toward base—manganese (?)
8	45–50	R = 1.1 ft
		0–0.3 ft; sand, with some silt, mostly fine sand with a little medium sand
		0.3–1.1 ft; silt, some oxidation at 1 ft, fairly weathered surface
9	50–60	R = 6.2 ft
		0–3.1 ft; silt, some sand and organic matter
		3.1–6.1 ft; sand, fine to medium, some silt, more black material (manganese?), some gravel
10	60–60.3	R = 0.5 ft
		0–4.8 ft; sand with some silt and gravel, highly oxidized at base, micaceous
11	60.3–70	R = 5.0 ft
		0–4.8 ft; sandstone, very soft, weathered, transition between soft sediment and bedrock, very friable
		4.8–5.0 ft; sand with gravel and some silt, silty material is maroon
12	70–76	R = 5.8 ft
		0–4.6 ft; sandstone, fine to medium, weathered, black material spread throughout (fairly soft)
		4.6–4.9 ft; sandstone, weathered, oxidized, transition zone
		4.9–5.8 ft; siltstone with inter-bedded sandstone, fine-grained
13	76–80	R = 3.4 ft
		0–3.4 ft; sandstone with interbedded siltstone, fine-grained sand, cross-bedded and wavy beds, color is gray to dark gray
14	80–85	R = 6.0 ft
		0–1 ft; sand and silt (probably fell in from borehole overnight)
		1–6 ft; siltstone, with interbedded sandstone, very fine sand, some cross-bedding, some deformed bedding, thinly bedded
15	85–93.6	R = 8.6 ft
		0–2.5 ft; siltstone, with interbedded sandstone, very fine sand, thin bedding, gray color
		2.5–8.6 ft; siltstone, clayey from 2.5–4.00 ft; no bedding visible, fairly soft, gray color

Core	Depth (ft)	Sample description (recovery, texture, color, structure)
16	93.6–104	R = 7.9 ft
		0–6.0 ft; siltstone, thinly bedded, fairly hard, greenish gray color
		6.0–6.4 ft; limestone, fairly hard, gray color
		6.4–7.9 ft; siltstone, thinly bedded, fairly hard, greenish gray color
17	104–110	R = 6.0 ft
		0–6.0 ft; shale, thinly bedded, gray in color, fairly hard, some pyrite
18	110–120	R = 7.8 ft
		0–7.8 ft; shale, thinly bedded, gray, fairly hard, pyrite and fossils throughout, some fine sand interbedded from 4.5–7.8 ft
19	120–128.9	R = 10.0 ft
		0–4.1 ft; shale, same as core 16, transition from shale to limestone from 4.0–4.1 ft
		4.1–10.0 ft; limestone, some horizontal fractures, fossils throughout, transition back to shale from 9.8–10.0 ft
20	128.9–135	R = 5.3 ft
		0–1.1 ft; shale, black, thinly bedded, organic-rich
		1.1–1.3 ft; coal, black, blocky
		1.3–5.3 ft; siltstone, gray, thinly bedded, deformed bedding
21	135–140	R = 5.9 ft
		0–5.9 ft; siltstone, thinly bedded, plant fragments (fossilized wood at 3.7 ft), horizontal fracture at 2.0 ft, a little fine sand towards base of core, gray in color
22	140–150	R = 10.0 ft
		0–10.0 ft; siltstone, with some interbedded fine sand, deformed bedding, plant fragments throughout, horizontal fracture with mineralization at 4.5 ft; increased sand content at very base of core
23	150–160	R = 10.0 ft
		0–10.0 ft; sandstone, with interbedded siltstone, deformed beds, some horizontal fracturing, mostly sandstone from 4.5–10 ft, fine sand from 4.5–9.0 ft, picking up some coarser sand from 9.0–10 ft, plant fragments
24	160–170	R = 10.2 ft
		0–10.2 ft; sandstone, with interbedded siltstone, deformed beds, nice sandstone interval from 1.2–2.0 ft, 2.3–2.9 ft, 3.3–4.2 ft, 6.4–7.0 ft, 7.4–8.0 ft; sand is mostly fine-medium grained in these intervals

Table A4-3 Well construction details for MH-1. Some fields were intentionally left blank.

Well Name: Mumford1

API: 131290000100

Personnel: Aud, Padilla, Bryant, Wimmer, Mehnert

Date well constructed: 7-16-09

Final Depth of Hole: 175'

Surface completion: stick-up

Backfilled?: no

Depth and thickness of aquifer: 174.7'–164.7'

Depth of water in well: 83.6'

Screened interval: 10' (174.7'–164.7') 10 slot screen

Lbs. of sand added: 435

Depth: 174.7'–134.7'

Lbs. of sand added:

Depth:

Lbs. of sand added:

Depth:

Lbs. of Bentonite added: 250 lbs. Benseal

Depth: 134.7'–8'

Depth of backfill: N/A

Texture of backfill: N/A

Any additional Bentonite? 250 lbs. Holeplug

Depth: 8'–1'

Lbs. of concrete: 50 lbs. (1 bag)

2'–surface

Was well developed at time of construction? no

Was well logged (natural gamma) at time of construction? yes

Table A4-4 Well construction details for MH-2. Some fields were intentionally left blank.

Well Name: Mumford2

API: 131290000200

Personnel: Aud, Padilla, Bryant, Wimmer

Date well constructed: 7-22-09

Final Depth of Hole: 170'

Surface completion: stick-up

Backfilled?: no

Depth and thickness of aquifer: 150'–170'

Depth of water in well: 105.67'

Screened interval: 10' (160'–170') 10 slot screen

Lbs. of sand added: 275

Depth: 148.2'–170'

Lbs. of sand added:

Depth:

Lbs. of sand added:

Depth:

Bentonite added: 3 gallons pellets

Depth: 143.8'–148.2'

Bentonite added: 400 lbs. Benseal

Depth: 143.8'–6'

Depth of backfill: N/A

Texture of backfill: N/A

Any additional Bentonite? 87.5 lbs.

Holeplug Depth: 6'–3'

Lbs. of concrete: 80 lbs. (2 bags)

3'–surface

Was well developed at time of construction? no

Was well logged (natural gamma) at time of construction? yes

Table A4-5 Well construction details for MH-3. Some fields were intentionally left blank.

Well Name: Mumford3

API: 131290000300

Personnel: Aud, Padilla, Bryant, Wimmer

Date well constructed: 7-29-09

Final Depth of Hole: 177.7'

Surface completion: stick-up

Backfilled?: no

Depth and thickness of aquifer: 138'–175'

Depth of water in well: 99.37'

Screened interval: 10' (165'–175') 10 slot screen

Lbs. of sand added: 425

Depth: 138.3'–175'

Lbs. of sand added:

Depth:

Lbs. of sand added:

Depth:

Bentonite added: 4 gallons pellets

Depth: 143.8'–138.3'

Bentonite added: 400 lbs. Benseal

Depth: 143.8'–4'

Depth of backfill: N/A

Texture of backfill: N/A

Any additional Bentonite? 150 lbs. Holeplug

Depth: 4'–2'

Lbs. of concrete: 120 lbs. (3 bags)

2'–surface

Was well developed at time of construction? no

Was well logged (natural gamma) at time of construction? yes

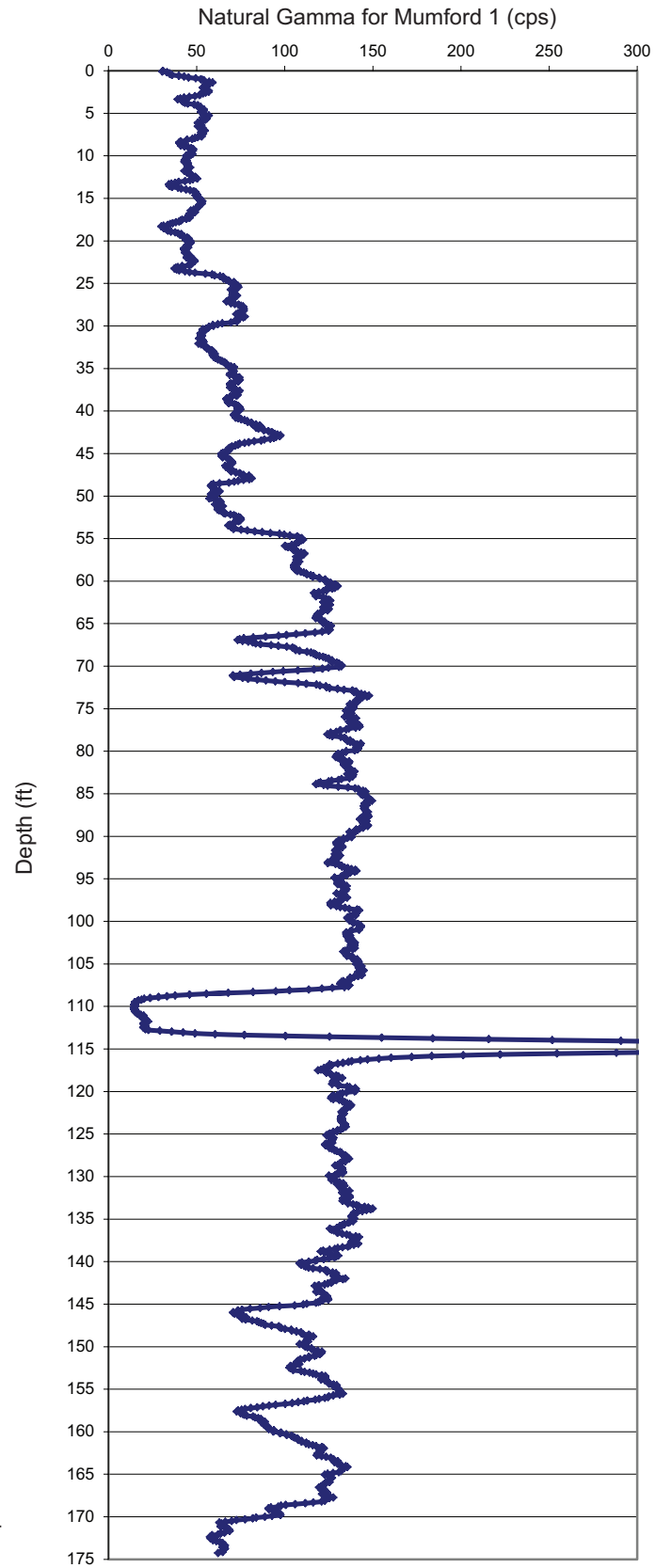


Figure A4-1 Natural gamma log for Mumford 1 (MH-1) groundwater monitoring well.

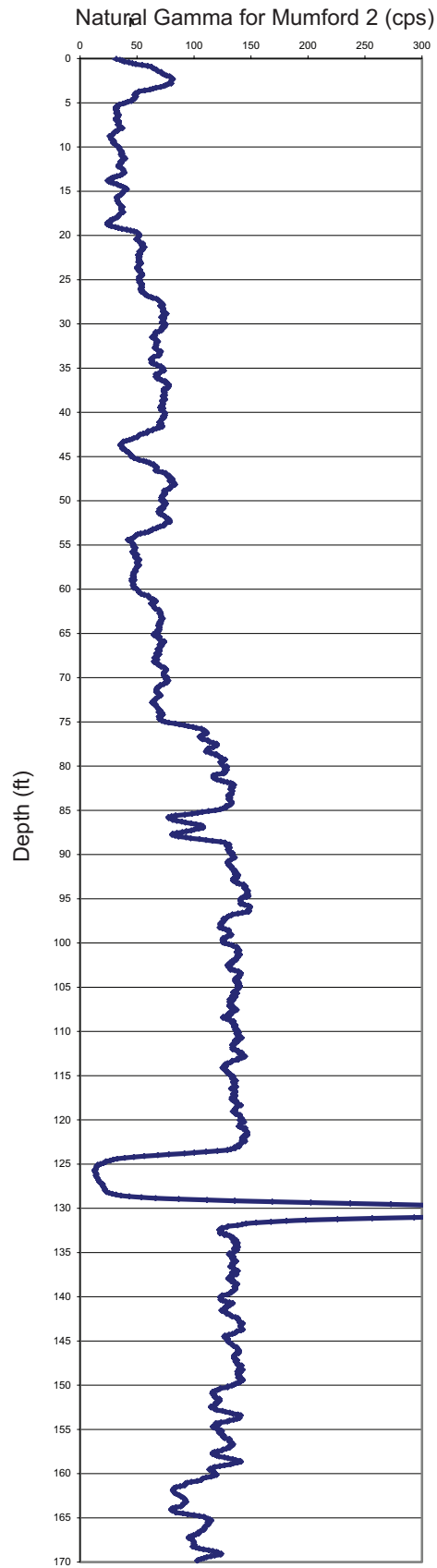


Figure A4-2 Natural gamma log for Mumford 2 (MH-2) ground-water monitoring well.

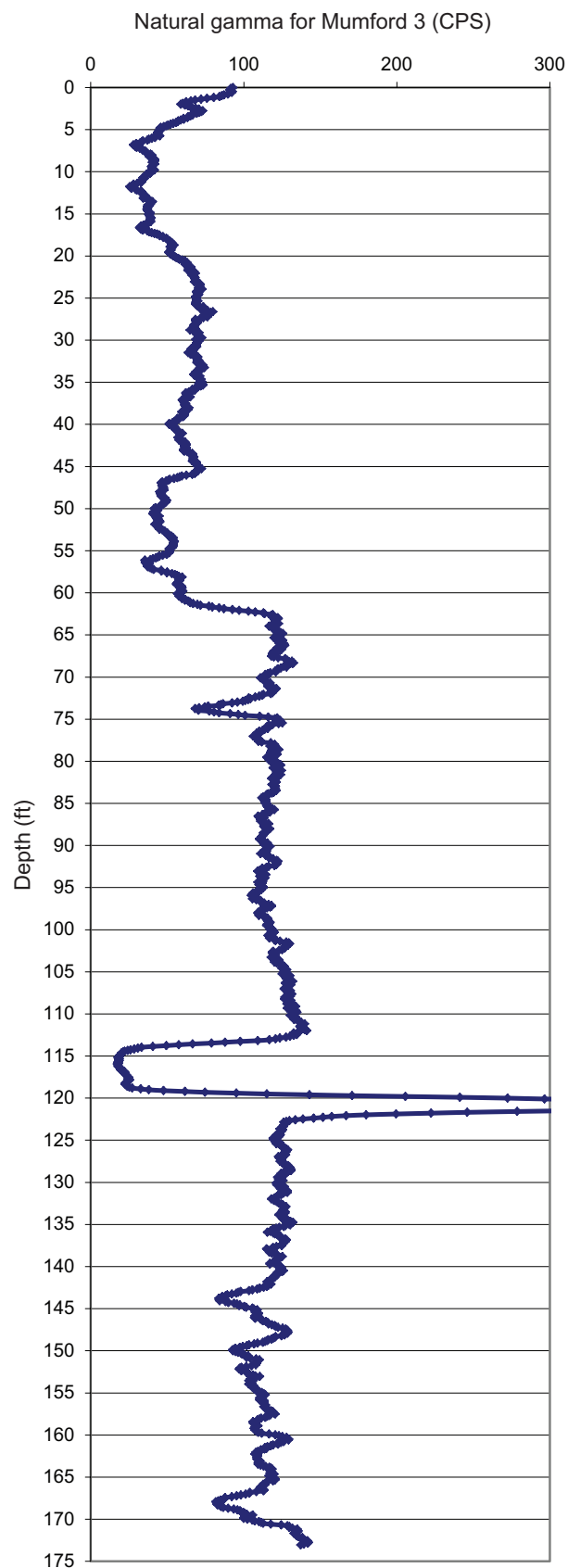


Figure A4-3 Natural gamma log for Mumford 3 (MH-3) groundwater monitoring well.

API # 131290000100

Date installed 7/16/09

Hole # MW Ford #1

Well T.D to top of riser 177.2

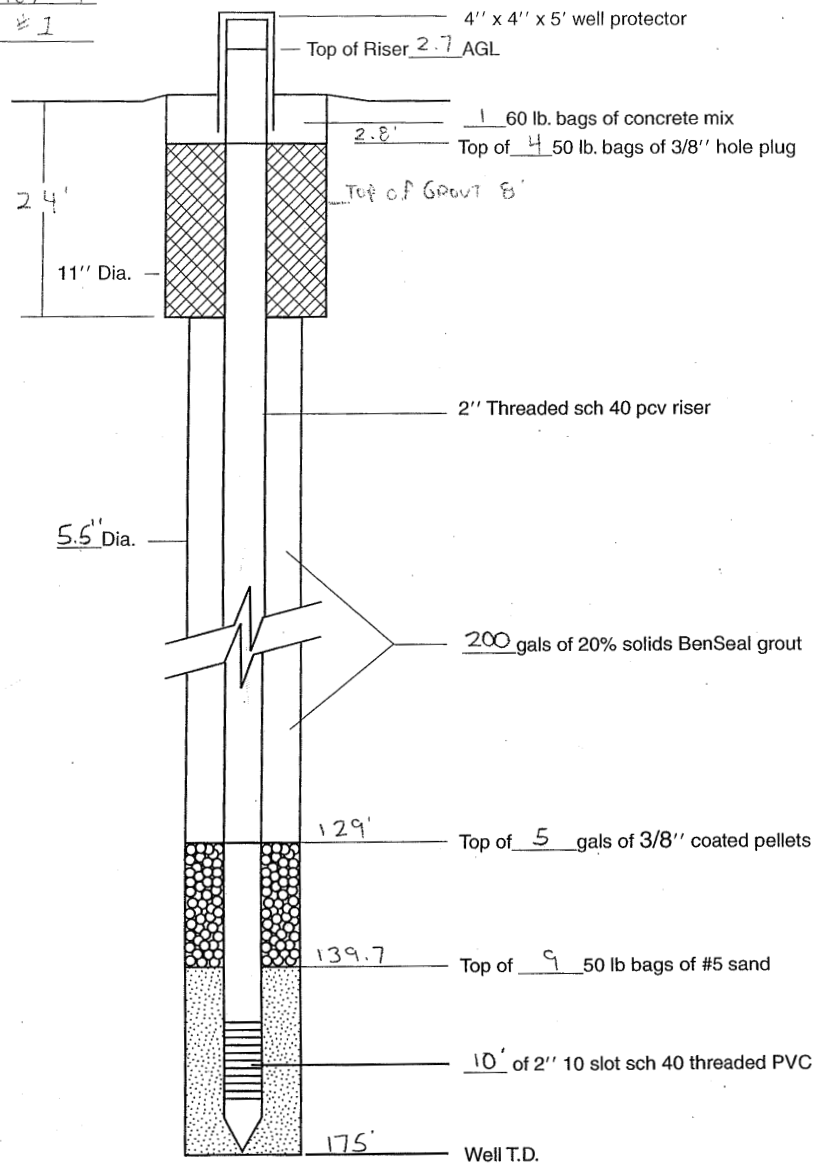


Figure A4-4 Details of groundwater monitoring well construction, MH-1.

API # 131290000200

Date installed 7/22/09

Hole # Mumford #2

Well T.D to top of riser 172.7

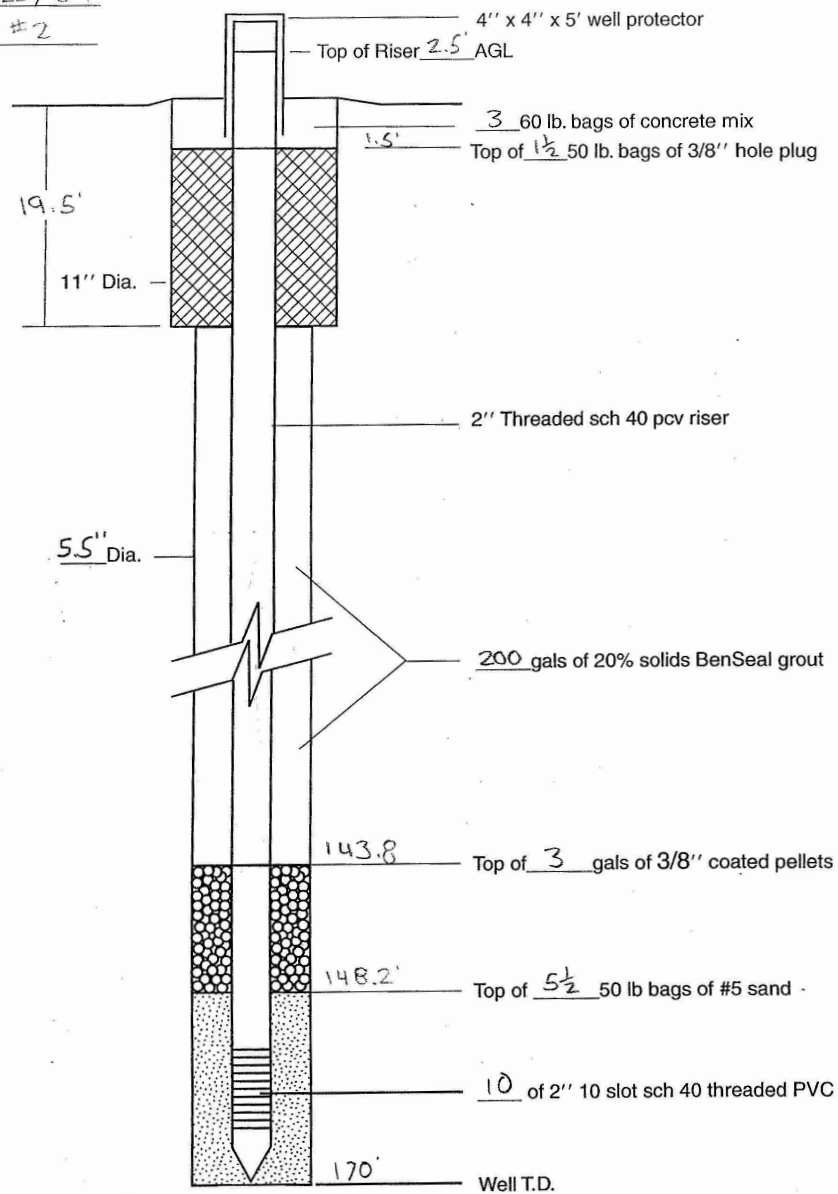


Figure A4-5 Details of groundwater monitoring well construction, MH-2.

API # 131290000300
 Date installed 7/29/09
 Hole # Mumford #3

Well T.D to top of riser 177.7

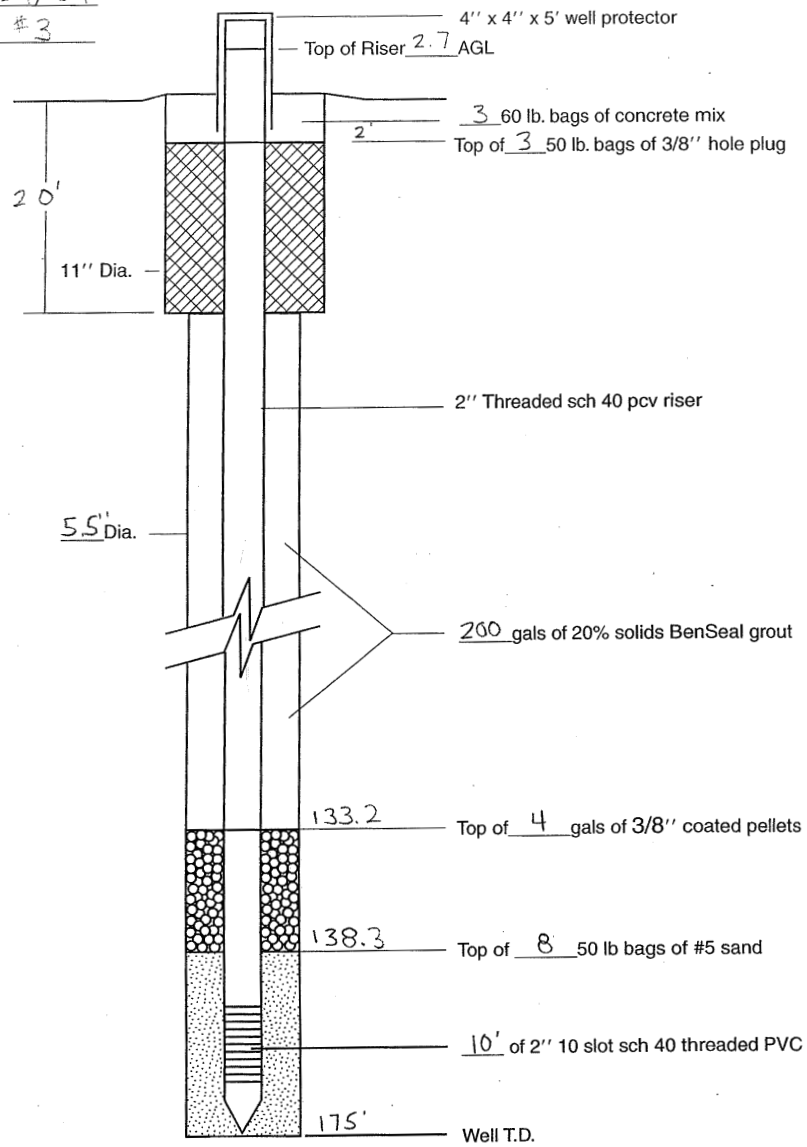


Figure A4-6 Details of groundwater monitoring well construction, MH-3.

Appendix 5 Chemistry of Reservoir Brine

Table A5-1 Concentrations (in mg/L) of constituents detected in reservoir brine samples from wells BA-1 and BA-2.

Sample Date	Source ID	B	Ba	Br	Ca	Cl	F	Fe	K	Li	Mg	Mn	Na
08/11/09	BA-1	2.2	2.5	29.3	244	12,936	0.76	1.0	26.9	0.32	123	0.2	7,952
09/01/09	BA-1	2.2	2.5	33.1	251	12,786	1.10	0.8	28.6	0.76	128	0.5	8,137
09/17/09	BA-1	2.2	2.4	33.0	254	14,692	0.76	0.6	28.1	0.35	125	0.4	7,827
10/14/09	BA-1	2.2	2.2	33.2	265	12,875	0.88	0.6	32.5	0.37	124	0.5	7,786
11/12/09	BA-1	2.2	1.9	33.2	282	12,905	1.30	0.4	28.1	0.35	130	0.6	7,983
12/22/09	BA-1	2.2	2.1	33.9	268	12,916	0.74	28.5	26.6	0.62	125	0.6	7,444
02/03/10	BA-1	2.2	3.3	26.8	320	14,069	1.15	75.8	24.1	0.36	132	1.3	8,151
03/18/10	BA-1	2.1	3.0	33.7	334	13,235	<0.1	19.5	25.0	0.45	124	1.3	7,950
06/09/10	BA-1	2.3	2.9	36.8	365	12,667	0.00	82.6	41.7	0.40	139	2.6	8,041
08/27/10	BA-1	2.5	3.4	27.1	355	12,970	3.40	129.0	43.1	0.40	144	2.4	7,868
11/04/10	BA-1	2.3	2.8	27.9	338	12,680	3.30	84.0	40.9	0.43	134	2.3	7,486
01/06/11	BA-1	2.1	2.1	26.0	338	12,790	<0.8	99.1	36.6	0.38	132	2.1	7,555
03/03/11	BA-1	2.2	2.0	26.0	352	13,060	<0.8	75.6	30.8	0.32	146	2.1	7,960
04/07/11	BA-1	2.2	2.0	30.0	315	12,960	<0.8	40.4	28.2	-	135	1.7	8,022
05/25/11	BA-1	2.2	2.1	29.0	343	12,510	<0.8	49.5	27.6	0.33	141	2.0	7,710
08/02/11	BA-1	2.2	2.2	29.0	343	12,690	1.00	59.1	42.4	0.43	141	2.3	7,687
08/11/09	BA-2	2.9	0.4	47.2	358	22,925	0.98	28.1	47.3	0.56	214	0.9	12,190
09/01/09	BA-2	2.9	0.5	50.9	343	20,703	1.34	18.2	45.8	0.54	187	0.8	11,490
09/17/09	BA-2	2.9	0.5	47.6	353	22,838	0.94	11.0	45.5	0.55	188	0.7	12,158
10/14/09	BA-2	2.7	0.6	47.7	375	19,656	<0.1	9.5	46.8	0.49	193	0.7	11,627
11/12/09	BA-2	2.8	0.7	46.5	374	19,087	0.93	8.9	41.7	0.51	185	0.7	11,112
12/22/09	BA-2	2.6	0.8	46.4	339	18,895	<0.1	11.6	35.7	0.86	178	0.8	10,283
02/03/10	BA-2	2.5	1.0	127.5	325	19,298	<0.1	15.1	30.7	0.44	174	0.7	10,856
03/18/10	BA-2	2.6	0.2	44.2	312	18,517	<0.1	0.1	44.7	0.53	226	0.3	12,430
06/09/10	BA-2	3.1	1.9	3.9	437	20,800	0.00	14.9	69.0	0.70	214	0.8	12,743
08/27/10	BA-2	2.9	1.2	34.8	349	16,710	3.60	0.8	56.7	0.50	174	0.6	10,089
11/04/10	BA-2	2.4	1.2	32.0	323	15,230	3.80	0.1	46.3	0.43	155	0.5	8,825
01/06/11	BA-2	2.4	1.3	28.8	272	14,370	<0.8	0.2	42.9	0.42	145	0.5	8,701
03/03/11	BA-2	2.2	1.3	28.0	298	14,120	<0.8	0.1	34.0	0.33	159	0.5	8,860
04/07/11	BA-2	2.3	1.4	32.0	256	13,900	<0.8	0.1	30.4	-	137	0.5	8,277
05/25/11	BA-2	2.2	1.5	31.0	277	13,600	<0.8	0.0	28.6	0.35	146	0.5	8,445
08/02/11	BA-2	2.2	1.5	31.0	279	14,180	1.00	0.1	46.3	0.44	144	0.5	8,050
12/08/11	BA-2	2.2	1.63	34.8	268	13,592	<0.8	0.4	28.9	0.33	143	0.453	8,619

¹Due to measurements below detection limits, values for constituents As, Be, Cd, Co, Cr, and Cu are not listed.

Table A5-2 Concentrations (in mg/L) of constituents detected in reservoir brine samples from wells BA-1 and BA-2 (continued).

Sample date	Source ID	Ni	NO ₃ -N	P	Pb	S	Se	Si	SO ₄	Sr	Tl	Zn
08/11/09	BA-1	0.07	<0.1	0.10	0.05	83.6	0.14	6.40	75.5	14.5	0.02	0.02
09/01/09	BA-1	0.06	<0.1	0.07	0.05	41.1	<0.131	6.40	70.7	14.8	0.02	<0.0073
09/17/09	BA-1	0.06	<0.1	0.10	<0.041	54.8	<0.131	6.38	75.8	14.4	0.02	<0.0073
10/14/09	BA-1	0.05	2.18	0.07	<0.041	45.6	0.15	6.44	75.5	14.3	0.05	<0.0073
11/12/09	BA-1	0.06	<0.1	<0.063	0.05	59.0	<0.131	6.56	90.2	14.7	0.03	<0.0073
12/22/09	BA-1	0.05	2.45	<0.063	<0.041	72.4	0.15	6.29	93.6	13.6	0.03	0.02
02/03/10	BA-1	0.05	<0.1	0.11	0.05	32.4	<0.131	7.72	90.2	13.1	<0.017	0.03
03/18/10	BA-1	0.04	<0.1	0.22	<0.041	29.4	<0.131	7.82	91.2	13.5	<0.017	0.02
06/09/10	BA-1	0.08	0.91	0.07	<0.041	62.1	0.18	7.27	94.2	14.4	<0.017	0.04
08/27/10	BA-1	0.07	<0.7	<0.06	0.06	30.8	0.17	7.91	76.2	14.0	0.02	0.05
11/04/10	BA-1	0.08	<0.7	<0.073	<0.041	81.0	0.44	7.44	75.0	13.1	<0.017	0.03
01/06/11	BA-1	<0.014	<0.7	<0.073	<0.041	53.1	0.21	6.90	72.7	13.5	<0.017	0.02
03/03/11	BA-1	<0.014	<0.7	0.09	<0.041	27.3	<0.13	7.29	70.0	14.0	<0.017	0.03
04/07/11	BA-1	<0.043	<0.7	<0.073	<0.041	29.1	0.17	7.55	72.0	13.8	0.03	0.04
05/25/11	BA-1	<0.043	<0.7	<0.073	<0.041	71.9	0.17	7.76	71.0	14.2	<0.017	0.02
08/02/11	BA-1	<0.043	<1	<0.073	0.05	37.7	0.14	7.47	71.0	13.9	<0.017	0.02
08/11/09	BA-2	0.09	2.26	<0.063	0.07	85.3	<0.131	5.52	206.7	20.0	0.03	0.04
09/01/09	BA-2	0.09	<0.1	0.08	0.05	77.9	<0.131	6.13	212.1	19.3	0.02	<0.0073
09/17/09	BA-2	0.09	<0.1	0.06	0.04	74.4	<0.131	6.47	188.2	20.7	0.04	<0.0073
10/14/09	BA-2	0.09	<0.1	<0.063	<0.041	74.7	<0.131	6.31	171.4	20.0	0.04	0.01
11/12/09	BA-2	0.08	2.50	<0.063	0.06	71.1	<0.131	6.77	163.6	19.1	0.04	<0.0073
12/22/09	BA-2	0.07	<0.1	<0.063	0.06	62.6	0.14	6.02	144.5	17.7	0.03	0.02
02/03/10	BA-2	0.06	<0.1	<0.063	0.06	50.1	<0.131	6.83	723.9	15.9	0.02	0.01
03/18/10	BA-2	0.06	<0.1	0.23	0.09	199.7	<0.131	6.72	119.2	20.5	0.04	0.02
06/09/10	BA-2	0.12	1.42	0.40	0.05	71.7	0.18	6.56	186.1	20.8	0.04	0.02
08/27/10	BA-2	0.08	0.96	0.18	0.05	50.9	0.15	6.88	117.0	16.3	0.01	0.03
11/04/10	BA-2	0.09	<0.7	0.13	0.05	117.9	0.19	6.24	95.1	14.2	0.05	0.02
01/06/11	BA-2	<0.014	<0.7	0.12	<0.041	75.5	0.37	6.24	88.8	14.5	<0.017	0.01
03/03/11	BA-2	<0.014	<0.7	0.14	<0.041	59.6	0.16	6.26	65.0	14.8	0.05	0.01
04/07/11	BA-2	<0.043	<0.7	0.10	0.05	131.0	0.18	6.71	62.0	14.2	0.03	0.01
05/25/11	BA-2	<0.043	<0.7	0.09	0.05	114.0	0.18	6.57	59.0	14.6	0.02	0.02
08/02/11	BA-2	<0.043	<0.7	0.10	0.07	42.9	0.19	6.26	69.0	14.1	0.04	0.02
12/08/11	BA-2	<0.043	<0.7	<0.063	<0.041	82.8	0.26	6.17	82.9	14.9	0.03	<0.0073

¹Due to measurements below detection limits, values for constituents PO₄, Sp, Sb, Sn, and V are not listed.

Table A5-3 Measurements of water quality parameters from reservoir brine samples from wells BA-1 and BA-2.

Sample date	Source ID	pH	DO ¹ (mg/L)	EC (mS/cm)	Eh (mV)	Temperature (°C)	Alkalinity (mg/L)	TDS (mg/L)	Dissolved CO ₂ (mg/L)
08/11/09	BA-1	7.08	0.7	34.77	-105	23.4	496	20,962	444
09/01/09	BA-1	7.27	2.8	27.80	-55	21.4	528	22,110	468
09/17/09	BA-1	7.33	1.7	30.66	-91	21.4	502	22,390	449
10/14/09	BA-1	7.23	-	37.15	-126	14.2	500	22,736	447
11/12/09	BA-1	7.33	0.3	52.41	-187	18.3	520	22,516	-
12/22/09	BA-1	5.65	0.3	52.69	-130	9.8	600	22,396	613
02/03/10	BA-1	5.43	0.6	38.15	-38	1.9	784	23,008	890
03/18/10	BA-1	5.48	0.2	32.50	-64	15.6	756	22,808	675
06/09/10	BA-1	5.92	0.1	39.96	-97	21.7	892	21,964	908
08/27/10	BA-1	5.82	0.1	33.29	-21	21.6	900	22,952	969
11/04/10	BA-1	5.82	0.2	35.59	5	14.1	880	23,616	2,080
01/06/11	BA-1	5.71	0.2	33.79	-66	8.5	984	22,600	2,557
03/03/11	BA-1	5.28	0.2	46.84	-18	11.2	904	22,100	2,329
04/07/11	BA-1	5.69	0.1	46.74	-62	16.6	852	22,960	1,882
05/25/11	BA-1	5.61	0.2	35.56	-70	20.4	864	22,790	1,608
08/02/11	BA-1	5.79	0.1	36.04	162	26.9	864	22,390	1,575
08/11/09	BA-2	7.49	0.3	46.43	-36	23.1	360	34,610	334
09/01/09	BA-2	7.26	0.7	35.56	17	21.5	400	33,529	348
09/17/09	BA-2	7.48	0.7	26.23	7	20.7	424	33,610	395
10/14/09	BA-2	7.52	-	39.89	-55	14.0	404	34,372	731
11/12/09	BA-2	6.73	0.3	49.67	-156	17.0	454	32,056	-
12/22/09	BA-2	6.35	0.5	53.16	-130	9.5	474	31,740	419
02/03/10	BA-2	6.65	1.1	41.14	-13	2.3	452	30,836	372
03/18/10	BA-2	6.11	0.5	37.48	-25	13.0	460	30,460	384
06/09/10	BA-2	7.38	0.4	50.02	-23	20.8	436	35,672	399
08/27/10	BA-2	7.11	0.1	28.45	-44	23.4	448	29,436	445
11/04/10	BA-2	7.01	0.2	36.72	-72	17.5	514	26,464	445
01/06/11	BA-2	7.20	0.3	38.71	-109	13.7	528	24,896	473
03/03/11	BA-2	6.72	0.2	48.26	-99	15.4	564	24,500	464
04/07/11	BA-2	7.18	0.3	48.97	-99	18.6	514	24,120	468
05/25/11	BA-2	7.19	0.3	38.94	-101	21.0	520	24,120	460
08/02/11	BA-2	6.82	0.2	34.48	99	32.2	524	23,780	482
12/08/11	BA-2	6.86	0.5	44.32	-126	6.6	544	-	480

¹Abbreviations: DO, dissolved oxygen; EC, electrical conductivity; EH, redox potential; TDS, total dissolved solids.

Table A5-4 Concentrations of constituents detected in reservoir brine samples from wells IB-2 and IB-3. All measurements in mg/L.

Sample date	Source ID	B	Ba	Br	Ca	Cl	F	Fe	K	Li	Mg	Mn	Na
08/11/09	IB-2	1.5	0.9	57.3	108	28,383	2.43	6.0	66.1	1.05	159	1.4	15,890
09/01/09	IB-2	3.1	0.4	60.1	336	25,903	1.76	16.5	60.0	0.70	305	1.0	15,406
09/17/09	IB-2	2.9	0.3	57.7	365	28,480	<0.1	4.7	53.7	0.60	291	0.8	14,570
10/14/09	IB-2	2.9	0.2	56.9	357	24,427	<0.1	0.3	59.3	0.64	279	0.6	14,719
11/12/09	IB-2	3.0	0.2	55.6	392	23,704	<0.1	0.1	51.5	0.62	268	0.6	13,921
12/22/09	IB-2	2.8	0.2	54.4	353	21,811	<0.1	0.3	46.8	1.09	248	0.5	12,910
02/03/10	IB-2	2.7	0.1	30.3	341	23,249	1.54	0.2	39.0	0.54	239	0.3	13,103
03/18/10	IB-2	2.6	0.2	49.5	312	21,060	<0.1	0.1	44.7	0.53	226	0.3	12,430
06/09/10	IB-2	2.9	0.2	53.9	337	19,354	3.60	20.9	69.9	0.70	239	1.4	12,296
08/27/10	IB-2	2.9	0.8	38.2	278	18,610	3.70	0.1	157.0	0.60	215	0.8	11,397
11/04/10	IB-2	2.6	0.4	36.8	267	18,080	<0.8	0.3	80.8	0.56	204	0.5	10,688
01/06/11	IB-2	2.7	0.3	34.6	233	18,030	<0.8	2.8	86.0	0.57	199	0.4	11,022
03/03/11	IB-2	2.5	0.4	34.0	226	18,460	<0.8	1.6	45.6	0.47	207	0.3	11,000
04/07/11	IB-2	2.6	0.4	41.0	240	18,210	<0.8	0.1	41.7	-	207	0.3	10,990
05/25/11	IB-2	2.5	0.4	39.0	229	17,530	1.00	0.1	40.6	0.45	204	0.2	10,670
08/02/11	IB-2	2.6	0.5	40.0	216	17,040	<0.8	0.2	63.9	0.61	195	0.2	10,670
12/08/11	IB-2	2.66	0.555	46.5	202	18,353	<2	9.7	43.4	0.47	215	0.661	11,697
08/11/09	IB-3	3.0	1.2	54.5	320	26,801	1.43	63.0	60.6	0.66	278	1.4	14,375
09/01/09	IB-3	2.9	1.6	57.8	343	24,500	1.80	31.3	49.6	0.56	245	1.0	12,827
09/17/09	IB-3	3.0	1.4	54.8	354	27,189	1.40	28.6	54.9	0.62	263	1.1	13,938
10/14/09	IB-3	2.9	1.4	52.7	358	22,990	1.84	32.0	56.0	0.59	248	1.2	13,495
11/12/09	IB-3	2.9	1.3	52.1	364	21,777	2.38	23.7	47.5	0.55	243	1.1	12,755
12/22/09	IB-3	2.8	1.3	51.2	338	21,936	1.44	20.5	42.9	0.99	222	1.0	11,994
02/03/10	IB-3	2.6	1.1	33.5	336	22,353	1.88	15.7	34.4	0.49	224	0.9	12,525
03/18/10	IB-3	2.5	0.9	48.7	322	20,914	0.44	14.8	37.2	0.52	224	0.9	12,133
06/09/10	IB-3	2.8	0.4	51.7	339	18,037	0.00	20.1	62.7	0.60	215	1.5	11,330
08/27/10	IB-3	2.8	1.0	36.5	315	17,890	4.10	7.9	62.6	0.60	197	0.6	10,649
11/04/10	IB-3	2.5	1.0	35.5	290	17,270	4.20	5.3	54.0	0.51	197	0.4	9,783
01/06/11	IB-3	2.5	1.1	33.3	257	16,280	<0.8	6.9	52.1	0.50	191	0.3	10,078
03/03/11	IB-3	2.4	1.3	33.0	266	17,250	<0.8	18.6	41.6	0.42	194	0.4	10,500
04/07/11	IB-3	2.5	1.3	39.0	253	16,890	<0.8	8.8	36.4	-	183	0.3	10,310
05/25/11	IB-3	2.5	1.4	37.0	248	16,720	<0.8	2.2	37.7	0.43	192	0.2	10,030
08/02/11	IB-3	2.6	1.9	38.0	244	17,270	2.00	2.9	60.0	0.58	199	0.3	9,901
12/08/11	IB-3	2.58	2.06	47.6	242	17,393	<2	4.13	37.5	0.42	182	0.664	10,946

¹Due to measurements below detection limits, values for constituents As, Be, Cd, Co, Cr, Cu, and Mo are not listed.

Table A5-5 Concentrations of constituents detected in reservoir brine samples from wells IB-2 and IB-3 (continued). All measurements in mg/L.

Sample date	Source ID	Ni	NO ₃ -N	P	Pb	S	Se	Si	SO ₄	Sr	Tl	Zn
08/11/09	IB-2	0.08	<1	0.14	0.06	2.8	<0.131	0.13	10.8	8.4	0.02	0.01
09/01/09	IB-2	0.11	<0.1	0.06	<0.041	310.2	<0.131	5.69	868.3	27.3	0.03	<0.0073
09/17/09	IB-2	0.12	<0.1	0.08	0.05	306.4	<0.131	5.54	867.7	26.5	0.04	<0.0073
10/14/09	IB-2	0.11	2.19	0.08	<0.041	297.9	0.16	5.99	851.4	27.2	0.04	<0.0073
11/12/09	IB-2	0.11	<0.1	<0.063	0.05	359.9	0.19	6.28	840.5	26.1	0.04	<0.0073
12/22/09	IB-2	0.10	<0.1	<0.063	0.04	316.7	0.21	5.61	813.4	22.9	0.05	0.02
02/03/10	IB-2	0.08	<0.1	0.13	<0.041	256.6	0.18	6.43	126.7	21.1	0.04	<0.0073
03/18/10	IB-2	0.06	<0.1	0.23	0.09	199.7	<0.131	6.72	670.7	20.5	0.04	0.02
06/09/10	IB-2	0.12	0.00	0.11	<0.041	224.0	0.16	6.27	612.1	19.4	0.04	0.02
08/27/10	IB-2	0.09	<0.7	0.21	<0.041	178.0	0.21	6.01	427.0	17.0	0.03	0.02
11/04/10	IB-2	0.12	<0.7	0.25	<0.041	204.9	0.14	5.89	417.0	17.1	0.03	0.01
01/06/11	IB-2	<0.014	<0.7	0.16	<0.041	161.0	<0.13	5.95	431.0	17.7	0.02	0.01
03/03/11	IB-2	<0.014	<0.7	0.08	<0.041	154.0	<0.13	5.60	407.0	17.9	0.04	0.01
04/07/11	IB-2	<0.043	<0.7	0.09	<0.041	183.0	0.14	6.11	402.0	18.1	0.04	0.01
05/25/11	IB-2	<0.043	<0.7	0.08	0.06	159.0	<0.13	6.14	370.0	18.5	0.05	0.02
08/02/11	IB-2	<0.043	<1	<0.073	<0.041	141.6	0.31	5.80	335.0	17.7	0.02	0.02
12/08/11	IB-2	<0.043	<0.7	0.86	<0.041	135	0.31	6.08	407	17.2	0.05	0.03
08/11/09	IB-3	0.11	<0.1	<0.063	0.05	167.6	0.18	4.85	441.2	22.4	0.02	0.02
09/01/09	IB-3	0.10	<0.1	<0.063	0.06	131.5	0.16	7.93	438.9	22.8	0.05	0.01
09/17/09	IB-3	0.10	<0.1	<0.063	0.05	157.1	<0.131	9.34	417.7	24.6	0.03	0.01
10/14/09	IB-3	0.10	<0.1	<0.063	<0.041	145.9	0.13	9.31	357.8	23.0	0.04	<0.0073
11/12/09	IB-3	0.10	<0.1	<0.063	0.06	139.4	<0.131	9.39	388.9	22.1	0.03	<0.0073
12/22/09	IB-3	0.09	<0.1	<0.063	<0.041	117.4	<0.131	8.45	310.5	20.1	<0.017	0.03
02/03/10	IB-3	0.07	<0.1	0.09	0.08	110.0	0.15	9.19	299.0	19.1	0.02	<0.0073
03/18/10	IB-3	0.06	<0.1	0.13	0.09	91.8	<0.131	9.73	291.3	19.1	<0.017	0.05
06/09/10	IB-3	0.11	0.00	0.09	<0.041	134.0	<0.131	9.11	367.0	18.0	0.03	0.02
08/27/10	IB-3	0.10	<0.7	0.10	0.04	91.9	<0.131	9.36	216.0	17.8	0.04	0.03
11/04/10	IB-3	0.12	<0.7	0.11	<0.041	162.2	0.16	8.22	179.0	16.8	0.04	0.01
01/06/11	IB-3	<0.014	<0.7	<0.073	<0.041	98.9	0.18	7.98	154.0	17.5	<0.017	0.01
03/03/11	IB-3	<0.014	<0.7	0.10	<0.041	54.2	<0.13	8.01	130.0	17.8	0.03	0.02
04/07/11	IB-3	<0.043	<0.7	<0.073	<0.041	94.2	<0.13	8.57	120.0	17.3	<0.017	0.01
05/25/11	IB-3	<0.043	<0.7	<0.073	0.05	81.5	0.18	8.52	95.0	17.7	0.04	0.02
08/02/11	IB-3	<0.043	<0.7	<0.073	0.05	25.6	0.14	8.34	55.0	16.5	0.05	0.02
12/08/11	IB-3	<0.043	<0.7	<0.073	0.06	32.3	<0.13	8.65	102	18.2	0.028	0.01

¹Due to measurements below detection limits, values for constituents PO₄, Sp, Sb, Sn, and V are not listed.

Table A5-6 Measurements of water quality parameters from reservoir brine samples from wells IB-2 and IB-3.

Date	Source ID	pH	DO ¹ (mg/L)	EC (mS/cm)	Eh (mV)	Temperature (°C)	Alkalinity (mg/L)	TDS (mg/L)	Dissolved CO ₂ (mg/L)
08/11/09	IB-2	7.53	0.2	50.84	-30	25.8	64	42,520	69
09/01/09	IB-2	7.47	0.2	41.04	-49	20.4	536	41,900	470
09/17/09	IB-2	7.65	0.2	38.97	-27	23.2	524	43,050	620
10/14/09	IB-2	7.61	-	51.66	-131	11.2	564	41,824	502
11/12/09	IB-2	7.58	0.2	56.54	-191	16.4	556	40,324	-
12/22/09	IB-2	6.50	1.1	53.15	-156	8.1	552	38,312	493
02/03/10	IB-2	6.81	0.6	33.07	-57	4.9	532	36,980	460
03/18/10	IB-2	5.98	0.2	44.13	-71	10.5	552	35,648	457
06/09/10	IB-2	7.50	0.1	45.39	-87	25.1	512	34,084	449
08/27/10	IB-2	7.75	0.1	35.06	-73	25.2	444	32,708	419
11/04/10	IB-2	7.40	0.2	43.06	-19	14.5	484	31,796	427
01/06/11	IB-2	6.91	0.1	31.96	273	7.1	484	31,516	464
03/03/11	IB-2	6.44	0.4	50.70	48	8.8	460	31,000	417
04/07/11	IB-2	6.91	0.2	55.42	42	13.8	446	31,300	427
05/25/11	IB-2	7.08	0.2	36.71	-19	20.7	432	30,880	390
08/02/11	IB-2	5.63	0.1	47.02	17	26.1	428	30,630	916
12/08/11	IB-2	7.11	1.6	44.04	-14	8.3	436	-	381
08/11/09	IB-3	7.39	0.1	62.80	-52	25.4	420	40,960	390
09/01/09	IB-3	7.34	0.2	45.83	-78	23.8	544	40,790	516
09/17/09	IB-3	7.49	0.1	47.98	-97	23.5	564	39,920	527
10/14/09	IB-3	7.44	-	59.90	-127	14.4	532	38,612	503
11/12/09	IB-3	7.47	0.1	53.86	-174	17.1	548	37,172	-
12/22/09	IB-3	6.23	0.4	58.86	-142	9.6	590	35,988	513
02/03/10	IB-3	6.25	0.4	44.03	-43	5.0	608	35,632	516
03/18/10	IB-3	6.28	0.2	49.24	-27	13.6	600	34,644	500
06/09/10	IB-3	6.82	0.5	52.18	-50	21.3	564	31,412	507
08/27/10	IB-3	6.38	0.1	44.17	-78	24.6	512	31,020	525
11/04/10	IB-3	6.19	0.2	34.75	-57	14.9	584	30,700	605
01/06/11	IB-3	6.32	0.4	29.17	-117	8.6	604	29,364	703
03/03/11	IB-3	5.65	0.2	60.27	-67	11.1	612	29,300	708
04/07/11	IB-3	6.37	0.2	64.94	-111	15.2	588	28,990	639
05/25/11	IB-3	6.57	0.2	47.42	-126	19.7	604	29,580	572
08/02/11	IB-3	6.44	0.1	47.82	130	29.0	572	29,370	583
12/08/11	IB-3	7.25	0.4	42.67	-90	7.4	612	-	549

¹Abbreviations: DO, dissolved oxygen; EC, electrical conductivity; Eh, redox potential; TDS, total dissolved solids.

Table A5-7 Concentration (in mg/L) of constituents detected in reservoir brine samples from well BD-3 and the tank battery (TB-1).

Sample date	Source ID	B	Ba	Br	Ca	Cl	F	Fe	K	Li	Mg	Mn	Na
08/13/09	BD-3	1.1	1.5	4.6	10	1,084	2.01	0.3	3.4	0.04	6	0.0	1,105
09/01/09	BD-3	1.1	1.4	8.1	9	1,287	1.88	0.2	3.7	<0.018	5	0.0	1,108
11/12/09	BD-3	1.1	1.4	6.7	9	1,288	1.77	0.5	3.4	<0.058	5	0.0	1,054
02/02/10	BD-3	1.1	1.3	3.6	9	1,300	1.63	0.2	3.0	<0.2	5	0.0	1,073
03/17/10	BD-3	1.1	1.4	7.3	9	1,305	1.60	0.2	3.0	<0.058	5	0.0	1,115
08/26/10	BD-3	1.2	1.4	1.7	10	1,182	1.70	0.2	4.1	0.05	5	0.0	1,097
11/03/10	BD-3	1.1	1.4	2.9	9	1,253	1.93	0.2	3.6	<0.11	5	0.0	1,011
01/05/11	BD-3	1.1	1.3	2.9	9	1,258	1.84	0.2	3.3	<0.11	5	0.0	1,128
03/02/11	BD-3	1.1	1.3	3.1	9	1,279	1.72	0.2	3.4	<0.11	6	0.0	1,160
04/06/11	BD-3	1.1	1.4	3.0	9	1,319	2.00	0.1	3.3	-	5	0.0	1,064
05/25/11	BD-3	1.1	1.3	3.0	9	1,207	2.00	0.3	3.2	<0.11	5	0.0	1,012
08/01/11	BD-3	1.1	1.4	3.0	9	1,327	2.00	0.3	3.8	<0.11	5	0.0	1,078
08/11/09	TB-1	2.3	2.5	31.3	249	14,908	0.66	0.7	30.5	0.36	131	0.3	8,007
09/01/09	TB-1	2.3	2.3	35.9	270	14,557	1.20	2.0	31.1	0.37	142	0.6	8,795
09/17/09	TB-1	2.3	2.1	38.1	272	18,022	0.84	1.2	31.1	0.37	143	0.5	8,875
10/14/09	TB-1	2.3	1.9	36.2	279	14,291	0.89	2.0	35.3	0.39	139	0.5	9,020
11/12/09	TB-1	2.4	1.6	36.7	304	14,372	1.14	4.1	33.7	0.41	156	0.7	9,074
12/22/09	TB-1	2.3	1.8	38.5	307	14,765	0.65	27.1	29.9	0.70	146	0.6	8,323
02/03/10	TB-1	2.3	2.6	28.2	332	15,706	1.22	60.6	27.1	0.39	147	1.1	9,223
03/18/10	TB-1	2.2	2.4	36.8	340	15,029	<0.1	16.6	26.7	0.39	139	1.2	9,040
06/09/10	TB-1	2.8	2.0	47.0	391	17,858	0.00	38.8	61.7	0.60	193	1.4	11,041
08/27/10	TB-1	2.7	1.7	32.9	339	15,740	3.60	37.6	54.1	0.50	170	1.1	9,434
11/04/10	TB-1	2.4	1.6	31.2	321	14,790	3.50	24.0	47.1	0.45	156	1.0	8,575
01/06/11	TB-1	2.4	1.4	28.2	281	13,880	<0.8	19.3	43.2	0.42	141	0.8	8,581
03/03/11	TB-1	2.2	1.5	28.0	300	14,430	<0.8	15.6	34.3	0.34	161	0.8	8,970
04/07/11	TB-1	2.3	1.5	32.0	266	14,230	<0.8	10.0	30.5	-	143	0.7	8,544

¹Due to measurements below detection limits, values for constituents As, Be, Cd, Co, Cr, Cu, and Mo are not listed.

Table A5-8 Concentration (in mg/L) of constituents detected in reservoir brine samples from well BD-3 and the tank battery (TB-1).

Sample date	Source ID	Ni	NO ₃ -N	P	Pb	S	Se	Si	SO ₄	Sr	Tl	Zn
08/13/09	BD-3	<0.014	<0.1	0.09	<0.041	0.5	<0.131	4.00	<0.1	0.8	<0.017	<0.0073
09/01/09	BD-3	<0.014	<0.1	0.10	<0.041	<0.217	<0.131	3.99	<0.1	0.7	<0.017	<0.0073
11/12/09	BD-3	0.01	<0.1	0.06	<0.041	0.3	<0.131	3.99	<0.1	0.7	<0.017	0.06
02/02/10	BD-3	<0.014	<0.1	0.07	<0.041	<0.217	<0.131	3.96	<0.1	0.6	<0.017	<0.0073
03/17/10	BD-3	<0.014	<0.1	<0.063	<0.041	<0.217	<0.131	4.04	<0.1	0.7	<0.017	0.02
08/26/10	BD-3	<0.014	0.00	0.06	<0.041	<0.217	<0.131	4.10	0.0	0.7	<0.017	0.02
11/03/10	BD-3	<0.014	<0.07	0.26	<0.041	<0.217	<0.131	3.89	<0.3	0.7	<0.017	0.01
01/05/11	BD-3	<0.014	<0.07	<0.073	<0.041	<0.22	<0.13	3.77	<0.3	0.7	<0.017	<0.0073
03/02/11	BD-3	<0.014	<0.07	0.08	<0.041	<0.22	<0.13	4.19	<0.31	0.7	<0.017	0.01
04/06/11	BD-3	<0.043	<0.07	<0.073	<0.041	0.3	<0.13	4.04	5.0	0.7	<0.017	0.01
05/25/11	BD-3	<0.043	<0.07	0.08	<0.041	0.2	<0.13	4.06	<0.31	0.7	<0.017	<0.0097
08/01/11	BD-3	<0.043	0.00	0.08	<0.041	<0.22	<0.13	4.08	0.0	0.7	<0.017	<0.0097
08/11/09	TB-1	0.06	<0.1	0.08	0.05	63.2	0.17	6.41	7.8	14.3	0.02	0.02
09/01/09	TB-1	0.07	<0.1	<0.063	<0.041	54.9	0.15	6.46	124.8	15.7	0.03	0.03
09/17/09	TB-1	0.07	<0.1	0.07	0.04	62.0	0.14	6.45	161.1	15.9	0.03	0.01
10/14/09	TB-1	0.08	<0.1	0.07	<0.041	58.8	<0.131	6.49	123.1	16.7	0.02	0.01
11/12/09	TB-1	0.07	<0.1	<0.063	0.05	71.5	0.15	7.02	135.8	16.4	0.03	0.03
12/22/09	TB-1	0.07	<0.1	0.09	<0.041	80.1	0.16	6.39	163.2	15.3	0.03	0.02
02/03/10	TB-1	0.05	<0.1	0.13	<0.041	57.7	<0.131	7.69	153.9	14.5	<0.017	0.14
03/18/10	TB-1	0.05	<0.1	0.18	0.06	46.8	0.15	7.86	152.9	15.1	0.03	0.09
06/09/10	TB-1	0.09	0.00	0.29	0.06	74.9	0.15	6.99	210.3	18.4	<0.017	0.03
08/27/10	TB-1	0.08	<0.7	0.07	<0.041	55.3	<0.131	7.30	131.0	15.7	0.03	0.05
11/04/10	TB-1	0.10	<0.7	<0.073	<0.041	116.3	0.18	6.70	127.0	14.2	<0.017	0.07
01/06/11	TB-1	<0.014	<0.7	<0.073	<0.041	56.4	0.21	6.43	96.9	14.6	<0.017	0.02
03/03/11	TB-1	<0.014	<0.7	0.12	0.05	61.0	0.22	6.57	84.0	15.2	0.04	0.02
04/07/11	TB-1	<0.043	<0.7	<0.073	<0.041	108.0	0.16	7.06	81.0	14.6	0.04	0.02

¹Due to measurements below detection limits, values for constituents PO₄, Sp, Sb, Sn, and V are not listed.

Table A5-9 Measurements of water quality parameters from well BD-3 and the tank battery (TB-1).

Sample date	Source ID	pH	DO ¹ (mg/L)	EC (mS/cm)	Eh (mV)	Temperature (°C)	Alkalinity (mg/L)	TDS (mg/L)	Dissolved CO ₂ (mg/L)
08/13/09	BD-3	8.59	0.2	5.14	-111	15.8	672	2,924	574
09/01/09	BD-3	8.48	0.2	4.89	-71	15.7	672	2,780	571
11/12/09	BD-3	8.64	0.2	4.14	-149	14.9	656	2,780	-
02/02/10	BD-3	8.39	0.2	5.22	291	14.8	672	2,762	561
03/17/10	BD-3	8.57	0.1	5.41	-78	15.6	658	2,779	570
08/26/10	BD-3	8.60	0.2	4.56	-36	15.6	600	2,840	579
11/03/10	BD-3	8.40	0.2	4.88	-25	15.2	666	2,888	556
01/05/11	BD-3	8.75	0.3	4.65	357	5.5	652	2,823	552
03/02/11	BD-3	8.36	0.2	7.62	-59	11.6	656	2,780	551
04/06/11	BD-3	8.49	0.2	6.76	-60	14.3	652	3,052	555
05/25/11	BD-3	8.63	0.1	-	-116	20.9	664	2,672	554
08/01/11	BD-3	8.37	0.1	5.34	126	28.6	668	2,908	546
12/07/11	BD-3	7.94	0.2	8.72	-50	15.1	644	-	569
08/11/09	TB-1	7.00	0.1	37.35	-127	23.7	476	23,560	-
09/01/09	TB-1	7.04	0.2	39.69	-100	22.7	512	23,867	-
09/17/09	TB-1	7.23	0.2	30.18	-121	22.2	452	24,027	-
10/14/09	TB-1	7.20	-	40.01	-151	15.2	488	24,804	-
11/12/09	TB-1	7.28	0.3	38.33	-189	16.2	528	25,140	-
12/22/09	TB-1	5.64	0.3	47.29	-144	11.5	584	25,192	580
02/03/10	TB-1	5.42	0.2	39.72	-52	8.8	720	25,292	796
03/18/10	TB-1	5.56	1.7	37.31	-30	14.4	672	24,108	666
06/09/10	TB-1	6.00	0.2	48.23	-97	21.4	628	30,032	590
08/27/10	TB-1	5.60	0.1	39.86	-41	22.8	572	28,288	1,000
11/04/10	TB-1	5.53	0.2	29.71	-38	15.6	628	26,772	1,407
01/06/11	TB-1	5.79	0.4	26.03	-93	11.4	604	25,272	1,633
03/03/11	TB-1	5.31	0.2	42.47	-57	13.5	588	24,000	1,303
04/07/11	TB-1	5.80	0.9	54.97	-53	16.6	584	24,980	1,088

¹Abbreviations: DO, dissolved oxygen; EC, electrical conductivity; Eh, redox potential; TDS, total dissolved solids.

Appendix 6 Chemistry of groundwater.

Concentrations of constituents detected in groundwater samples collected from monitoring wells (MH-1, MH-2, MH-3) for the Mumford Hills CO₂-EOR project. Concentrations for As, Be, Cd, Co, Cr, Cu, Li, Mo, Ni, Pb, PO₄, Se, Sp, Sb, Sn, Ti, V, and Zn were below detection limits in all samples and are not listed in table.

Table A6-1 Concentrations (in mg/L) of constituents detected in groundwater samples collected from monitoring wells.

Sample date	Source ID	B	Ba	Br	Ca	Cl	F	Fe	K	Mg
08/13/09	MH-1	0.81	0.04	1.31	8.20	244	1.73	0.02	5.46	3.41
09/02/09	MH-1	0.85	0.03	0.71	5.42	291	1.62	0.01	4.17	1.96
09/18/09	MH-1	0.86	0.02	0.74	4.12	300	1.67	0.02	3.51	1.43
10/14/09	MH-1	0.88	0.02	1.63	3.67	334	1.37	0.01	3.19	1.19
11/13/09	MH-1	0.87	0.04	1.63	4.12	372	1.24	<0.0059	3.31	1.43
12/23/09	MH-1	0.85	0.06	2.28	3.83	425	1.40	0.02	2.44	1.30
02/02/10	MH-1	0.90	0.08	1.44	4.27	549	1.26	0.01	2.49	1.36
03/18/10	MH-1	0.90	0.12	3.23	5.06	631	1.12	0.01	2.34	1.72
06/09/10	MH-1	0.96	0.19	2.13	6.32	752	1.25	0.03	2.55	1.98
08/26/10	MH-1	0.98	0.22	1.67	6.42	787	1.47	0.02	2.56	2.08
11/03/10	MH-1	0.92	0.24	1.65	5.77	761	1.51	0.03	2.41	1.87
01/05/11	MH-1	0.89	0.24	1.59	6.07	754	1.29	0.05	2.27	2.06
03/02/11	MH-1	0.87	0.28	1.72	6.97	872	1.32	0.06	2.53	2.29
04/06/11	MH-1	0.92	0.31	2.10	7.76	922	1.25	0.06	2.51	2.75
05/25/11	MH-1	0.92	0.42	2.40	8.61	1,043	1.22	0.05	2.48	3.04
08/01/11	MH-1	0.94	0.46	2.52	10.12	1,127	1.21	<0.024	3.26	3.43
08/14/09	MH-2	1.08	0.02	<0.1	1.30	11	3.30	0.05	2.52	0.67
09/02/09	MH-2	1.00	0.02	<0.1	1.36	10	2.82	0.01	3.17	0.81
09/18/09	MH-2	0.95	0.02	<0.1	1.45	10	2.76	0.02	3.83	0.90
10/14/09	MH-2	0.97	0.02	<0.1	1.47	10	2.39	0.05	3.85	0.88
11/13/09	MH-2	0.97	0.02	0.17	1.57	10	2.22	0.15	3.60	0.91
12/23/09	MH-2	0.96	0.03	0.06	1.67	10	2.74	0.71	3.30	1.05
02/02/10	MH-2	1.05	0.02	<0.1	1.92	10	2.52	1.51	3.56	1.14
03/17/10	MH-2	1.05	0.02	<0.1	1.49	10	1.14	0.30	2.61	0.87
06/09/10	MH-2	1.09	0.02	0.00	1.66	46	2.93	0.01	2.56	0.84
08/26/10	MH-2	1.10	0.01	<0.08	2.01	10	2.90	0.85	2.58	0.95
11/03/10	MH-2	1.02	0.02	<0.08	1.59	9	2.92	0.02	2.15	0.73
01/05/11	MH-2	1.02	0.01	<0.08	1.43	9	3.04	<0.0059	1.87	0.74
03/02/11	MH-2	1.01	0.01	<0.08	1.39	10	3.02	0.01	1.93	0.70
04/06/11	MH-2	1.04	0.01	<0.08	1.38	9	3.10	<0.024	1.83	0.75
05/25/11	MH-2	1.05	0.02	<0.08	1.55	9	2.99	<0.024	1.80	0.80
08/01/11	MH-2	1.06	0.04	<0.08	1.97	10	3.11	1.57	3.22	1.21
09/18/09	MH-3	1.03	0.02	<0.1	3.01	9	2.30	0.06	4.89	1.31
10/16/09	MH-3	1.06	0.03	<0.1	2.99	9	2.14	0.45	4.97	1.34
11/13/09	MH-3	1.12	0.02	<0.1	2.35	9	2.10	0.07	3.40	0.97
12/23/09	MH-3	1.10	0.02	<0.1	2.28	9	2.49	0.07	2.94	0.98
02/02/10	MH-3	1.17	0.02	<0.1	2.12	9	2.19	0.19	2.78	0.87
03/17/10	MH-3	1.17	0.02	<0.1	1.90	9	1.12	0.11	2.28	0.78
06/09/10	MH-3	1.21	0.02	0.00	2.11	11	2.66	0.03	2.08	0.73
08/26/10	MH-3	1.24	0.01	<0.08	1.77	9	2.63	<0.0059	1.69	0.58
11/03/10	MH-3	1.16	0.02	<0.08	1.76	8	2.62	0.01	1.82	0.63
01/05/11	MH-3	1.14	0.02	<0.08	1.42	8	2.72	<0.0059	1.41	0.47
05/25/11	MH-3	1.13	0.02	<0.08	1.29	8	2.68	<0.024	1.46	0.45

Table A6-2 Concentrations (in mg/L) of constituents detected in groundwater samples collected from monitoring wells (continued).

Sample Date	Source ID	Mn	Na	NO ₃ -N	P	S	Si	SO ₄	Sr
08/13/09	MH-1	0.01		1.39	0.16	2.86	4.81	7.78	0.10
09/02/09	MH-1	0.01	414	0.98	0.18	2.14	4.58	5.19	0.09
09/18/09	MH-1	0.02	411	0.80	0.25	1.28	4.50	4.09	0.08
10/14/09	MH-1	0.01	442	0.52	0.25	1.13	4.50	2.63	0.08
11/13/09	MH-1	0.01	438	0.42	0.22	1.55	4.23	3.53	0.09
12/23/09	MH-1	0.02	465	<0.1	0.27	0.89	4.04	2.57	0.10
02/02/10	MH-1	0.01	552	<0.1	0.23	1.02	4.65	2.13	0.12
03/18/10	MH-1	0.01	602	<0.1	0.21	0.85	4.16	2.98	0.15
06/09/10	MH-1	0.01	671	0.00	0.15	1.06	4.07	2.13	0.20
08/26/10	MH-1	0.01	706	<0.07	0.17	1.05	4.18	2.51	0.21
11/03/10	MH-1	0.01	665	<0.07	0.19	1.09	3.97	2.31	0.21
01/05/11	MH-1	0.01	663	<0.07	0.13	1.07	3.78	2.44	0.22
03/02/11	MH-1	0.01	700	<0.07	0.12	1.25	3.99	2.77	0.25
04/06/11	MH-1	0.01	762	<0.07	0.14	1.19	4.14	2.50	0.29
05/25/11	MH-1	0.01	806	<0.07	0.15	0.94	4.13	2.27	0.34
08/01/11	MH-1	0.01	890	<0.07	0.16	0.83	4.16	2.41	0.40
08/14/09	MH-2	0.00	329	0.95	0.45	3.44	3.99	10.91	0.03
09/02/09	MH-2	0.00	348	1.03	0.44	7.32	3.80	19.72	0.04
09/18/09	MH-2	0.01	358	1.01	0.37	8.91	3.50	25.60	0.04
10/14/09	MH-2	0.01	353	0.59	0.40	6.59	3.50	17.14	0.04
11/13/09	MH-2	0.02	328	0.87	0.38	4.47	3.90	13.43	0.04
12/23/09	MH-2	0.03	314	0.53	0.39	2.89	5.18	9.07	0.04
02/02/10	MH-2	0.04	348	0.39	0.40	2.56	7.66	5.08	0.04
03/17/10	MH-2	0.02	328	<0.1	0.37	1.43	4.29	3.79	0.04
06/09/10	MH-2	0.01	319	0.00	0.40	1.41	3.37	2.48	0.04
08/26/10	MH-2	0.02	320	<0.07	0.48	0.90	3.82	1.92	0.03
11/03/10	MH-2	0.01	307	<0.07	0.40	0.87	3.25	1.44	0.03
01/05/11	MH-2	0.01	295	<0.07	0.41	0.83	3.12	1.90	0.03
03/02/11	MH-2	0.01	306	<0.07	0.38	0.99	3.27	2.11	0.03
04/06/11	MH-2	0.01	312	<0.07	0.43	0.68	3.41	1.53	0.03
05/25/11	MH-2	0.01	330	<0.07	0.40	0.98	3.39	1.32	0.04
08/01/11	MH-2	0.03	306	<0.07	0.47	1.13	10.73	2.49	0.04
09/18/09	MH-3	0.02	302	0.99	0.23	3.94	3.88	11.22	0.06
10/16/09	MH-3	0.01	303	0.46	0.25	2.43	5.34	6.54	0.06
11/13/09	MH-3	0.01	288	<0.1	0.31	1.33	3.55	3.77	0.05
12/23/09	MH-3	0.01	286	<0.1	0.33	1.34	3.54	4.09	0.05
02/02/10	MH-3	0.01	314	<0.1	0.36	1.19	4.69	2.25	0.05
03/17/10	MH-3	0.01	306	<0.1	0.32	1.14	3.79	3.17	0.04
06/09/10	MH-3	0.00	303	0.00	0.34	1.20	3.56	2.40	0.04
08/26/10	MH-3	0.00	305	<0.07	0.42	0.44	3.46	1.03	0.03
11/03/10	MH-3	0.00	297	<0.07	0.35	0.33	3.34	0.63	0.04
01/05/11	MH-3	0.00	286	<0.07	0.40	0.40	3.23	0.77	0.03
05/25/11	MH-3	0.00	294	<0.07	0.38	0.55	3.40	1.22	0.03

Table A6-3 Groundwater properties measured at monitoring wells.

Sample date	Source ID	pH (units)	DO (mg/L)	EC (mS/cm)	Eh (mV)	Temp (°C)	Alkalinity (mg/L)	TDS (mg/L)	Dissolved CO ₂ (mg/L)
08/14/09	MH-1	8.37	0.8	1.44	189	16.0	528	916	448.00
09/02/09	MH-1	8.31	0.4	1.19	198	15.2	548	1,027	440.00
09/18/09	MH-1	8.57	0.9	1.60	256	15.3	504	1,045	465.00
10/15/09	MH-1	8.60	-	1.83	-74	14.0	496	1,108	456.00
11/13/09	MH-1	8.42	0.4	1.48	142	14.8	480	1,152	-
12/23/09	MH-1	8.53	0.4	2.59	383	13.6	488	1,252	426.26
02/02/10	MH-1	8.35	0.3	2.85	374	13.1	552	1,386	404.52
03/17/10	MH-1	8.46	0.4	3.49	294	15.2	442	1,551	368.94
06/09/10	MH-1	8.66	0.6	3.35	78	15.3	436	1,713	372.13
08/26/10	MH-1	8.47	0.3	2.94	68	16.0	392	1,569	370.11
11/03/10	MH-1	8.36	0.7	2.92	182	14.4	444	1,699	378.85
01/05/11	MH-1	8.56	0.4	2.93	276	13.5	448	1,766	379.02
03/02/11	MH-1	8.05	0.3	4.41	37	13.8	432	1,810	-
04/06/11	MH-1	8.33	0.3	4.13	88	18.3	432	1,978	365.95
05/25/11	MH-1	8.55	0.5	3.54	50	15.8	392	2,220	346.29
08/01/11	MH-1	8.36	0.7	4.66	89	16.5	400	2,284	349.42
12/07/11	MH-1	8.28	0.6	4.39	8	13.8	380	-	328.08
08/14/09	MH-2	8.94	0.6	1.29	294	15.2	-	806	662.00
09/02/09	MH-2	8.75	0.7	1.24	180	15.7	732	850	594.00
09/18/09	MH-2	8.84	0.6	1.29	258	16.6	752	906	670.00
10/15/09	MH-2	8.85	-	1.32	-72	14.3	732	856	747.00
11/13/09	MH-2	8.70	0.4	1.22	110	15.6	716	845	-
12/23/09	MH-2	8.85	0.3	1.55	339	14.0	716	803	612.92
02/02/10	MH-2	8.65	0.8	1.58	356	12.3	712	804	593.54
03/17/10	MH-2	8.85	0.2	1.55	252	16.5	692	791	583.99
06/09/10	MH-2	8.91	0.2	1.40	226	18.1	692	761	585.22
08/26/10	MH-2	8.55	0.2	1.23	225	16.2	628	758	582.13
11/03/10	MH-2	8.52	0.2	1.23	283	15.2	680	757	578.87
01/05/11	MH-2	8.82	1.0	1.29	364	12.3	682	755	564.24
03/02/11	MH-2	8.44	0.3	1.93	343	13.6	672	756	-
04/06/11	MH-2	8.33	0.3	1.62	390	18.0	678	753	568.78
05/25/11	MH-2	8.83	0.5	1.24	181	17.2	628	749	560.21
08/01/11	MH-2	8.50	0.3	1.38	218	21.2	668	1377	565.34
12/07/11	MH-2	-	-	-	-	-	-	-	-
08/14/09	MH-3	-	-	-	-	-	-	-	-
09/02/09	MH-3	-	-	-	-	-	-	-	-
09/18/09	MH-3	8.57	2.6	1.12	260	15.3	648	754	620.00
10/15/09	MH-3	8.52	-	1.14	-47	13.5	644	732	644.00
11/13/09	MH-3	8.40	0.4	1.04	132	14.1	644	733	-
12/23/09	MH-3	8.56	0.4	1.43	331	13.3	666	733	559.14
02/02/10	MH-3	8.50	0.5	1.46	355	11.7	664	727	566.74
03/17/10	MH-3	8.72	0.3	1.43	220	14.8	652	748	548.30
06/09/10	MH-3	8.86	0.2	1.34	219	18.2	668	734	557.64
08/26/10	MH-3	8.72	0.8	1.17	66	17.1	608	724	581.30
11/03/10	MH-3	8.55	0.8	1.17	163	14.0	648	736	554.57
01/05/11	MH-3	8.96	0.4	1.21	303	11.9	660	718	551.99
03/02/11	MH-3	8.53	0.2	1.83	250	13.3	648	-	-
04/06/11	MH-3	-	-	-	-	-	-	-	-
05/25/11	MH-3	8.91	0.4	1.20	117	14.8	600	729	547.25
08/01/11	MH-3	8.59	0.9	1.28	104	17.6	-	-	-
12/07/11	MH-3	-	-	-	-	-	-	-	-

¹Abbreviations: DO, dissolved oxygen; EC, electrical conductivity; Eh, redox potential; TDS, total dissolved solids.

Appendix 7 Gas composition corrected for air contamination.

Table A7-1 Composition (%) of gas samples collected at Bald Unit wellheads and tank battery, corrected for air contamination.

Sample date	Source ID	N	O	CO	H ₂ (%)	CH ₄ (%)	C ₂ H ₆ (%)	C ₃ H ₈ (%)	iC ₄ H ₁₀ (%)	nC ₄ H ₁₀ (%)	C ₅ H ₁₂ (%)	C ₆ H ₁₄ (%)
03/18/10	BA-1	1.18	0.23	96.18	0.14	0.16	0.26	0.92	0.27	1.13	1.02	0.59
06/09/10	BA-1	1.85	0.42	82.00	0.48	2.02	0.64	3.69	1.21	3.79	2.70	1.21
08/27/10	BA-1	1.18	0.21	95.80	0.00	0.03	0.09	0.46	0.14	0.80	0.86	0.43
11/04/10	BA-1	2.02	0.21	93.76	0.00	0.10	0.14	0.65	0.31	1.22	1.12	0.48
01/06/11	BA-1	1.88	0.21	96.07	0.43	0.19	0.08	0.24	0.09	0.31	0.31	0.18
03/03/11	BA-1	0.11	0.22	97.68	0.58	0.13	0.12	0.29	0.08	0.32	0.32	0.16
04/07/11	BA-1	2.73	0.21	92.38	1.11	0.36	0.24	0.68	0.22	0.83	0.78	0.45
05/25/11	BA-1	1.18	0.36	95.92	0.00	0.44	0.44	1.90	0.75	2.49	1.90	0.83
08/02/11	BA-1	0.75	0.23	95.94	0.00	0.61	0.28	0.59	0.17	0.62	0.52	0.29
03/18/10	BA-2	2.83	0.59	78.40	0.68	0.68	1.04	5.35	1.13	4.37	3.41	1.52
06/09/10	BA-2	25.66	1.02	4.17	0.00	7.17	3.97	23.01	6.05	17.24	9.35	2.37
08/27/10	BA-2	47.93	0.25	14.76	0.00	2.67	3.22	12.44	3.28	9.88	3.94	1.63
11/04/10	BA-2	1.18	1.06	9.91	0.00	5.04	6.08	24.12	8.96	25.60	15.02	4.83
01/06/11	BA-2	21.85	1.30	10.88	0.00	4.37	4.20	20.87	6.22	17.44	10.11	2.76
03/03/11	BA-2	29.44	0.85	5.14	0.79	3.84	4.28	20.28	5.72	17.34	9.55	2.76
04/07/11	BA-2	24.93	1.05	4.47	0.00	4.14	4.93	23.63	6.88	16.93	10.25	2.79
05/25/11	BA-2	14.32	0.99	4.47	0.00	3.85	5.63	28.57	7.66	21.61	9.15	3.75
08/02/11	BA-2	14.97	0.61	50.98	0.00	2.12	2.08	7.73	1.46	10.13	6.57	3.37
03/18/10	IB-2	5.91	0.21	82.16	0.73	0.71	0.89	4.01	0.92	2.50	1.37	0.59
06/09/10	IB-2	11.01	0.35	35.69	0.65	3.30	3.62	20.43	4.72	14.11	4.98	1.15
08/27/10	IB-2	47.96	0.25	14.77	0.00	2.66	3.21	12.44	3.27	9.88	3.93	1.62
11/04/10	IB-2	54.09	0.24	1.00	0.00	5.71	4.26	14.45	4.64	9.65	4.93	1.04
01/06/11	IB-2	41.85	0.48	12.24	0.00	5.32	4.09	15.78	3.94	10.47	4.68	1.14
03/03/11	IB-2	20.42	0.64	17.95	3.52	3.47	4.74	20.99	5.21	14.38	6.68	2.01
04/07/11	IB-2	21.53	1.32	10.28	0.00	3.11	4.37	21.54	6.43	17.85	10.55	3.01
05/25/11	IB-2	25.22	0.84	5.31	0.00	4.65	5.26	24.96	6.25	16.47	8.69	2.34
08/02/11	IB-2	6.42	0.21	75.58	0.00	1.46	1.06	4.74	1.38	4.96	2.66	1.55
02/03/10	IB-3	1.18	0.39	76.35	0.00	0.24	1.62	10.22	2.52	7.83	3.26	1.03
03/18/10	IB-3	3.68	0.48	48.72	0.00	0.97	2.79	17.07	4.15	13.31	6.02	2.81
06/09/10	IB-3	2.23	0.57	37.55	0.00	4.57	3.07	20.62	5.22	16.85	7.31	2.01
08/27/10	IB-3	4.95	0.45	49.01	0.00	1.80	3.42	16.41	3.34	11.32	7.21	2.10
11/04/10	IB-3	27.47	0.30	36.25	0.00	2.79	3.67	13.11	3.10	8.66	3.65	1.00
01/06/11	IB-3	6.17	0.74	48.03	0.00	2.33	4.79	18.18	4.00	10.21	4.58	0.98
03/03/11	IB-3	22.92	0.29	41.97	1.08	2.69	3.84	12.41	2.74	7.86	3.36	0.83
04/07/11	IB-3	3.43	0.43	49.33	0.64	1.79	4.52	17.17	4.03	12.25	5.17	1.25
05/25/11	IB-3	1.18	0.63	67.95	0.00	0.98	2.14	11.38	3.23	9.68	5.94	2.18
08/02/11	IB-3	4.46	0.40	33.41	0.00	1.47	4.69	22.42	5.43	18.20	6.67	2.85
02/03/10	TB-1	1.18	0.33	90.20	0.00	0.20	0.37	3.20	1.15	4.37	2.94	1.51
03/18/10	TB-1	1.18	1.14	61.19	0.00	0.33	0.92	8.41	3.63	12.48	8.95	3.69
06/09/10	TB-1	4.31	0.73	29.96	0.00	1.88	2.40	19.95	5.87	19.99	10.64	4.28
01/06/11	TB-1	1.18	0.62	80.06	0.00	0.40	0.87	4.92	2.11	6.23	3.94	0.96
03/03/11	TB-1	1.18	1.23	57.82	0.00	0.58	1.38	6.80	9.29	13.21	10.49	3.30
04/07/11	TB-1	7.99	1.07	37.01	0.92	2.12	2.33	14.16	5.20	15.51	10.33	3.36
08/01/11	TB-1	16.58	0.81	18.91	0.00	1.52	2.97	17.52	5.51	19.65	11.14	5.39

Appendix 8 Interpretation of the reservoir saturation tool logging data from the Bald Unit.

SUMMARY

The RST logs were run at the Bald Unit to determine whether the CO₂ injected was migrating into zones above the injection zone. The RST is one of the tools used to monitor the possible movement of CO₂ into the zones above the injection. It is a wireline pulsed neutron logging tool that has as its main measurements the macroscopic capture cross section as well as the neutron porosity of the formation. Other measurements useful to the monitoring of CO₂ in the borehole, as well as in the formation, were also made and are described later in this document. This report is related primarily to the analysis of the RST data collected on one CO₂ injector well and four oil-producing wells. Conclusions are most accurate within feet from the wellbore and diminish in relevance laterally from the wellbore in any direction.

The wireline logging process used to determine CO₂ containment consisted of running two passes of the RST and then overlaying the pertinent data to detect any changes in the fluids in the wellbore or in the formation. The first logging runs (base pass) of the RST were made in late July 2009 prior to injection. After CO₂ injection, in early October 2011, the monitor run of the RST log was made in each well.

After making the logging passes, all data was reviewed and reprocessed as necessary to ensure the correct parameters were being used. Next, displays were made to overlay key data from the two logging runs; we looked for indications that the fluids in the borehole or formation had changed. Changes in the fluids are indicated by separations in the overlaid curves. A general interpretation of the data is that the CO₂ remained in the primary zone of injection.

DETAILED DESCRIPTION

Reservoir Saturation Tool Pulsed Neutron Capture

This mode of the RST can also be referred to as the “Sigma mode”. In the capture mode the tool is measuring the rate at which thermal neutrons are captured by the formation. This measurement is called Sigma (SIGM) and is the macroscopic capture cross section. Because chlorine has the greatest ability to capture thermal neutrons and hydrogen has the greatest ability to slow the high energy neutrons to the thermal level, this measurement is very responsive to the saltwater in the porosity. If the amount of saltwater decreases and is replaced by hydrocarbon or CO₂ then the capture cross section of the formation will decrease since hydrocarbons and CO₂ have low sigma values compared to saltwater. The tool also measures thermal neutron porosity very similar to the open-hole neutron porosity tools. The RST porosity is called TPHI. This porosity will respond to CO₂ very much like gas since they both have a very low hydrogen index. Gas and CO₂ both cause neutron porosity to be too low as the neutron porosity measurement is primarily responding to hydrogen index. Because of these differences the Sigma measurement and the porosity measurement from the RST tool can be combined in an analysis to determine the saturation of saltwater and the gas/CO₂ in the formation porosity. Gas and CO₂ cannot be differentiated because their neutron porosity response is the same, and there is not enough difference between their SIGM values to provide adequate differentiation. Both the SIGM and TPHI measurements are intended to be related to the formation properties. Although much has been done to characterize these measurements for changing borehole conditions, the condition where the borehole contains either gas or CO₂ remains as a difficult situation to consistently make the borehole corrections. For this reason, additional calculations of Sigma and porosity are also made. The log presentation will also include SIGM_TDTL, which is the computation of TPHI Sigma using the same algorithm that was used by the TDT-P tool. This computation is not as robust as the RST sigma computation under normal conditions, but it is a bit more consistent under some unusual borehole conditions. Therefore, both will be presented for analysis with the belief that if there is a difference between the two runs and the changes in SIGM and SIGM_TDTL are consistent with each other, the change is in the formation. If there is a difference between the two runs and the changes in SIGM and SIGM_TDTL are not consistent with each other, the change is in the borehole fluids. The additional porosity that is presented on the logs is

PHIC, which is a porosity that was developed for the pulsed neutron tools and is able to provide a porosity computation even in a gas-filled borehole. In a gas-filled borehole, the TPHI porosity will be considerably lower than it should be, even going to zero in larger borehole sizes. As mentioned before, CO₂ and methane cause similar responses to the SIGM and porosity from the RST; therefore, in a CO₂ filled borehole the TPHI porosity will be much too low. The PHIC porosity allows for measurement of a neutron porosity that is responsive to changes in the formation fluids rather than being dominated by changes in the borehole fluids in gas or CO₂ filled boreholes.

Other Measurements Used from RST

The RST provides other data that can be valuable for monitoring changes in the borehole, especially borehole fluids. The capture cross section of the borehole (SBNA) and the inelastic counts from the far detector (INFD_TDTL) are two of these measurements. Just as SIGM is a measurement of the capture cross section of the formation, SBNA is a measurement of the capture cross section of the borehole. To pulsed neutron tools, the borehole is everything that is not formation. Therefore, the SBNA measurement includes the capture cross section of all of the cement, all of the different strings of casing and tubing, all of the other hardware such as packers, and all of the fluids in the different casing and tubing strings. In a monitoring case such as this, if the wellbore configuration is not changed, and there are changes in either the SBNA or INFD_TDTL between runs, then the fluids have likely been changed. If CO₂ or gas has entered the borehole where water once was, both of these measurements would respond to the CO₂. As discussed with CO₂ in the formation, the capture cross section of CO₂ is low, and with CO₂ anywhere in the borehole, SBNA would be lower than if water of any salinity was in the wellbore. This relationship may also be true with fluids that have a lower capture cross section; however, the magnitude of the change would be less. INFD_TDTL responds to both the hydrogen index and density of the materials in place. It would then not respond to changes in water salinity, and any change in fluid, such as water to oil, would be so small as to not be detectable, if any change occurs at all. However, CO₂ is a complete change from both water and oil. It has no hydrogen, and it has a lower density. With CO₂ anywhere in the borehole, INFD_TDTL will increase. This response is very similar to that of methane; so again, gas and CO₂ cannot be differentiated.

GENERAL INTERPRETATION

The interpretation of pulsed neutron data is normally done by calculating the saturations of the different fluids that may be in the reservoir. In the case of monitoring analysis, a change in saturation can be computed using the change in SIGM measured by the tool. For the wells in the Bald Unit, a cursory look at the data reveals that both SIGM and SIGM_TDTL repeat very well from the base pass to the monitor run, indicating that there is no change in the formation fluids and that CO₂ is not migrating upward into other zones. Only the Bailey #2 well requires some explanation, which is in the Detailed Interpretation of Results section. Since SIGM is the primary measurement from the RST this forms the basis for the analysis. The TPHI and PHIC can be used as well but SIGM has less uncertainty and better statistical precision than does the porosity measurement. Also, TPHI will be affected by CO₂ in the wellbore, and this may cause slight changes in PHIC as well.

For identifying fluid changes in the borehole, the SBNA and INFD_TDTL data will be the main source of information. In several wells, the top of liquid in the borehole can be identified where the INFD_TDTL curve increases dramatically. SBNA also decreases as just discussed, but the magnitude of the decrease is much less. A more detailed discussion of the data on each well follows the figures showing the log data.

Description of log curves

Depth Track

Depth

Zone Track

Zone tops (injection zone indicated with shading where deep enough)

Gamma Ray – Tension

GR_2009 – Gamma ray from the RST base run in 2009

GR_2011 – Gamma ray from the RST run in 2011

TENS_2009 – Tension from the RST base run in 2009

TENS_2011 – Tension from the RST run in 2011

Sigma Borehole – Far Inelastic, TPMI Porosity

SBNA_2009 – Sigma borehole from the RST base run in 2009

SBNA_2011 – Sigma borehole from the RST run in 2011

INFD_TDTL_2009 – Inelastic far detector counts (TDT-Like) from the RST base run in 2009

INFD_TDTL_2011 – Inelastic far detector counts (TDT-Like) from the RST base run in 2011

TPHI porosity

TPHI_2009 – TPHI ratio porosity from the RST base run in 2009

TPHI_2011 – TPHI ratio porosity from the RST run in 2011

PHIC porosity

PHIC_2009 – PHIC difference based porosity from the RST base run in 2009

PHIC_2011 – PHIC difference based porosity from the RST base run in 2011

Sigma Track

SIGM_2009 – Sigma from the RST base run in 2009

SIGM_2011 – Sigma from the RST run in 2011

Sigma_TDTL Track

Sigma (TDT-Like) from the RST base run in 2009

Sigma (TDT-Like) from the RST base run in 2011

Note: Shading is applied such that an increase of CO₂ (also gas or air) in the monitor run would be indicated by yellow shading.

DETAILED INTERPRETATION OF RESULTS

Bailey-Alexander #1 (Figures A8-1 and A8-2)

As seen in Figure A8-1, all data from the monitor run in October 2011 match the same data from the base pass in March 2009, which indicates no change in formation fluid saturation. The log for Bailey-Alexander #1 included part of the injection zone, as seen in a closer view in Figure A8-2. (The top of the Clore may be at 577.6 or 577.9 m [1895 or 1896 feet], i.e., higher than is shown in Figure A8-2.) On both runs of the RST, the tension device (TENS) indicates that the tool picked up at 591.9 m (1942 ft). The measure point of the tool is 4.0 m (13 ft) above the bottom of the tool, which puts the first reading of the RST measurements at 588.0 m (1929 ft). The PHIC porosity was computed on a sand matrix, and numerical values have been put in the same track as the curves to make it easier to read. The average porosity is about 21 pu.

Bailey-Alexander #2 (Figure A8-3)

All data from the monitor run in October 2011 match the same data from the base pass in March 2009, which indicates no change in formation fluid saturation.

Inez Bailey #2 (Figures A8-4 and A8-5)

In Figure A8-4 all data from the monitor run in October 2011 match the same data from the base pass in March 2009 down to a depth of 573.6 m (1,882 ft), indicating no change in formation fluid saturations in this part of the wellbore. However, below this point it seems that there may be some indication of change as SIGM and the other curves display a difference in the base pass and the monitor pass. A closer look at this interval in Figure A8-5 reveals that the first reading of the base pass is at 573.6 m (1,882 ft) and the first reading of the monitor pass is at 581.3 m (1,907 ft). The tension measurement (TENS) indicates where the tool pick-up for each run is, and the first reading is 4.0 m (13 ft) above this point for each run. Because the log data for the base pass is not valid below 573.6 m (1,882 ft), there is no indication of any change in formation fluid saturation.

Inez Bailey #3 (Figure A8-6)

All data from the monitor run in October 2011 matches the same data from the base pass in March 2009, which indicates no change in formation fluid saturation.

Bald Unit #1 (Figure A8-7)

The Bald Unit #1 was only logged for the base run in 2009 and is included as a reference and for correlation to the other wells.

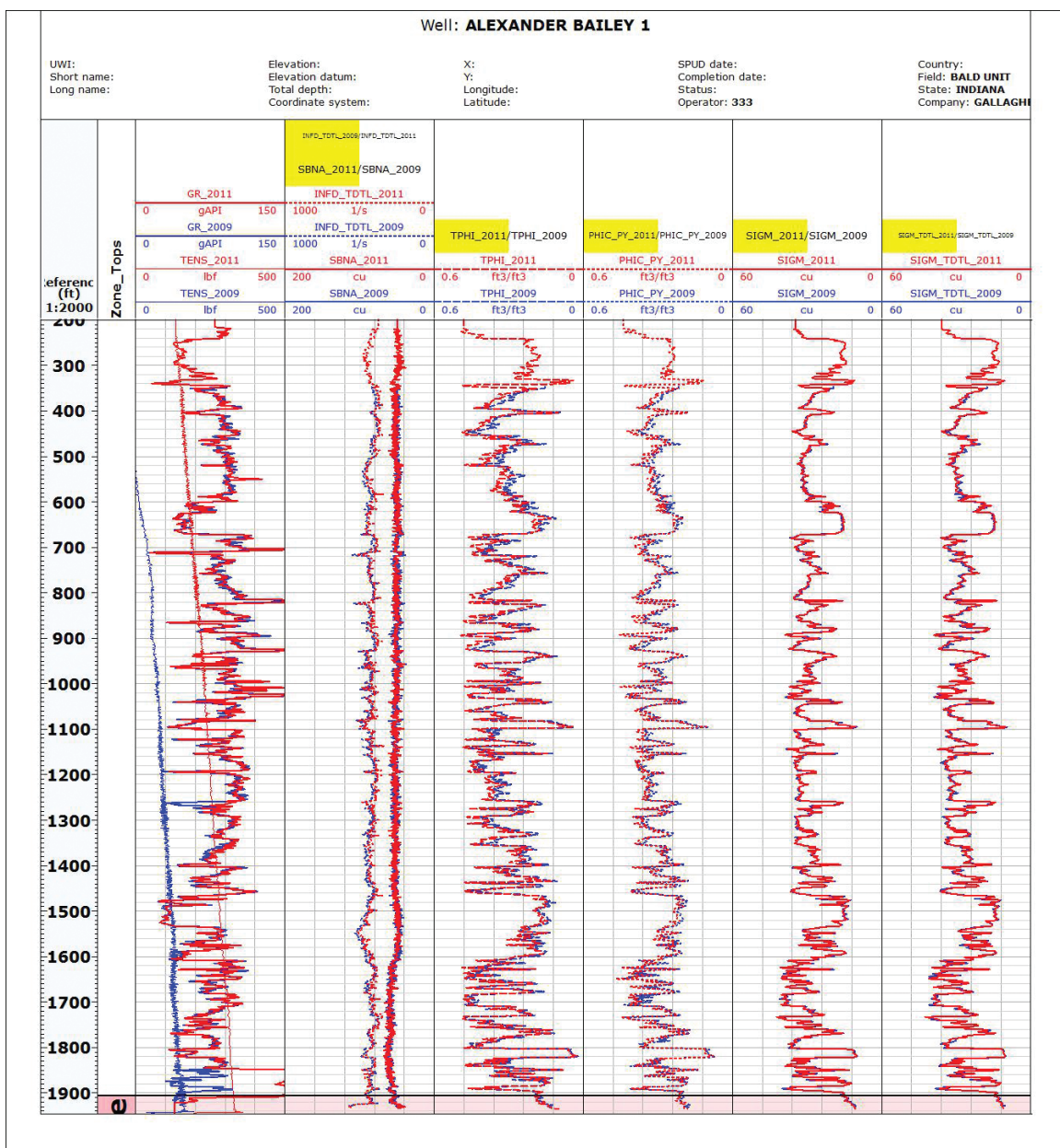


Figure A8-1 Log analysis for well BA-1.

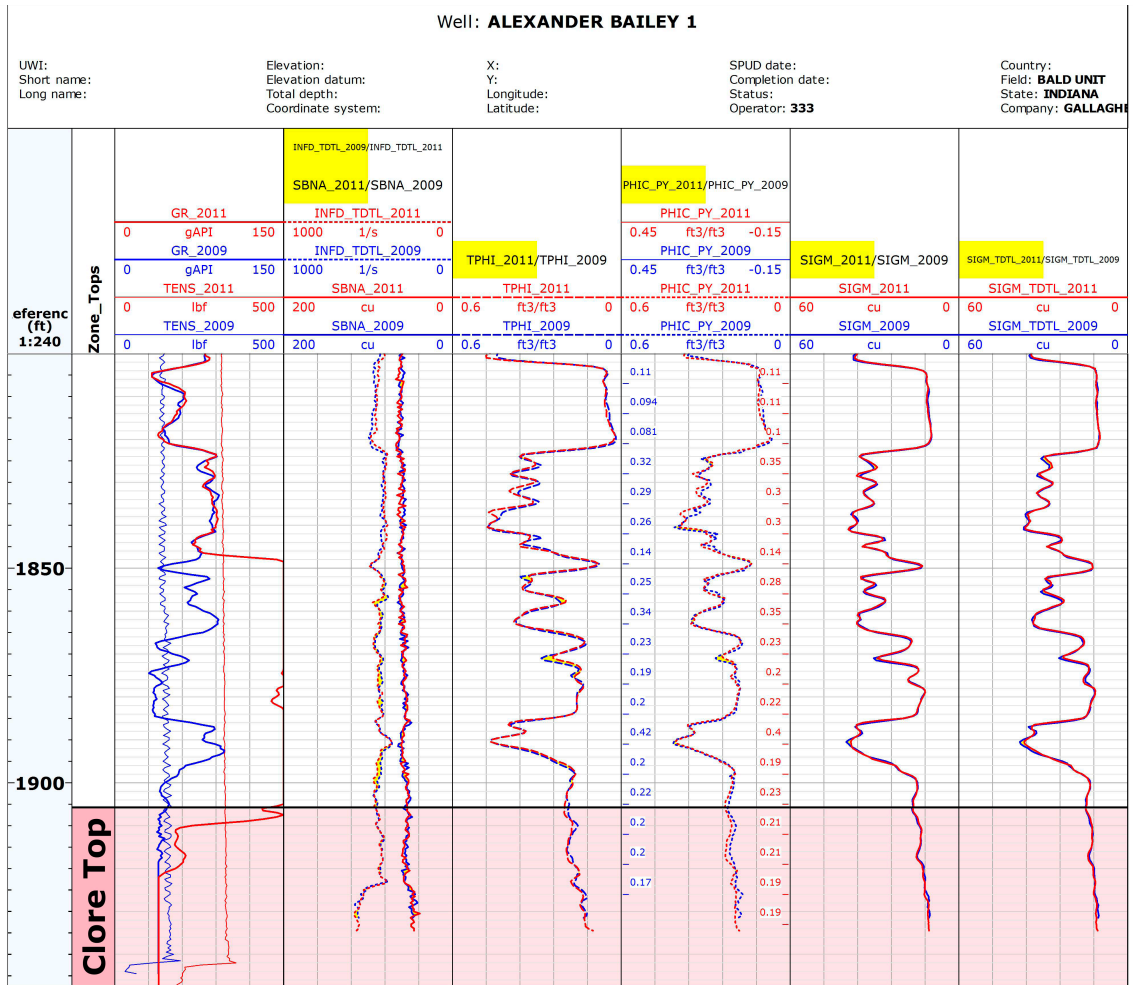


Figure A8-2 Log analysis for well BA-1 (magnified, showing a portion of the injection zone).

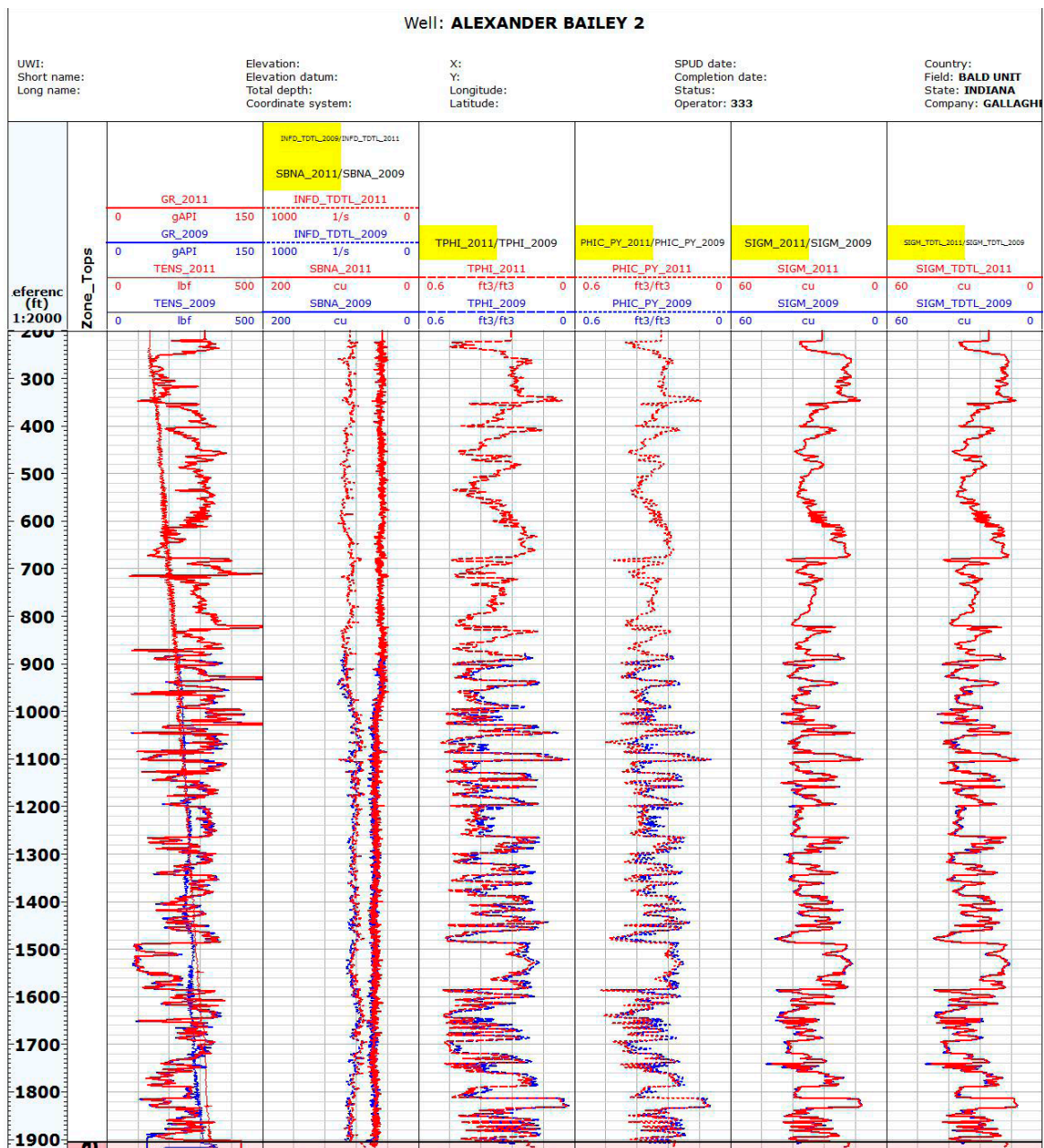


Figure A8-3 Log analysis for well BA-2.

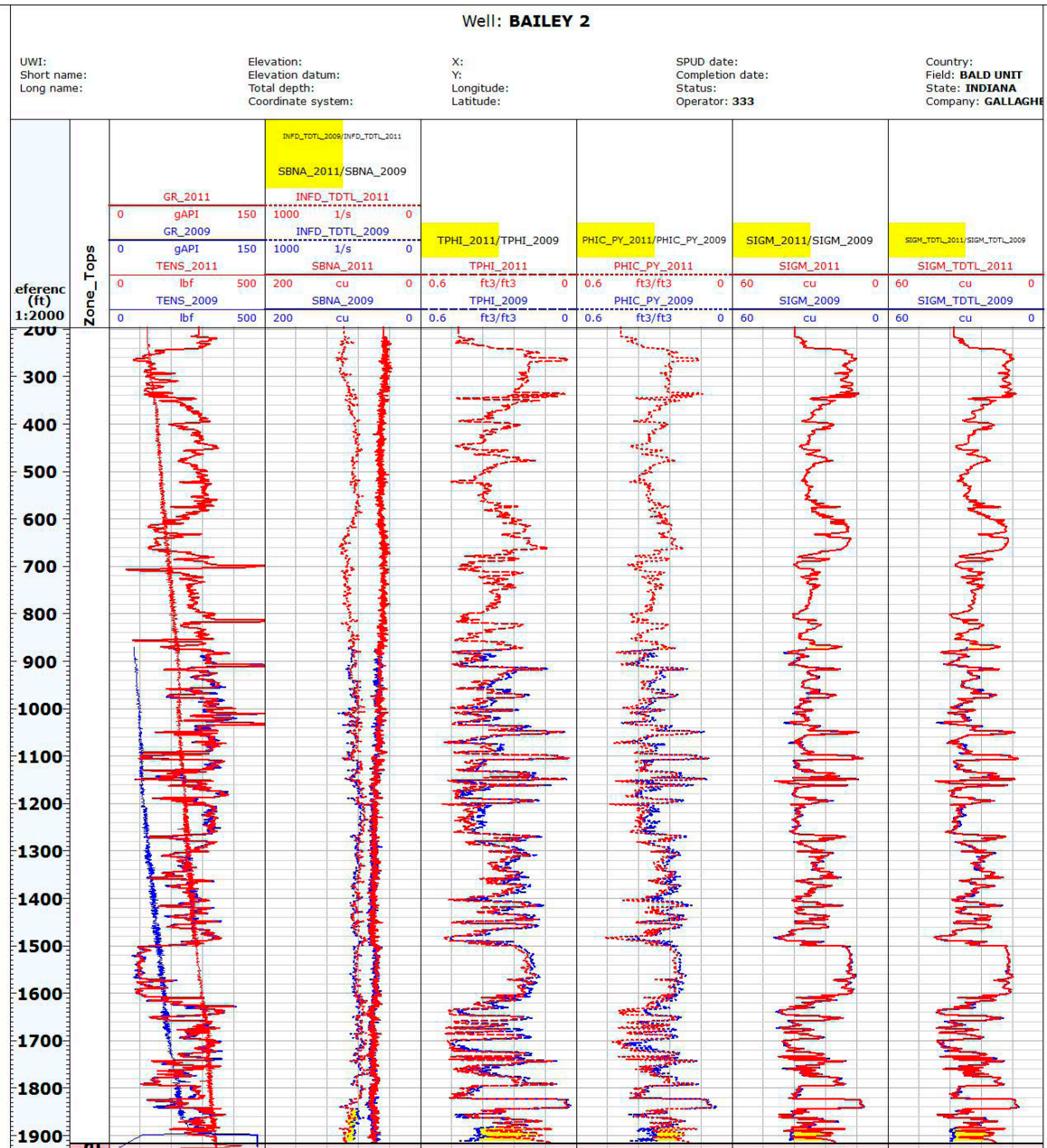


Figure A8-4 Log analysis for well IB-2.

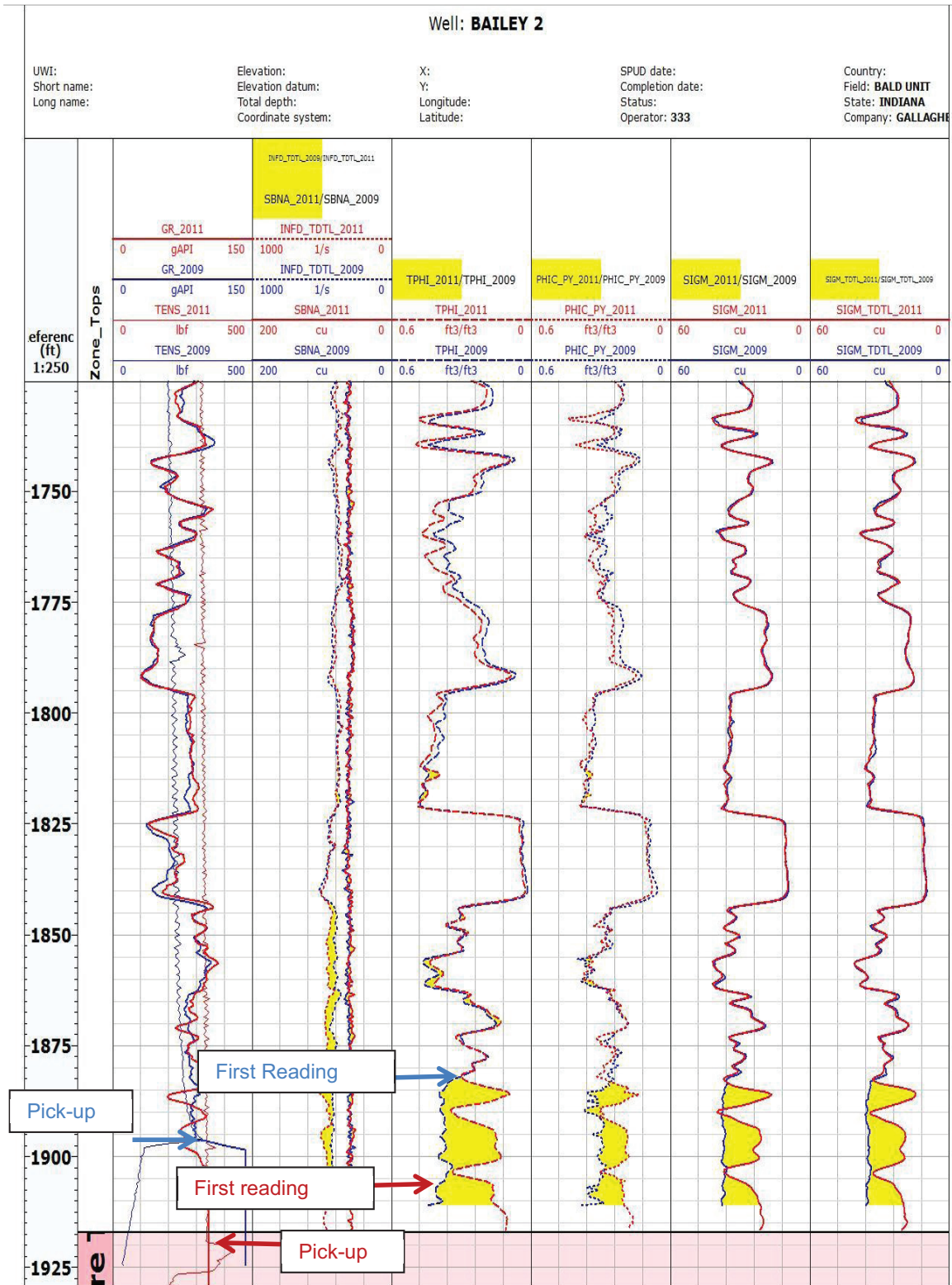


Figure A8-5 Log analysis for well IB-2 (magnification).

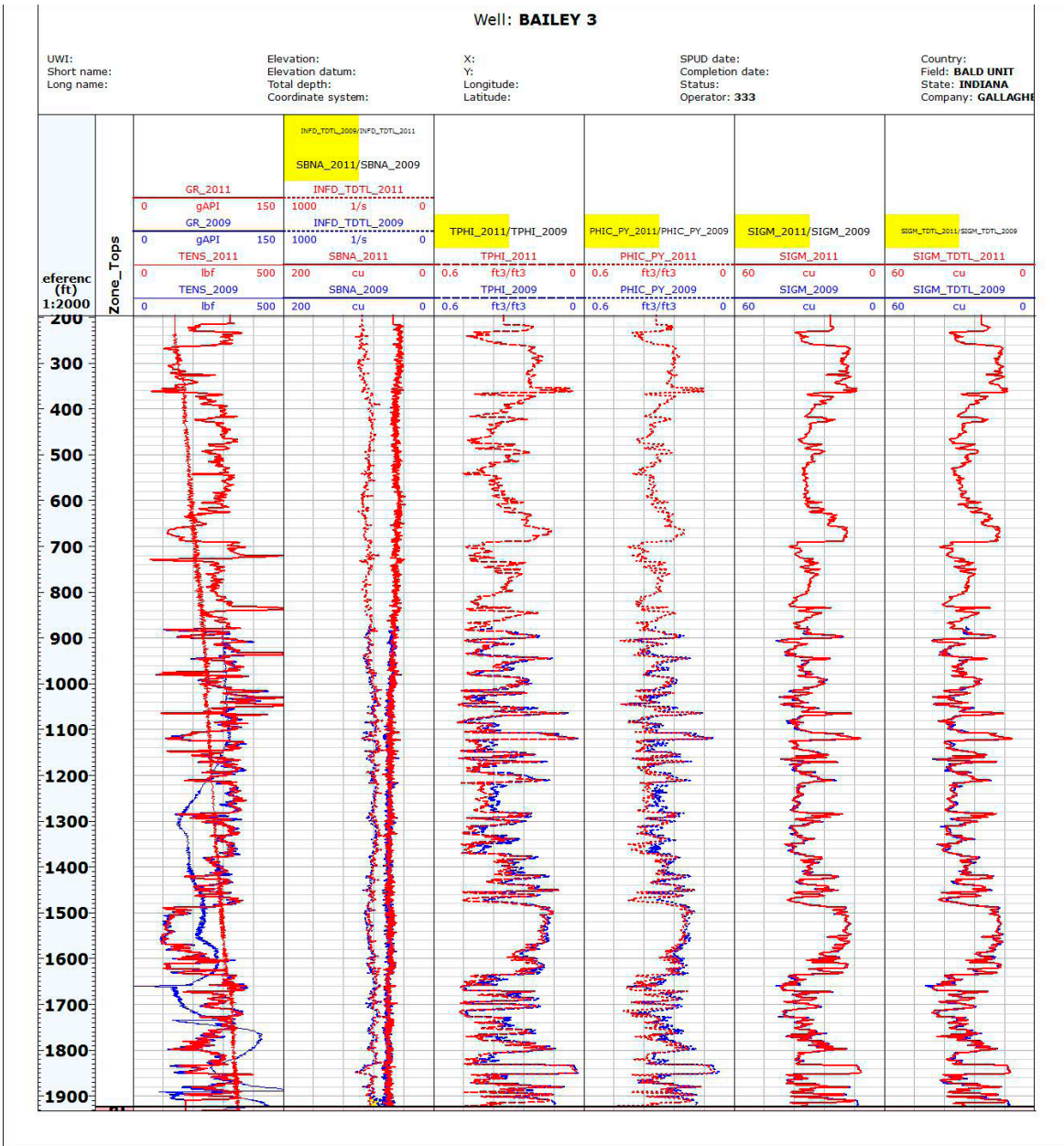


Figure A8-6 Log analysis for well IB-3.

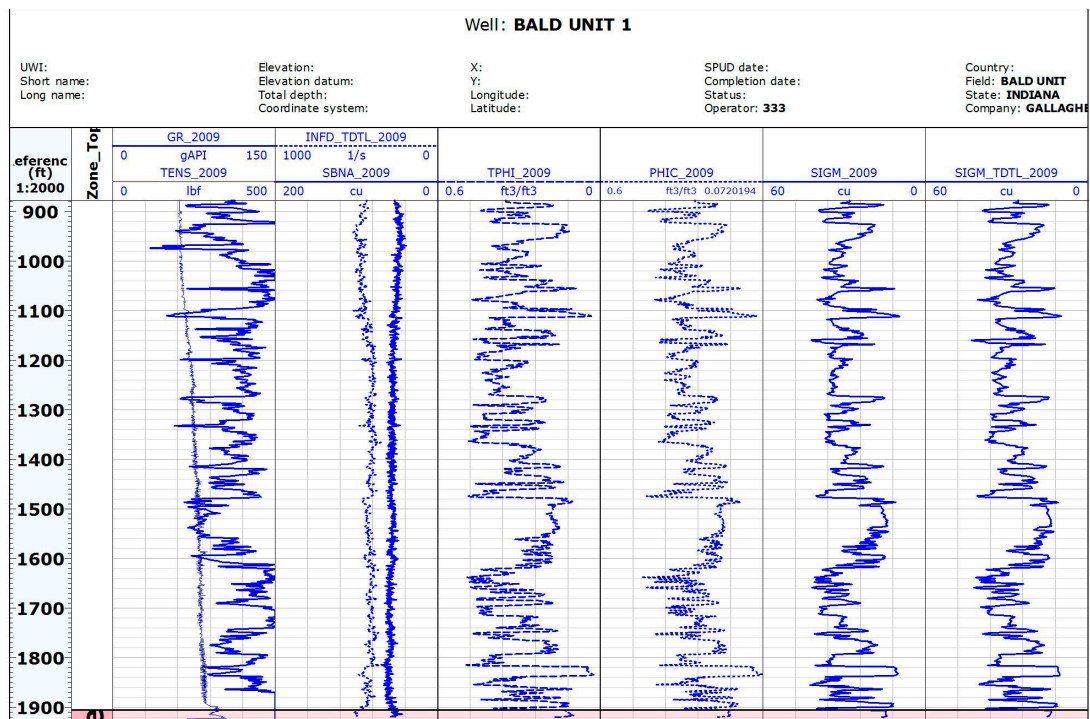


Figure A8-7 Log analysis for well BU-1.

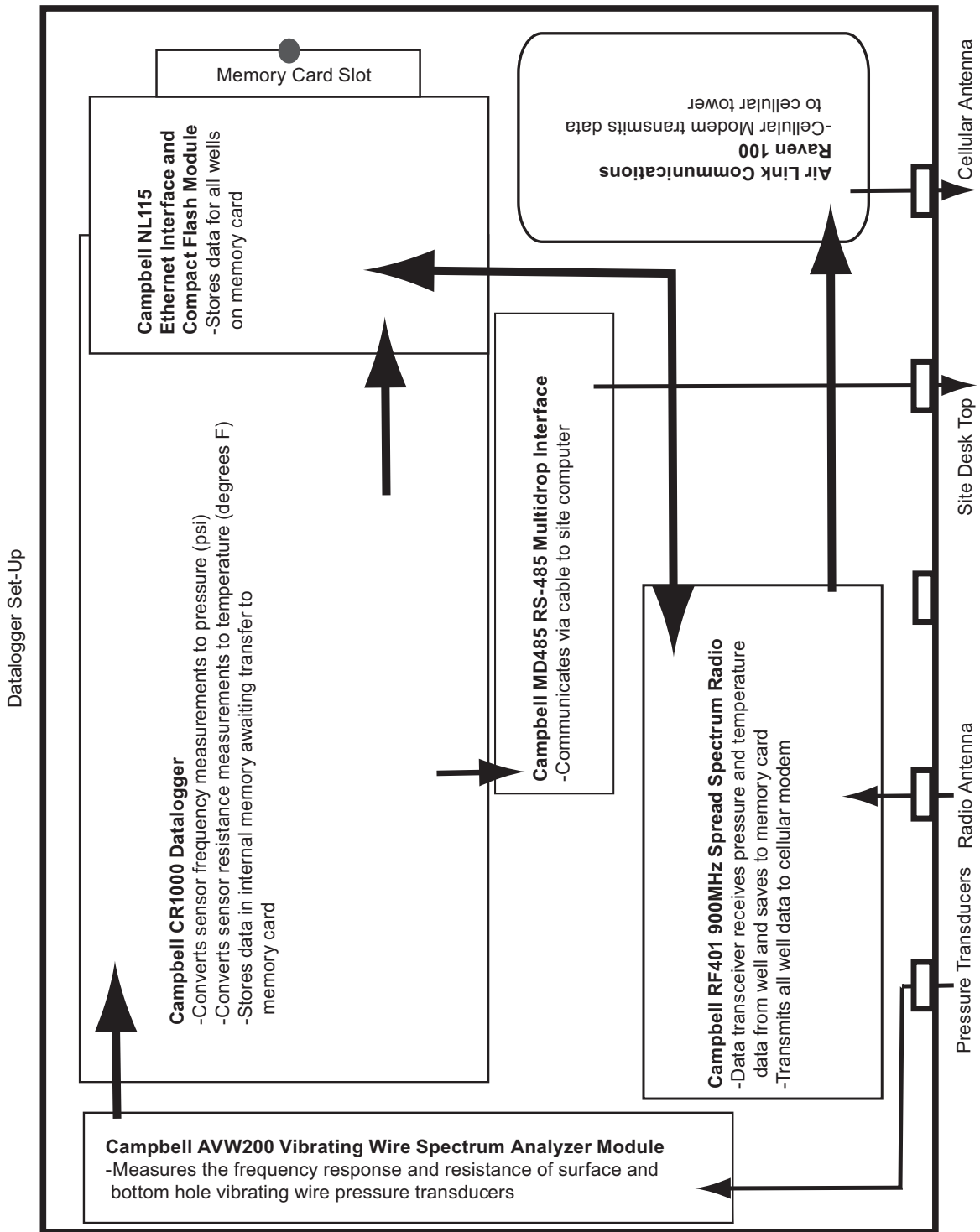
Appendix 9 Equipment.

Table A9-1 Data monitoring and logging equipment used at the Bald Unit pilot.

Description	Well	Position	Pressure range	Temperature range
Geokon 4500SH Vibrating Wire Pressure Transducer	BA-1, BA-2, IB-3	Surface	0–10 MPa	–20°C to +80°C
Geokon 4500SH Vibrating Wire Pressure Transducer	BU-1	Surface	0–20 MPa	–20°C to +80°C
Geokon 4500SHI Vibrating Wire Pressure Transducer	BA-1, BA-2, IB-2, IB-3, BU-1	Downhole	0–20 MPa	–20°C to +80°C
Geokon 4580-1 (Barometer) Vibrating Wire Pressure Transducer	IB-2	Surface	0–2.5 psi	–20°C to +80°C
Siemens Sitrans P Pressure Transmitter	IB-4, BU-2	Surface	0.4–5800 psi	
Campbell Scientific CD295 Display for Enclosure Lid	BA-1, BA-2, IB-2, IB-3, BU-1, PS ¹			
Campbell Scientific CR1000 Datalogger	BA-1, BA-2, IB-2, IB-3, IB-4, BU-1, BU-2, PS ¹			
Campbell Scientific AVW200 2-Channel Vibrating Wire Spectrum Analyzer Module	BA-1, BA-2, IB-2, IB-3, BU-1			
Campbell Scientific NL115 Ethernet Interface and CompactFlash Module	BA-2			
Campbell Scientific CFM100 CompactFlash Module	BA-1, IB-2, IB-3, IB-4, BU-1, BU-2, PS ¹			
Sierra Wireless Communications Raven XT V2221-V Cellular Modem	IB-3			
Campbell Scientific RF401 900MHz Spread Spectrum Radio Data Transceiver	BA-1, BA-2, IB-2, IB-3, IB-4, BU-1, BU-2, PS ¹			
Campbell Scientific MD485 RS-485 Multidrop Interface	PS ¹			
Siemens Sitrans P Pressure Transmitter		Upstream and downstream of first pump	0–900 psi	
Siemens Sitrans P Pressure Transmitter		Downstream of second pump	0–1,500 psi	
Siemens Sitrans TK-H Temperature Transmitter		Upstream and downstream from pumps		–30°C to +50°C
Siemens Sitrans TK-H Temperature Transmitter		Downstream from line heater (exit temperature)		–27.5°C to +48.2°C
Cameron NuFlo Liquid Turbine Flowmeter		Downstream from pumps	0–14.6 gpm	

¹PS=pump skid.

Appendix 10 Schematics of data logger equipment.



Appendix 11 Scale treatment.

An analysis by Baker Petrolite yielded the following information on scale at Bald Unit flowing wells.

For wells IB-1, IB-2, and IB-3 North, the major portion of the scale makeup was CaCO_3 , and the minor portion was FeS. The analysis was performed following the de-oiling and washing of all samples. The scale was acid soluble following the washing and de-oiling. The major portion of the scale (>85%) was identified as calcium carbonate, and the remainder (<15%) was identified as iron sulfide.

Baker recommended (based on the scale analysis and the method of producing, i.e., flowing) that each well be squeezed with 2 drums (110 gal) of SCW4755, which is effective in controlling calcium carbonate scale when placed in the formation.

Suggested treatment procedure:

1. Pre-mix 2 drums of SCW4755 with 10 bbl of water.
2. Displace the produced fluid in the tubing with a pre-flush of clean water. (Note: After step #2 SCW4755 may be slipped streamed into 10 bbl of water as water is pumped down the tubing.)
3. Pump the pre-mixed solution of SCW4755 and water down the tubing.
4. Displace the solution with a minimum of 10 bbl of clean water.
5. Close in each well for a minimum of 12 to 24 hours.

Appendix 12 Description of fracture stimulation treatment.

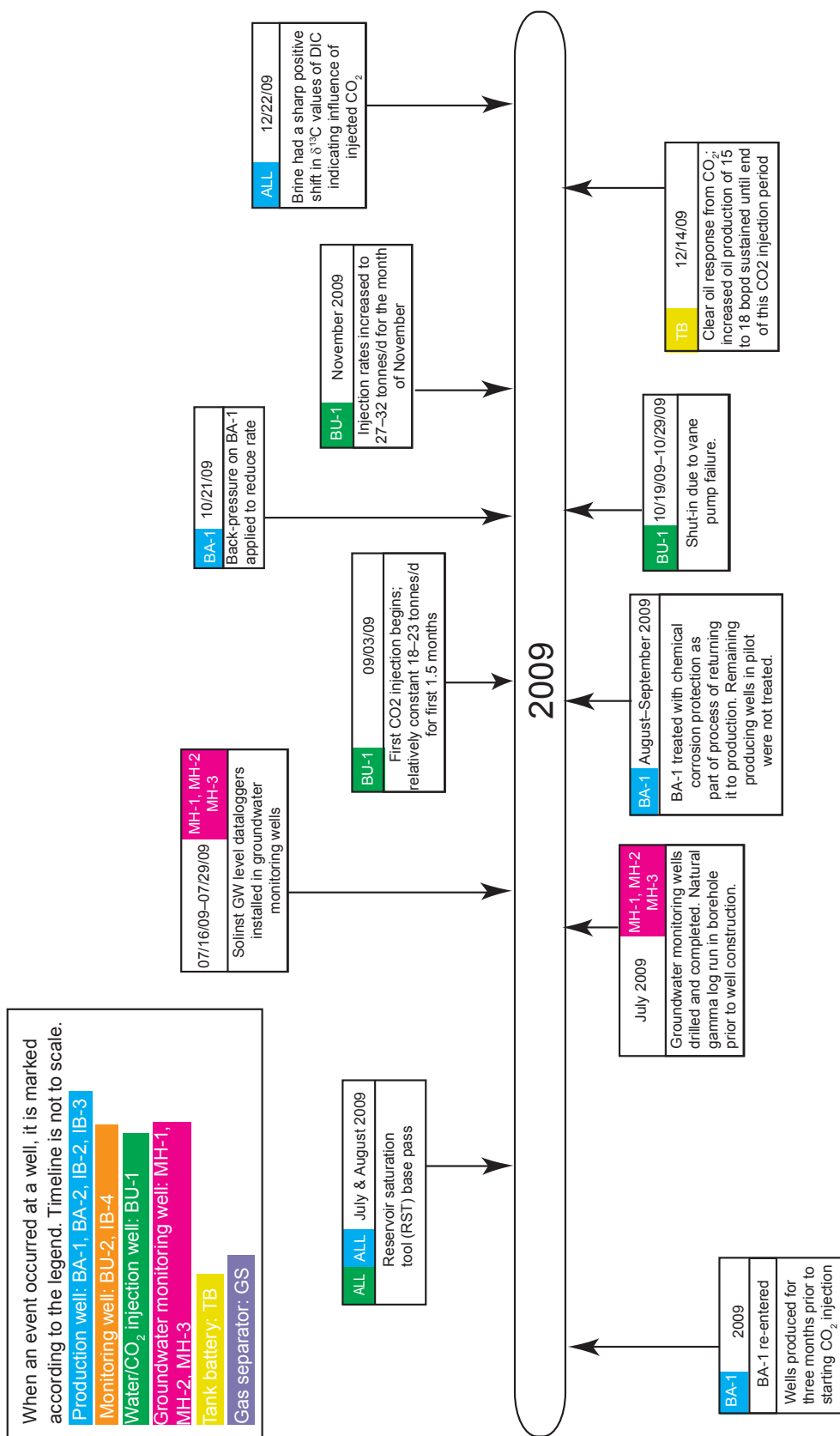
A staged fracture stimulation treatment was administered. The tubing was removed, and the well was cleaned out. The tubing and packer were then returned to the well. A 20/40 mesh sand was used at a surface injection pressure of 8.62 MPag (1,250 psig). Table A12-1 has the injection stages in chronological order.

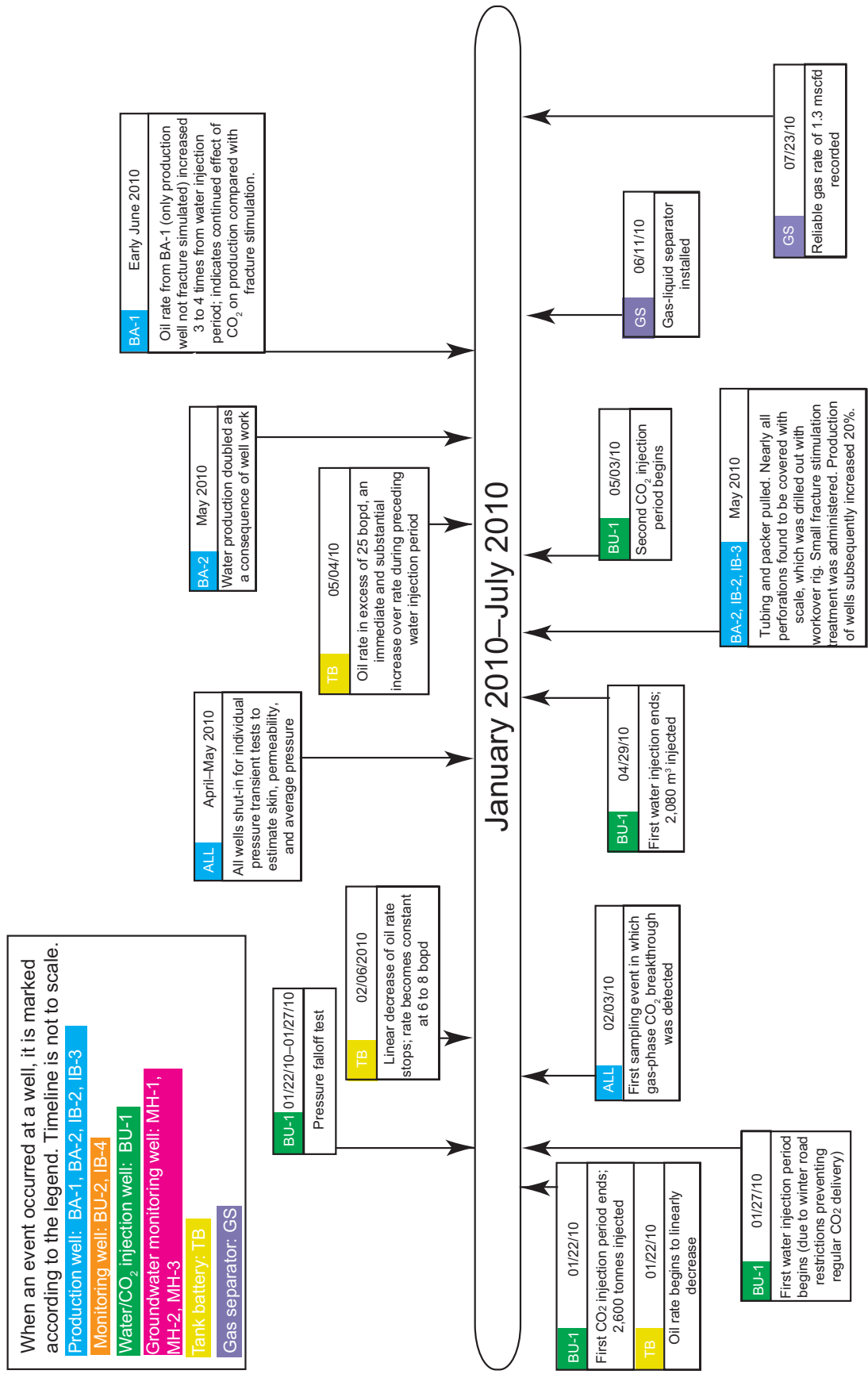
Table A12-1 Stages of fracture stimulation treatment.

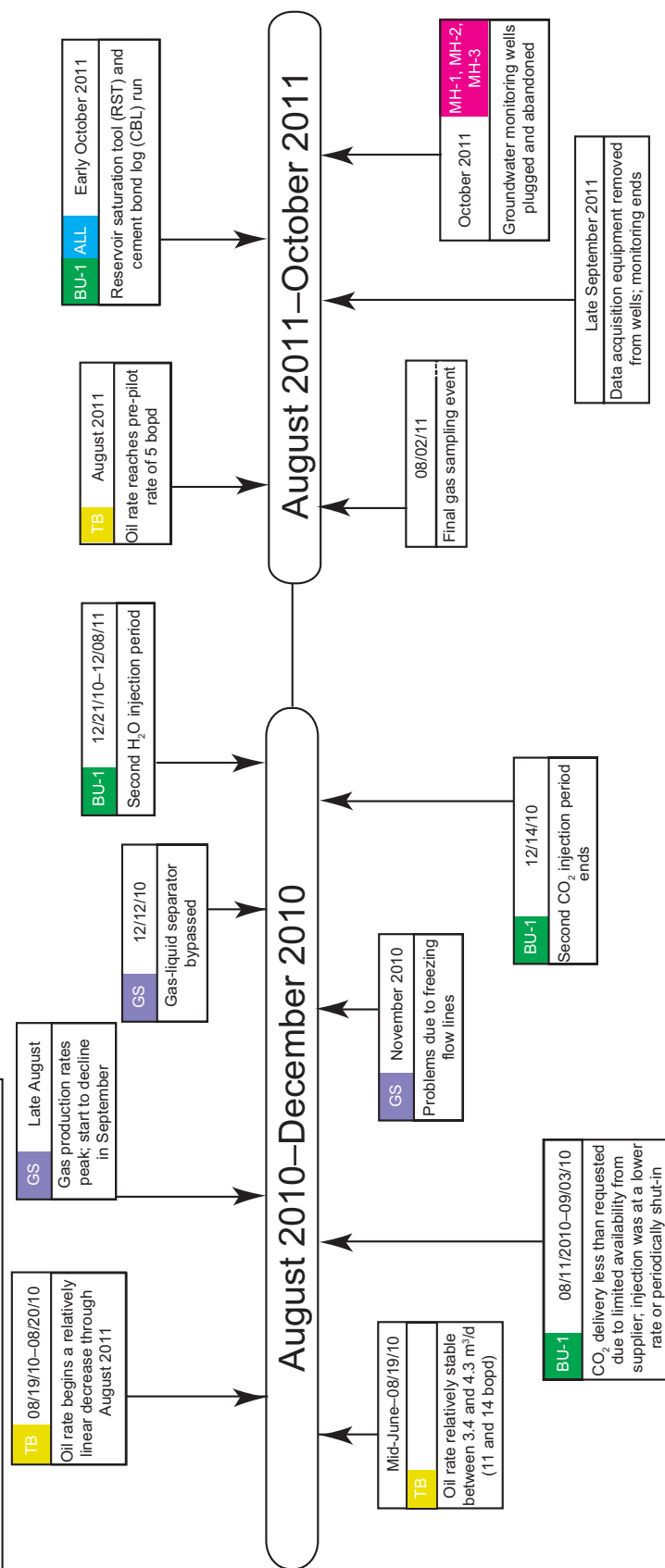
Stage	Volume, m ³ (gallons)	Description
1	3.8 (1,000)	Gelled pad
2	1.9 (500)	Proppant at 0.12 kg/L (1 lb/gal)
3	0.95 (250)	Proppant at 0.24 kg/L (2 lb/gal)
4	0.95 (250)	Proppant at 0.36 kg/L (3 lb/gal)
5	0.95 (250)	Proppant at 0.48 kg/L (4 lb/gal)
6	2.3 (610)	Flush

After this treatment, the well had 3.1 MPag (450 psig) measured on the tubing at the surface. The well was flowed 1.2 m³ (7.6 bbl) in the first hour to a tank. In the next hour, 1.0 m³ (6.5 bbls) were swabbed. Afterward the tubing and packer were removed, and sand was bailed from the bottom of the well. The tubing and packer were returned to the well and the flow line was hooked back up to the wellhead.

Appendix 13 Sequence of events







Appendix 14 Results of all isotopic analyses.

Abbreviations used for well names in this appendix may differ from those used elsewhere in report. AB1 and AB2=BA-1 and BA-2; B2 and B3=IB-2 and IB-3; D3=BD-3.

Table A14-1 Isotopic composition of brines from production wells at Mumford Hills site.

Sample ID	Date	$\delta^{13}\text{C}_{\text{DIC}}$ (‰)	$\delta^{18}\text{O}_{\text{H}_2\text{O}}$ (‰)	$\delta\text{D}_{\text{H}_2\text{O}}$ (‰)
MH-AB1-01	8/11/2009	-11.36	-4.63	-31.0
MH-AB2-01	8/11/2009	-14.36	-4.52	-27.8
MH-B2-01	8/11/2009		-4.02	-24.9
MH-B2-01 (Redo)	8/11/2009	3.75		
MH-B3-01	8/11/2009	-19.37	-4.15	-25.5
MH-B3-01 (Dup)	8/11/2009	-19.35		
MH-TB1-01	8/11/2009	-11.90	-5.06	-31.0
MH-BU1-01	8/13/2009	-15.93	-4.99	-31.1
MH-D3-01	8/13/2009	-4.36	-5.82	-37.3
MH-D3-02	9/1/2009	-4.74	-6.53	-38.6
MH-B3-02	9/1/2009	-20.33	-4.30	-26.0
MH-AB2-02	9/1/2009	-14.68	-4.64	-28.6
MH-AB1-02	9/1/2009	-11.99	-5.25	-32.1
MH-AB1-02 (Dup)	9/1/2009	-12.04		
MH-TB1-02	9/1/2009	-12.98	-5.23	-31.2
MH-B2-02	9/1/2009	-23.68	-4.15	-25.5
MH-AB1-03	9/17/2009	-11.66	-5.21	-32.6
MH-AB2-03	9/17/2009	-14.58	-4.78	-29.8
MH-B2-03	9/17/2009	-21.98	-4.18	-26.1
MH-B3-03	9/17/2009	-19.54	-4.16	-26.6
MH-B3-03 (Dup)	9/17/2009	-19.70		
MH-D3-03 (Redo)	9/17/2009	-11.05	-5.41	-35.4
MH-TB1-03	9/17/2009	-12.17	-4.96	-31.6
MH-AB1-04	10/14/2009	-11.40	-5.01	-32.1
MH-AB2-04	10/14/2009	-14.09	-4.48	-29.7
MH-B2-04	10/14/2009	-22.18	-4.23	-26.7
MH-B3-04	10/14/2009	-18.66	-4.08	-27.4
MH-D3-04	10/14/2009	-13.99	-4.57	-31.1
MH-D3-04 (Dup)	10/14/2009	-14.11		
MH-TB1-04	10/14/2009	-11.94	-4.98	-32.1
MH-AB1-05	11/12/2009	-12.31	-4.83	-32.3
MH-AB2-05	11/12/2009	-14.72	-4.51	-29.5
MH-B2-05	11/12/2009	-22.09	-4.09	-26.9
MH-B3-05	11/12/2009	-19.36	-4.41	-29.3
MH-B3-05 (Dup)	11/12/2009	-19.34		
MH-D3-05 (Redo)	11/12/2009	-4.60	-6.41	-39.9
MH-TB1-05	11/12/2009	-13.12	-4.94	-31.7
MH-AB1-06A	12/22/2009	-6.05	-4.68	-32.4
MH-AB1-06A (Dup)	12/22/2009	-6.09		
MH-AB2-06A (Redo)	12/22/2009	-11.09	-4.60	-29.2
MH-B2-06A	12/22/2009	-17.27	-4.00	-27.6
MH-B3-06A	12/22/2009	-14.22	-3.47	-28.2
MH-D3-06A	12/22/2009	-7.99	-4.71	-33.3
MH-D3-06A (Redo)	12/22/2009	-7.94		
MH-TB1-06A (Redo)	12/22/2009	-6.50	-4.92	-31.2

Sample ID	Date	$\delta^{13}\text{C}_{\text{DIC}}$ (‰)	$\delta^{18}\text{O}_{\text{H}_2\text{O}}$ (‰)	$\delta\text{D}_{\text{H}_2\text{O}}$ (‰)
MH-AB1-07A	2/3/2010	-9.32	-4.80	-32.1
MH-AB2-07A (Redo)	2/3/2010	-13.16	-4.67	-29.4
MH-B2-07A (Redo)	2/3/2010	-18.87	-4.38	-26.5
MH-B3-07A	2/3/2010	-16.11	-4.26	-28.7
MH-B3-07A (Dup)	2/3/2010	-16.24		
MH-D3-07A	2/2/2010	-4.74	-6.17	-39.8
MH-TB1-07A	2/3/2010	-9.36	-4.93	-32.7
MH-AB1-08A	3/18/2010	-5.78	-5.26	-34.7
MH-AB2-08A	3/18/2010	-10.77	-4.70	-30.8
MH-B2-08A	3/18/2010	-13.67	-4.43	-29.3
MH-B2-08A (Dup)	3/18/2010	-13.69		
MH-B3-08A	3/18/2010	-15.42	-4.56	-28.9
MH-D3-08A	3/17/2010	-4.67	-6.46	-40.3
MH-TB1-08A	3/18/2010	-6.07	-4.86	-32.4
MH-AB1-09A	6/9/2010	-8.9	-5.11	-33.4
MH-AB2-09A	6/9/2010	-15.2	-4.43	-28.9
MH-B2-09A	6/9/2010	-17.8	-4.62	-29.6
MH-B3-09A	6/9/2010	-16.7	-4.72	-29.9
MH-TB1-09A	6/9/2010	-10.3	-4.77	-32.1
MH-AB1-09A (Dup)	6/9/2010	-8.8		
MH-AB1-10A	8/27/2010	-3.8	-5.10	-32.7
MH-AB2-10A	8/27/2010	-14.0	-4.84	-30.3
MH-B2-10A	8/27/2010	-18.3	-4.78	-30.9
MH-B3-10A	8/27/2010	-13.5	-4.69	-30.5
MH-D3-10A	8/27/2010	-4.6	-6.47	-40.3
MH-TB1-10A	8/27/2010	-5.2	-4.87	-31.5
MH-B3-10A (Dup)	8/27/2010	-13.5		
MH-AB1-11A	11/4/2010	-7.3	-4.98	-33.0
MH-AB2-11A	11/4/2010	-14.1	-4.92	-31.8
MH-B2-11A	11/4/2010	-17.1	-4.43	-29.6
MH-B3-11A	11/4/2010	-14.9	-4.47	-29.8
MH-D3-11A	11/3/2010	-4.7	-6.26	-39.8
MH-TB1-11A	11/4/2010	-8.9	-4.90	-32.2
MH-D3-11A (Dup)	11/3/2010	-4.7		
MH-AB1-13A	1/6/2011	-4.6	-5.36	-34.4
MH-AB2-13A	1/6/2011	-14.1	-5.63	-32.5
MH-B2-13A	1/6/2011	-16.9	-4.89	-32.2
MH-B3-13A	1/6/2011	-13.8	-4.95	-29.3
MH-D3-13A	1/5/2011	-4.6	-6.83	-42.4
MH-TB1-13A	1/6/2011	-6.3	-5.08	-32.1
MH-AB2-13A (Dup)	1/6/2011	-14.1		
MH-AB1-14A	3/3/2011	-3.8	-4.94	-31.4
MH-AB2-14A	3/3/2011	-14.2	-5.17	-31.9
MH-B2-14A	3/3/2011	-17.5	-4.77	-31.9
MH-B3-14A	3/3/2011	-12.2	-4.78	-30.0
MH-D3-14A (Redo)	3/2/2011	-4.6	-6.32	-38.6
MH-TB1-14A	3/3/2011	-6.0	-5.12	-32.9
MH-B2-14A (Dup)	3/3/2011	-17.5		

Sample ID	Date	$\delta^{13}\text{C}_{\text{DIC}}$ (‰)	$\delta^{18}\text{O}_{\text{H}_2\text{O}}$ (‰)	$\delta\text{D}_{\text{H}_2\text{O}}$ (‰)
Ref STD-1645				
MH-AB1-15A	4/7/2011	-4.8	-5.21	-32.1
MH-AB2-15A	4/7/2011	-13.3	-5.25	-35.4
MH-B2-15A	4/7/2011	-16.6	-5.26	-34.4
MH-B3-15A	4/7/2011	-13.1	-4.87	-30.5
MH-D3-15A	4/6/2011	-4.5	-6.31	-40.0
MH-TB1-15A	4/7/2011	-6.3	-5.06	-32.9
MH-B3-15A (Dup)	4/7/2011	-13.0		
MH-AB1-16A	5/26/2011	-7.4	-5.21	-33.2
MH-AB2-16A	5/26/2011	-14.1	-5.04	-32.1
MH-B2-16A	5/26/2011	-18.0	-4.79	-30.4
MH-B3-16A	5/26/2011	-16.9	-4.78	-32.3
MH-D3-16A	5/25/2011	-4.7	-6.37	-40.6
MH-D3-16A (Dup)	5/25/2011	-4.8		
MH-AB1-17A	8/1/2011	-8.4	-5.15	-33.8
MH-AB2-17A	8/2/2011	-13.7	-5.06	-34.5
MH-B2-17A	8/2/2011	-12.6	-4.61	-29.0
MH-B3-17A	8/2/2011	-15.6	-4.64	-28.7
MH-D3-17A	8/2/2011	-4.3	-6.31	-38.5
MH-AB1-17A (Dup)	8/1/2011	-8.2		
MH-AB2-18A	12/8/2011	-13.8	-4.96	-31.4
MH-B2-18A	12/8/2011	-18.0	-4.84	-32.9
MH-B3-18A	12/8/2011	-18.3	-4.63	-29.4
MH-D3-18A	12/7/2011	2.0	-5.63	-35.3
MH-B2-18A (Dup)	12/7/2011	-18.1		
MH-D3-18A (REDO)	12/7/2011	2.0		

Table A14-2 Isotopic composition of freshwater samples from monitoring wells at Mumford Hills.

Sample ID	Date	$\delta^{13}\text{C}_{\text{DIC}}$ (‰)	$\delta^{18}\text{O}_{\text{H}_2\text{O}}$ (‰)	$\delta\text{D}_{\text{H}_2\text{O}}$ (‰)
MH-FB1-02 ¹			-7.06	-44.9
MH-FB1-03			-7.03	-44.6
MH-FB1-04			-6.90	-44.6
MH-BA1MW-01	8/13/2009	-5.91	-6.69	-41.9
MH-BA1MW-02	9/2/2009	-5.99	-6.72	-42.1
MH-AB1MW-03	9/18/2009	-5.92	-6.64	-42.0
MH-AB2MW-03	9/18/2009	-5.63	-6.82	-42.8
MH-BU1MW-01	8/14/2009	-5.14	-6.62	-42.4
MH-BU1MW-02	9/2/2009	-5.25	-6.53	-42.4
MH-BU1MW-03	9/18/2009	-5.27	-6.76	-42.0
MH-Mumford1-04	10/14/2009	-5.73	-6.52	-42.2
MH-Mumford2-04	10/14/2009	-5.16	-6.64	-42.4
MH-Mumford3-04	10/14/2009	-5.50	-6.73	-43.8
MH-Mumford3-04 Dup	10/14/2009	-5.55		
MH-FB1-05			-7.13	-44.6
MH-Mumford1-05	11/13/2009	-6.53	-6.79	-42.0
MH-Mumford2-05	11/13/2009	-5.28	-6.95	-42.9
MH-Mumford2-05 (Dup)	11/13/2009	-5.28		
MH-Mumford3-05	11/13/2009	-5.62	-7.05	-43.6
MH-FB1-06A			-7.07	-44.7
MH-Mumford1-06A	12/23/2009	-5.84	-6.75	-43.1
MH-Mumford2-06A	12/23/2009	-5.28	-6.81	-43.4
MH-Mumford3-06A	12/23/2009	-5.44	-6.77	-44.4
MH-Mumford3-06A (Dup)	12/23/2009	-5.46		
MH-FB1-07A			-6.93	-44.4
MH-Mumford1-07A	2/2/2010	-5.85	-6.60	-42.4
MH-Mumford1-07A (Dup)	2/2/2010	-5.86		
MH-Mumford2-07A	2/2/2010	-5.73	-6.64	-42.7
MH-Mumford3-07A	2/2/2010	-5.48	-6.68	-42.9
MH-FB1-08A			-7.16	-45.0
MH-Mumford1-08A	3/17/2010	-5.56	-6.79	-41.6
MH-Mumford2-08A	3/17/2010	-5.48	-6.82	-42.8
MH-Mumford3-08A	3/17/2010	-5.56	-6.89	-42.9
MH-Mumford1-09A	6/9/2010	-5.53	-6.68	-42.3
MH-Mumford2-09A	6/9/2010	-5.78	-6.90	-42.5
MH-Mumford3-09A	6/9/2010	-5.49	-6.79	-43.1
MH-Mumford1-10A	8/26/2010	-5.69	-6.42	-40.5
MH-Mumford2-10A	8/26/2010	-6.01	-6.42	-41.1
MH-Mumford3-10A	8/26/2010	-5.68	-6.57	-42.3
MH-Mumford1-11A	11/3/2010	-5.55	-6.81	-42.6
MH-Mumford2-11A	11/3/2010	-6.13	-6.99	-42.5
MH-Mumford3-11A	11/3/2010	-5.70	-6.88	-42.6

Sample ID	Date	$\delta^{13}\text{C}_{\text{DIC}}$ (‰)	$\delta^{18}\text{O}_{\text{H}_2\text{O}}$ (‰)	$\delta\text{D}_{\text{H}_2\text{O}}$ (‰)
MH-FieldBlank1-13A	1/6/2011		-6.89	-44.2
MH-Mumford1-13A	1/5/2011	-6.39	-6.64	-41.3
MH-Mumford2-13A	1/5/2011	-6.19	-6.72	-42.4
MH-Mumford3-13A	1/5/2011	-5.71	-6.79	-42.2
MH-Mumford2-13A (Dup)	1/5/2011	-6.19		
MH-FieldBlank1-14A	3/2/2011		-6.96	-45.7
MH-Mumford1-14A	3/2/2011	-5.79	-6.59	-41.4
MH-Mumford2-14A	3/2/2011	-6.02	-6.71	-41.9
MH-FieldBlank1-15A	4/6/2011		-6.78	-43.3
MH-Mumford1-15A	4/6/2011	-5.57	-6.70	-40.9
MH-Mumford2-15A	4/6/2011	-6.13	-6.73	-42.9
MH-FieldBlank1-16A	5/26/2011		-6.97	-45.6
MH-Mumford1-16A	5/25/2011	-1.73	-6.71	-42.1
MH-Mumford2-16A	5/25/2011	-5.92	-6.79	-43.1
MH-Mumford3-16A	5/25/2011	-5.49	-6.78	-43.5
MH-FieldBlank1-17A	8/2/2011		-7.08	-44.6
MH-Mumford1-17A	8/1/2011	-5.42	-6.61	-41.8
MH-Mumford2-17A	8/1/2011	-7.16	-6.78	-42.6
MH-Mumford1-18A	12/7/2011	-5.49		
MH-FieldBlank1-18A	12/8/2011			

¹Field Blanks did not contain enough DIC for isotope measurement.

Table A14-3 Isotopic analyses of CO₂ and CH₄ for selected gas samples from Mumford Hills site.

Sample ID	Date	$\delta^{13}\text{C}_{\text{CO}_2}$ (‰)	$\delta^{13}\text{C}_{\text{CH}_4}$ (‰)	$\delta\text{DC}_{\text{CH}_4}$ (‰)	$^{14}\text{C}_{\text{CO}_2}$ (pMC)	^{14}C (± pMC)
MH-BA1-G1	2/3/10	-12.2			92.6	0.17
MH-AB1-08A	3/18/10	-12.6			86.7	0.16
MH-AB1-08A Dup	3/18/10					
MH-AB1-09A	6/9/10	-13.2			84.4	0.2
MH-AB1-10A	8/27/10	-13.4			88.8	0.22
MH-AB1-11A	11/4/10	-14.5			85.3	0.21
MH-AB1-13A	1/6/11	-14.0			52.3	0.21
MH-AB1-14A	3/3/11	-10.1				
MH-AB1-15A	4/7/11	-14.7				
MH-AB1-16A	5/25/11	-15.0				
MH-AB1-17A	8/2/11	-14.7				
MH-TB1-G1	2/3/10	-11.6				
MH-TB1-08A	3/18/10	-12.8				
MH-TB1-09A	6/9/10					
MH-TB1-11A	11/4/10					
MH-TB1-13A	1/6/11					
MH-TB1-14A	3/3/11	-14.3				
MH-TB1-14A Dup	3/3/11					
MH-TB1-15A	4/7/11	-14.9				
MH-TB1-17A	8/2/11	-16.0				
MH-B3-G1	2/3/10	-12.3	-50.0	-198	92.2	0.16
MH-B3-G1 Dup	2/3/10					
MH-B3-08A	3/18/10	-13.1	-49.7		84.2	0.16
MH-B3-09A	6/9/10	-13.3	-58.8	-214		
MH-B3-09A Dup	6/9/10					
MH-B3-10A	8/27/10	-13.4				
MH-B3-10A Dup	8/27/10					
MH-B3-11A	11/4/10					
MH-B3-13A	1/6/11	-14.3				
MH-B3-13A Dup	1/6/11					
MH-B3-14A	3/3/11	-14.5	-48.8	-209		
MH-B3-15A	4/7/11	-12.4				
MH-B3-16A	5/25/11	-14.4				
MH-B3-17A	8/2/11	-15.5				
MH-B3-17A Dup	8/2/11					
MH-B2-08A	3/18/10	-12.5	-47.4	-197	85.4	0.15
MH-B2-09A	6/9/10	-11.4	50.9	-210		
MH-B2-10A	8/27/10	-13.6				
MH-B2-11A	11/4/10	-19.6	-48.8	-220		
MH-B2-13A	1/6/11	-14.1				
MH-B2-14A	3/3/11	-10.9				
MH-B2-15A	4/7/11	-12.7				
MH-B2-16A	5/25/11	-12.5	-51.8	-225		
MH-B2-16A Dup	5/25/11					
MH-B2-17A	8/2/11	-14.4	-58.0	-269	75.8	0.21

Sample ID	Date	$\delta^{13}\text{C}_{\text{CO}_2}$ (‰)	$\delta^{13}\text{C}_{\text{CH}_4}$ (‰)	$\delta\text{DC}_{\text{CH}_4}$ (‰)	$^{14}\text{C}_{\text{CO}_2}$ (pMC)	^{14}C (± pMC)
MH-BA2-08A	3/18/10	-12.8	-47.6			
MH-AB2-09A	6/9/10	-15.0	-56.8	-210		
MH-AB2-11A	11/4/10	-17.4	-47.9	-207	55.2	
MH-AB2-13A	1/6/11	-14.1				
MH-AB2-14A	3/3/11	-14.6				
MH-AB2-15A	4/7/11	-16.9	-50.4	-212	49.3	
MH-AB2-15A (Dup.)	4/7/11					
MH-AB2-16A	5/25/11	-18.5				
MH-AB2-17A	8/2/11	-14.7	-53.3	-235	76.0	
MH-D3-09A	6/9/10	-15.4	-67.7	-202		
MH-SP-10A	8/27/10	-13.3				
MH-SP-11A	11/4/10	-14.0				
MH-SP-13A	1/6/11					

